ibvt
Institut für Bioverfahrenstechnik

Technische Universität Braunschweig

Band 59
ibvt-Schriftenreihe

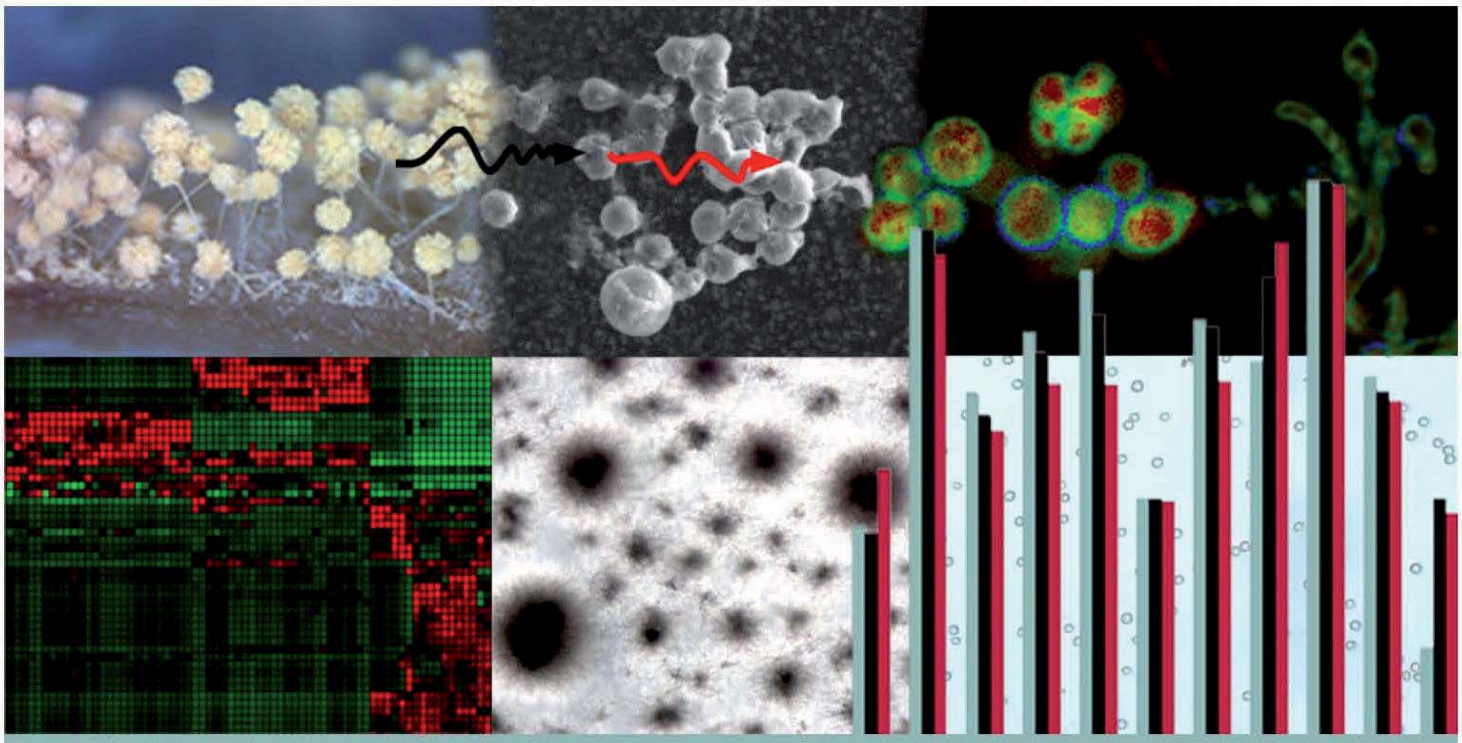

Development and Validation of Indicators for the Production and Quality of Seed Cultures

Matthias Gehder

Cuvillier-Verlag

ibvt-Schriftenreihe

Schriftenreihe des Institutes für Bioverfahrenstechnik
der Technischen Universität Braunschweig

Herausgegeben von Prof. Dr. Christoph Wittmann

Band 59

Cuvillier-Verlag
Göttingen, Deutschland

Herausgeber
Prof. Dr. Christoph Wittmann
Institut für Bioverfahrenstechnik
TU Braunschweig
Gaußstraße 17, 38106 Braunschweig
www.ibvt.de

Hinweis: Obgleich alle Anstrengungen unternommen wurden, um richtige und aktuelle Angaben in diesem Werk zum Ausdruck zu bringen, übernehmen weder der Herausgeber, noch der Autor oder andere an der Arbeit beteiligten Personen eine Verantwortung für fehlerhafte Angaben oder deren Folgen. Eventuelle Berichtigungen können erst in der nächsten Auflage berücksichtigt werden.

Bibliographische Informationen der Deutschen Nationalbibliothek
Die Deutsche Nationalbibliothek verzeichnet diese Publikation in der Deutschen Nationalbibliographie; detaillierte bibliographische Daten sind im Internet über *http://dnb.d-nb.de* abrufbar.
1. Aufl. – Göttingen: Cuvillier, 2011

© Cuvillier-Verlag · Göttingen 2011
Nonnenstieg 8, 37075 Göttingen
Telefon: 0551-54724-0
Telefax: 0551-54724-21
www.cuvillier.de

Alle Rechte, auch das der Übersetzung, vorbehalten
Dieses Werk – oder Teile daraus – darf nicht vervielfältigt werden, in Datenbanken gespeichert oder in irgendeiner Form – elektronisch, fotomechanisch, auf Tonträger oder sonst wie – übertragen werden ohne die schriftliche Genehmigung des Verlages.

1. Auflage, 2011
Gedruckt auf säurefreiem Papier

ISBN 978-3-86955-847-9
ISSN 1431-7230

Abstract

Cultivations of filamentous fungi are of large industrial and scientific interest. However, the utmost starting point of the majority of those cultivations, the inoculum consisting of fungal spores, has previously been neglected. This work hence introduces a total of nine spore quality indicators and subsequently correlates the sporulation environome to the properties of the generated spores and their performance in submerged cultivation. The model organism is *Aspergillus ochraceus* while the model process is the hydroxylation of a steroid. A positive correlation between the spore yield and the substrate's carbon content on solid medium was found with oat bran agar giving best yields of $26 \cdot 10^7$ spores/mL. The assessment of the conidial metabolome revealed the presence of 126 metabolites. Particularly, polyols, such as glycerol, erythritol and ribitol, are found at high concentrations of up to 55 ng/10^5 spores. They show a strong correlation to the storage resistance of conidia and also to the performance of the spores in cultivations where reactant turnover is approx. 80 % after 72 h cultivation. The culture performance is further a function of the portion of protein bound NAD(P)H and the aggregation behavior of the spores, strongly affecting the morphology of the culture. Surprisingly, severe alterations of spore properties were observed after storing the same in suspension for 7 d at 4 °C.

Zusammenfassung

Die Kultivierung filamentöser Pilze ist von großer wirtschaftlicher und wissenschaftlicher Bedeutung. Dennoch wurde der Zustand von Pilzsporen, die als Inokulum den Startpunkt der meisten Pilzkultivierungen darstellen, bislang vernachlässigt. In dieser Arbeit werden daher neun Qualitätsindikatoren für die Charakterisierung von Konidien vorgestellt. Diese ermöglichen, das Sporulationsenvironom, die Sporeneigenschaften sowie die Ergebnisse einer anschließenden Submerskultivierung zu korrelieren. Als Modellorganismus dient *Aspergillus ochraceus*, der exemplarische Produktionsprozess ist die Hydroxylierung eines Steroids. Zwischen dem Kohlenstoffgehalt des Sporulationsmediums und der Konidienausbeute wurde ein positiver Zusammenhang festgestellt. Die höchste Konzentration ergab Haferkleie-Agar mit Ausbeuten von $26 \cdot 10^7$ Sporen/mL. Des Weiteren wurden 126 Metabolite in Sporen detektiert, die größtenteils zur Gruppe der Polyole gehören und in Konzentrationen von bis zu 55 ng/10^5 Sporen vorliegen. Eine enge Verbindung zur Lagerungsfestigkeit und der Aktivität der Sporen konnte auch hier gezeigt werden. Der Eduktumsatz liegt nach 72 h maximal bei ca. 80 %. Weitere wichtige Einflussfaktoren für die Kulturausbeute sind der Gehalt an Protein gebundenem NAD(P)H sowie das Aggregationsverhalten, welches die Morphologie beeinflusst. Sehr starke Veränderungen der Sporen wurden bereits während der Lagerung in Suspension bei 4 °C für 7 Tage festgestellt.

Table of contents

Acknowledgments

First of all, I would like to sincerely thank my supervisor Prof. Dr. Rainer Krull for supporting me throughout this entire project, for always having an open ear for my ideas and problems as well as for the very helpful corrections of the manuscript.

Just as cordially, I would like to thank Prof. Dr.-Ing. Dietmar C. Hempel for setting up the project, for supporting me during the course of this work, for his helpful advice, for chairing the committee and for being my mentor for many years.

Many thanks also go to Prof. Dr. Siegmund Lang (Inst. for Biochemistry and Biotechnology, TU Braunschweig), not only for his co-supervision but also for accompanying me during all my years in Braunschweig, right from the beginning.

I also thank Dr. Simone Kardinahl (Bayer HealthCare Pharmaceuticals, Bergkamen) for the interesting insights, the good collaboration, the positive atmosphere and the financial support.

Prof. Dr. Karl-Heinz Gericke and Dipl.-Chem. Sebastian Herbrich (Inst. for Physical and Theoretical Chemistry, TU Braunschweig) I want to thank for their tremendous help as well as their expertise during the measurement and even more during the mathematical interpretation of the TCSPC data.

Many thanks go to Dr. Christian Scherling (Inst. for Biochemistry and Biotechnology, TU Braunschweig) for his expert help, his profound knowledge, his helpful advice and the always joyful collaboration during the metabolite profiling.

Further I would like to thank Jan-Michael Blum, Jakub Gabrielczyk, Felix Krujatz and Jan-Hendrik Sachs for their invaluable help with all the work in the laboratory, most of all for their willingness to assist me with even the strangest experimental setups and their hard work regardless of season and day- or nighttime.

Becky Sommer I would like to thank for the always positive atmosphere, the great collaboration and the interesting discussions we shared throughout the entire project.

Thanks also go to Yvonne Göcke for her help with the HPLC analysis as well as all other technicians without whose help any scientific work would not be possible: Sandra Hübner, Cord Hullmann, Rochus Jonas and Detlev Rasch.

Further, I want to thank Ewald Priegnitz (Inst. for Genetics, TU Braunschweig) for his help with the silanization as well as Michael Hust and Thomas Schirrmann (Inst. for Biochemistry and Biotechnology, TU Braunschweig) for the possibility to use their facilities for the ATP analysis.

I would also like to thank my colleagues in the subproject B3 of the SFB 578 as well as the team of the ibvt for the good working environment.

My thanks further go to Prof. Dr. Rainer Löwen of the German National Academic Foundation for accompanying me several years as well as Dr. Hans-Ottmar Weyand for the generous financial support and many inspiring meetings.

Very special and heartfelt thanks go to my family and friends. For all their love, their help, their patience, their motivation, their inspiration and for their faith they have always had in me.

Matthias Gehder Braunschweig im Juli 2011

Publications

Gehder, M., Krujatz, F., Gabrielczyk, J., Herbrich, S., Scherling, C., Gericke, K.-H., Krull, R.
Comprehensive analysis of fungal spore properties and how they impact the subsequent cultivation process
1st European Congress on Applied Biotechnology, Berlin, September 2011
Accepted

Label-free spatial analysis of free and enzyme-bound NAD(P)H in the presence of high concentrations of melanin
Herbrich, S., Gehder, M., Krull, R., Gericke, K.-H.
Journal of Fluorescence, submitted

Sommer, B., Gehder, M., Kardinahl, S., Hempel, D. C., Krull, R.
Charakterisierung von Aspergillus-Seedingkulturen
100. SFB 578-Kolloquium Vom Gen zum Produkt, Haus der Wissenschaft, Braunschweig, Juni 2010

Gehder, M., Sachs, J.-H., Kardinahl, S., Hempel, D. C., Krull R.
Bestimmung der Viabilität von Pilzinokula mittels Autofluoreszenz von Sporen
Proc. GVC/DECHEMA-Vortrags- und Diskussionstagung „Bioprozessorientiertes Anlagendesign“, P33, 105, Nürnberg, Mai 2010

Gehder, M., Sachs J.-H., Hempel, D.C., Kardinahl, S., Krull, R.
Using spore autofluorescence to measure viability of fungal inocula
European Conference ECFG10, 10th European Conference on Fungal Genetics, Meeting abstracts, Fungal Biotechnology PR8.44, 176, Leeuwenhorst, The Netherlands, März 2010

Supervised works of students that were conducted within the scope of the project and contributed to the work:

Jan-Hendrik Sachs, Diplomarbeit:
Durchflusszytometrische Analyse von Sporen filamentöser Pilze
June of 2009

Felix Krujatz, Master thesis:
Charakterisierung von Sporen für den industriellen Einsatz
November of 2010

Jakub Gabrielczyk, Bachelor thesis:
Einfluss von Sporulationsbedingungen auf die Submerskultivierung
October of 2010

List of abbreviations and symbols

2PFM	Two-photon fluorescence microscopy
19-NorAD	Norandrostenedione
ANOVA	Analysis of variance
ATP	Adenosine triphosphate
BAA	Banana agar
BSA	Bovine serum albumin
BSI	Biomass sink index
CFU	Colony forming unit
CLSM	Confocal laser scanning microscopy
CSL	Corn steep liquor
CSLA	Corn steep liquor agar
CSL-SP	Medium for shake flask culture
CYEA	Czapecks yeast extract agar
d	Day(s)
Da	Dalton
DBM	Dry biomass (see eq. 3.3)
DMF	Dimethylformamide
DMSO	Dimethyl sulfoxide
FACS	Fluorescence activated cell sorting
FLIM	Fluorescence lifetime imaging
GABA	Gamma-aminobutyric acid
g	Gramm
GPI	Glycosylphosphatidylinositol
h	Hour(s)
HPLC	High pressure liquid chromatography
L	Liter
LLD	Lower level discriminator
M	Molar
MEA	Malt extract agar
MEL	Malt extract liquid medium
MES	2-(N-Mopholin)-ethansulfonic acid
MI	Morphology index (see eq. 3.4)
min	Minute(s)
MSTFA	N-methyl-N-trimethylsilyl-trifluoroacetamide
MYEGA	Malt extract yeast extract agar
NAD(P)H	Nicotinamide adenine dinucleotide (phosphate), reduced form
OD	Optical density
OBA	Oat bran agar
OH-19-NorAD	11-alpha-Hydroxy-19-Norandrostenedione
p	p-value for statistical significance according to t-test
PAGE	Polyacrylamide gel electrophoresis
PCA	Principle component analysis
PDA	Potato dextrose agar
PMSF	Phenylmethylsulfonylfluoride
PMT	Photo multiplier tube
ROS	Reactive oxygen species
s	Second(s)
SAF	Specific autofluorescence
SEM	Standard error of the mean
SDS	Sodium dodecyl sulfate
STEM	Scanning transmission electron microscopy
TAE	Tris base, acetic acid, EDTA
TCA cycle	Tricarboxylic acid cycle
TCSPC	Time correlated single photon counting
Ti:Sa	Titanium-sapphire crystal
ULD	Upper level discriminator
WBA	Wheat bran agar
WVB	Wet volume of biomass
YESA	Yeast extract sucrose agar
YEPGA	Yeast extract peptone glucose agar

SI prefixes

k	kilo
m	milli
μ	micro
n	nano
p	pico
f	femto

Greek symbols

τ	Fluorescence life time
λ	Wavelength

1 Introduction and theoretical background

1.1 Aim and structure of the thesis

Filamentous fungi are of tremendous interest in research and industry. Their ability to produce a large spectrum of economically relevant substances makes them appealing organisms for the entire biotechnological community. Their use hence ranges from large scale applications like the production of citric acid all the way to therapeutic proteins requiring complex glycosylation patterns (Demain, 2000; Grimm et al., 2005a; Punt et al., 2002). Furthermore, filamentous fungi are widely used in bioremediation and biotransformation (Da Costa et al., 2007). In fact, the 11-alpha hydroxylation of progesterone by the filamentous fungus *Mucorales* spp. shown by Peterson and Murray (1952), the same biotransformation that is in the focus of this work, is today considered the first 'green chemistry' process as this single step cultivation process replaced a 31-step chemical synthesis (Dunn et al., 2010).

The increasing awareness for ecologically clean production alternatives, the rising application of technical enzymes and the growing demand for protein-based therapeutics have hence raised the interest in filamentous fungi dramatically. Tremendous efforts are being invested to understand and optimize the complex cultivation processes. Power input through stirring and aeration, initial pH and pH shift of the cultivation broth, addition of microparticles to the medium, aggregation behavior of spores, hyphae and steel as well as rupture resistance of hyphae walls have been investigated, only to name a few, recently reviewed in Wucherpfennig et al. (2010). Advances in this field have been contributed especially from the collaborative research center SFB 578, based in Braunschweig, Germany.

The inoculum, however, has been neglected throughout most of those studies. If at all, the effect of the concentration of the inoculum was assessed. But disregarding the inoculum in the holistic analysis jeopardizes the entire scrutiny as the seed culture marks the absolute starting point of any cultivation. Without detailed knowledge of the characteristics of the inoculum, the cultivation outcome cannot be interpreted properly. As with any process, the output is an immediate function of the input and hence maximum care has to be taken with the inoculum. Inferior seed cultures will result in suboptimal products and an inoculation with spores of unknown properties will turn the result of any cultivation into a game of 'trial and error' while also strongly hindering the correct interpretation of the same. Overcoming of these two immense stumbling blocks, i.e. usage of mediocre inocula and working with inocula of unknown properties, is the overall goal of this investigation.

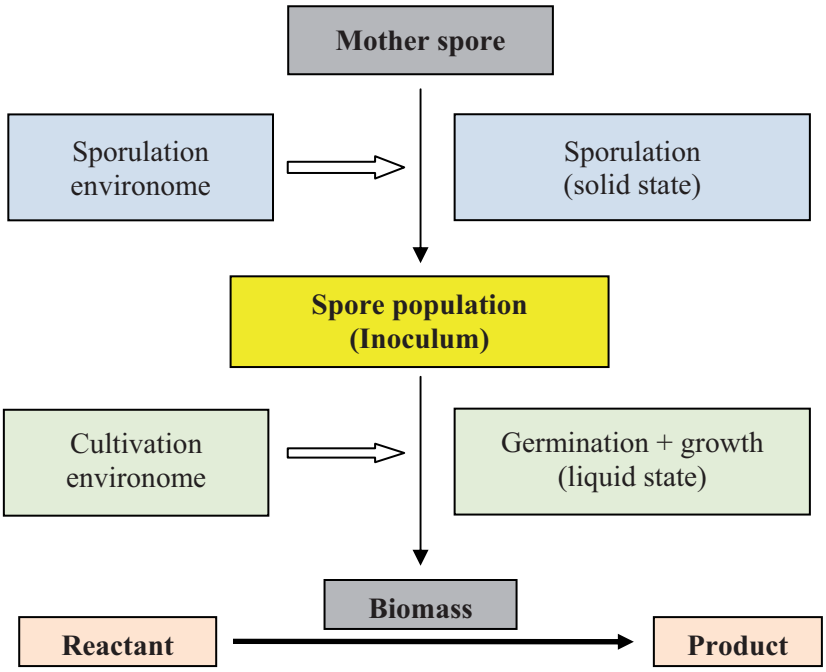

Fig. 1.1. Schematic illustration of the process sequence for cultivations with filamentous fungi including the often neglected inoculum generation.

Figure 1.1 schematically illustrates the process sequence for cultivations including the generation of the inoculum which is strongly affected by the sporulation environome. Previously reported studies, however, often focused exclusively on the cultivation part of the process, i.e. the actual cultivation while the inoculum was regarded as a 'black box'. Hence, the first step has to be the establishment of indicators that allow the assessment of spore quality. Only very little is known about the constitution of spores even though it has been shown very early that spores are capable of conducting biotransformations (Vezina et al., 1963).

Analysis of conidial properties such as cell wall characteristics and the resulting aggregation behavior, determination of intra-conidial carbon reservoirs and stress-protectors as well as metabolic characteristics are possible starting points. However, the methods for the proper analyses of the here suggested criteria need to be established as hardly any work has previously been conducted in this field. Possible means for their analysis are biochemical and spectroscopic techniques as well as extraction of key compounds and consecutive analysis by means of chromatography.

Subsequently, in a second step, the methods have to be validated as indicators are only meaningful if they exhibit biological responses upon changing parameters during the sporulation. Further, at least for industrial applications, they are additionally interesting when showing correlations to properties of the cultivation inoculated with the respective spore population. This validation can be combined with the assessment

of typical sporulation parameters such as solid medium, incubation duration and storage which together resemble a part of the ‘sporulation environome’. Summarized, spore characterization indicators have to be established and consequently validated. This hence represents the structure of the presented work:

In the first results section (chapter three) nine methods are introduced which have been set up and employed throughout this work. As the establishment of these methods represents a significant part of the results of this work, they are reported there rather than in the standard ‘materials and methods’ section. Further, the significance is exemplified for every assessment and, where applicable, possible relevant correlations to other criteria are illustrated.

In the second results section (chapter four), the nine previously presented methods are applied to spore populations generated under alternating conditions (where reasonable). This hence represents a permutation of the nine methods and five parameters of relevance, i.e. sporulation media, sporulation duration, inoculum concentration, storage and initiating germination.

Regardless of the section, the focus throughout the entire study is the introduction of novel meaningful methods to facilitate the assessment of spore characteristics in order to avoid working with mediocre inocula and/or inocula of unknown quality. As it has been increasingly difficult to interpret the escalating details of submerged cultivations, this study may foster the understanding of these processes by elucidating the influence of the inoculum and therefore eliminating an unknown but important parameter in this multivariant system. Further, determination of the requirements for the generation of optimal seed cultures will result in more homogenous and improved cultivations and eventually lower production costs.

1.2 Biology of *Aspergillus ochraceus*

Aspergillus ochraceus is a wide spread filamentous fungus. It is typically found in soil of tropical and subtropical regions but also in cereals, nuts and many more food products. It was first characterized in 1877 and is best known as a feed spoiler due to his production of the mycotoxin Ochratoxin A (Al-Anati and Petzinger, 2006; Kozakiewicz, 1990; O'Callaghan et al., 2006; Van Der Merwe et al., 1965). *A. ochraceus* can be classified as follows (Schwantes, 1996):

- Phylum: Ascomycota
- Class: Ascomycetes, Subclass: Eurotiomycetes
- Order: Eurotiales
- Family: Trichocomaceae
- Genus: *Aspergillus*
- Species: *Aspergillus ochraceus*

A. ochraceus is in many aspects a typical representative of the Ascomycota. This phylum contains numerous very common fungi covering several thousand species, including famous edible fungi like morels and truffles. The Phylum received its name from the typical ascus-cell where the ascospores, the spores for sexual reproduction, are produced. However, not all fungi categorized as Ascomycota actually form an ascus. The categorization can therefore be misleading. In fact, for many fungi, including the majority of Aspergilli, no sexual propagation has been witnessed so far. These species only reproduce asexually by the formation of conidiospores and were therefore formerly united in the informal taxon Deuteromycota and denoted as fungi imperfecti for not having a sexual stage (Geiser, 2009; Hibbett et al., 2007; Schwantes, 1996).

A close investigation of the current literature reveals an equivocal use of the numerous terms for the entire spore developing process even amongst mycologists. Therefore, the notions employed in this work are briefly shown below summarizing the definitions given by Axelrod (1972), Champe et al. (1987), Cahagenier et al. (1993) and Davis and Perkins (2002):

- Ascospore: haploid spore for sexual reproduction
- Conidiophore: specialized fungal hypha that bears and generates the conidiospores
- Conidiospore: synonym for conidium
- Conidium (pl. conidia): spore for asexual reproduction, generally haploid
- Macrospore / Microspore: synonym for conidium, used to differentiate between smaller and larger spores from the same organism
- Mitospore: synonym for conidium

For this study, ‘conidium’ and ‘spore’ are used synonymously.

Fig. 1.2. On this cross section of an A. ochraceus *colony grown on malt extract agar the substrate penetrating hyphae, the aerial hyphae and the conidiophores carrying the spores can be identified.*

Figure 1.2 shows a cross section of *A. ochraceus* growing and sporulating on solid substrate. The spores are of ocher to brown color, giving the species its name. They are spherical with a diameter of approx. 3.5 µm and a slightly rough surface. Their generation is identical to the typical spore formation of Ascomycota and involves the following seven steps (Adams et al., 1998; Broderick and Greenshields, 1981; Christensen, 1982; Schwantes, 1996):

- Formation of thick-walled footcells on the solid medium.
- Development of conidiophores, aerial unbranched stalks that elongate by apical extension on top of each footcell.
- Growth of the conidiophores orthogonally to the medium surface up to 1.5 mm in length.
- Formation of a conidiophore vesicle at the distal end of each conidiophore.
- Development of metulae surrounding the conidiophore vesicles.
- Budding of metulae to produce a layer of uninucleate sterigmata termed phialides.
- Phialides then continuously produce a chain of conidia.

As phialides undergo repeated asymmetric division to produce chains of spores while maintaining their own identity, they have been considered ‘fungal stem cells’. The spore chain growing from each phialide can contain several hundred spores with the youngest conidium being located immediately next to the phialide-cell at the bottom of the spore chain and the oldest spore at the distal end of the tip (Timberlake, 1990).

The spore formation in *A. ochraceus* can be categorized as blastic conidiogenesis as the spores are constricted after conidiation (i.e. the spore is evident before it separates

from the phialide), in contrast to thallic conidiogenesis where constriction occurs before conidiation. In all cases, ripening of the conidia occurs after constriction and like in most Ascomycota the spores as well as the vegetative cells of *A. ochraceus* are haploid (Schwantes, 1996).

Further, international research groups are currently combining efforts to understand the complex role of light for conidiogenesis. However, the results for the different genera and even for different species within some genera seem to differ significantly and are still very equivocal (Friedl et al., 2008). First regulatory mechanisms are just being revealed for *A. nidulans* and *Neurospora crassa* but no publications were found examining the effect in *A. ochraceus*. The role of light is hence not discussed deeply within this work.

Before the availability of rapid rRNA analysis for the establishment of phylogenetic trees, *A. ochraceus* was considered as a group of fungi containing 15 species, the key representative being '*Aspergillus alutaceus* var. *alutaceus* Berkeley et Curtis'. After 1990 some regrouping efforts were undertaken and strains were renamed. Hence, some older references referring to *A. alutaceus* are now ascribed to *A. ochraceus* Wilhelm (Chelack et al., 1991; Christensen, 1982; El-Kady and Youssef, 1993).

1.3 Industrial relevance of *A. ochraceus* and the synthesis of steroids

The first documented utilization of fungi for the production or enhancement of food dates back to the early settlements in the Middle East and Egypt some 5 000 years ago. The production of bread, beer, wine and fermented meat are well known examples how microorganisms were exploited yet in ancient times and their use has been broadened since then. Today, filamentous fungi are well established biocatalysts for various reactions like condensations, oxidations, reductions and isomerizations. (Bennett, 1998). The commercially most important example for the industrial employment of fungi is the production of citric acid with a volume of approx. one million tons by *A. niger* and the synthesis of numerous antibiotics with a market volume of approx. 25 billion US$ by a multitude of species (Crolla and Kennedy, 2001; Janssen, 2006).

Lately, the expression of heterologous proteins has gained significant interest as well. Most fungi are unpretentious with respect to their growth conditions on the one hand, but at the same time capable to introduce complex glycosylation patterns. This fact makes them promising production hosts for technical enzymes and therapeutic proteins

alike filling the gap between bacteria and cell culture (Punt et al., 2002; Sharma et al., 2009). Furthermore, the use of fungi, especially spores of fungi, as a biological pest control has gained broad attention during the last years. Particularly, conidia of *Trichoderma* spp. are widely used to protect crops from other fungi, nematodes, insects and weeds (Verma et al., 2007).

The relevant commercial use of *A. ochraceus* focuses on two applications: the decomposition of the xenobioticum triphenylmethane which accumulates during staining in the textile industry (Parshetti et al., 2007; Saratale et al., 2006) and the enantioselective hydroxylation of various steroids and similar substances which has been exploited and expanded for more than fifty years (Dulaney et al., 1955a; He et al., 2010). The chemical family of steroids comprises a variety of naturally occurring substances in fungi, plants and animals that all share the same structure depicted in **figure 1.3**.

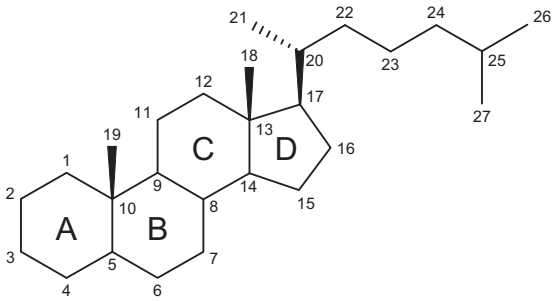

Fig. 1.3. Steroid skeleton including the IUPAC recommended ring lettering and atom numbering.

Steroids can be categorized into the following four major groups (Berg et al., 2003):

- Sterols, e.g. Cholesterol
- Bile acids
- Steroid hormones, i.e. steroids that function as hormones
  These are again divided into five groups according to the type of receptor they typically bind to:
    - Glucocorticoids, e.g. Cortisone*
    - Mineralocorticoids, e.g. Aldosterone*
    - Androgens, e.g. Testosterone*
    - Estrogens, e.g. Estradiol*
    - Progestagens, e.g. Progesterone*
- Other steroid derived molecules
    - Secosteroids, e.g. Calcitriol*
    - Insect hormones, e.g. Ecdyson
    - Heart active steroids, e.g. Digitoxin
    - Steroid alkaloids, e.g. Solanidin

The steroid hormones indicated with an asterisk (*) are found in humans. Glucocorticoids and mineralocorticoids are often summarized as ‘corticosteroids’. This super-group contains the hormones naturally synthesized in the adrenal cortex as well as similar synthetic substances. The biosynthesis of all steroid hormones initiates at cholesterol. With the exception of calcitriol they carry no or only small side chains of two carbon atoms. Characteristic is an oxo-group at C-3 and the conjugated double-bond between C-4/C-5 in ring A. Only estradiol is aromatic in ring A, its hydroxyl-group is hence of phenolic tendency. Characteristic differences between the hormones can be found in the residues of rings C and D. Calcitriol, however, differs from this scheme that is conserved throughout the vertebrates. It contains the entire carbon skeleton from the cholesterol but ring B has been opened through a light dependent reaction transforming it into a secosteroid (Koolman and Röhm, 1998).

It is true for all steroid hormones that they play an important role in the regulation of the human body. They are relevant for the carbohydrate and electrolyte metabolism, the circulatory system and the blood pressure, sexual development, the nervous system, the regulation of inflammations and the immune system. They are hence prescribed for a wide range of indications such as rheumatism, arthritis, allergies, asthma, gastrointestinal diseases, anemia, leukemia, meningitis and many more (Hildebrandt, 1994).

Here it quickly becomes evident that there is a tremendous demand for synthetically produced steroids in medicine. Due to their complex structure, however, their chemical synthesis has been limited for many years and was a tedious, expensive undertaking. Starting from ox bile acid, a 31 step chemical synthesis was necessary to produce cortisone, twelve of those only for the rearrangement of the hydroxyl group from position 12 to position 11 (Kardinahl et al., 2006).

After Peterson and Murray in 1952 discovered the ability of several *Rhizopus* spp. to directly introduce an 11-alpha-hydroxyl group to progesterone, i.e. the one step bio-synthesis of 11-alpha-OH-progesterone, biotransformations have rapidly replaced the unthrifty chemical process (Peterson and Murray, 1952). The reaction is depicted in **figure 1.4**.

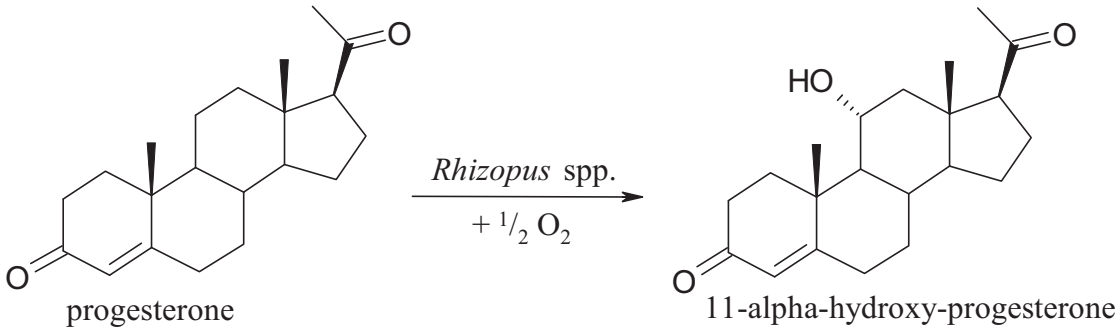

Fig. 1.4. Hydroxylation of progesterone by Rhizopus nigricans *marks the beginning of green chemistry in 1952, long before the term was coined (Dunn et al. 2010).*

Soon variations were presented for similar molecules and a growing number of fungi: Fried and colleagues (1952) demonstrated the ability of *A. niger* to introduce the 11-alpha-hydroxyl-group to progesterone, deoxycorticosterone and others in higher quantities. Shull and Kita (1955) then used *C. lunata* to directly synthesize 11-beta-OH-progesterone from progesterone which was a breakthrough as the beta-configuration is also required for several pharmaceuticals.

The same year an even higher yield was reported for conversions catalyzed by *A. ochraceus* outpacing 129 *Aspergillus* and *Penicillium* species. The tested strain rapidly transformed progesterone to 11-alpha-hydroxyprogesterone and further to 6-beta,11-alpha-dihydroxyprogesterone creating a yield of 96 % of the latter after 35 h of submerged culture. Later, the same group demonstrated the opportunity to prevent the consecutive reaction by a zinc deficiency (Dulaney et al., 1955a; Dulaney et al., 1955b). However, significant variations with respect to transformation yield between different strains of the same species (i.e. *A. ochraceus* NRRL 405 vs. *A. ochraceus* NRRL 398) were described afterwards (Vezina et al., 1963). In total, the combination of these improvements resulted in the simplification of the synthesis from 30 to 15 steps and hence price reductions from approx. 500 US$ per gram in 1948 to 3.50 US$ in 1955 (Kardinahl et al., 2006).

In the following years, numerous groups investigated the option to not only utilize free mycelium as a catalyst but also cell free extracts (Shibahara et al., 1970), spores (Schleg and Knight, 1962), immobilized spores (Dutta et al., 1993) or immobilized, activated spores (Dutta and Samanta, 1999; Wolken et al., 2003). Today, the hydroxylation of progesterone and other steroids is catalyzed exclusively microbially (Mahato and Garai, 1997).

The reaction is catalyzed by progesterone 11-alpha-monooxygenase. It is classified as an oxidoreductase (EC class 1), acting on two electron-donors, each receiving one atom of oxygen (EC subclass 1.14). It is not further categorized and hence a member of the 'miscellaneous group' (EC 1.14.99) where it carries number 14, giving it the code EC 1.14.99.14. It is also known as progesterone 11-alpha-hydroxylase (Koolman and Röhm, 1998; Shibahara et al., 1970).

While the categorization as a monooxygenase refers to its catalytic activity, phylogenetically it is a member of the cytochrome P450 superfamily (CYP). Because most (but not all) members of this family have monooxygenase activity, the two categorizations are often misleadingly used interchangeably.

As all cytochrome P450 monooxygenases (Cyt P450), the enzyme contains a heme cofactor. It catalyzes the reductive cleavage of molecular oxygen. One of the two oxygen atoms is transferred to the substrate, the second is discharged as water. The required reduction equivalents are transferred through an FAD-containing helper protein from the co-enzyme NADPH to the actual monooxygenase. The function of the heme group is to provide atomic oxygen in its reactive form: While the iron within the heme is trivalent in its non-activated status, it becomes bivalent when the substrate (progesterone) is bound to the enzyme close to the catalytic center. Now molecular oxygen can be bound. Hydrogen and one electron are added and a peroxide forms from which a hydroxide ion is released. Another proton is added to this intermediate and water is formed. The remaining oxygen (still bound to the now tetravalent iron) is thus activated and hence capable to insert into a C-H bond of the substrate forming the hydroxyl group (Berg et al., 2003; Nelson and Cox, 2005). The *A. ochraceus* progesterone 11-alpha-hydroxylase was first extensively characterized in 1987 (Samanta and Ghosh, 1987). The structure of a key intermediate in this reaction, the heme iron bearing a single oxygen atom, has just been unraveled in 2010 illustrating the unbroken relevance of the enzyme (Rittle and Green, 2010).

As indicated, *A. ochraceus* is not only capable of catalyzing the biotransformation of progesterone but many more steroids, one of them being the hydroxylation of 19-Norandrostenedione (19-NorAD) to 11-alpha-OH-norandrostenedione (OH-19-NorAD) (Diassi and Westfield, 1970; Dutta et al., 1983; Mahato and Garai, 1997) which will be the exemplary reaction throughout this study.

1.4 Influence of sporulation conditions on the properties of conidia

The production of spores serves two objectives: propagation and survival under adverse conditions. However, as both purposes overlap in most cases, it is impossible to treat them independently. It is generally accepted that sporulation is hindered under optimal growth conditions while it initiates as growth rates decrease. Nevertheless, conidiation has also been reported under favorable conditions for several fungi (Dahlberg and Etten, 1982; Vega et al., 2003). Sporulation is, like any biological process, a function of the environome. Nutrient concentration, particularly the form and availability of carbon and nitrogen as well as water activity, temperature, pH and light have been identified as the most important factors (Larroche and Gros, 1997).

1.4.1 Solid and liquid culture

Sporulation can occur on solid and liquid media alike. However, while most production and transformation processes are carried out as submerged fermentations (SmF), generation of conidia has proven to be more efficient on solid substrates. Even though scale up and reproducibility are harder to manage in solid state culture, higher volumetric yields on firm substrates have turned solid state fermentation (SSF) conidiation into the industrial standard (Hölker and Lenz, 2005; Moo-Young et al., 1983; Ooijkaas et al., 1998).

A certain gradient in nutrient provision to the fungus seems to be necessary. As the colony growths radially, young hyphae constantly have access to a fresh, nutrient-rich substrate while older hyphae remain on spent ground where nutrient limitations can be witnessed. According to the intensive studies of Georgiou and Shuler (1986), this limitation is the trigger for sporulation. This, as they suggest, also implies the possibility to influence sporulation by a variation of substrate thickness.

It had been shown that spores from solid media were more resistant to storage and UV radiation along with increased overall viability when compared to conidia from SmF. Muñoz et al. (1995) attribute this to the thicker cell wall and the tremendously increased abundance of hydrophobins on the surface of the conidia. Hydrophobins are small, highly conserved, extracellular proteins (< 14 kDa), often covering the entire spore, rendering it hydrophobic. These findings have been confirmed multiple times emphasizing the better resistance (expressed as continued high viabilities) of aerial spores against a multitude of harsh treatments like UV irradiation, freeze drying and

uncooled storage when compared to the submerged counterpart (Pascual et al., 2000). Nevertheless, spores produced in SmF have shown superior behavior with respect to germination speed and metabolic activity during early cultivation (Dillon and Charnley, 1990). For the conversion of sensitive reactants, they might hence still be of interest.

Finally, the use of membranes placed on liquid substrates, on which conidiation is observed, represents a hybrid of SSF and SmF. It has been stated that this option combines the best of both worlds while also facilitating the harvest. Filter paper, cellophane and cloths of linen have been tested, all showing satisfactory results when applied to *Penicillium* spp. (Larsen et al., 2002; Ludemann et al., 2010). However, beneficial properties of this method are still being discussed and will most likely be species specific as negative effects on spore metabolism have been reported as well (Rahardjo et al., 2004).

1.4.2 The role of carbon, nitrogen and trace elements

Not only the aggregate state of the sporulation medium has a significant effect on the produced conidia but also the ingredients. Carbon and nitrogen content play a role for both, the amount of spores produced and even more for their properties. It has been shown that the use of oligo- and polysaccharides instead of monosaccharides as the carbon and energy source has a positive effect on spore yield, viability and stability (Chen et al., 2005; Engelkes et al., 1997; Ooijkaas et al., 1998). Also, the carbon concentration is important: Impaired heat tolerance has been described for *Beauveria bassiana* spores generated on media containing carbon concentrations above 24 g/L (Ying and Feng, 2006). The superiority of starch compared to glucose can most likely be attributed to the necessary degradation of starch. As the hydrolysis through secreted enzymes is slower than the uptake of glucose no catabolite repression, hindering conidiation, occurs.

A glimpse of the complex network regulating conidiation as a function of the environome can be seen in the study of Friedl et al. (2008): While light is necessary for conidiation in most cases, a few carbon sources allow conidiation in the dark. Growing on these substrates, conidiation of *Hypocrea atrovirids* (the ‘standard fungus’ for studies evaluating the effect of light) can be enhanced, reduced or unaffected by light, depending on the particular carbon source. Also, the contribution of the two conidiation regulators BRL-1 and BRL-2, both believed to be essential for conidiation, was only required on 80 and 68 of the 95 tested carbon sources, respectively. To make

things even more complicated, addition of c-AMP, a key player in the sporulation signaling pathway, had positive, negative or no effect on spore formation, again, depending on the carbon source. This brings understanding for the statement of Beyer et al. (2005), writing about 'mysterious' findings, in their report about the effect of humidity on sporulation.

Investigating the effect of nitrogen, it has been shown that ammonium sulfate at a concentration of 0.8 g/L nitrogen stimulates the conidiation of *Fusarium graminearum* (Larroche, 1996). The same concentration, however, delays formation of spores in *Conophytum truncatum* (Jackson and Bothast, 1990). Krasniewski et al. (2006) showed how potassium nitrate and ammonium phosphate stimulate conidiation in *Penicillium camemberti* while ammonium sulfate and sodium nitrate hinder the same. A simple generalization that reduced or oxidized nitrogen sources are preferred is hence not possible. For *C. truncatum*, however, it can be said that nitrogen from proteins and protein hydrolyzates enhances sporulation over inorganic nitrogen sources.

Also, the point where nitrogen enters the metabolism plays an important role. While nitrate and histidine resulted in low spore yields, supplementation of the medium with ammonium and glycine showed better results, possibly because less energy was required to incorporate those substrates into the fungal metabolism. Pyruvate as a side product of the breakdown of glycine may be of higher value for the organism than alpha-ketoglutarate from histidine catabolism (Ooijkaas et al., 1998).

Studying the literature, it has to be taken into account, however, that not all authors state their control for the pH of the medium sufficiently. Addition of ammonium nitrate for example increases the pH of the medium. It is hence possible that the change in conidiation behavior is a secondary effect and not directly related to the nitrogen source. Taking this into account, urea and corn steep liquor seem to be suitable sources of nitrogen for the conidiation of a large number of fungi.

For *P. fumosoroseus* a correlation between the nitrogen content of the sporulation medium and the protein content inside the spore could be demonstrated. On substrates with high casamino acid concentrations, a large number of spores was produced which also showed high protein concentrations resulting in faster germination and increased resistance to freeze drying (Cliquet and Jackson, 2005). This is partly in line with results for *P. camemberti* where high total concentrations of carbon and nitrogen increased spore yields while high C:N-ratios seem to be beneficial as well (Krasniewski et al., 2006). Nevertheless, too high concentrations have also been

reported various times to hinder sporulation (Chen et al., 2005; Engelkes et al., 1997). In fact, the addition of ammonium sulfate to *A. niger* SSFs, expressing technical enzymes on palm kernel cake, has been suggested to inhibit the, in this case undesired, formation of spores (Swe et al., 2009).

The results are also equivocal for trace elements. While some reports state beneficial effects of trace elements (Ooijkaas et al., 1999), others find increasing yields under starving conditions (Chen et al., 2005). Others specify varying effects depending on the respective trace element ($MgSO_4$ fosters, $FeCl_3$ hinders sporulation), the strain (*Colletotrichum coccodes* reacts differently than *Beauveria bassiana*) and the property under investigation (mycelial growth, sporulation or heat tolerance) (Ying and Feng, 2006; Yu et al., 1997).

It can hence be said that the roles of nitrogen and trace elements are just as complex as that of carbon and have to be assessed specifically for every species until the complex regulatory mechanisms at the junction between metabolisms and gene expression are fully understood.

With respect to the almost exclusive use of natural complex media as sporulation substrates in industrial applications, some authors have investigated their effect as well. Here, just like for the defined media described above, strong effects were observed but no general trend could be seen. Among others, wheat bran, corn kernel, soy bean, pea, rice, millet, corn steep liquor and potato have been used, generally providing fair results, although with variances depending on the respective strain (Bapat et al., 2003; Ludemann et al., 2010).

It has to be mentioned that also a few examples exist where a variation of the sporulation conditions had no detectable effect on the generated conidia. As explained before, the hydroxylation of progesterone is not only possible with active hyphae but also with spores of *A. ochraceus*. Vézina et al. (1963) found the activity per conidium to remain constant for all solid and liquid sporulation media. Also, pH, nitrogen source, presence of various metal ions, chelating agents and metabolic activators in the sporulation medium had no significant effect within wide limits on the subsequent biotransformation activity of the resulting spores.

1.5 Metabolite profiling

1.5.1 Relevance and application of metabolome analysis

Out of the multitude of 'omics' mushrooming during the last two decades, four technologies attract significant interest as they build upon each other and cover the majority of the information in a cell: While the genome describes the entire genetic information, typically encoded in DNA, the transcriptome is derived there from and includes all transcribed information, typically in the form of RNA. The proteome is again a result of the transcriptome as all proteins are translated from RNA information. These proteins eventually catalyze biochemical reactions in each cell building up the metabolome, i.e. the complete pool of small metabolites in a cell at any given time. As the pool of molecules can be increased or diminished at any of these interconnections, the flux of information is not strictly linear. Additional signals may be incorporated, others may be lost through a multitude of regulatory pathways. The metabolome can therefore be seen as ultimate execution of the genetic information in the pathway described and represents the molecular phenotype of a given organism (Lodish et al., 2000). A schematic overview is provided in **figure 1.5**.

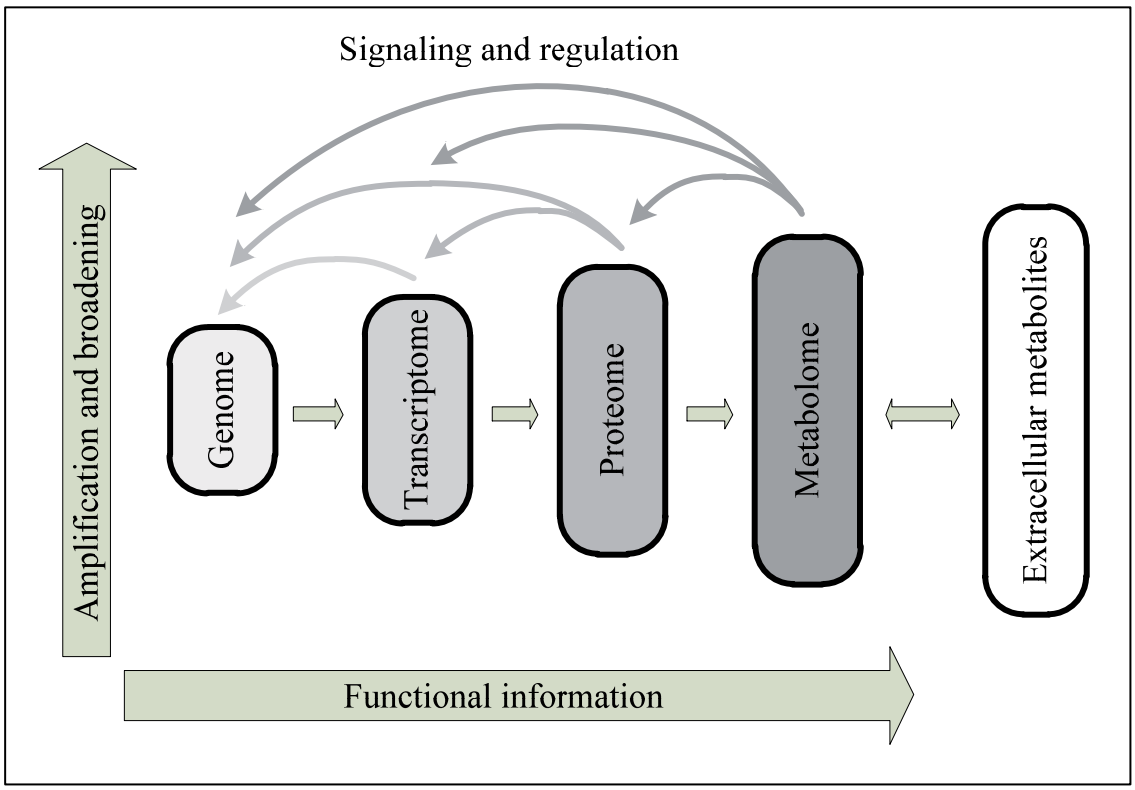

Fig. 1.5. Succession of information passing through the four major 'omes' in a cell (adapted from Smedsgaard and Nielsen, 2005).

The metabolome represents the ultimate answer of a cell to external signals and therefore provides the best insight into the relevant changes a cell experiences during certain conditions. Nevertheless, metabolite profiling has also proven efficient in identifying fundamental capabilities of putative production organisms. The applications of metabolome analysis hence range from cancer diagnostics through biotechnological engineering all the way to the taxonomic classification of organisms and systems biology (Nielsen et al., 1999; Sumner et al., 2003; Tyo et al., 2007). By means of metabolome analysis, it is possible to discover bio- and diagnostical markers, to classify organisms in phenotypes, ecotypes and genotypes as well as to reveal changes in metabotypes even with no phenotype visible.

Aiming to structure the various forms of metabolome analysis, the following four types have been defined (Fiehn, 2002), thou the mere differentiation between targeted and untargeted approaches is also well accepted today:

- Target analysis: A small number of metabolites is assessed to study the effect of a certain change, e.g. growth conditions, mutations, etc. on the organism.
- Metabolic profiling: A larger number of metabolites is selected and quantified in order to clarify metabolic pathways. This is the link to studies of the fluxome.
- Metabolomics: In order to elucidate pleiotropic effects, all metabolites of an organisms have to be assessed.
- Metabolic fingerprinting: Here the whole metabolome is measured, but only analyzed statistically, e.g. to find differences in samples. Individual metabolites are not investigated.

As no preliminary investigations on the metabolome of *A. ochraceus*, the investigated host organism in this study, are known in the literature, its genome is not sequenced and the elucidation of detailed relationships between particular genes, pathways and metabolites is beyond the scope of this work, the methods applied herein will focus on the first and the last category: target analysis and metabolite fingerprinting.

1.5.2 Available technology for metabolite profiling

Even though the idea of analyzing the ingredients of cells is as old as the knowledge of the existence of cells, metabolome analyses as we understand it today has seen a tremendous boost during the last two decades. To a large extend this has been fostered by increasing separation and detection technologies. The most important analysis techniques are liquid and gas chromatography (LC and GC, respectively) with all the

available types of detectors as well as mass spectrometry (MS) and any serial combination thereof.

While LC-MS is primarily used for the detection of secondary metabolites, GC-MS is ideal for the analysis of primary metabolites. The latter is one of the most common setups and will also be applied during this study. Hence, the basic principle will be briefly explained. The first step in any analysis is the drawing of the sample and the extraction of the metabolites from the cells, i.e. in this case spores. This step is of tremendous importance as any bias introduced at this point influences all further analyses. Most of all, it has to be ensured that the extraction method chosen, especially solvent, time and temperature, does not favor certain substances over others, e.g. by selective solubility or substance loss due to thermal instabilities (Bolten et al., 2007).

For GC-MS analysis, the extracted substances are evaporated as they are injected into the current of the carrier gas, typically an inert gas such as helium or nitrogen that does not interfere with the molecules of interest. This mobile phase carries the mixture in a continuous flow over the separation column where the ingredients are partitioned according to their interaction with the stationary phase, commonly of fused quartz capillaries with a polysiloxan coating. The separation is hence based on the NERNST's distribution law describing the concentration ratio of a given substance under specified conditions between any two phases. As this ratio is substance specific and differs depending on the functional groups, the molecular structure and the overall hydrophobicity of each constituent, some substances are carried through the column faster while others bind stronger to the stationary phase and subsequently move slower. The exit of any substance is detected at the end of the column. Every substance can then be described by its retention time which is typically corrected and converted to the retention index for better comparability between different setups.

After separation, the molecules are transferred directly to a mass spectrometer. Due to the minute flow rates it is possible to connect the two directly without compromising the high vacuum in the MS ionization chamber. While electrospray ionization (ESI) is most common for LC-MS setups, the ionization after a GC is typically achieved by electron impact (EI) with high energies of 70 eV creating reproducible fragments. The now charged molecules are accelerated in an electromagnetic field and after quadrupole filtering and possibly reflecton detouring eventually arrive at the detector. The time of flight (TOF) which is the actual measure depends on the mass to charge ratio and the drift time to the detector.

The described combination of gas chromatography and mass spectrometry (GC-MS) not only covers a large separation and detection bandwidth, it also provides information about the relative concentration in the mixture, the retention time as well as the molecular weight of the molecule fragments. Typically, this is sufficient to identify the substances in a library of known chemicals.

The disadvantage of GC of only being suitable for the separation of volatile substances is overcome by preceding derivatization of the samples with N-methyl-N-trimethylsilyl-trifluoroacetamide (MSTFA). Silylation increases volatility and thermostability of most compounds, is applicable to a broad range of molecules and generates reproducible results (Lottspeich and Engels, 2006; Morgenthal et al., 2005; Villas-Bôas et al., 2003; Villas-Bôas et al., 2005).

As most compounds exist in an equilibrium of different isoforms, silylation would uncomely manifest these isoforms into different derivatives. This unwanted, artificial enlargement of the chromatogram is restricted by methoxymation of the carbonyl group prior to silylation inhibiting the ring closure of the sugars (Roessner et al., 2000). This is of particular interest when analyzing the metabolome of spores as high concentrations of sugars, polyols and other compatible solutes have previously been shown to be present in these dormant bodies (Solomon et al., 2007).

1.5.3 Compatible solutes and other metabolites in conidia

Even though only very few studies of comprehensive metabolic profiling or target analysis in filamentous fungi in general and none for conidia have been reported (Kouskoumvekaki et al., 2008), some groups investigated the role of individual compatible solutes in fungal spores. As the findings for all of those are still being controversially discussed, only the most important will be presented here with a brief description of their currently ascribed, putative roles.

Glycerol is one of the smallest compatible solutes relevant in fungi and has been shown previously to be upregulated in osmotic stress conditions (Hallsworth and Magan, 1995). Together with other low molecular weight compatible solutes such as erythritol, it has been shown to support germination when water activity is low. Mannitol and sorbitol are the least soluble of the linear poly-alcohols and sugar alcohols typically found in the cell. They are hence not as suitable for osmoregulation as the smaller ones. In fact, a shift from mannitol towards low molecular weight compounds under osmotic stress has been observed (Clark et al., 2003; Hallsworth and Magan, 1994). It has therefore been suggested that mannitol's role as an osmoregulator

is only of minor importance but it serves as a carbon store. This, however, could not be proven or confuted as equivocal findings for different strains were reported. It seems likely that mannitol can act as a carbon store but its presence is not essential (Solomon et al., 2007). Also, mannitol may protect pathogenic fungi against reactive oxygen species involved in plants' defense mechanisms after infection as well as against damage after repeated freeze-thawing and lyophilization (Solomon et al., 2007). Its involvement in the so called mannitol cycle and the regeneration of NADPH has recently been confuted (Velez et al., 2007). Mannitol has also been shown to be required for the formation of spores. However, this seems to be species specific (Ruijter et al., 2003; Solomon et al., 2006). Also, its precise function in the spore after conidiation remains unclear.

Similar findings have been reported for sugar compatible solutes like trehalose and sucrose. While their ability to allow germination and growth under hyper-osmotic conditions is inferior compared to glycerol and eryhtritol, they have been shown to be up- or downregulated during conidiogenesis, depending on the species under investigation (Harman et al., 1991; Pascual et al., 2003).

As shown in chapter 1.3, spores are much more than just a dormant state. They are, without germination, capable of catalyzing complex reactions. It can hence be expected that they carry a variety of metabolites that may show changes depending on the history as well as biological responses to the environment of the spore.

1.6 Fluorescence

The underlying phenomenon for all the analysis techniques described in this chapter is fluorescence. Simplified, that is the emission of light by a molecule that has absorbed light of a different wavelength before. Prerequisite for any fluorescence is a match between the transition dipole moment of the molecule under investigation, the so called fluorophore, and the plane as well as the frequency of the electromagnetic radiation (i.e. light). This will result in the electronic excitation of the fluorophore, i.e. the transition of electrons from their stationary state into an excited state. Because electrons can only be excited to discrete energy levels, they only absorb energy of the precise difference between the ground and the excited state. However, as fluorophores typically have more than one possible excited state, they are capable of absorbing more than one precise energy portion, a so called quantum, of the electromagnetic wave, i.e. photons. Nevertheless, a match of the energy of the absorbed photon and the

energy difference between the ground and the elevated level of the electron of the fluorophore is essential for fluorescence to occur (with one exception that will be explained later in this chapter).

As the excited state is instable, the electron will rather quickly fall back into its ground state and emit light while doing so. This second step is described by three fluorophore specific characteristics: First, the fluorescence lifetime which is the average time between the excitation and the return to the ground state of the fluorophore, generally in the range of nanoseconds. Second, the wavelength of the emitted light. Because a proportion of the excited state energy is dissipated as heat, the emitted photon is of less energy and hence of a larger wavelength. This effect, known as the STOKES shift (sometimes 'green shift' or 'red shift'), is the reason why many famous fluorophores absorbing in the UV range emit visible radiation of green and orange color. Third, the quantum yield, i.e. the number of emitted photons relative to the number of absorbed photons (Atkins and de Paula, 2006; Lakowicz, 2006). The process is schematically illustrated in **figure 1.6**.

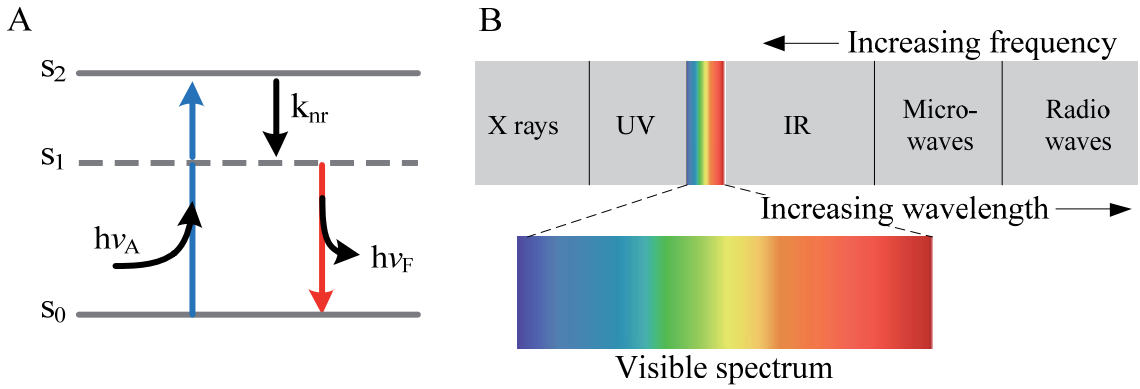

Fig. 1.6. (A) Electron transitions in the context of fluorescence can be divided in three phases. First, energy in form of a photon of the absorbance energy ($h\nu_a$) is absorbed and the electron is excited. Second, non-radiative energy dissipation to the surrounding molecules (k_{nr}). Third, spontaneous fall back to the ground level and emission of the energy difference as light ($h\nu_F$). (B) Spectrum of visible light. Photons of increasing wavelengths have decreasing frequencies and hence decreasing energy.

1.6.1 Fluorescent dyes and autofluorescence

A vast number of fluorescent dyes is available for a multitude of scientific uses (Haugland, 2005). Often the experiment makes use of a physical property of the fluorophore directly. This can be related to its ability or inability to penetrate particular membranes (e.g. propidium iodine and Syto-9), to its preferred distribution in a particular solvent (e.g. nonyl-acridinium-orange-chloride) or to its specific degradation

rate under defined conditions (e.g. fluorescein). Newer applications couple the fluorophore to other functional molecules and hence tremendously enlarging their field of application. The most common in life sciences is certainly immunofluorescence where a fluorophore is coupled to an antibody (Giepmans et al., 2006).

However, imaging technology is not necessarily connected to the need for an additional fluorophore as a number of intrinsic cell components show fluorescence themselves. This is known as autofluorescence and is the basis for the imaging applications in this work. The advantage of autofluorescence over the use of external fluorophores is the reduced probability of introducing artifacts during sample preparation. Furthermore, autofluorescence analyses are still possible when the application of a fluorophore is restricted (Chance et al., 1962; Zipfel et al., 2003a).

The most relevant biological intrinsic fluorophores responsible for autofluorescence of cells are NADPH, retinol, indoleamines, collagen, melanin and chlorophyll (Baker, 2008; Imanishi et al., 2007; Tran et al., 2006). As the majority of those fluorophores absorb and emit over a broad wavelength range with overlapping spectra, they cannot be discriminated by their spectra alone (Mizeret, 1998). What therefore becomes important is their fluorescence lifetime, i.e. the average time between the excitation and the return to the ground level of a molecule. This allows the discrimination of fluorophores in a mixture even with identical emission spectra (Hirshfield et al., 1993). As, unlike with artificial dyes, the spectrum of intrinsic fluorophores cannot be altered to individual needs, this is of particular interest for the measurement of autofluorescence.

1.6.2 Fluorescence lifetime

The lifetime of a fluorophore is a statistical concept as not all the fluorescence light is emitted at one time. Moreover, the decay of the fluorescence intensity is exponential and can be described by:

$$F(t) = F_0 e^{-\frac{t}{\tau}} \qquad (1.1)$$

where F is the fluorescence intensity and τ is the lifetime of the particular fluorophore. Now it becomes obvious that the lifetime is defined as the time point where 63 % of the excited fluorophores have returned to their ground state (Lakowicz, 2006). Exceptions, however, have also been reported (Nofsinger and Simon, 2001). **Figure 1.7** illustrates the phenomenon with two hypothetical fluorophores and their respective lifetimes, the resulting decay curves and the superimposition of the two.

The fluorescence lifetime τ depends not only on the nature of the molecule itself but also on its surrounding environment, i.e. solvent, pH, polarity, ion concentration, refractivity, temperature and most of all interaction with macromolecules. For example, the decay time for free NADPH is 400 ps in solution and 1 000 ps for bound NADPH (Lakowicz et al., 1992; Scott et al., 1970). This is a result of the folding of the molecule after its association with an enzyme. However, as the lifetime depends on a multitude of factors, absolute values are only relevant in combination with a detailed description of the setting. It is hence not surprising that fluorescence lifetimes for NADPH of 1 081 and 2 530 ns have also been reliably reported (Yu and Heikal, 2009).

The availability of superfast light detectors allows for the measurement of decay curves in so called fluorescent decay time measurements, also known as time correlated single photon counting (TCSPC). Here the photons are not integrated over a large time span generating an intensity image. Instead, the number of photons is counted in small time intervals individually generating a decay curve, typically with a resolution in the picosecond range (Maus et al., 2001).

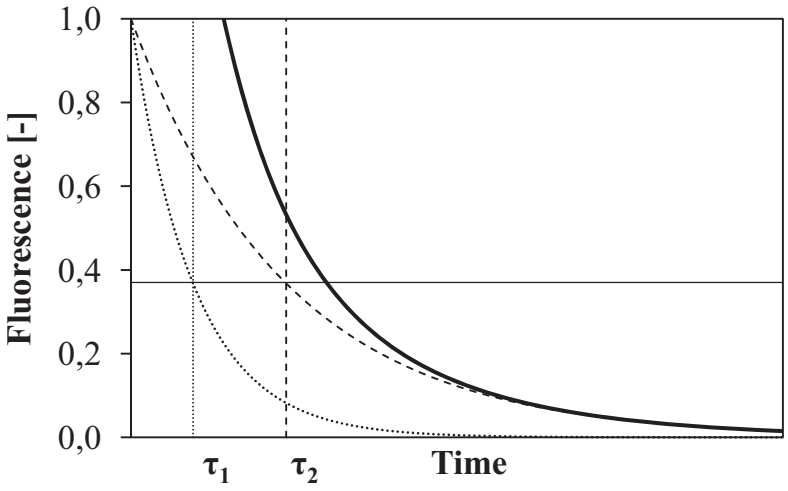

Fig. 1.7. Decay curves of two hypothetical fluorophores (dotted and dashed line) with their respective fluorescence lifetimes (dotted and dashed vertical lines, τ_1 and τ_2,). The bold line represents the hypothetically detected signal, assuming fluorophore 1 is twice as abundant in the mixed sample as fluorophore 2. 63 % of the excited fluorophores have returned to the ground state, i.e. 37 % remain excited at $t = \tau$ (vertical continuous line).

1.6.3 Spatial information and fluorescence lifetime imaging (FLIM)

All the technologies described above allow the precise determination of the fluorescence in a single spatial point, the focus of the laser beam. However, the analysis of two-dimensional samples may be of even greater interest, especially in biomedical research. This can be achieved by the combination of the described technique with either highly sensitive charge coupled device (CCD) cameras

(Lakowicz et al., 1992) or raster-scanning technology (Wang et al., 1990). For the latter, movement of the sample and of the beam have both proven suitable. Eventually this will produce images where every pixel not only contains information about the intensity and wavelength of the light at those particular coordinates, but an entire decay curve. This technology is hence known as fluorescence lifetime imaging (FLIM) (Chang et al., 2007).

Analysis of FLIM data requires the interpretation of the decay curve. In simpler cases, knowing the underlying exponential principle, the curve is easily fitted and the desired information, most of all the decay time, is obtained. However, when investigating mixed samples, which is generally the case for biological experiments, the measurement will always give the heterodyne combination of the underlying fluorescence decay curves. The most important (and sometimes most difficult) part is hence the subsequent mathematical separation of the contained unknown decays in order to determine the lifetimes and concentrations of the involved fluorophores. The measured data have hence to be fitted with a sum of exponential functions. Numerous approaches such as nonlinear least squares, the method of moments, Laplace transformation, maximum entropy method and Prony method, to name a few, have been developed and are continuously being improved. Many of them have been included in commercial and academic analysis software (Lakowicz, 2006). The first noniterative, nonrestrictive method applied in FLIM for approximations of multiexponential decays was developed by Gericke and colleagues in 2004 for the analysis of biexponential decays resulting from protein bound and free NAD(P)H (Niesner et al., 2004).

In any case, a sum of exponential decays (as given in equation 1.1 for one component) is assumed and fitted against the measured data. The number of terms is adjusted for as many compounds as can reasonably be expected in the sample though a fit with more than three free parameters has to be questioned. Depending on the analysis method of choice, this can be performed for every pixel yielding a spatial resolution of the fluorescence lifetime and the concentration ratio. Eventually, a false color image is produced where each color represents a determined lifetime (Sugata et al., 2010).

1.6.4 Two-photon fluorescence

With two-photon fluorescence a tremendous exception is introduced to the concept stated before that a photon can only be absorbed if it carries the exact energy that marks the difference between the ground and the elevated stage of the electron of the fluorophore: In a *Gedanken* experiment Maria Göppert-Mayer in 1931 postulated the

possibility that the energy may also be conveyed by two (or possibly even more) photons if only they reach the fluorophore 'simultaneously' that is within 0.5 fs (Dunn and Young, 2006). Their energy can then be added incrementally until the fluorophore reaches the elevated state (Göppert-Mayer, 1931; Yuste, 2005). This is the underlying principle of two-photon fluorescence microscopy (2PFM), also known as two-photon excitation (2PE) as it has been suggested in 1978 and first actualized in 1990 (Denk et al., 1990). As each photon is now only required to transfer half the energy, i.e. half the frequency, the excitation wavelength to work with is twice as high compared to conventional fluorescence. Typical UV or blue light excitation is hence replaced by near infrared stimulation. This means that in contrast to the above mentioned STOKES shift, the emitted light in 2PFM is shifted towards the blue range compared to the excitation light. The phenomena is not to be confused with anti-STOKES-behavior though.

The phenomenon is also often referred to as 'nonlinear optical microscopy' which palpably describes the nature of the phenomenon: As now two photons are required to interact with the fluorophore at once, a quadratic dependence of fluorescence is found. Doubling the intensity of the excitation light generates four times the fluorescence (Zipfel et al., 2003b). However, the energy typically applied during single photon fluorescence would not be enough to generate measurable signals when scanning a sample. However, any further intensification would rapidly destroy the sample. The solution is to combine the intensity increase with the implementation of a pulsed laser. This setup allows the average power to remain low while peak energy is sufficient to provoke electron excitation. The fluorescence is then a function of average squared intensity and no longer of squared average intensity (Helmchen and Denk, 2005).

Figure 1.8 shows the standardized experimental setup for 2PFM. It is almost identical to traditional confocal laser (scanning) microscopy. Since excitation is conveyed in the near infrared range, i.e. at wavelengths between 700 and 1 000 nm, the optical equipment should be optimized for this range. The heart of the technology and the most important difference to conventional fluorescence microscopy is the need for an ultrafast pulsed laser which is typically achieved by mode locked Titanium-sapphire crystals (Ti:Sa). They generate pulses with a duration of 100 fs and a frequency of up to 100 MHz (i.e. 'gaps' between the pulses of 10 ns) which is important, as described above, to achieve sufficient excitation at the laser peak without destroying the sample through a high continuous intensity. They can be trimmed to generate light with a wavelength between 670 and 1 070 nm (Helmchen and Denk, 2005). In a way, a 2PFM setup can be even simpler than the conventional arrangement: As the entire

signal can be expected to originate from the focal volume, the only place where excitation occurs, confocal detection is not necessary. Instead whole area detection is carried out by photo multiplier tubes (PMTs) which allow the recognition of minute intensities in an epi-collection setup (Beaurepaire and Mertz, 2002).

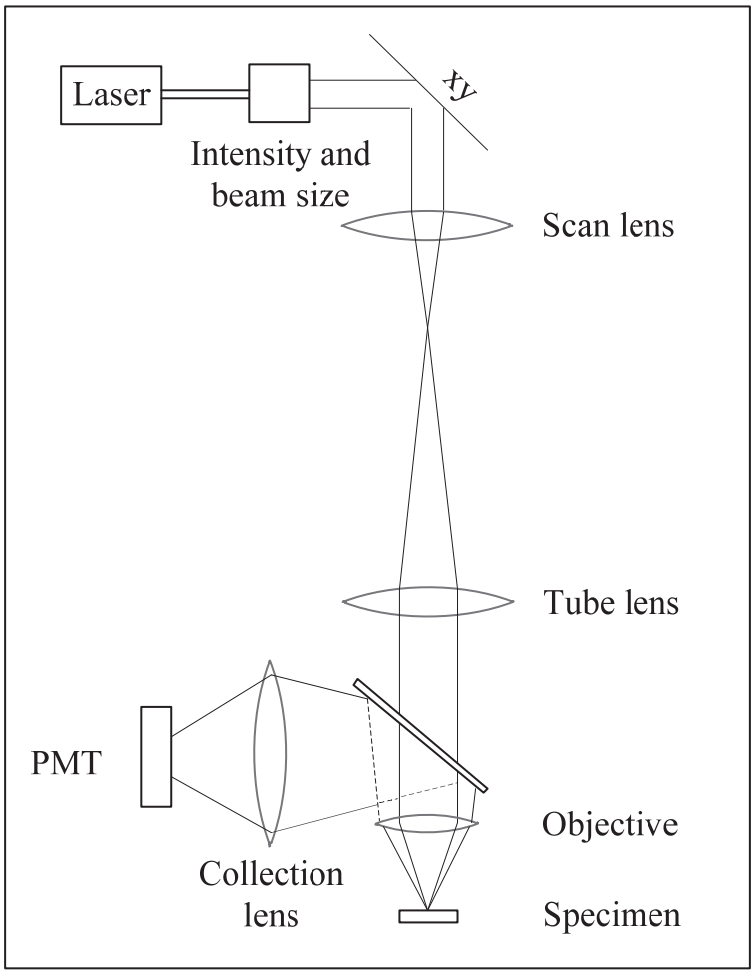

Fig. 1.8. Principal technical setup for two-photon fluorescence microscopy. The beam generated by the laser is adjusted for intensity and size and is redirected by a moveable x-y-scanning mirror. After passing the scan lens, the tube lens, a dichroitic mirror and the objective it reaches the sample. The subsequently emitted fluorescence is reflected by the mirror, then collected and generally detected by a photo multiplier tube (PMT).

As the molecular emission spectra can vary between one- and two-photon fluorescence, it is difficult to predict the spectra based on one-photon data (Xu et al., 1996). However, it has also been stated that the emission spectra are somewhat independent of the photon order of excitation. For interpretation or at least prediction, one can therefore rely on the data obtained with one-photon excitation (Zipfel et al., 2003a).

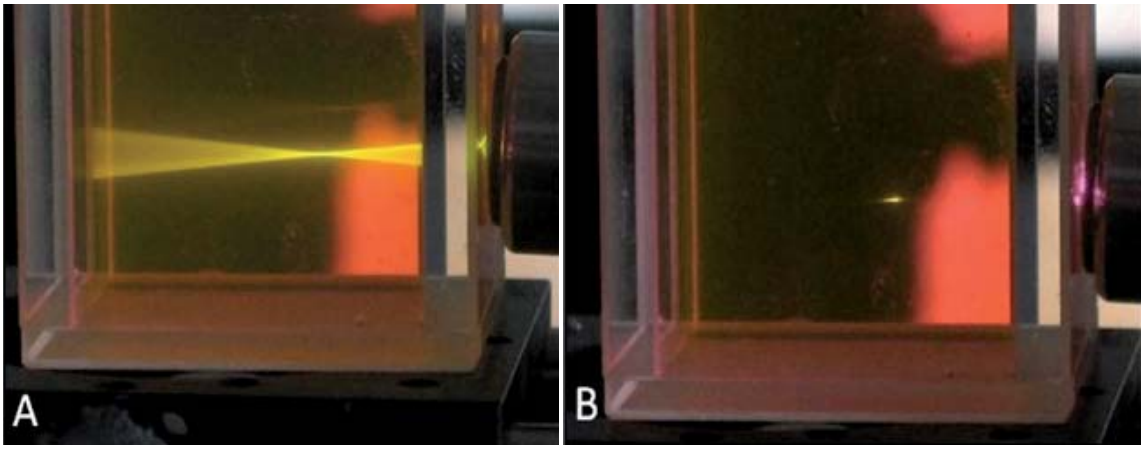

Fig. 1.9. Fluorescence obtained through conventional (A) and two-photon excitation (B).

While unsuccessful single photon absorption occurs within the entire light cone, multiphoton absorption is confined to the perifocal region of the beam where the density of photons is high enough. 2PFM therefore has better resolution, reduced photo damage and is less sensitive to light scattering as the density of scattered photons is too low to generate a measureable signal as palpably illustrated in **figure 1.9**. Two-photon fluorescence microscopy is hence well suited for the investigation of intrinsic cell constituents and has found its largest application in brain research (Mainen et al., 1999; Svoboda and Yasuda, 2006). However, the development of compact, more affordable devices has fostered their introduction into a broader group of users.

1.6.5 Fluorescence of NAD(P)H and melanin

Nicotinamide adenine dinucleotide (NAD) and its phosphorylated form (NADP) as well as their reduced forms (together abbreviated as NAD(P)H) are crucial coenzymes in cellular processes. NAD(P)H has been described as an excellent biomarker for the overall state of a cell as it is known to be involved in energy metabolism, mitochondrial functions, calcium homeostasis, gene expression, immunological functions and cell death (reviewed in Ying, 2008; reviewed in Yu and Heikal, 2009).

As the reduced form NAD(P)H (but not the oxidized form $NAD(P)^+$) shows fluorescence, it can be exploited for analyzing the metabolic activity of a given cell in a nondestructive manner. **Figure 1.10** shows the absorption and emission spectrum of NADPH. While the determination of absolute concentrations of the four species has proven difficult and error-prone, yet alone the relative concentrations and ratios between them are meaningful. It has been shown that under physiological conditions the cellular $[NADP^+]/[NADPH]$ ratio is approx. 10^{-3}. The $[NAD^+]/[NADH]$ ratio,

however, is in the range of 10^2 (Veech et al., 1969). There is hence significantly more NADPH which fluoresces than $NADP^+$ which does not show fluorescence. Of the unphosphorylated form there is considerably more NAD^+ which does not appear in fluorescence measurements than of its fluorescing reduced counterpart. Even though more recent studies found $[NAD^+]$/[NADH] ratios to vary between 10 and 600, it can still be concluded that the majority of the fluorescence signal is generated by NADPH even though the absolute concentration of NAD(H) is higher than that of NADP(H) (Lin and Guarente, 2003; Pollak et al., 2007).

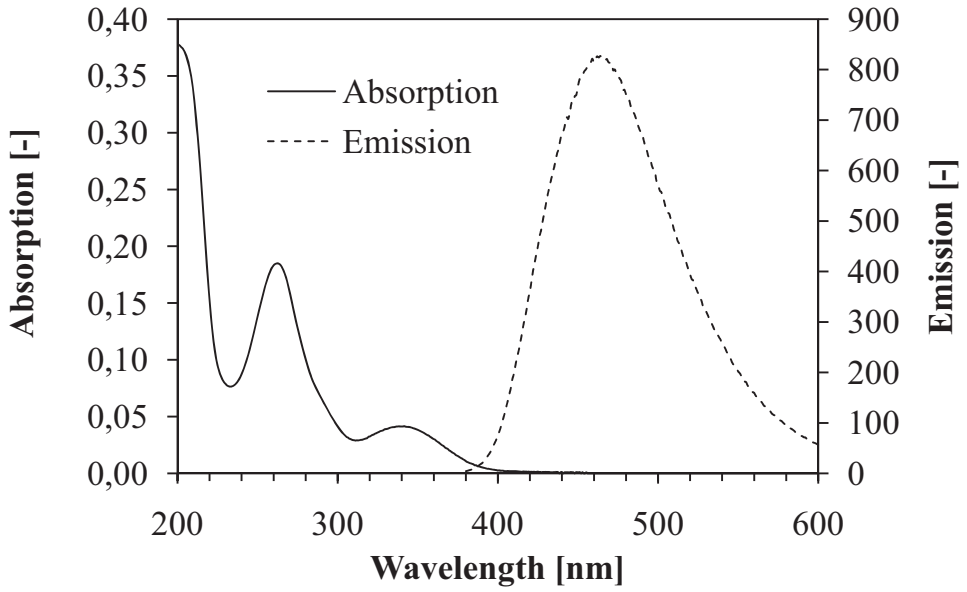

Fig. 1.10. Absorption and emission spectrum of NAD(P)H for conventional (single photon) fluorescence. Intensities are detected in relative units.

Further, as a coenzyme, NAD(P)H is only relevant in conjunction with the appropriate enzyme. It has hence been shown that the majority of the cellular NADP pools are not free but protein bound. In turn, an increase in free NAD(P)H is to be interpreted as a decreased metabolic activity of the cells while a shift towards the bound cofactor is associated with 'healthy' cells (Canepa et al., 1991; Zhang et al., 2002). As described in the previous subchapter, the free and the bound form of NAD(P)H can be distinguished by their differing fluorescence lifetimes.

The recent analysis of NAD(P)H has therefore shown very promising results and has been employed on a relatively large number of cell types. Effects of cellular oxygen concentration, enzyme rearrangement and even rotational mobility of single molecules (so called anisotropy) have been shown, mainly exploiting the autofluorescence of intrinsic NAD(P)H (Vishwasrao et al., 2005).

Also, the fluorescence of melanin has been studied extensively, primarily to understand its effect in human skin protection. As melanin is a complex macromolecule that can exist in various polymerization forms made from various monomers, interpretation and combination of the results has proven difficult (Nighswander-Rempel et al., 2005).

1.6.6 Fluorescence in flow cytometry

Even though flow cytometry makes use of the exact same principles as the fluorescence techniques described above, it covers a different area of application. While fluorescence microscopy and in particular multi-photon investigations require intensive sample preparation, often time-consuming measurement and complex data analysis, flow cytometry is a high throughput method. Once a suitable setup is found for a particular question, a sample consisting of a suspension of cells or other particles of interest can be measured within minutes. The price for such high throughput rates, however, is the loss of detailed information, particularly about the localization of cell constituents.

Rather than being characterized under a microscope, the particles of interest, i.e. in our case spores, are now investigated as they pass through a flow chamber. Here, they are typically exposed to a laser beam, whole-cell-fluorescence is generated and detected and the cell yet again exits the flow chamber making room for the next particle. Due to the high flow rates, thousands of spores can be measured per minute. In fact, some devices are even capable of sorting the particle as it leaves the chamber into one of two or more channels. Those devices hence allow fluorescence activated cell sorting (FACS). However, as not all of the available instruments provide this feature calling any flow cytometric analysis ‘FACS’, it is not only a generalization of the trademark of the manufacturer Becton-Dickinson but moreover a misleading description that should hence be avoided (Herzenberg et al., 2002; Ormerod, 2000).

Developed in the late 1960s, flow cytometry has soon found significant applications in clinical research and practice. The combination of this technology with the rapid development of monoclonal antibody technique has allowed not only for the analysis but even the separation of the most complex mixtures of cells, typically from blood samples, opening doors for instantaneous diagnosis or customized stem cell transplants. The development and the application, however, were long focused primarily on medical purposes (Tung et al., 2007).

In 2000, Stopa presented a methodology for the reliable detection of *Bacillus anthracis* spores based on their conjugation to fluorescently labeled monoclonal antibodies (Stopa, 2000). Already two years later, the applicability of Invitrogens Live/Dead BacLight Kit was shown for spores of various fungal strains by means of flow cytometry (Chen and Seguin-Swartz, 2002). Another three years passed, though hastened by the 2001 anthrax attacks in the USA, until autofluorescence of spores was introduced as a measure for viability (Laflamme et al., 2005). Now for the first time, autofluorescence was no longer considered a disturbance when assessing the signal emitted by fluorescent dyes but it actually carried the information gathered in flow cytometry. It was presented that spore populations with higher autofluorescence show significantly increased viability as determined by plate counts, i.e. by means of colony forming units. They also exhibit higher dipicolinic acid content, which is responsible for heat resistance, and higher membrane potential, which is an indicator for metabolic activity, as well as better membrane integrity, which causes a decreased permeability for propidium iodide when compared to the subpopulation with lower autofluorescence (Laflamme et al., 2006). It is speculated that the increased autofluorescence for more viable spores results from higher NADH levels which, however, could not be proven within the presented publication. Nevertheless, the overall findings have been verified multiple times (Ammor, 2007; Huffman et al., 2009).

In 2006, eventually autofluorescence of fungal spores was determined with a flow cytometer and again showed a positive correlation to viability. Here fungi, typically found in the mycorrhiza of palm trees, were investigated. Variances between different species as well as between spores of differing age were detected and it was proven that the intrinsic fluorophores were easily hydrolyzed suggesting their sensitive properties. Most interestingly, a shift in the fluorescence spectrum towards red was found during the maturation of spores. However, subsequent classical fluorescence microscopy found the fluorophores to be localized primarily in the spore wall rather than the interior opposing the signal to arise from NAD(P)H. The origin of the autofluorescence could hence not be securely identified (Dreyer et al., 2006).

2 Materials and methods

As many of the methods employed throughout this work were non-standard methods and hand therefore to be established, they represent partly the results of this work. They are hence not discussed in this chapter but in section 3 where a detailed description of the established methods is given.

2.1 Microorganism

All investigations were undertaken with *Aspergillus ochraceus* Wilhelm, catalogue number DSM 63304. The strain was freshly ordered as dry, cryogenic culture from the 'Deutsche Sammlung für Mikroorganismen und Zellkulturen' (DSMZ) in Braunschweig.

2.2 Instruments

Tab. 2.1. Instruments employed throughout this study and their manufacturer.

Instrument	**Type**	**Manufacturer**
Autoclave	5075 ELV 150 V	Systec Systec
Balance	CP 225 D LA 5200 P K-09	Sartorius Sartorius CMC
Centrifuges	5415 R Varifuge 3.0R	Eppendorf Heraeus
Cleanbench	HS-18	Heraeus
Drying cabinet	UT 6420	Heraeus
Electron Microscope	EVO LS 25	Zeiss
Filter 0.2 µm	Reference No.: FT-3-102-050	Sartorius
Filter paper	Miracloth	Calbiochem
Flow cytometer	Cell Lab Quanta*TM* SC MPL	Beckmann Coulter
GC system	Pegasus IV	Leco
Gel chamber	XCell Sure Lock*TM* Mini Cell	Invitrogen
Growth chamber	Certomat IS and BS-1 with cooling	Sartorius
Homogenizer	Ultra-Turrax T25	Janke & Kunkel IKA Labortechnik
HPLC system	ELITE LaChrome	Hitachi
Incubator	Certomat BS-1	Sartorius
Microscope	Axioskop and Stemi 2000C	Zeiss
Microtiter plate (white)	Reference No.: 655094	Greiner Bio-One
Microtiter plate reader	Sunrise Tecan-Ultra	Tecan Tecan
Petri dishes	145 mm	Greiner Bio-One

pH-Meter	CG 840	Schott
Photo detector	Avalanche Photodiode Detector	MicroPhotonDevices
Photometer	SmartSpecTM 3000	Bio-Rad
Platform shaker	Polymax 1040	Heidolph Instruments
Pumplaser	10WNd:YVO4 Verdi V10	Coherent
Pure water system	MilliQ-Gradient A10	Millipore
Ti:Sa Laser	Mira 900 D	Coherent
Ultrasound bath	Sonorex Super RK 255	Bandelin
Vortex	Reax top	Heidolph Instruments

2.3 Chemicals, solutions and media

2.3.1 Chemicals and disposables

Tab. 2.2. Chemicals and disposables employed throughout this study, their supplier and, where applicable, their abbreviation.

Chemical	**Supplier**
11-alpha-hydroxy Norandrostenedione (OH-19-NorAD)	Bayer
19-Norandrostenedione (19-NorAD)	Bayer
Acetic acid	Roth
Acetonitril	Fisher Scientific
Agar	Roth
ATP Determination Kit A22066	Invitrogen
Bananas	Standard Reseller (Bio-Grade)
Biomass filter	Sartorius (Grade 389)
Chloroform (HPLC grade)	Fisher Scientific
Corn steep liquor	Bayer
Dimethylformamide (DMF)	Sigma-Aldrich
Dimethyl sulfoxide (DMSO)	Merck
Ethanol	Sigma-Aldrich
Malt extract	Becton, Dickinson & Co.
Methanol	Fisher Scientific (HPLC-Grade)
Miracloth filter - 20microns	Merck
Oat bran	Standard Reseller (Bio-Gut & Gerne)
Peptone from soybean	Fluka
Petri dishes	Greiner Bio One, 145mm with vents
Potassium carbonate	Merck
Potato dextrose agar	Becton, Dickinson & Co.
Protein size standard	Invitrogen, Mark12 Unstained Standard
Roti-Quant Staining solution	Roth
Sodium chloride	Roth
Trichloroacetic acid (TCA)	Merck
Wheat bran	Standard Reseller (Schneekoppe)
Zymolyase 20T	US-Biological

2.3.2 Media

Tab. 2.3. Media employed throughout this study and their composition.

Medium (Abbreviation)	Ingredients	
Banana agar (BAA)	Homogenized banana	80 g/L
	Agar	15 g/L
Corn steep liquor agar (CSLA)	Corn steep liquor	9 g/L
	Peptone from soybean	10 g/L
	Agar	20 g/L
Czapeck yeast extract agar (CYEA, adapted from Atlas 2004)	Sucrose	30 g/L
	Yeast extract	5 g/L
	Czapeck Concentrate	10 mL/L
	$NaNO_3$ 30.00 g/L	
	KCl 5.00 g/L	
	$MgSO_4 \cdot 7\ H_2O$ 5.00 g/L	
	$FeSO_4 \cdot 7\ H_2O$ 0.10 g/L	
	$ZnSO_4 \cdot 7\ H_2O$ 0.10 g/L	
	$CuSO_4 \cdot 5\ H_2O$ 0.05 g/L	
	KH_2PO_4	1 g/L
	Agar	20 g/L
Malt extract agar (MEA)	Malt extract	30 g/L
	Peptone from soybean	3 g/L
	Agar	15 g/L
Malt extract liquid medium (MEL)	Malt extract	30 g/L
	Peptone from soybean	3 g/L
Medium for shake flask culture (CSL-SP), Technical cultivation medium	Corn steep liquor	10 g/L
	Peptone from soybean	3 g/L
Malt extract yeast extract agar supplemented with 40% glucose (MYEGA)	Glucose mono hydrate	440 g/L
	Malt extract	12 g/L
	Yeast extract	3 g/L
	Agar	20 g/L
Oat bran agar (OBA)	Oat bran	50 g/L
	Agar	15 g/L
Potato dextrose agar (PDA)	Potato dextrose agar	39 g/L
	Uridin	1 g/L
	Agar	5 g/L
Wheat bran agar (WBA)	Wheat bran	30 g/L
	Agar	15 g/L
Yeast extract sucrose agar (YESA)	Sucrose	20 g/L
	Yeast extract	4 g/L
	KH_2PO_4	1 g/L
	$MgSO_4 \cdot 7\ H_2O$	0.5 g/L
	Agar	20 g/L
Yeast extract peptone glucose agar (YPGA)	Glucose mono hydrate	22 g/L
	NaCl	20 g/L
	Peptone from soybean	10 g/L
	Yeast extract	10 g/L
	Agar	20 g/L

2.3.3 Preparation of solid media, liquid media and additives

All media were prepared as shown in the ingredient list above. The required amount of added agar for OBA, WBA and BAA media were experimentally optimized according to their flow behavior. pH was adjusted with 2 and 5 M HCl and NaOH to 5.6, when necessary, prior to sterilization. Culture media and saline solution were steam sterilized at 121 °C for 25 to 35 min and stored at room temperature in the dark for no more than 7 d. Media were subsequently poured into sterile Petri dishes or Erlenmeyer flasks with baffles. During preliminary investigations, alternative media, e.g. bananas and tomatoes, were used as a sporulation medium pure with no prior treatment except steam sterilization.

For the preparation of agar plates of alternative sources, fruits and vegetables were blended in deionized water using the high performance homogenizer IKA Ultra-Turrax T25 for 2 min at 13 500 min^{-1}. The homogenate was then used like standard media ingredients.

1 g of reactant 19-NorAD was dissolved in 6 mL DMF. For shake flask cultivations, the reactant solution was added to the sterilized medium before aliquotation into Erlenmeyer flasks to a final concentration of 2 g/L 19-NorAD, i.e. 12 mL solution, unless stated differently. Vigorous shaking is crucial as the reactant is hardly soluble in water.

2.4 Production of spores on agar plates

Working cell bank: The initial lyophilizated DSMZ stock culture was resuspended, distributed evenly on MEA agar plates and incubated for 5 d. Spores were harvested through plate flooding with sterile saline solution and sheering with a metal rod. The harvest suspension was mixed with the same volume of 30 % glycerol, shock frosted in liquid nitrogen and subsequently stored at -80 °C representing the working cell bank.

Preliminary solid state culture and main culture: To minimize effects through cryodemage, spores from the working cell bank were plated as preliminary culture. The thereof harvested spores were subsequently used for seeding the main solid culture. Preparatory culture and main culture were conducted using the same media composition.

Inoculation: For spore production, solid media in Petri dishes or 1 000 mL shake flasks ('agar flasks') were inoculated with 1.5 mL of spore suspension with a concentration of $2.8 \cdot 10^6$ spores/mL, unless stated differently. Petri dishes and flasks were chosen to have identical media surfaces (inner diameter of 13 cm), inoculation density was hence 320 spores/mm² agar surface. Distribution of the seed suspension was conducted with sterile glass spatulas on Petri dishes and by platform shaking at 10 min^{-1} for 3 min.

Incubation: Unless stated differently, solid cultures were left for sporulation in the dark at 24 °C for 8 d. Glass flasks employed for solid state cultivation were sealed with aluminum caps. For Petri dishes, lids were sealed to 95 % with parafilm.

Harvest: Unless stated differently, spores were harvested 8 d post inoculation by the addition of 15 g glass beads (5 mm diameter) and 25 mL sterile saline solution through vigorous shaking at 100 min^{-1} for 20 min. The obtained suspension was gravity strained into a sterile container through a miracloth filter, holding back the glass beads, pieces of agar and mycelium. Spores from the main solid culture were subsequently analyzed for their quality indicators, used to inoculate shake flask cultures or stored and analyzed after a defined period of time.

Storage: Storage of spores was conducted at 4 °C in the dark in Schott glass bottles or plastic tubes, unless stated differently.

2.5 Characterization of spores

2.5.1 Concentration and aggregation

For the determination of concentration and aggregation behavior, 1:20, 1:50 and 1:100 dilutions of harvest suspension were counted manually in a 'THOMA (Neu)'-haemocytometer (area: 0.0025 mm^2, depth: 0.1 mm). Enumeration of single spores as well as spore aggregates of 2, 3, 4, 5 and > 5 spores was conducted. The optical density at λ = 600 nm was determined as well. Further details are provided in sections 3.1 and 3.2.

2.5.2 Proteome analysis

Spore wall degradation and protein extraction: After centrifugation of 5 mL spore suspension at 4 000 g for 5 min, the supernatant was discarded and the wet weight of the spores determined. Afterwards, a spore suspension containing 2.5 g of spores was centrifuged again and the pellet resuspended in 20 mL digestion buffer containing 17.22 mL S-buffer (10 mM pipes, 1.2 M sorbitol, 0.5 M $CaCl_2$), 1 mM 1,10-

phenanthroline and 1 µM PMSF both in ethanol, 1 µM pepstatin A and 1 µM chymostatin both dissolved in DMSO, 1 µM E-64, 1 µM leupeptin hemisulfate and 50 mg zymolyase. The digestion was performed in a 100 mL conical flask at 45 °C and 100 min^{-1} for 90 min. Afterwards, the digestion suspension was centrifuged at 4 000 g for 15 min. The supernatant was filtrated through a 0.2 µM filter and 100 µL 0.15 % deoxycholic acid per mL filtrate were added. After incubation for 15 min, the soluble proteins were precipitated overnight on ice with 100 % trichloroacetic acid used in a 1:10 ratio. The next day, the proteins were pelleted at 4 °C and 4 000 g for 15 min. The protein pellet was resuspended in 5 mL Tris/HCl buffer (pH 7) and a few drops of 1 M NaOH and incubated on a shaker at 150 min^{-1} for 1 h. The protein solution was pipetted in a vivaspin 20 concentrator tube, concentrated to 1 000 µL and then in a vivaspin 2 concentrator tube to concentrate it to 100 µL.

Gel electrophoresis: NuPAGE Novex BisTris Mini gels (4 – 12 %) and an XCell SureLockTM Mini-Cell system (Invitrogen) were used, chemicals purchased from Invitrogen, chambers filled with 1x MES-Puffer and 500 µL of antioxidans pipetted in the inner chamber. 6.5 µL of the protein solution, 2.5 µL NuPage 4x LDS sample buffer und 1 µL reducing agent were incubated at 70 °C for 10 min and then pipetted in the gel pockets. The gel electrophoresis was performed at 200 V for 45 min. Afterwards, the gel was washed with water three times for 5 min each and stained with a Coomassie solution for 1 h. Before analyzing the protein bands, the gel was destained with water, in a first step for 1 h and then for 12 h, and stored in water at 4 °C for no more than 4 d.

2.5.3 Metabolome analysis

Extraction of metabolites: 2 mL of a $2 \cdot 10^8$ spores/mL suspension were centrifuged at 13 000 min^{-1} and 4 °C for 15 min. The supernatant was discharged, the pellet resuspended in 1 mL cold saline solution. This was added to 1 ml preheated (90 °C) extraction buffer (9:9:1 DMSO:Methanol:1xTAE v/v/v) and incubated at 90 °C for 75 s followed by immediate cooling on ice. Centrifugation at 13 000 min^{-1} and 4 °C yielded a clear supernatant containing the metabolites. This solution was transferred to a new vial, dried in an Eppendorf SpeedVac over night (Program 1, 30 °C, Rotation) and kept at -80 °C for no longer than 7 d until analysis. EDTA (from TAE) served as the internal standard.

Derivatisation for GC-MS: Pellets were redissolved and derivatized for 90 min at 30 °C in 20 µl of 40 mg/mL methoxyamine hydrochloride in dry pyridine each

followed by addition of 32 µL MSTFA. Subsequently, the samples were incubated at 37 °C for 30 min and at 25 °C for 120 min. A standard retention time index marker (n-alkanes ranging from C10 to C36, each 200 µg/ml in pyridine) added.

GC-MS settings: Samples were analyzed by a GC coupled to a LECO® Pegasus IV TOF (Leco Corp Inc., St. Joseph, USA) mass analyzer. GC-TOF-MS analysis was performed on a 7890A gas chromatograph with deactivated standard split/splitless liners containing glass wool (Agilent, Böblingen, Germany).

Sample volumes of 1 µl were injected with a split ratio of 1:25 at 230 °C injector temperature. GC was operated on a VF-5ms capillary column, 30 m in length, 0.25 mm inner diameter and 25 µm film thickness (VARIAN, Palo Alto, USA) at constant flow of 1 mL/min helium. The temperature program started isocratic with 1 min at 70 °C followed by temperature ramping at 10 °C/min and a final temperature of 330 °C held for 8 min. Scan rates of 20 s^{-1} and mass ranges of 70-600 Da were used.

GC-MS targeted profiling: Data were analyzed with the ChromaTOF® software (LECO®) supporting automated deconvolution of all mass spectra of a chromatogram and mass-spectral correction for co-eluting metabolites. Further, the retention indices (RI`s) are calculated and suitable fragment mass-to-charge ratios for selective quantification were identified. The obtained data were analyzed by defining a reference chromatogram with the maximum number of detected peaks over a signal-to-noise threshold of 50. Second, all chromatograms were matched against the reference with a minimum match factor of 800. Compounds were annotated by RI and mass spectra comparison to a user defined spectra library. Selected fragment ions specific for each individual metabolite were used for peak area quantification. Each compound was normalized by the peak area from the internal standard EDTA. Quantification of concentration was obtained by analyzing samples with known concentrations for selected compounds and subsequent comparison of the peak areas. Finally, results were corrected by division through spore concentrations.

2.5.4 ATP analysis

Extraction of ATP: The concentration of the harvest suspension was adjusted to $2 \cdot 10^7$ spores/mL. 500 µL thereof were added to the same volume of preheated DMSO-1xTAE extraction buffer (9:1 v/v). The mixture was incubated at 100 °C for 60 s followed by immediate cooling on ice. Spores and debris were pelleted with a table top centrifuge at 13 000 min^{-1} for 15 min. Extraction was conducted in triplicate.

Bioluminescence assay: Standard reaction solution of 'Invitrogen ATP Determination Kit' was prepared according to manufacturer's instructions (8.9 mL deionized water, 0.5 mL 20x reaction buffer, 0.1 mL dithithreitol, 0.5 mL 10 mM D-luciferin and 2.5 µL recombinant luciferase). 10 µL of the ATP containing supernatant from above were combined with 90 µL reaction solution in white microtiter plates. Generated bioluminescence was determined within 60 s at $\lambda = 560$ nm with a Tecan-Ultra (Institute for Biochemistry and Biotechnology, Technische Universität Braunschweig).

Due to excess of luciferin and luciferase, the reaction is linearly dependent on the ATP concentration and can readily be determined. Tests were conducted in triplicate resulting in 3 biological and 9 technical replicates. Mock extraction of saline solution served as the negative control and 5 point calibration with known concentrations of ATP (Sigma) was conducted for every analysis. Subtraction of negative control is mandatory. Further details provided in section 3.

2.5.5 Two-photon fluorescence microscopy

Instrument setup and measurements:

Tab. 2.4. Setup of two-photon fluorescence instrumentation.

Parameters and characteristics	**Model and/or setting**
Pumplaser10 W Nd:YVO4	Verdi V10, Coherent, USA Output: 532 nm
Ti:Sa Laser	Mira 900 D, Coherent, USA 780 nm
Avalanche photodiode detectors	MPD Micro Photon Devices, Italy
Time Correlated Single Photon Counting (TCSPC)	Picoharp 300, PicQuant GmbH, Germany Temporal resolution: 32 ps
Laser power for: - stored and fresh spores - germinated spores - heat inactivated spores	 113 mW 300 mW 132 mW
Resolution	200 nm/Pixel
Filter	460/80
Software	SymPhoTime, PicoQuant, Germany ‚Lab' (Prof. Dr. K.-H. Gericke, Technische Universität Braunschweig)

Sample preparation: Microscope slides and cover slips were silanized for increased hydrophobicity with chloroform containing 5 % dimethyldichlorosilane, dried overnight and heated at 180 °C for 2 h. Spores were analyzed freshly harvested, stored

or after germination at 24 °C in MEL medium. Germinated spores were pelleted at 4 000 g for 15 min and washed twice with cold 0.9 % NaCl solution prior to analysis.

Fluorescence detection: To measure the fluorescent life time, the time correlated single photon counting (TCSPC) method was used including a triexponential fitting as shown in:

$$F = a_0 + a_1 e^{-\frac{x-b_1}{\tau_1}} + a_2 e^{-\frac{x-b_2}{\tau_2}} + a_3 e^{-\frac{x-b_3}{\tau_3}} \qquad (2.1)$$

with $a_0 = 10$ and $b_1 = b_2 = b_3 = 27.1$

FLIM: A color was assigned to each of the three obtained lifetimes (shortest blue, intermediate green, longest red). This allowed generation of false color images where the color of every pixel represents the proportion of the three fluorophores present at that particular position.

2.5.6 Flow cytometric analysis (fluorescence and size)

Instrument and sample preparation: The concentration of the harvest suspension was adjusted to approx. $5 \cdot 10^6$ spores/mL. Flow cytometric analysis was conducted using a 'Beckman Coulter Cell Lab Quanta SC MPL' with the following settings.

- Shaking intensity: 5
- Shaking duration: 5 s
- Excitation source: Mercury-vapor lamp (λ = 366 nm)
- Flow rate: 13.57 µL/min
- Low level discriminator: 76 eV
- Upper level discriminator: 1 000 eV
- Trigger: Electronic volume
- Gain volume detection: 6.00
- Gain fluorescence detection: 4.00
- PMT voltage fluorescence detection: 10.30
- Stop criterion: 10 000 events

Size determination is conducted by means of the COULTER principle. A two point calibration was conducted before every other analysis using beads of a defined diameter of 3.6 µm (Beckman Coulter, Flow Set Beads), allowing direct conversion of the generated raw data (electronic equivalent volume) to diameters.

Fluorescence determination is carried out in parallel allowing direct assignments of fluorescence signals and sizes per individual spore. In lack of fluorescence calibration for UV excitation, fluorescence intensities are provided as arbitrary units. Correlation

to spore size, precisely spore projected area, generates the specific fluorescence SAF though. The instruments' events lists are transformed into histograms where the x-coordinate of the maximum is determined and subsequently serves as the characteristic value of the population. Further relevant analysis of raw data is explained in chapter 3.

2.5.7 Viability

Viability assessment in submerged culture: 100 mL shake flasks with 30 mL MEL medium were aseptically inoculated to have 10^6 spores/mL and incubated at 24 °C and 130 min^{-1} in the dark in triplicate. Samples of 1 000 µL were taken every 2 h. Germination was stopped through the addition of 1 drop of 2 M HCl per sample. These were assessed immediately microscopically. Standard or cavity microscope slides proofed superior over the haemocytometer as towards the later phase of the cultivation aggregates did not fit under the cover slip of the haemocytometer swaying the analysis. 100 spores were counted. Conidia with germ tubes equal to or greater than the diameter of the spore were counted as germinated. Percentage of germinated spores was subsequently determined.

Viability assessment on solid culture: Harvest suspension was diluted $1{:}2 \cdot 10^4$, $1{:}2 \cdot 10^5$ and $1{:}2 \cdot 10^6$ and spread on MEA plates in triplicate in Petri dishes and incubated at 24 °C in the dark. Spore concentration in the suspension was determined as described above. Subsequently, colonies were enumerated after 72 h incubation and related to the initial spore concentration. In the subsequent determination of the arithmetic mean, highest dilutions (lowest concentrations) were weighted double. Ratio of grown colonies per spores represents viability. Further details are provided in chapter 3.

2.5.8 Shake flask culture

Culture conditions: Liquid cultures were conducted in 100 mL shake flasks with three baffles and a working volume of 30 mL. Unless stated differently, all shake flask cultivations were carried out with CSL-SP medium supplemented with 2 g/L 19-NorAD in DMF as described above. A target concentration of 10^6 spores/mL was adjusted by the addition of $3{\cdot}10^6$ suspended spores to each flask. Cultures were incubated at 24 °C for 72 h with orbital shaking of 130 min^{-1}.

Sampling and sample preparation: At 0, 48 and 72 h, the liquid culture was analyzed with respect to pH, dry biomass, wet volume of biomass, morphology, reactant

consumption and product formation. To ensure that no bias between the different time points would be introduced through the depletion of the cultivation broth after sampling, a flask was only sampled once and for subsequent analyses at later time points, new flasks were chosen.

Morphology: Morphology was determined visually through comparison of the morphology with representative images of known morphologies and determination of the clearing time as an indicator for the sedimentation velocity.

pH: pH of the cultivation broth was determined before and after homogenization with the Ultra-Turrax.

Wet biomass: While shaking, 10 mL of cultivation broth were sampled and transferred to 15 mL centrifugation tubes. Centrifugation at 1 000 g for 10 min and subsequent comparison of the pelleted biomass with calibrated containers yielded the wet biomass [mL/mL].

Dry biomass: The biomass in the culture broth was homogenized by means of an Ultra-Turrax for 2 min at 13 500 min^{-1}. 10 mL of the homogenized cultivation broth were filtered through 0.22 µm filters. These were rinsed with deionized water once. The loaded filters were then dried at 105 °C for 3 d before the net dry mass was determined. Correction terms were introduced accounting for insoluble remaining reactant concentrations and corn steep liquor particles as described in chapter 3.9.

2.5.9 HPLC reactant and product analysis

Sample preparation: 5 mL homogenized culture broth and 15 mL ice cold methanol containing 1 % acetic acid were mixed and exposed to 15 min ultrasound for cell disruption. 1.5 mL sample solution was centrifuged at 13 000 min^{-1} at 4 °C for 5 min. 500 µL supernatant and 1 350 µL methanol containing 1 % acetic acid were centrifuged again for 1 min. Clear supernatant was subsequently analyzed by HPLC. All steps were conducted on ice. Total dilution factor: 14.7.

Analysis by means of HPLC: HPLC was used to determine the quantity of products by comparing the peak areas with the standards (0.10, 0.15, 0.20, 0.25, 0.30, 0.35, 0.40 and 0.50 g/L 19-NorAD and OH-19-NorAD in methanol/acetic acid/water (89:1:10 v/v/v). Samples were kept on ice during handling and at -24 °C when stored until analysis.

Instrument properties and settings (ELITE LaChrome, Hitachi):

- Pump: ELITE LaChrome L-2130
- Autosampler: ELITE LaChrome L-2200
- Column: Hypersil ODS 2 (Thermo), 250 x 4.6 mm
- Pre-column: Hypersil ODS 2 (Thermo), 50 x 4.6 mm
- Detector: ELITE LaChrome L-2455 PDA (Photodiode array)
- Detection wavelength: 245 nm
- Flow rate: 1.5 mL/min
- Column temperature: 40 °C
- Sampler temperature: 15 °C
- Injected volume: 5 µl
- Eluent: 75 % deionized water + 25 % acetonitrile, no gradient
- Duration of analysis: reactant approx. 18.9 min; product approx. 9.2 min

2.6 Statistical Analysis

All experiments where performed in biological triplicate and wherever possible repeated in the same manner three times yielding a total of nine biological samples. For each sample, the characterization was then performed in triplicates itself again (technical replicates) resulting in a total of 27 measurements per given set of parameters. Unless stated differently, all 27 assessments were pooled and outliers were, when necessary, identified with Walsh's outlier test (Walsh, 1950).

Student's t-test for paired samples was used for statistical analysis (Carlin and Doyle, 2001). Data were compared at a significance level of 0.01, unless stated differently.

3 Establishing methods for spore characterization

The primary objective of this study was the establishment of a bouquet of indicators allowing the characterization of spores of filamentous fungi. Previously, spore production was optimized, if at all, only with respect to the quantity of harvestable spores. This is not sufficient as spores may differ tremendously in quality and hence influence the outcome of the subsequent submerged cultivation. The quality of spores, however, could not be readily analyzed as no adequate methods existed. Characterization of spores was hence limited to light microscopical assessment of overall integrity and rarely also germination efficacy on solid medium was analyzed.

Therefore, the establishment of efficient methods to determine relevant spore quality indicators represents a major result of this work. Each method together with the corresponding indicator of spore quality is accordingly presented in the following nine subchapters. In the section thereafter, those methods will be applied to assess the effect of the sporulation environome, sporulation duration and storage on the constitution and performance of spores. Also, detectable changes during early germination will be analyzed there. The obtained results regarding the spore proteome analysis, however, are the only exception to this structure as these findings are hence presented exemplarily in chapter 3.2.

3.1 Determination of spore yield with microscopy, optical density and automated counting

The amount of harvestable spores per area of the solid state cultivation is of utmost interest as it is well known that the inoculum concentration for the subsequent submerged cultivation has significant impact on the germination speed and the morphology (Papagianni and Moo-Young, 2002). A method for the quick and reliable determination of spore concentration was therefore identified.

3.1.1 Manual haemocytometer count (microscopical determination)

Manual cell count with a THOMA chamber served as the reference for the evaluation of any other method. Because the microscopical cell count is conducted manually, it is considered the most reliable. It shows strong resistance against biases through possibly varying spore color, aggregation and sizes as well as through a putative ‘non-linear’ measuring range and software misinterpretation. Also, manual counting shows good resistance against a bias through possible residual non-spore particles. The microscopic image is exemplarily illustrated in **figure 3.1**.

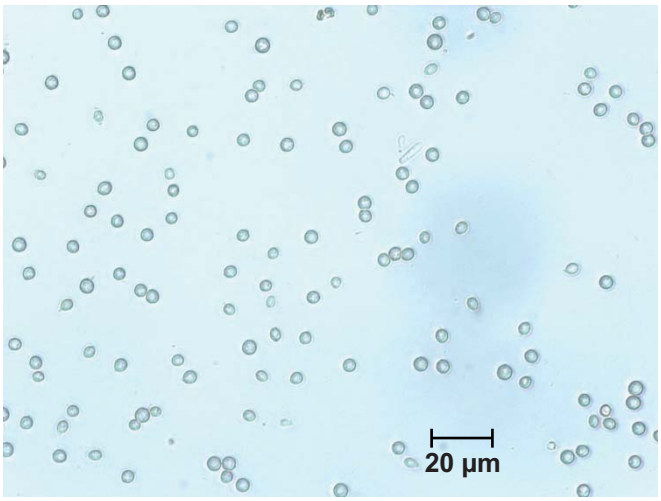

Fig. 3.1. Microscopic view of spores as usually seen for manual cell count. Discrimination of spores, harvest residues and aggregates is readily possible.

Conducting each determination in two or more dilutions, in technical triplicate and in assessing the entire THOMA area with 256 squares resulted in sufficient statistical validation. The results obtained through manual cell count are therefore regarded as safe. The disadvantage is the relatively tedious and time consuming work. Also, a certain experience is needed for the correct interpretation of particles as spores or debris in bright field as well as phase contrast. Another advantage of the method is the possibility for concomitant determination of conidial aggregation behavior.

3.1.2 Determination of spore concentration by optical density

It has been shown previously that the turbidity of a spore suspension may serve as a rapid and reliable method to determine its concentration (Fujita et al., 1994). Higher wavelengths > 500 nm have proven to be most trustworthy as those measurements are independent of particle size and pigmentation. Nevertheless, filtering and vigorous stirring to get rid of hyphae and to break up aggregates, respectively, is important in any case (Morris and Nicholls, 1978).

Figure 3.2 shows the correlation of the solutions' spore concentration determined by manual count and the optical density at 600 nm for approx. 500 samples. A stability index of 96 % and linear behavior throughout the entire absorbance range between 0.0 and 1.0 relative absorbance units demonstrates the reliability of the method. It is interesting to note that even though the suspension was measured against clear NaCl solution, the regression fits best when not constraint to pass through the origin. This finding, however, is in line with results by Morris and Nicholls (1978). Measurements were conducted with spores harvested from malt extract agar as described above.

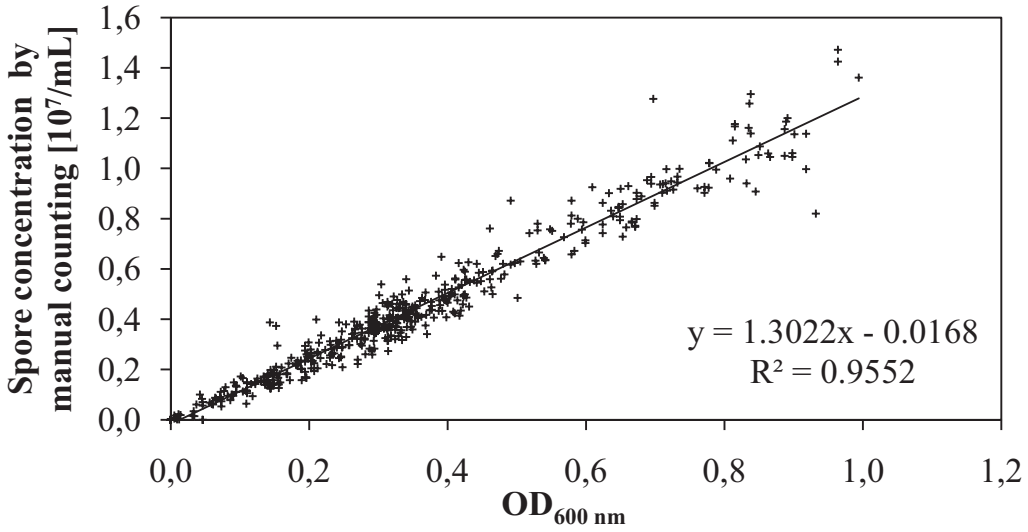

Fig. 3.2. Spore concentration as determined by manual count over optical density of the suspension at 600 nm (n = 496; data best fit: solid line, spores from malt extract agar).

Different pigmentation of spores from different solid media is noticeable with the naked eye. The method therefore had to be validated with spores of lighter and darker color as well. **Figure 3.3** shows the comparison of concentrations determined by turbidity and haemocytometer counts for spores from wheat bran agar (stronger pigmentation) and oat bran agar (less pigmentation). No bias through spore color is noticeable. This can be attributed to measuring at a wavelength of 600 nm where particle pigmentation and size is less relevant (Morris and Nicholls, 1978).

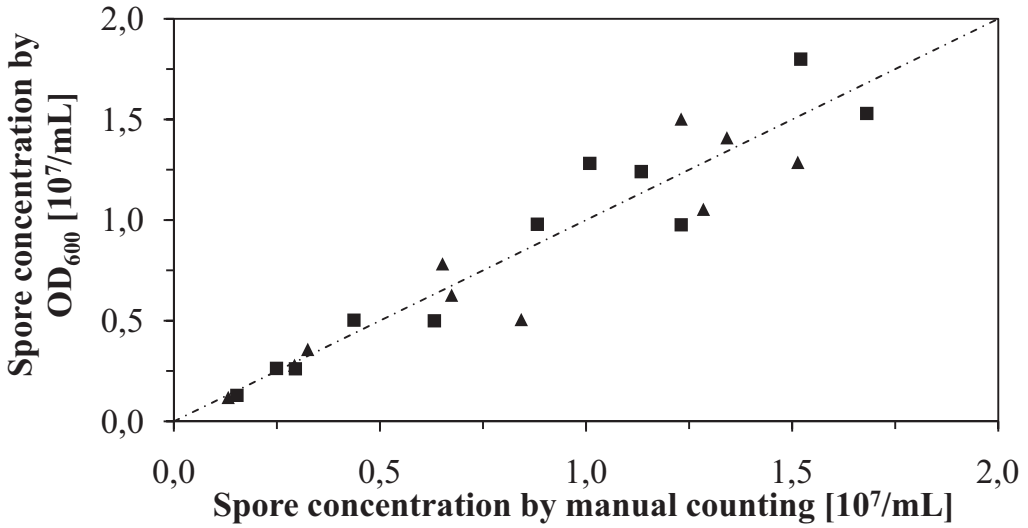

Fig. 3.3. Correlation of spore concentration based on optical density calibrated with spores from malt extract agar and manual count. Results for spores grown on oat bran agar (triangles) and wheat bran agar (squares) fit well. Theoretical correlation, dashed line.

Future analyses of spore concentration (see subchapters 4.1.1, 4.2.1 and 4.3.1) were conducted applying exclusively this method and the obtained calibration parameters.

3.1.3 Determination of spore concentration by flow cytometry

For automated cell count, a flow cytometer equipped with a COULTER counter was validated. The idea of counting spores with a high throughput instrument and hence increasing statistical significance while minimizing manual labor seems appealing. However, as can be seen in **figure 3.4**, the method did not prove to be reliable as the measurements are heavily inconsistent.

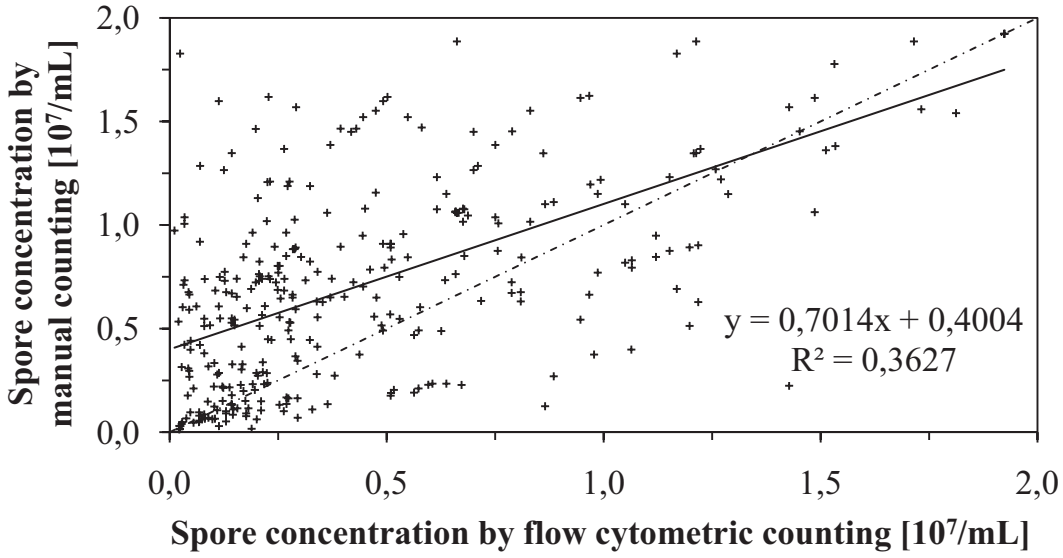

Fig. 3.4. Spore concentration determined manually and with a flow cytometer. Poor correlation and a low stability index can be noticed. Data best fit: solid line; theoretical correlation: dashed line.

It is shown that the application of automated cell counting for spore concentration determination is inappropriate. The stability index of 36 % as well as 10-fold positive and negative deflection render this method not suitable. The error should not be attributed to the instruments inability to correctly count particles but to the imprecise measurement of suspension volume. The fact that the values calculated by the flow cytometer are in average 12 % below the manually determined concentration also suggests the presence of small aggregates in the suspension which were not sufficiently separated in the instrument and hence not resolved by the applied COULTER counter. Manual determination, however, readily differentiates between single spores and aggregates accounting for each spore individually. Considering furthermore the expense and the complex setup of a flow cytometer, it becomes obvious that the determination of the spore harvest concentration by means of flow cytometry is not recommendable.

3.2 Determination of spore aggregation and wall constitution

3.2.1 Aggregation analysis by means of microscopy

Filamentous fungi can be categorized in coagulating and non-coagulating types. While non-coagulating species form pellets from hyphae growing from single spores, formation of pellets in coagulating species like Aspergilli is a result of spore-spore and spore-hyphae aggregation, i.e. primary and secondary aggregation, respectively (Metz and Kossen, 1977; Takahashi and Yamada, 1959). Even though the impact of secondary aggregation for the resulting morphology can be expected to be higher (Grimm et al., 2004), spore-spore interactions have recently been shown to be relevant as well (Fontaine et al., 2010). The aggregation behavior of spores in the saline harvest suspension is hence meaningful and was therefore analyzed.

The main difficulty for the determination of spore aggregation is the coincidental swelling of spores with diameter increases of up to factor 2 (see the following chapter ‘spore size’). Automated determination of aggregation based on size distribution is hence not possible as the volume increase per particle due to swelling often exceeds the increase caused by aggregation. Also, software supported analysis of microscopic images did not prove efficient because automated spore detection was not reliable. The determination of a spore sets tendency to form aggregates had therefore to be determined manually in a haemocytometer.

The number of spores existing individually, in groups of two, groups of three etc. was documented. The fraction hence always refers to the total number of spores and not the number of particles. This allows the declaration of proportions of spores as single spores, spores in aggregates of two, three etc. It is further noteworthy that the harvest suspension was free of detergents and buffers. The pH of the suspension was generally 5.5, irrespective of the sporulation medium. This pH typically fosters spore aggregation and pellet formation as compared to a lower pH (around 3) where aggregation is decreased and mycelial growth is the predominant morphology (Obaidi and Berry, 1980). The addition of surfactants and buffers was avoided in order to reduce potential impact on further analyses. Also, spores were not washed with deionized water as this as well would have impaired the measurement and shifted results away from standard industry procedures. However, if pH values of sporulation media differed, control of pH would be necessary for comparable results. It is also of critical importance that sample treatment is absolutely standardized. Due to the fact that aggregation is generally too high for manual counting, suspensions have to be

vortexed prior to analyses. 5 s vortexing at maximum speed prior to manual counting has proven to show best results. This was hence conducted throughout the entire study and is recommended for industrial applications.

As can be seen in **figure 3.5**, the tendency to form aggregates differs considerably between spores from different substrates as well as between freshly harvested spores and those that have been stored. While 96 % of the freshly harvested spores from potato dextrose agar (PDA) exist as single spores, only 42 % of all stored spores from malt extract agar (MEA) are single spores. Instead 21 % of the spores can be found in aggregates of six or more conidia. The aggregation behavior is hence meaningful. In subchapters 4.1.2, 4.3.2 and 4.4.1, it is discussed in detail how environmental parameters affect spore aggregation.

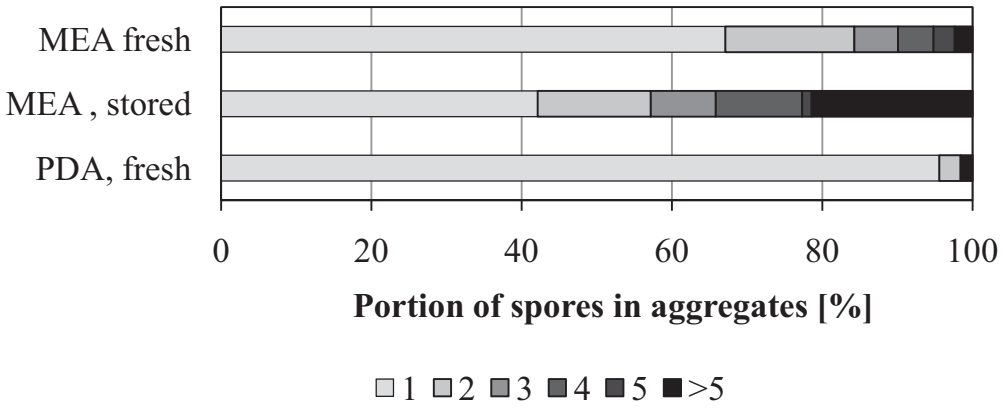

Fig. 3.5. Aggregation behavior of spores. Shown are the fractions of spores found as single spores, aggregates of two, three, four, five and more. Tested spores were obtained from MEA (fresh), MEA (stored, 21 d, 20 °C) and PDA (fresh). Results represent means from 6 biological and 3 technical replicates.

It became obvious that the aggregation behavior of spores differs tremendously. Hence the cell wall, as the mediator for aggregation, was investigated further by means of protein analysis and electron microscopy. Even though those two techniques represent methods for the characterization of spores themselves, they are presented within this chapter as they here serve the purpose of further elucidating the aggregation behavior. They will therefore also not be included in chapter 4.

While the wall of the growing hyphae is well described, less is known about the constitution of the conidial wall. However, it has been reported that the overall structure is more species specific than it is growth-state specific (Bowman and Free, 2006). The main components of the fungal cell wall are polysaccharides. Especially chitin forms the strong but dynamic exoskeleton from linearly linked beta-1,4-N-

acetylglucosamine. The chitin layer provides mechanical stability and is located immediately on top of the plasma membrane. A second layer of the fungal wall is made of branched alpha- and beta-glucans. These represent the matrix material and are linked via beta-1,4-glycosidic bonds to the inner chitin layer. It was shown recently that precisely those glucans are responsible for the spore-spore recognition and aggregation, once further coats (see below) have been lost during early germination. Included in this glucan matrix is a multitude of proteins that themselves show significant glycosylation. These cell wall proteins can be divided into soluble proteins, which show no or only loose glycosidic attachment to other components of the cell wall, and insoluble proteins, which are linked to the plasma membrane via GPI anchorage (Fontaine et al., 2010; Fontaine et al., 2003; Fontaine et al., 2000; Latgé, 2007).

On top of this three layer structure is the hydrophobic outer coat which is, in contrast to the inner ensemble, opaque to electron transmission. It consists of melanin and hydrophobins. While melanin, a heteropolymer pigment, accomplishes UV protection, hydrophobins render the surface hydrophobic. They are short, amphipathic proteins of approx. 100 amino acids that form a dense, crystal coat covering the entire spore. Hydrophobins hence account for facilitated spore dispersal through wind and insects, provide further structure, mediate spore-spore aggregation in aqueous solution and mask immunogenic spore antigens (Aimanianda et al., 2009; Bruneau et al., 2001; Wessels et al., 1991; Wösten, 2001).

3.2.2 Analysis of spore wall proteins

The difficulty in the analysis of spore wall proteins is the extraction of intact proteins from the polysaccharide network of the wall. It has been reported that this can be achieved through enzymatic digestion of the glucan structure or chemical hydrolysis (Aimanianda et al., 2009; Asif et al., 2006; Kniemeyer et al., 2006). For enzymatic digest, ‘Zymolase 20T’, a recombinant glucanase cocktail, has proven applicable. Addition of protease inhibitors is crucial because Aspergilli, like all saprophytic organisms, produce large amounts of proteases which are likely to rapidly degrade the proteins of interest after cell disruption. The mixture for protease inhibition hence consisted of phenylmethylsulfonylfluoride (PMSF), E-64 and leupeptine hemisulfate (all inhibiting cysteine and serine proteases). Further, pepstatin A (inhibiting acidic proteases), 1,10-phenanthroline (a chelating agent inhibiting metalloproteases) and chymostatin (a broad range protease inhibitor) were added to the inhibitory blend. Overall, this protocol represents an adaption of the combination of the methods

suggested previously (Allen et al., 2001; Apoga et al., 2001; Asif et al., 2006; Gil et al., 1991; Lopez-Ribot et al., 1991) and produced the best results for the analysis of *A. ochraceus* cell wall proteins. Generic protein preparation steps such as filtration, precipitation, solubilization, concentration and polyacrylamide gel electrophoresis (PAGE) separation are described in section 2.

Known quantities of bovine serum albumin (BSA) were also subjected to the procedure in order to determine possible protein loss. Recovery of BSA was 94 % for total treatment. Quantification of cell wall proteins was not possible as these are only soluble in an alkaline environment which heavily impaired common assays. Furthermore, it is important to include negative controls that also undergo the entire process in order to allow the discrimination of meaningful protein signals from samples and those from zymolyase showing distinct peptides of 55, 42, 30, 23, 17, 15, 13 and 12 kDa in accordance with the manufacturer's instructions.

The characterization of the spore wall has proven very difficult and results are not unequivocal. They have therefore to be considered preliminary. Further, very large amounts of spores are required for the preparation of sufficiently detectable amounts of the spore wall proteome. This required the spore production to be conducted in Petri dishes rather than shake flasks as applied for any other spore characterization. For these reasons, the results regarding the comparison of the proteome of different spore populations are presented within this chapter rather than in section 4 where the effects of the environome on the spores' constitution are discussed.

Figure 3.6 shows the protein pattern of freshly harvested spores from MEA and WBA as well as after 7 d of storage in suspension at 30 °C. For freshly harvested spores from MEA, protein bands of 40 (lane 2, green arrow), 20 (lane 2, red arrow), 14, 12 and 10 kDa (black arrows) were identified. Stored spores show a similar pattern with only the band at 40 kDa reduced (lane 2, green arrow). Freshly harvested spores from WBA show a comparable pattern of proteins in the range of 40 to 10 kDa though the 20 kDa protein was not detected. However, three additional bands were detected in fresh WBA spores that were not present in MEA spores and vanished during storage at approx. 80, 100 and 120 kDa (lane 3 and 5, red and green arrows).

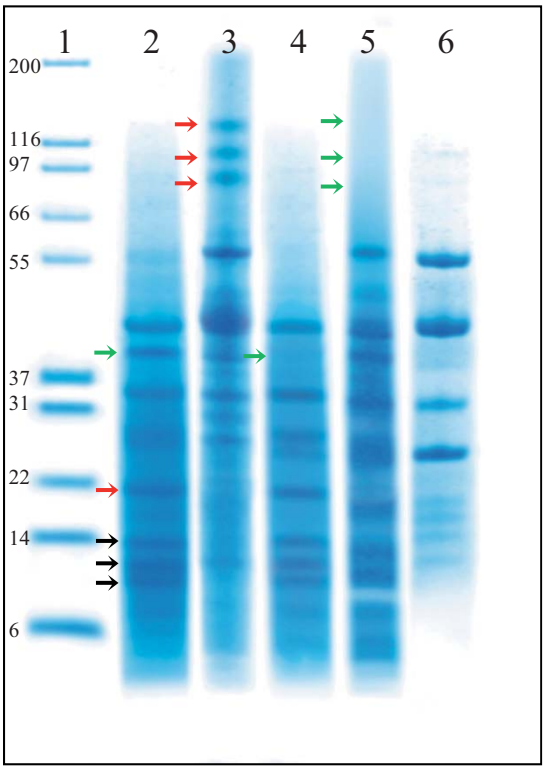

Fig. 3.6. Separated proteins from spores harvested from wheat bran agar (WBA) and malt extract agar (MEA) after enzymatic cell wall degradation. 1: Marker (protein mass in kDa), 2: MEA fresh, 3: WBA fresh, 4: MEA stored, 5: WBA stored, 6: degradation enzyme mix. Stored spores were kept at 30 °C for 7 d in suspension. Black arrows: general cell wall proteins; red arrows: only detected in MEA or WBA spores; green arrow: protein changes during storage. Image represents digital combination of separately ran protein gels at different time points.

Even though the separated proteins could not be purified nor identified, these findings can be summarized in the way that spores from MEA and WBA show differing protein patterns with a 20 kDa protein only present in MEA spores and the three additional bands at 80, 100 and 120 kDa in WBA spores. Also, storing the spores in suspension at 30 °C for 7 d has differing effects on the cell wall proteome of the conidia depending on the original substrate: While MEA spores hardly change, it leads to the loss of the three high molecular weight proteins in WBA spores.

As mentioned before, cell wall analysis of *A. ochraceus* has proven difficult and these results shall be regarded as preliminary results indicating the principal existing option to assess the proteins of the cell wall. It could be shown that protein composition of spores differs depending on the conidiation substrate. Also, changes in the protein pattern during storage of spores could be visualized. Here it became noticeable that proteins not only change during the storage period but that these changes also differed depending on the conidiation substrate.

The large unidentifiable protein continuum between 10 and 40 kDa can be expected to be a result of hydrophobin breakdown. As the molecular weight of hydrophobin isomers from *A. fumigatus* was determined to be 14, 16 and 20 kDa and they are known to aggregate to form larger structures, it is very likely that products of hydrophobin breakdown account for the apparent contamination in the lower half of the gel (Paris et al., 2003; Sulc et al., 2009). Also, the overall distribution of protein sizes is well in line with findings presented previously for the conidial wall of *A. fumigatus*. Here, several proteins with molecular weights between 10 and 100 kDa could be detected. The highest concentration, however, was found in the range between 10 and 20 kDa (Asif et al., 2006).

3.2.3 Electron microscopic imaging of spores

The final coat on the outside of spores consists of hydrophobins, small amphiphatic proteins that arrange in a highly organized manner covering the entire spore. These highly conserved proteins thereby form so called rodlets which appear like needles lying flat on the spore. As mentioned before, this crystalline structure is, in contrast to the inner layers, opaque to electron transmission and has been shown previously by means of electron microscopy (Hawker, 1965; Rydjord et al., 2007).

Within this work, it was therefore postulated that spores whose rodlet layer is altered, can be differentiated from inert spores with an uncompromised hydrophobin coat. This might serve as a further indicator for spore wall constitution though also not as a routine measure for industrial applications.

Figure 3.7 shows that freshly harvested spores from malt extract agar appear relatively dark in scanning electron microscopy images, affirming the prediction that the layer of crystalline hydrophobins is opaque for electron transmission. Spores that have been stored for 7 d in saline solution at 4 °C, however, appear with more light spots of variable size. Here, the rodlet layer has been altered and no longer forms the smooth, continuous coat as in freshly harvested spores. Detection of secondary electrons (data not shown) also affirms this finding as stored spores reflect electrons not as smoothly as fresh spores. This is in line with previously reported findings where the disruption of the rodlet layer was monitored by means of real-time atomic force microscopy (Dague et al., 2008). However, it is noteworthy that stored spores from *A. ochraceus* were found to have a compromised rodlet layer yet after storage whereas breakage of the outer coat was previously reported only for germinating spores (Aimanianda et al., 2009; Hobot and Gull, 1981b; van der Aa et al., 2002). As no emerging germ tubes

were apparent on the spores, it has to be speculated that spores stored in saline suspension are in a 'pre-germination-arrest' where they are only awaiting the provision of nutrients or other favorable conditions in order to rapidly germinate.

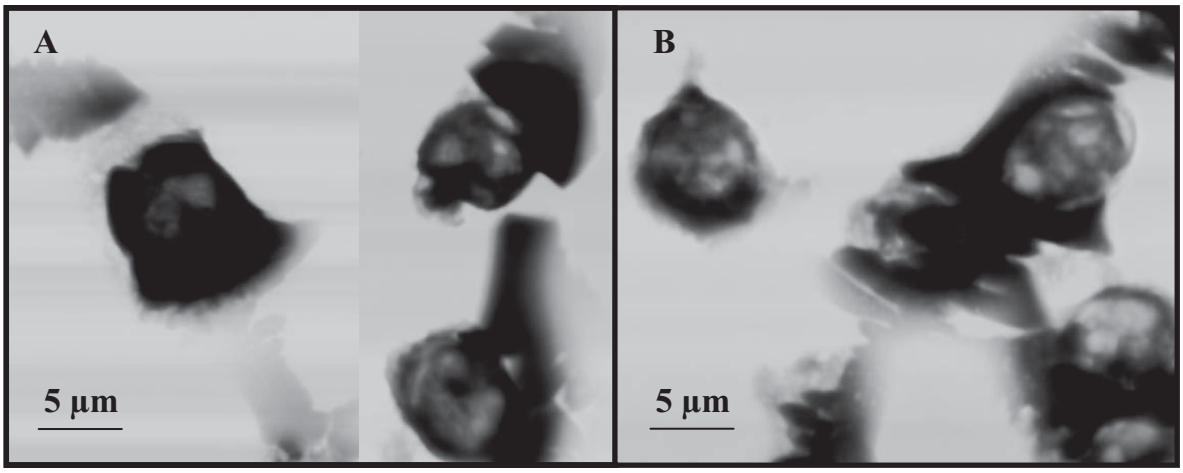

Fig. 3.7. Scanning transmission electron microscopy (STEM) images of freshly harvested spores from malt extract agar medium (MEA; (A)) and those that have been stored at 4 °C for 7 d (B).

This is coherent with literature findings emphasizing that spores show significant metabolic activity (reviewed in Wolken et al., 2003). As an immediate consequence of an active metabolism it can be expected that spores interact with their environment by the uptake of water and oxygen or by the release of carbon dioxide. Therefore, partly ruptured hydrophobin coats of stored spores are well allegeable.

Despite the shown interesting results it has to be stated that analysis of conidial cell wall proteins and electron microscopic imaging of spores cannot be recommended as a routine assessment to measure spore quality. The acquired information does not justify the required labor for routine analyses. Further, the obtained results are not clear enough to be introduced into further correlation.

Nevertheless, analysis of spore wall proteins was regarded as an additional information to the aggregation behavior which, entirely uncompromised, can readily be determined. Spore aggregation alone can hence certainly be assessed and gives evocative results that correlate well with a given population's performance in submerged culture as will be presented later in this work.

3.3 Determination of spore size with the COULTER principle

It has been suggested that spores swell prior to germination. Spore size may therefore be a relevant indicator for spore quality assessments. Spore size was hence determined by means of a COULTER counter built into the flow cytometer which allows the determination of the electronic volume. For statistical significance 10 000 particles were analyzed per measurement. An electronic lower level discriminator was set to 2 µm blocking signals from debris and other noise, simplifying later analysis and enlarging the data base, as thus all 10 000 measured events are particles of interest.

A two point calibration with beads of a known diameter of 3.6 µm was conducted and the obtained data were fitted with a four parameter non-linear regression to a GAUSSian normal distribution according to:

$$y = y_0 + a\, e^{-0.5\left(\frac{x-x_0}{b}\right)^2} \qquad (3.1)$$

The x-coordinate of the maximum subsequently served as the reference volume. Based on this calibration and the assumption that spores resemble spheres, the diameter is calculated thereof. The mere list of diameters is subsequently transformed into a histogram with a class width of 0.05 µm, the instruments resolution limit, as recommended by the manufacturer and Scott (1979). The x-coordinate of the resulting maximum is regarded as the characteristic diameter and a suitable tool because it describes the majority of the conidia in the sample.

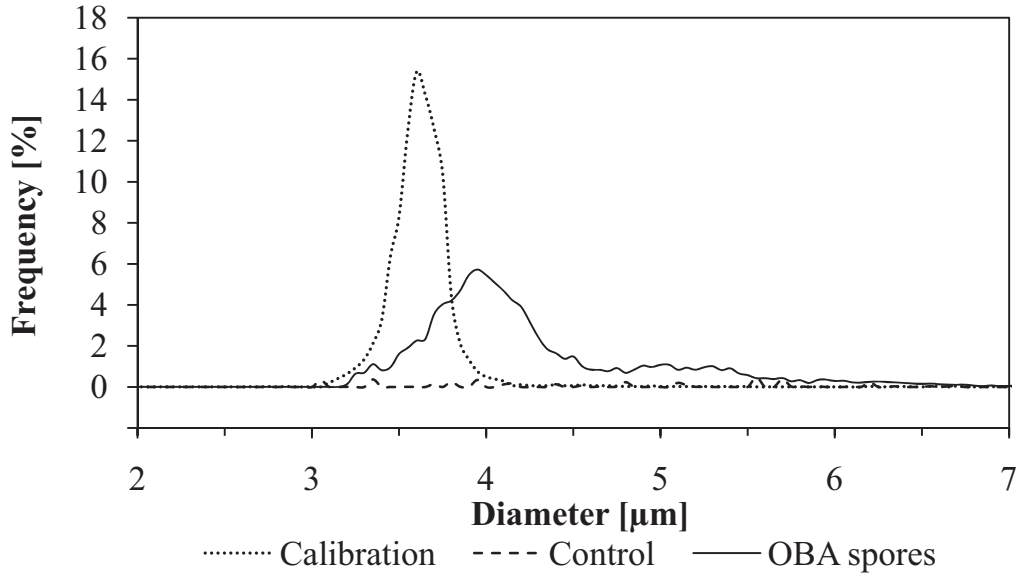

Fig. 3.8. Diameter distribution density histogram of fresh spores from oat bran agar (OBA, solid line), calibration spheres (3.6 µm diameter, dotted line) and a negative control (sterile saline solution, dashed line).

Figure 3.8 shows the results of a typical measurement conducted with the COULTER counter as well as a calibration and a negative control. The calibration is characterized by a narrow distribution and a maximum at 3.6 µm. The measured spores show a much broader distribution with their maximum at 3.95 µm. The negative control was aborted after 10 min, only showing 201 counted particles, compared to 10 000 events for both of the other measurements in less than 5 min. The finding that spores show a broad size distribution is confirmed by electron microscopy images, as shown in **figure 3.9**.

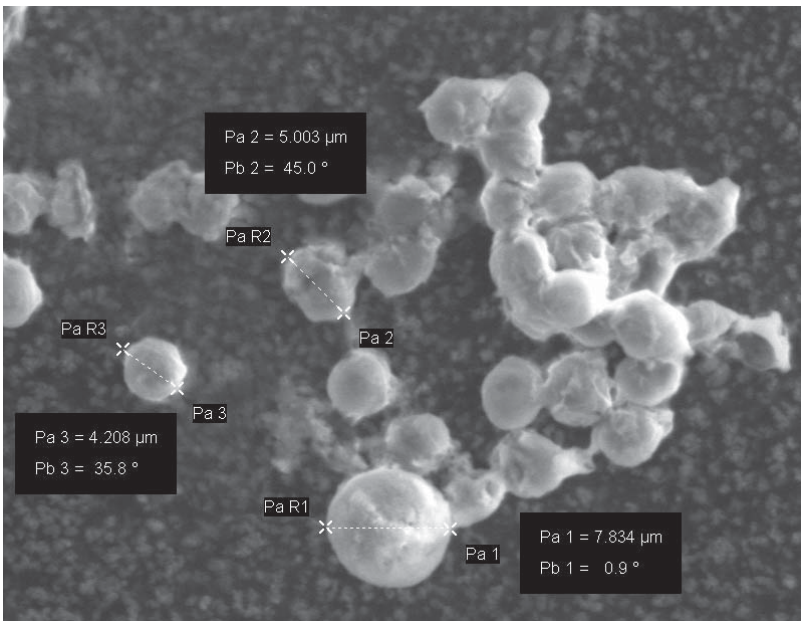

Fig. 3.9. Electron microscopy image illustrating the large differences between spores of the same population (Spores from MEA, stored for 7 d at 4 °C).

It is hence important to relate spore specific findings like the autofluorescence to the spore size. At the same time, this broad distribution prohibits automated aggregation detection and further meaningful interpretation. Despite large amounts of data, spore size is therefore also not included in the assessments in chapter 4.

3.4 Determination of spore composition with metabolite profiling

In this study, for the first time, metabolites of the primary metabolism of spores of a filamentous fungus were profiled. It was speculated that the differences observed between the different sets of spores are also mirrored in their metabolome. Hence, a protocol for the preservative extraction and the subsequent separation and identification of metabolites from conidia was established.

After washing the spores, the metabolites were extracted with the above described mixture of DMSO, methanol and TAE for 75 s at 90 °C, dried overnight,

methoxymated, silylated and eventually analyzed by means of GC-TOF-MS. In an untargeted approach, 69 metabolites could be reproducibly detected in fresh spores while 126 metabolites were found in total over all spore stages. 65 of those were selected for a targeted analysis out of which 50 could be undoubtfully identified. Measures were related to initial spore concentrations for semi-quantitative analysis while 7 selected metabolites were absolutely quantified.

Of the 50 identified metabolites, 12 are related to the fundamental carbon metabolism, i.e. glycolysis and the TCA cycle, for example pyruvic acid and malic acid, though in very low concentrations. Also, 14 amino acids such as alanine and glutamic acid were identified and quantified. Hexadecanoic and octadecanoic acid are representatives related to the lipid metabolism. The largest group is composed of sugars and polyols with a total of 16 identified substances such as erythrose, threitol and inositol. Also, two polyamins known for their DNA stabilizing properties were identified: putrescine and spermidine. Finally, kojic acid, a metabolite specific to filamentous fungi, was determined (Berg et al., 2003; Kwak and Rhee, 1992).

Figure 3.10 shows a typical chromatogram found during the analysis of spores' metabolites. The most prevalent metabolites therein are glycerol and phosphate (co-eluting with a retention time of 518 and 519 s), erythritol (696 s), ribitol and xylitol (co-eluting at 843 s) and sorbitol (975 s). The two metabolites towards the end are trehalose (1 415 s) and a possible product of melanin breakdown. Identification was supported in all cases by MS patterns. The substances eluting at 420 s and 628 s are contaminants.

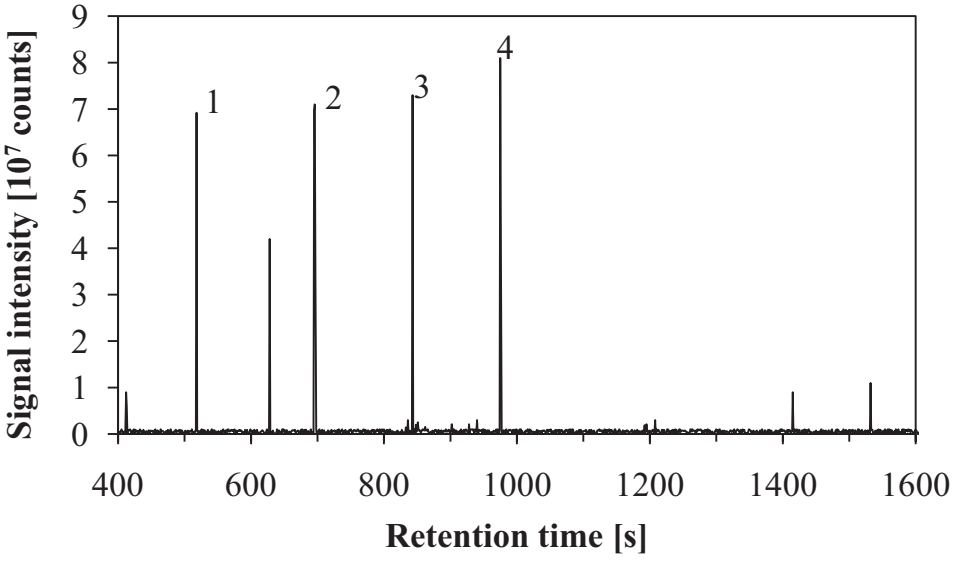

Fig. 3.10. Typical chromatogram detected during the analysis of a spore set's metabolome with a GC-TOF-MS. Most prominent are glycerol and phosphate (1), erythritol (2), ribitol and xylitol (3) and sorbitol (4).

Figure 3.11 shows a metabolic fingerprinting analysis (according to the classification given in the introduction). The detected metabolites of freshly harvested conidia from OBA, MEA and WBA were compared to those from spores stored for 7 d at 4 °C and those from spores germinated for 4 to 12 h. Principal component analysis (PCA) of normalized metabolite profiles illustrates strong effects of spore storage and early germination on the metabolome of the conidia, compared to the spores right after sporulation. The two leading PCA axes for the metabolite profiles cumulatively explain 49 % of the total metabolic variance.

It becomes visible how the samples group according to their history: Unstored spores form an obvious cluster in the second quadrant of the PCA plot. Each sample is represented by one square, i.e. each of the 27 blue marks represents one of the 27 spore sets generated. Biological and technical replicates cluster more closely than samples from different sporulation media. However, for better perceptibility, labels are not displayed on the plot. Conidia that have been kept in suspension at 4 °C for 7 d create an even more distinct group in the third quadrant shown in red (n = 25). Spores that have been left for germination are again well separated from the remainder clustering around the x-axis in the first and fourth quadrant shown in green (n = 18).

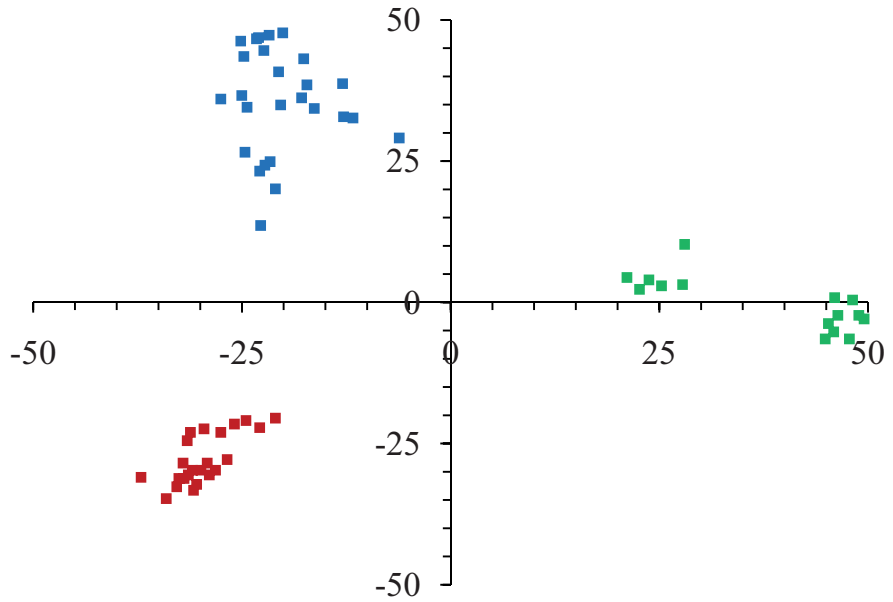

Fig. 3.11. Principal component analysis scatter plot of the scores for principal component 1 (PC1, x-axis) and PC 2 (y-axis) conducted on the metabolome of 70 sets of spores each consisting of 65 metabolites. Blue squares stand for untreated spores of oat bran ager, malt extract agar and wheat bran agar. Red squares represent spores from the same substrates stored for 7 d at 4 °C and green squares represent spores during early germination. These first two principal components explain 49 % of the variation of the original data.

However, clearly two groups can be identified. Closer analysis revealed that the six samples separated from the rest (for $20 < x < 30$) are those that germinated for 12 h (compared to 4 and 6) or in the presence of the reactant steroid 19-NorAD, again illustrating the closer correlation between spores with comparable treatments, evident in metabolic fingerprints.

The metabolic similarity between spores with similar histories becomes even more obvious when conducting ANalysis Of VAriance tests (ANOVA) and including the statistically changed metabolites into the resulting graphical display as can be seen in **figure 3.12**. Analysis of significant differences among the three groups of samples resulting from cluster analysis was performed with FISHER-distribution testing with an overall threshold p-value of 0.01 and BONFERRONI adjustment. The subsequent clustering was based on EUCLIDEAN distance and average linkage. 50 metabolites showed significant differences between all three spore groups, i.e. fresh, stored and germinated. The degree of relationship between samples is shown as EUCLIDEAN distance at the upper side of the graph while the relationship between metabolites is indicated at the left side.

Sample group 1 (blue) clusters freshly harvested spores from MEA, OBA and WBA. Of the 27 samples, 23 gather according to their sporulation substrate while only 4 (WBA-f-a2, OBA-f-a2, WBA-f-a3 and WBA-f-b3) group with conidia from other media though still within the class of freshly harvested spores. In most cases, EUCLIDEAN distance is also lower for technical replicates (digits 1, 2, 3) than for biological replicates (lower case letters a, b, c) emphasizing the results' significance. Sample group 2 (red) clusters stored spores. Here, all 25 samples cluster according to their initial sporulation substrate. This is noteworthy as it demonstrates that differences between the spores' metabolomes are not leveled off during storage but maintained and possibly even fortified. Sample group 3 (green) contains spores during early germination. Here, however, only biological replicates exist due to technical limitations. Still, it becomes evident that samples cluster according to their treatment and germinated spores differ tremendously from fresh and stored conidia while germinated spores from identical substrates still cluster together. This is outstanding as differences introduced during sporulation are hence conserved (and in part manifested) through germination of spores. Also, as expected the sporulation duration (4, 6 or 12 h) and the addition of reactant 19-NorAD (indicated with 'r') introduces significant effects. It is also notable that stored spores, although metabolically active, cluster over all closer to fresh spores than to spores during early germination.

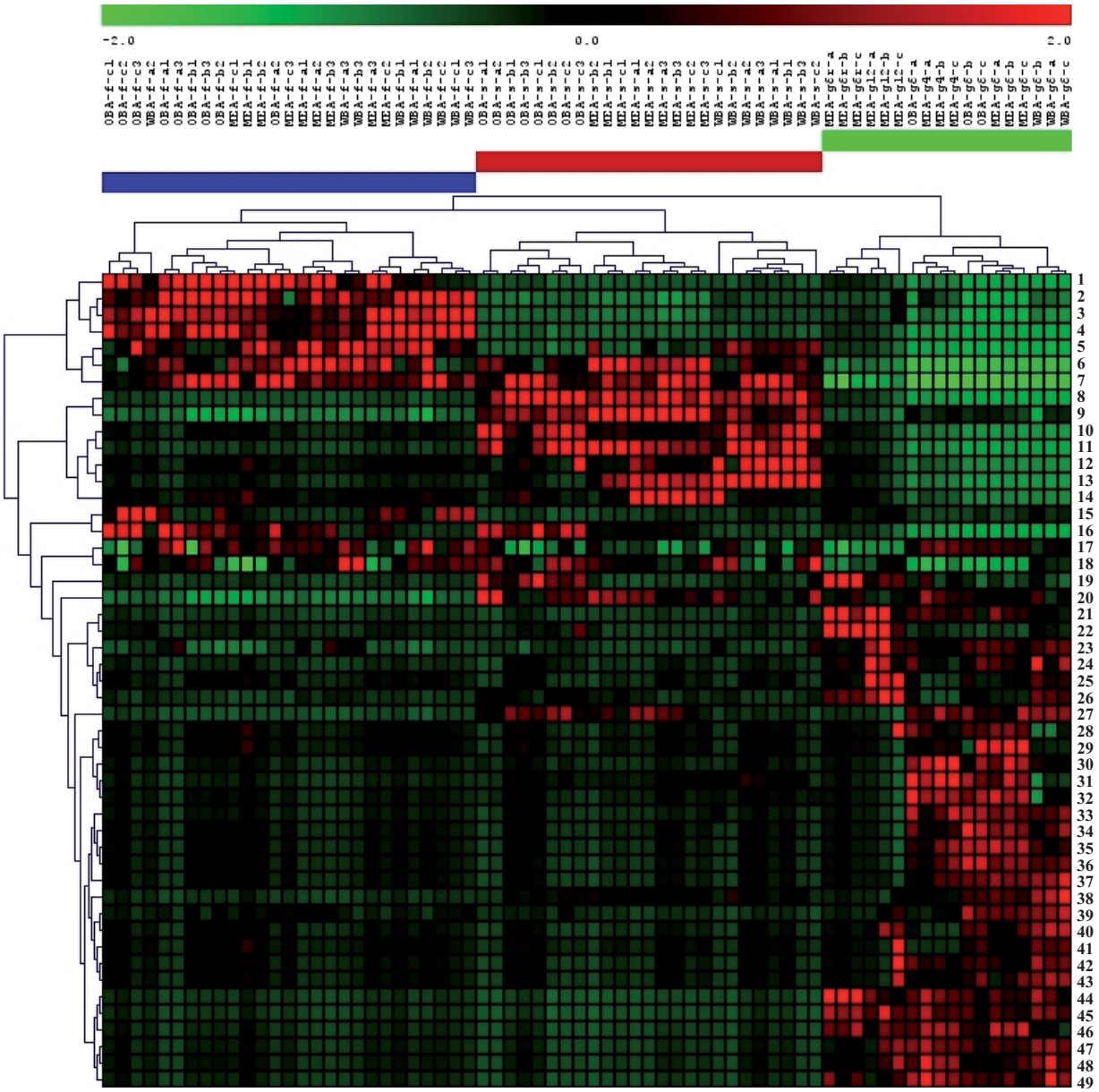

Fig. 3.12. Significant changes in metabolites of spores in response to sporulation substrate, storage and early germination (normalized data). Analysis of variance (ANOVA) was performed on F-distribution testing with Bonferroni adjustment separately for each metabolite and resulted in 49 significantly ($p < 0.01$) changed metabolites displayed herein. The relative changes of the metabolite level are given in a color-coded display where green indicates a down-regulation and red indicates an upregulation. Group 1 (blue, n = 27) summarizes freshly harvested spores; group 2 (red, n = 25) are spores stored for 7 d at 4 °C; group 3 (green, n = 18) contains spores during early germination. Sporulation substrates were oat bran ager (OBA), malt extract agar (MEA) and wheat bran agar (WBA). Biological replicates are indicated with lower case letters a, b and c; technical replicates are identified with digits 1 through 3. Freshly harvested spores (f), stored (s) and germinated (g). Germination duration 4, 6 and 12 h, (4), (6), (12), respectively. Addition of reactant (r). 1: Erythritol; 2: Nicotinic acid; 3: Unknown RI 1341; 4: Gluconic acid-1;5 lactone; 5: Xylitol; 6: Ribitol; 7: Sorbitol; 8: Phenylalanine; 9: Citric acid; 10: Butyro-1,4-lactam; 11: Aspartic acid; 12: Urea; 13: Shikimic acid; 14: Spermidine; 15: Glycolic acid; 16: Threitol; 17: Unknown RI 1401; 18: Trehalose; 19: Sucrose; 20: Hexadecanoic acid; 21: Pyruvic acid; 22: Fructose; 23: Phosphoric acid; 24: Lactic acid; 25: Butanoic acid; 26: myo-Inositol; 27: 4-Aminobutyric acid; 28: Unknown #sst-cgl-008; 29: Glutamic acid; 30: Pyroglutamic acid; 31: Glycine; 32: Putrescine; 33: Valine; 34: Alanine; 35: Serine; 36: Threonine; 37: alpha-Ketoglutarate; 38: 2-Hydroxyglutaric acid; 39: Malic acid; 40: Glycerol-3-phosphate; 41: Succinic acid; 42: Succinic semialdehyde; 43: Uridine; 44: Glucose; 45: Lactose; 46: Isomaltose; 47: Erythrose; 48: Kojic acid; 49: Maltotriose.

The described clustering palpably illustrates the differences between spores with a different background (fresh, stored, germinated) rendering metabolome analysis a meaningful tool for the assessment of spores and possibly connecting phenomenological changes to physiological evidence present in the spores themselves. Changes of individual, meaningful metabolites in response to sporulation medium, storage and early germination will be presented and discussed in the subchapters 4.1.3, 4.4.2 and 4.5.1, respectively. Conducting PCA and ANOVA with the data set obtained from the untargeted metabolome analysis generates similar results as the here presented illustration (hence not shown).

3.5 Determination of ATP concentration with an enzyme assay

ATP is one of the most important energy carriers and coenzymes in cells. As it could not be detected by means of metabolic profiling but is of greatest interest, a protocol was established for the assessment of ATP in fungal spores.

The extraction of ATP from conidia was optimized based on a protocol previously published (Rakotonirainy et al., 2003). Best ATP extraction results were obtained by the addition of 500 µL spore suspension ($2 \cdot 10^7$ spores/mL) to the same volume of preheated DMSO-1xTAE extraction buffer (9:1 v/v), 60 s incubation at 100 °C and subsequent, immediate cooling of the sample on ice. ATP extraction by means of polar, organic solvents at high temperatures with short exposure times had been reported previously to not be deteriorative (Przybylski and Bullerman, 1980). Due to the small volume subjected to the subsequent enzymatic assay, replacement of the solvent DMSO was found to be unnecessary.

In **figure 3.13** the determined ATP concentration is compared to results reported in the literature (Rakotonirainy et al., 2003). It can be seen that the ATP concentration in freshly harvested *A. ochraceus* conidia is with 1 699 ± 34 pg ATP/10^5 spores within the same range as previously reported findings for *A. niger* (1 560 pg/10^5 spores). However, *A. flavus* was reported to contain significantly decreased ATP concentrations with only 190 pg/10^5 spores. Furthermore, it can be seen that heat inactivation (100 °C, 30 min) of spores readily destroys ATP in conidia with reported concentrations of 3 and 7 pg ATP/10^5 spores for inactivated *A. niger* and *A. flavus* spores, respectively. Detected ATP content for heat inactivated *A. ochraceus* spores is with 84 ± 33 pg ATP/10^5 spores slightly higher. It becomes obvious that the ATP content is a meaningful indicator for the spore quality and significant responses to environmental conditions can be detected. However, it can also be seen that the ATP

content is highly strain specific. Even though concentrations are within the same order of magnitude for the presented *Aspergillus* species, differences are significant and comparisons between varying conditions can hence only be conducted for individual strains.

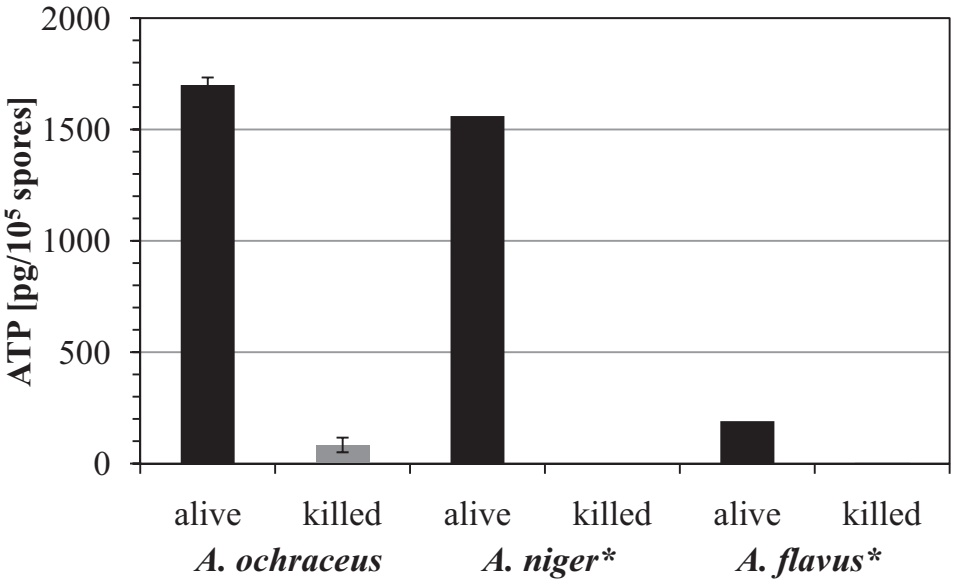

Fig. 3.13. ATP concentration in conidia from common Aspergillus *species. Black: freshly harvested, grey: heat inactivated (30 min, 100 °C),*reported in Rakotonirainy et al., 2003.*

It has previously been reported that ATP concentration can serve as an indicator for spore viability (Liewen and Marth, 1985). Newer studies suggest that exogenous stress causes ATP levels to decrease in cells. Particularly nitrogen monoxide (NO) and reactive oxygen species (ROS) are frequently involved in the defense mechanisms of infected plants against pathogenic fungi. They suppress germination and hyphae growth upon intrusion of the spore into the plant cell. Both, NO and ROS, inhibit cytochrome c oxidase and hence hamper the generation of ATP. The ATP reservoir of the spore is rapidly depleted and with the replenishing pathway being impaired, the fungus is incapable to profoundly infect the host organism (Giulivi et al., 2006; Lai et al., 2011). It can therefore be concluded that the size of the intrinsic ATP pool is relevant for both, the ability to withstand external stresses and the germination rate until the growing cell is capable to regenerate ATP. The detailed effect of conidiation substrate and storage on the ATP concentration in conidia of *A. ochraceus* will be presented in subchapters 4.1.4 and 4.4.3, respectively.

3.6 Determination of NAD(P)H composition in spores with two-photon fluorescence microscopy

After analysis of the ATP content in the previous chapter, a second cofactor of utmost importance is assessed in the following: The NAD(P)H composition of *A. ochraceus* spores was analyzed by means of two-photon fluorescence microscopy. Best results were obtained with an excitation wavelength of 780 nm which is equivalent to excitation at 390 nm in conventional single photon fluorescence. Even though absorption of NAD(P)H is very low at this point, it was found to generate less emission of melanin and hence improved the resolution of the NAD(P)H signal of interest. Laser excitation power was set to 120 ± 10 mW and 300 mW for germinated spores. Fluorescence signals were detected at 460 nm ± 40 nm with a temporal resolution of 32 ps per channel and an exposure time of 0.6 ms per pixel. Immobilization of spores was best achieved in aqueous saline solution through hydrophobic effects between the hydrophobic surface of the conidial wall and a silanized microscope slide. This is crucial as measurements cannot be conducted with dry samples and immobilization with polymers has proven impractical. Four representative images are summarized in **figure 3.14**.

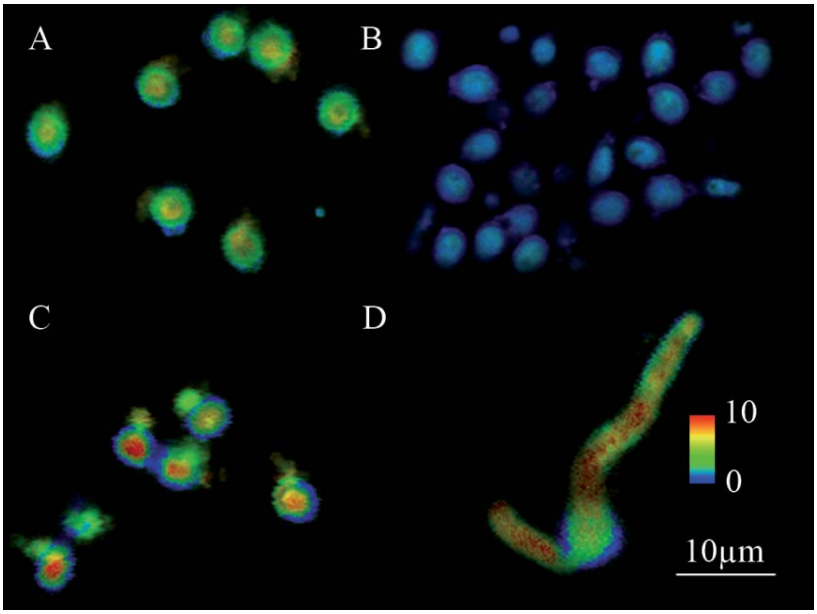

Fig. 3.14. Fluorescent lifetime images (FLIM) of A. ochraceus *spores.*
A: Freshly harvested after incubation on OBA at 24 °C for 8 d; B: Dead spores after autoclaving; C: stored for 7 d at 4 °C; D: germinated for 12 h. Color code represents average fluorescence lifetime per pixel in ns. Software for data acquisition and analysis: SymPhoTime.

Multiphoton fluorescence has been applied for the characterization of mammalian cells, primarily for the diagnosis of various cancer types and other abnormalities in readily accessible tissues (Paoli et al., 2007; Rubart, 2004; Schweitzer et al., 2010). The characterization of fungal spores by means of two-photon fluorescence microscopy has never been done before. With the technique presented in this work, it is now possible to investigate differences between fungal spores even of the same species. Although the application of multiphoton fluorescence was recently reported for the imaging of fungal structures, the technology was there merely deployed for the achievement of better image contrast (Lin et al., 2009). However, time correlated single photon counting (TCSPC) allows the nondestructive visualization of spore ingredients and reveals alterations between different spore populations. Moreover, the relative abundance of bound and free NAD(P)H is determined via fluorescence lifetime imaging where a decreasing average lifetime stands for decreasing amounts of protein bound NAD(P)H and hence impaired metabolic activity.

It can clearly be seen in figure 3.14-A that freshly harvested spores show an intermediate average lifetime between 2.5 and 7.5 ns, green and yellow, respectively, in the centre of the conidium indicating some metabolic activity. In contrast, the spore wall appears blue and hence with shorter lifetimes of approx. 1 ns. This signal can be attributed to melanin which is characterized by a multitude of lifetimes due to its hetero-random-polymeric character but is generally detected at approx. 0.1 ns (Bochenek and Gudowska-Nowak, 2003; Capozzi et al., 2006; Nighswander-Rempel et al., 2005). The fact that spores which have been killed through sterilization (100 °C, 30 min) appear entirely blue (figure 3.14-B) vividly shows how changes can be visualized by this technology. Most cellular structures have been destroyed and fluorescence lifetimes hence globally decrease to a minimum. Spores that have been stored at 4 °C for 7 d in suspension, however, appear even more active than freshly harvested conidia. Here, in the center of several spores average lifetimes of up to 10 ns are determined (shown in red) indicating the majority of the fluorophores to be bound to proteins. The blue appearing conidial wall is also distinctly visible. Finally, the germinating spore (figure 3.14-C) also shows significant differences to the previously mentioned. While the original conidium is still visible, two germ tubes can clearly be seen growing out of it (figure 3.14-D). The spore still shows melanin embedded into the wall in those areas where no germ tube has emerged while the plasma of the spore appears mostly green indicating intermediate average fluorescence lifetimes and hence some metabolic activity. The two germ tubes, however, show alternating areas of red (high fluorescence lifetimes of up to 10 ns and hence intense metabolic activity) as

well as green and yellow areas with intermediate biochemical activity. It can further be observed that the wall of the germ tube, particularly ca. 5 µm around the tip, shows a slight abundance of very short fluorescence suggesting melanin to be present in the growing hyphae wall as well.

It has to be emphasized though that results shown in figure 3.14 represent average lifetimes integrated over 13 ns per pixel. For detailed interpretation, the TCSPC raw data, exemplarily depicted in **figure 3.15**, have to be mathematically modeled.

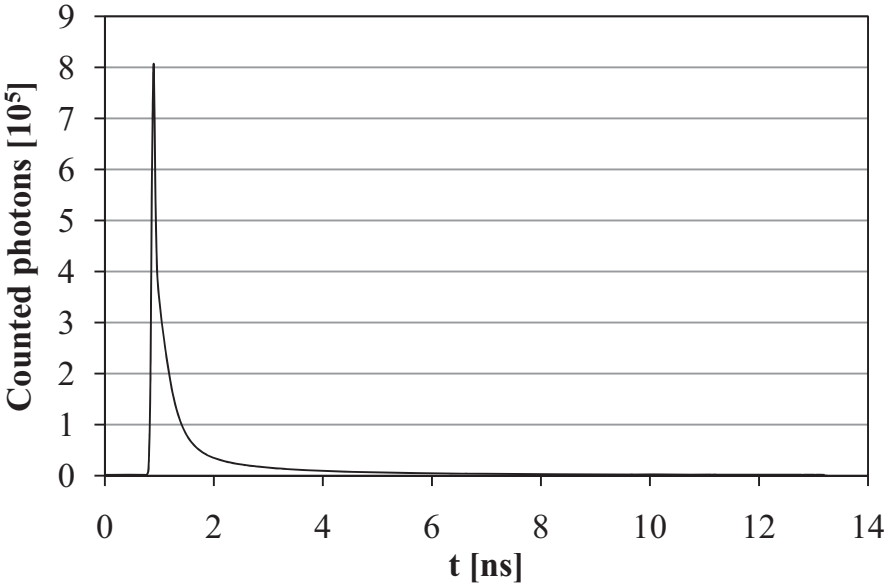

Fig. 3.15. Fluorescence decay of A. ochraceus *spores, freshly harvested from oat bran agar. Excitation at 780 nm, detection at 460 ± 40 nm, temporal resolution 32 ps, exposure 0.6 ms/pixel.*

Fitting of the two-dimensionally (x; y) integrated fluorescence decay curves over the time t has proven most appropriate with a tri-exponential function as explained in equation 2.1 in subchapter 2.5.5. Because the fluorescence signal can be expected to be generated by three fluorophores (melanin, free NAD(P)H and protein bound NAD(P)H), tri-exponential fitting is also mechanistically reasonable. The prefactor (a_1, a_2 and a_3) and the exponent of the three terms of the target function (2) can then be interpreted as the relative abundance and the decay time, respectively, each corresponding to one of the fluorophores.

These results then allow an interpretation of the relative concentration of melanin, free NAD(P)H and protein bound NAD(P)H. Detailed quantitative data will be presented and compared for conidia populations from different conidiation media, freshly harvested and stored spores as well as those that have been left for germination and combinations thereof in subchapters 4.1.5, 4.4.4 and 4.5.2, respectively.

Summarized, it can be stated that the assessment of fungal spores by means of two-photon fluorescence reveals tremendous differences between spores that have been subjected to different treatments but showed no observable difference in conventional optical microscopy with the exception of germinating spores. It was hence not only possible to establish FLIM for the visualization of fungal spores but the methodology was also proven meaningful as it discloses significant metabolic differences between conidial populations.

3.7 Determination of spore visible longwave fluorescence with flow cytometry

The results presented in the previous subchapter vividly illustrate the relevance of autofluorescence measurements in fungal spores. However, the routine assessment of the quality of seed culture conidia for industrial applications by means of two-photon fluorescence microscopy appears impractical. Also, the determination of further spore ingredients by means of fluorescence would be interesting. It was therefore assessed whether a high throughput fluorescence determination would provide valuable insight into the constitution of fungal conidia. Spores of *A. ochraceus* were therefore analyzed by means of flow cytometry. Analysis was conducted with a BeckmanCoulter Quanta SC MPL flow cytometer, measurements were triggered by size rather than fluorescence and the following instrument settings gave best results: flow rate = 13.57 µL/min, LLD = 76 eV, ULD = 1 000 eV, eV-gain = 6, FL-gain = 4, PMT-voltage = 10.3 mV, excitation $\lambda = 366$ nm, detection $\lambda = 525 \pm 15$ (FL-1), 575 ± 15 (FL-2) and > 670 nm (FL-3). Further, as described in chapter 3.3, spore size was determined in parallel which allows the determination of the specific autofluorescence SAF. As for the measurements in the flow cytometer, in contrast to the above described two-photon microscopy, the entire fluorescence signal for every particle is integrated, it is important to account for size differences between individual spores. The specific autofluorescence is hence the ratio of the fluorescence signal in relative units and the projected area of the spore. This is in line with a previously suggested procedure for the analysis of the fluorescence of growing hyphae (Agger et al., 1998; McIntyre et al., 2001). Further, this is most reasonable as the acquisition of the fluorescence signal in the given setup occurs two-dimensionally where the projected area of the particle is exposed to the excitation radiation and fluorescence radiation is detected in the same scheme. Ultimately, it is important to determine the specific autofluorescence per conidia before statistical analysis. Calculating the ratio of average fluorescence and average projected area will not yield meaningful results.

Figure 3.16 shows the typical histogram detected during the analysis of a spore population. The x-coordinate of the maximum of the distribution density subsequently served as the characteristic SAF for the particular population. The shape of the distribution did not show significant changes between populations. Further, focusing on the maximum of the distribution curve eliminates perturbations through debris and other unspecific particles in the suspension.

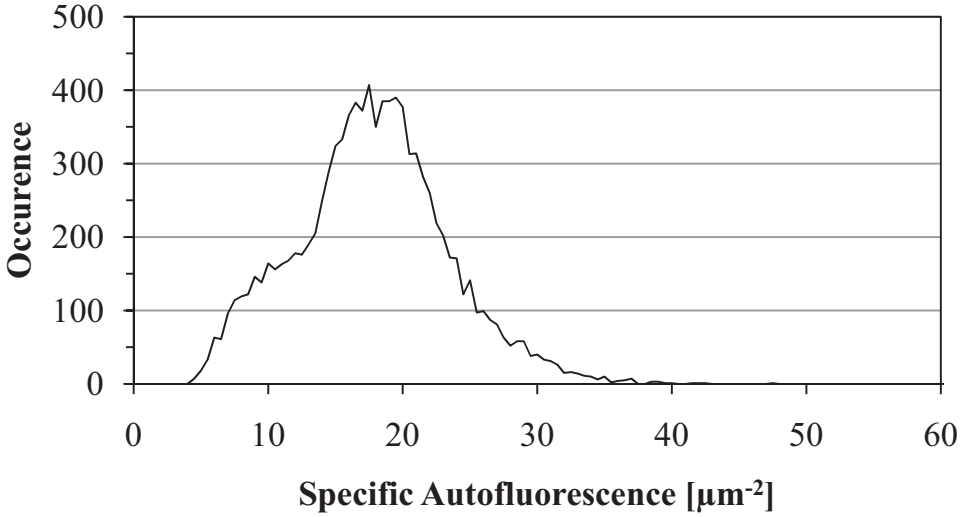

Fig. 3.16. Population distribution density of specific autofluorescence (SAF) of A. ochraceus *conidia analyzed by flow cytometry. Excitation: 366 nm, detection: > 670 nm.*

When analyzing fungal conidia, the most relevant information was found in the specific autofluorescence signal of wavelengths > 670 nm. Detection at 525 ± 15 and 575 ± 15 nm was carried out as well. However, no significant response to environmental changes was detected in those bandwidths. It has to be assumed that the quantum yield of NAD(P)H is too low to be detected through flow cytometry. Two-photon fluorescence microscopy can hence not be replaced by this high throughput technology for industrial applications. Moreover, flow cytometric analyses may serve as an additional measure for the assessment of fungal conidia. The analysis of heat inactivated spores (data not shown) showed an almost complete loss of intrinsic autofluorescence in all wavelengths. The initial hypothesis that conidial autofluorescence is positively correlated to viability, as suggested previously (Kanaani et al., 2008), could hence be confirmed.

The fact that fluorescence signals were best detected in the visible longwave range at wavelengths > 670 nm, even though excitation was conducted at 366 nm, indicates that drastic energy loss occurs, a result of melanin and secondary fluorescence phenomena: Melanin protects the spore from UV light. This is achieved through its complex heteropolymer structure causing the majority of the absorbed energy to be

dissipated by non-radiative means. The shift between the absorbed and the emitted wavelength is hence more substantial than in the majority of other fluorophores (Meredith and Riesz, 2004; Nighswander-Rempel et al., 2005).

The second reason can be found in the natural occurrence of FÖRSTER resonance energy transfer (FRET) within spores. The common denotation as fluorescence resonance energy transfer is incorrect as the energy transfer between the two involved fluorophores is of non-radiative nature. Summarized, FRET occurs in three steps: excitation of the first chromophore (donor), transfer of lower emission energy to the second chromophore (acceptor) which is thus excited; final emission of again lower radiation through the second chromophore. As the wavelength is shifted three times, instead of once in conventional fluorescence, the energy of the emitted light is considerably lower (Lakowicz, 2006). The phenomenon is schematically illustrated in **figure 3.17**.

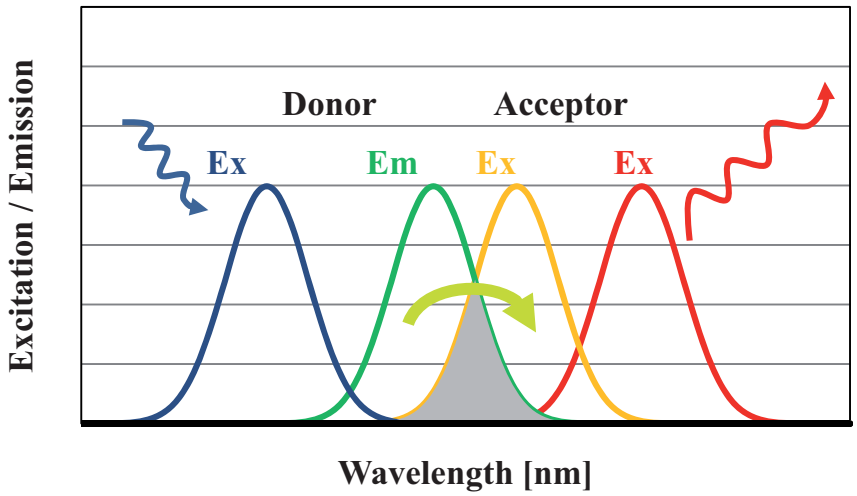

Fig. 3.17. Principle of FÖRSTER resonance energy transfer. The excited donor chromophore passes its emission energy non-radiative to the acceptor which subsequently emits visible longwave fluorescence.

Numerous common cellular compounds, primarily form secondary metabolism, have been reported to show intrinsic FRET behavior as well as absorption and emission in the bandwidth of interest, most of all but not exclusively various porphyrins and flavins as well as the respective associated proteins (Billinton and Knight, 2001; Dichtel et al., 2004; Gouterman, 1961; Laible et al., 1998). Even though intrinsic FRET has not been reported for fungi to this point, more than 60 fungal species are known to show bioluminescence which is tightly connected to the presence of FRET-capable molecules and may readily be achieved through minor changes of larger structures, for example ligand substitutions (Desjardin et al., 2008; Secrist et al., 1972). The existence of FRET and similar phenomena in fungal spores is hence very

likely. Determination of the specific visible longwave autofluorescence of conidia is therefore a valuable method for the determination of secondary metabolites.

These two effects cause the energy shift to be so drastic and are the reason why the most relevant changes in the autofluorescence behavior in fungal conidia determined by means of high throughput flow cytometry are detected in the visible longwave range, i.e. at wavelengths > 670 nm. It can be summarized that the specific visible longwave autofluorescence of spores is a function of the environome and measurable by means of flow cytometry. Relevant information regarding the composition of secondary metabolites can be obtained. The advantages of flow cytometry are the speed of measurement, the high statistical significance and the theoretical possibility to further utilize selected spores after their measurement. However, information about spatial distribution, concentrations ratios, fluorescence lifetimes and hence underlying fluorophores is not available. The influence of the sporulation substrate, sporulation duration as well as the storage will be discussed in subchapters 4.1.6, 4.3.3 and 4.4.5, respectively, with the most relevant effect determined for the incubation duration. It has to be emphasized though that a precise allocation of the fluorescence signal to individual chromophores, as conducted for NAD(P)H in two-photon fluorescence microscopy, requires knowledge of putative conidial secondary metabolites in spores. This, though tedious, may be achieved through the concerted application of HPLC-MS, multi-wavelength excitation and multi-wavelength emission microscopy. This would allow the molecular elucidation and the understanding of the underlying biophysical chemistry of the suggested phenomena.

3.8 Determination of spore viability on solid and liquid media

Spore viability is one of the most important characteristics. Previous spore quality analyses, if conducted at all, focused on the viability as the main criterion. Generally, the number of germinated spores is assessed after a predetermined interval post inoculation. This has been reported for liquid culture, where the incubation is typically in the range of few hours, as well as solid culture, where colony forming units (CFUs) are counted several days after inoculation of the agar plate (Araujo and Rodrigues, 2004; Vesper et al., 2008). Viability assessments in liquid culture have the advantage of investigating the property under more relevant conditions as conidia are typically industrially applied in submerged cultivations. Viability assessments on solid substrates, however, have the advantage of being easier to operate and less susceptible to external biases. Therefore, in order to establish a reliable but meaningful spore viability assessment, conidial viability was tested in solid *and* liquid culture.

Figure 3.18 shows the germination rate in liquid culture (**A**) and on solid medium (**B**). It can be seen that conidia in liquid culture are in the middle of the exponential phase 10 h after inoculation reaching 51 ± 10 % germinated spores. Germination on agar was assessed by naked eye observations and is hence based on countable CFUs. First colonies are detected 42 h after inoculation. The increase of enumerated CFU is almost linear in contrast to the exponential behavior in liquid culture. However, after approx. 72 h of incubation, 55 ± 11 % of the conidia have formed colonies. It is hence postulated that determination of CFU after 72 h is equivalent to the more laborious identification of germinated spores in liquid culture.

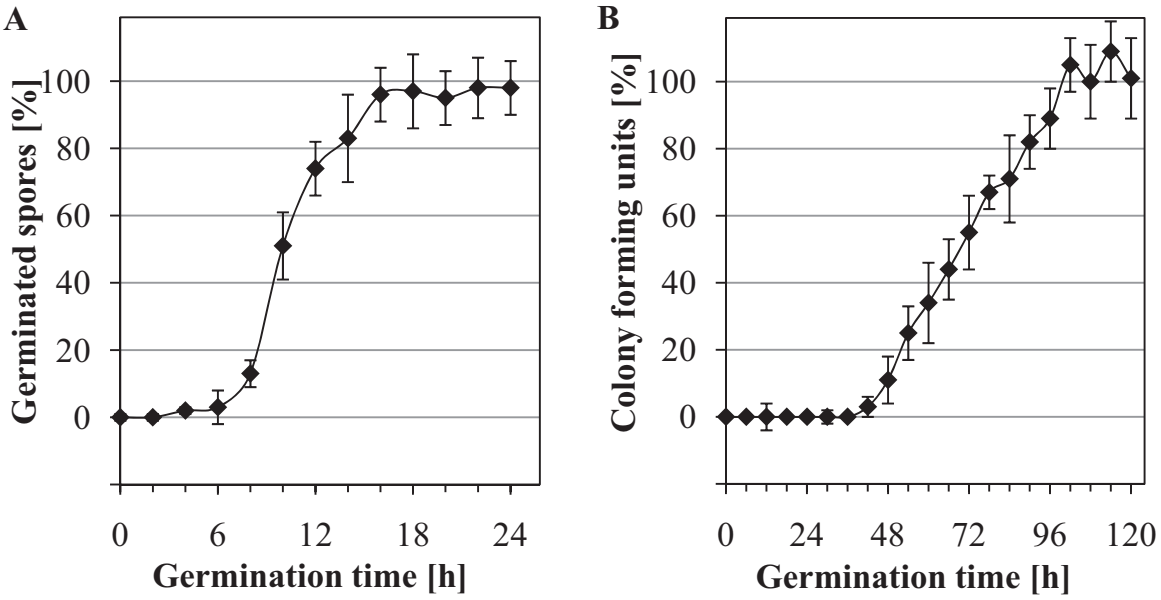

Fig. 3.18. Germination rate in liquid culture (A) and colony forming units on solid medium (CFU; B) as an indicator for viability of fungal conidia. Spores with germ tubes of the same length or larger as the spore diameter were counted as germinated.

This hypothesis was further affirmed by parallel assessments of populations with adjusted viable spore concentrations (addition of heat inactivated conidia to untreated spores in known quantities). **Figure 3.19** shows the strong correlation of both methods rendering the analysis of spore viability by means of CFU, a reliable and meaningful indicator. Further, viability characterization in this study is hence exclusively conducted by this method. Due to its strong correlation with liquid culture assessments on the one hand and its relatively uncomplicated handling procedure on the other, it is also recommended for industrial applications. It has to be emphasized though that the determined viability is not the absolute viability but the percentage of spores that germinated within a given time interval. This is more meaningful as otherwise spore populations generated on virtually any substrate would exhibit viabilities of almost 100 % as has been reported for spores from *Penicillium nalgiovense* (Ludemann et al.,

2010). The here suggested viability index moreover is a combination of mere viability and germination rate which is more meaningful because the relevant criterion for industrial applications is the space time yield not the hypothetical sporulation potential of the population.

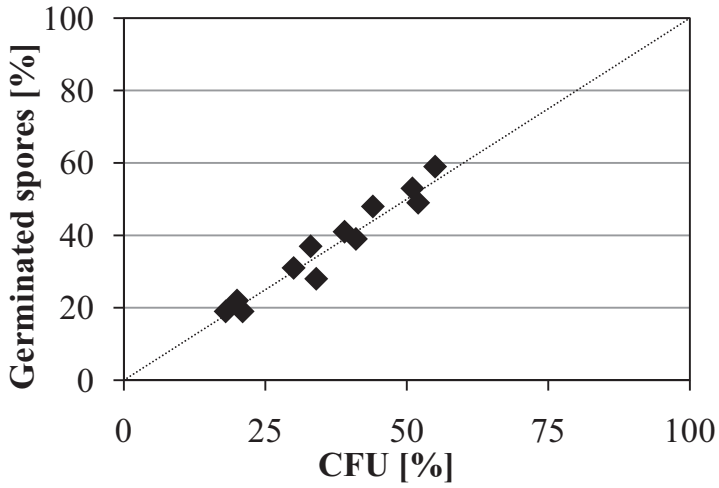

Fig. 3.19. Correlation of germination rate in liquid culture and colony forming units (CFU) on solid substrates for A. ochraceus *conidia.*

3.9 Determination of culture performance in submerged cultivation

Harvested spores were not only analyzed directly, their performance in subsequent submerged culture was assayed as well. Therefore, shake flask cultures were conducted as described in section 2 and analyzed at 48 and 72 h in triplicate. pH, biomass growth, morphology and product formation were identified as possible indicators for the characterization of the cultivation and hence the performance of the inoculum. Even though this analysis is beyond the characterization of the actual spore properties, it gives meaningful insights into the industrially most relevant characteristic, the productivity of the generated spore population.

3.9.1 pH of the cultivation broth

The pH of the cultivation broth was assayed before and after homogenization of the same. An alkalization of the culture broth during the cultivation of *A. ochraceus* was witnessed. This can be expected to be a result of feed-protein degradation, amino acid deamination and subsequent release of ammonia. It is hence an indicator for metabolic activity, particularly as the medium is rich in proteins (Nanou et al., 2007).

Figure 3.20 shows the course of the pH during the conducted cultivations. It can clearly be seen how the pH rose from initial 5.6 throughout the cultivation to an average of 8.5 before and 8.7 after homogenization. The fact that the pH rose not only over cultivation time but also as a result of homogenization, i.e. disruption of mycelia, indicates that ammonia and possibly further alkaline metabolites accumulate intracellularly and are only slowly released into the supernatant. For further analysis throughout this study, pH will hence be determined after homogenization to include intracellular activities in the assay.

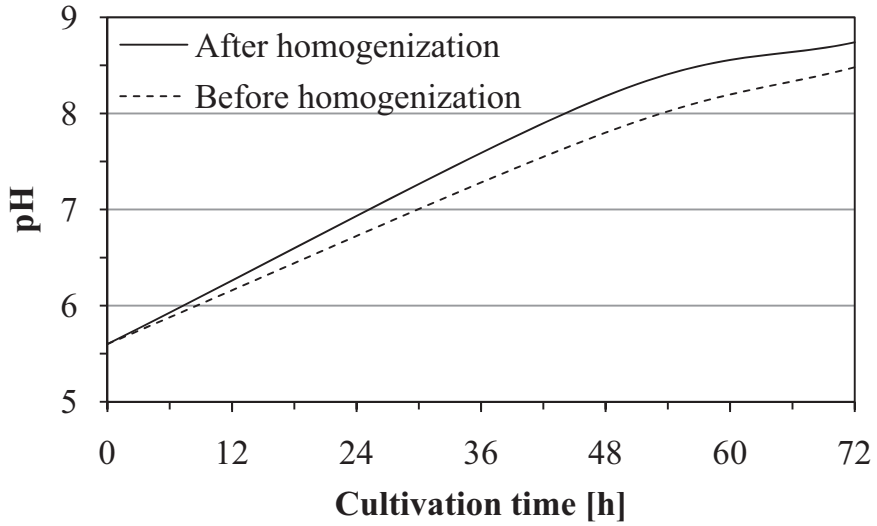

Fig. 3.20. Shake flask cultivations, 30 mL, 24 °C, 130 min^{-1}. Alkalization of the culture broth over cultivation time. Determination before and after homogenization (dashed and solid line, respectively). Averaged for all cultivations conducted, irrespective of sporulation environome.

3.9.2 Biomass formation and morphology

Dry biomass was determined after Ultra-Turrax treatment for 2 min at 13 500 min^{-1} and subsequent filtration of 10 mL cultivation broth through a filter. The loaded filter was dried at 105 °C for 3 d before the mass of the dry bio matter was measured.

However, as the reactant 19-NorAD is highly insoluble in water and hence forms crystals that are held back by the biomass filter, corrections had to be calculated. Based on the measured remaining 19-NorAD concentration in the broth (shown below), it was possible to distinguish between actual biomass and precipitated reactant. It had been shown previously that the product of the biotransformation OH-19-NorAD has a water solubility that is 40-times higher than that of the non-hydroxylated steroid (2000; Ruelle et al., 1997). These findings could be verified with a qualitative assay performed during this work inspecting the solubility of the given 19-NorAD and OH-19-NorAD. It is therefore reasonable to account for the reactant but not for the product.

Further, the medium additive corn steep liquor contains several insoluble compounds. They are, however, degraded through exo-enzymes produced by *A. ochraceus* throughout the cultivation and have therefore to be accounted for in the determination of dry biomass. From the initial concentration of 0.4 g/L the decay is exponential and best fitted with:

$$c = c_0 \, e^{-\frac{t}{22}} \qquad (3.2)$$

The dry biomass was hence determined as follows:

$$DBM = DBM_{std} - [r]_i - 0.4 \, e^{-\frac{t(i)}{22}} \qquad (3.3)$$

with DBM being the corrected dry biomass, DBM_{std} the dry biomass according to the standard procedure at a given time point t(i) in hours and $[r]_i$ the remaining concentration of the untransformed reactant at the same time. Throughout this study, 'dry biomass' will refer exclusively to the 'corrected dry biomass' as shown in eq. 3.3.

Further, wet volume of biomass was determined by centrifuging 10 mL of culture broth at 1 000 g for 10 min. The volume of the precipitate was determined by comparison with calibrated containers with known contents. In contrast to the dry biomass, the wet volume of biomass also takes into account the morphology as denser grown cultures may show increased dry biomass but decreased wet volume of biomass at the same time.

As can be seen in **figure 3.21**, there is no clear correlation between dry biomass and wet volume of biomass. The two indicators represent independent variables. It is hence recommended to not only correct the dry biomass by the residual reactant in the culture broth but to also measure wet volume of biomass for a more holistic understanding of the cultivation.

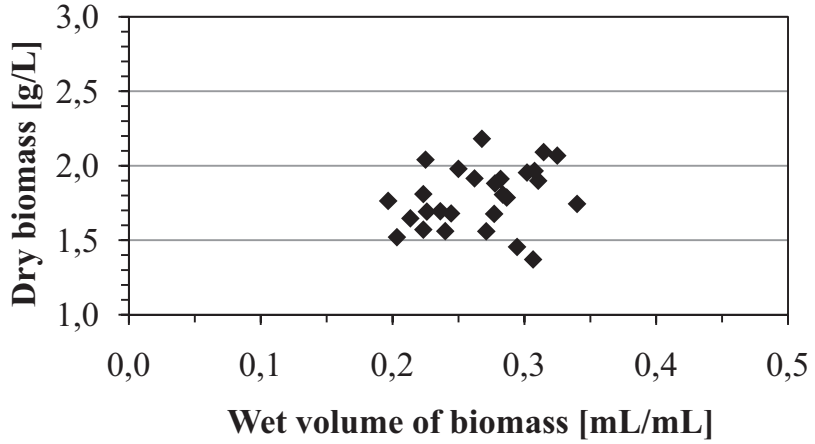

Fig. 3.21. Dry biomass and wet volume of biomass in shake flask cultivations. 30 mL corn steep liquor-soy peptone medium, 24 °C, 130 min^{-1}, pH 5.6. Each data point represents the arithmetic mean of 6 biological and 3 technical replicates.

Besides wet and dry biomass, also the morphology was analyzed over the course of the cultivations. Therefore, the morphology index (MI) was introduced consisting of 3 components: At first, the percentage of pellets in comparison to the total biomass was assessed visually. Second, the sedimentation velocity was evaluated as suggested by Lin et al. (2010) and converted into a biomass sink index (BSI) by categorizing the required time for the clearance of the non-agitated broth ($t > 3.5$ min: BSI = 0.5; $2.5 < t < 3.5$ min: BSI = 0.6; $1.5 < t < 2.5$ min: BSI = 0.7; $0.5 < t < 1.5$ min: BSI = 0.8; $t < 0.5$ min: BSI = 1). At last, a correction term, accounting for very small pellets, was introduced: If the average pellet diameter was below 1 mm and the overall behavior was therefore more comparable to dispersed growth, the pellet-fraction-number was multiplied by 0.8. This altogether is integrated into the morphology index MI which hence represents a corrected pellet-biomass-ratio:

$$MI = \begin{cases} \dfrac{pellet\ biomass}{total\ biomass} \cdot 0.8 \cdot BSI, \ d < 1\,mm \\ \\ \dfrac{pellet\ biomass}{total\ biomass} \cdot BSI, \ d \geq 1\,mm \end{cases} \qquad (3.4)$$

where d represents the average diameter of the cultivations' pellets and BSI the respective biomass sink index. An overview of possible morphologies and their characteristics is given in **table 3.1** and further illustrated in **figure 3.22**.

Tab. 3.1. Morphology indices, biomass sink index criteria and characteristics of shake flask cultures.

Morphology Index	Primary feature	Typical characteristics
0 – 0.2	Mycelium	Viscous broth Very few clumps or pellets Clearing > 3.5 min: BSI = 0.5
0.2 – 0.4	Mycelium with pellets	Viscous broth Few clumps and small pellets Clearing 2.5 to 3.5 min: BSI = 0.6
0.4 – 0.6	Mycelium-pellet-conglomerate	Intermediate viscosity Various small clumps and pellets Barely differentiated structures Clearing 1.5 to 2.5 min: BSI = 0.7
0.6 – 0.8	Small pellets	Low viscosity Clear broth with numerous small, fluffy pellets Clearing 0.5 to 1.5 min: BSI = 0.8
0.8 – 1	Large pellets	Low viscosity Clear with large and very large pellets Clearing < 30 s: BSI = 1

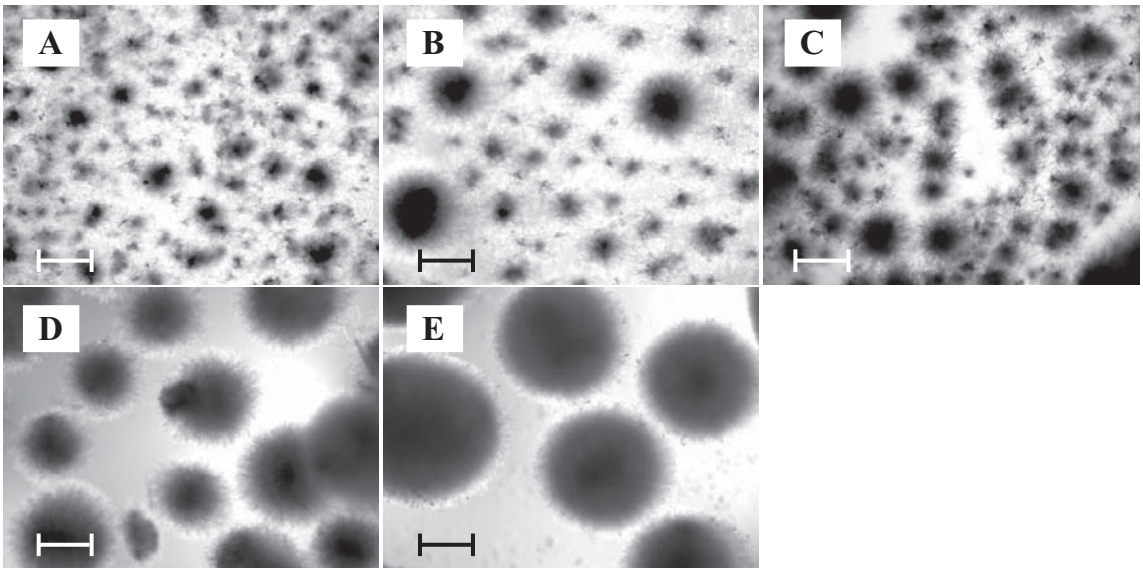

Fig. 3.22. Microscopic images of different cultivation broths after 72 h of incubation exemplarily illustrating the variety of morphologies observed throughout the cultivations: (A) mycelium; (B) mycelium with pellets; (C) mycelium-pellet-conglomerate; (D) mostly small pellets; (E) large pellets. Scale bar: 200 µm.

Investigating the dry biomass (DBM), wet volume of biomass (WVB) and morphology index (MI) over the course of the shake flask cultivations, it can be noticed that DBM steadily increases. WVB, however, increases during the first 48 h of cultivation and declines thereafter despite continued biomass formation. The reason for this phenomenon is the increasing tendency to form pellets as the cultivation progresses. I.e., the morphology shifts towards a more pellet-like growth over the course of the cultivation due to the ongoing alkalization of the cultivation broth. The biomass is hence denser which explains why the wet volume of biomass decreases even though dry biomass increases. This interrelationship is illustrated in **figure 3.23**.

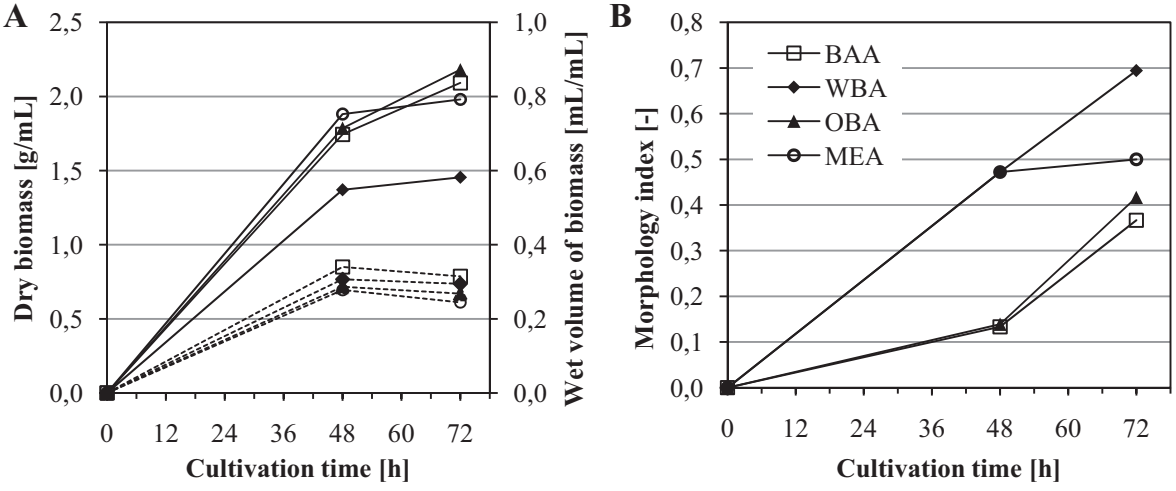

Fig. 3.23. Development of dry biomass (A, solid lines), wet volume of biomass (A, dashed lines) and morphology index (B) during shake flask cultivations with A. ochraceus. *30 mL CSL-SP medium, 24 °C, 130 min^{-1}, pH 5.6. Presented are arithmetic means of 6 biological and 3 technical replicates.*

As described above, the pH increases throughout the cultivation. It has also been shown previously that aggregation and pellet formation is increased at higher pH ranges (Papagianni, 2004) possibly due to increased desorption of melanin (Eisenman et al., 2007; Priegnitz, personal communication; Hagemann, personal communication). This contributes to the increasing morphology index. It is remarkable though as typically acidification and not alkalization of the medium occurs.

Figure 3.24 shows the correlation between the aggregation behavior and the resulting morphology of the submerged cultivation. It can be seen that the morphology of the culture is influenced by the aggregation tendency of the spores even though the stability index is with 58 % not very high. As described in chapters 3.2, 4.1.2 and 4.4.1, the aggregation of spores is not only a function of the pH of the surrounding solution but also of the media the spores were generated on and the storage of the spores. This is a result of melanin, glucan and hydrophobin interactions which form the spore wall and mediate spore aggregation. Among others, differing melanin concentrations, washout and breakage of the hydrophobin layer may hence strongly affect the aggregation behavior of a spore population. Here evidence is provided that additionally to the important role of secondary aggregation investigated by Grimm et al. (2004, 2005) the primary aggregation of the spores also strongly affects the resulting morphology and hence productivity of the culture: The higher the spores' tendency to form aggregates, the larger the fraction of pellets in the subsequent submerged cultivation.

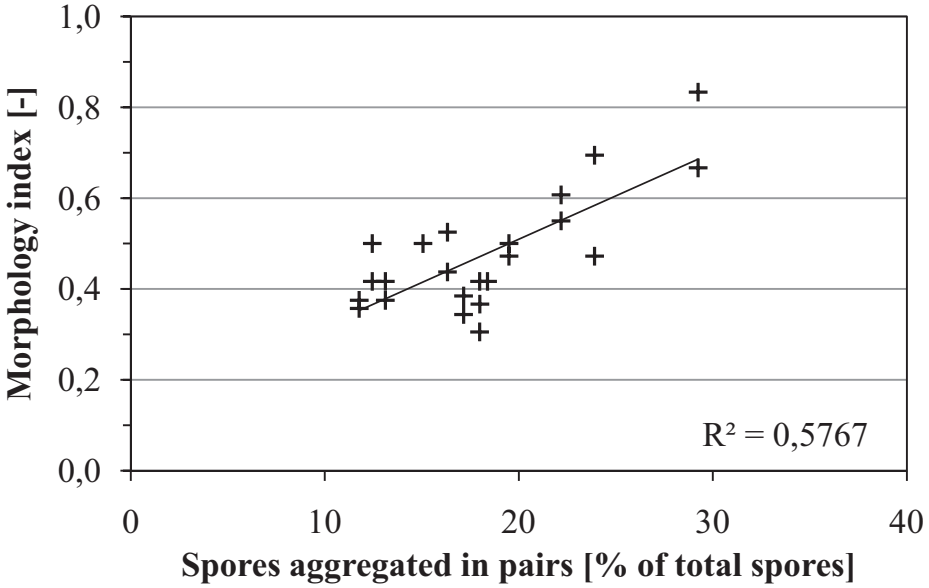

Fig. 3.24. Morphology index of shake flask cultivations (30 mL corn steep liquor-soy peptone medium, 24 °C, 130 min^{-1}, initial pH 5.6, 72 h) over the initial aggregation behavior in saline solution of the inoculum.

3.9.3 Product formation and reactant consumption

Shake flask cultivations were conducted under the presence of the reactant 19-NorAD at an initial concentration of 2 g/L. The formation of the hydroxylated steroid and the concomitant consumption of the reactant were monitored through quantitative HPLC analysis over the course of the cultivations. The continuous depletion of the reactant and the subsequent increase of the product could be witnessed.

It is well known that *A. ochraceus* has multiple closely related monooxygenases which hydroxylate not only progesterone but many similar reactants as well as aryl hydrocarbons. They all show tremendous differences with respect to the kinetics (K_m, v_{max}) and substrate specificity of the individual reactions (Dutta et al., 1983). While progesterone for example is converted entirely, the conversion of 19-nortestosterone stops at 14 %. Furthermore, these products can in most cases be substrates for further monooxygenases producing a multitude of mono- and polyhydroxylated steroids as a result of side- and consecutive reactions (Dulaney et al., 1955b; Holland and Weber, 2000). The three in the literature suggested options to overcome this problem (zinc depletion, preparation of cell free extracts only containing the monooxygenase of interest or using (immobilized) spores directly as catalysts (Dulaney et al., 1955b; Dutta et al., 1993; Dutta and Samanta, 1999; Shibahara et al., 1970)) were not realizable within this study as the original production conditions were to be resembled as closely as possible. The reactant product balance is not even, if only 19-NorAD and OH-19-NorAD are regarded. Formation of structurally similar side products was confirmed by HPLC analyses and has to be account. **Figure 3.25** exemplarily shows the HPLC chromatogram of a shake flask culture broth after 72 h of incubation.

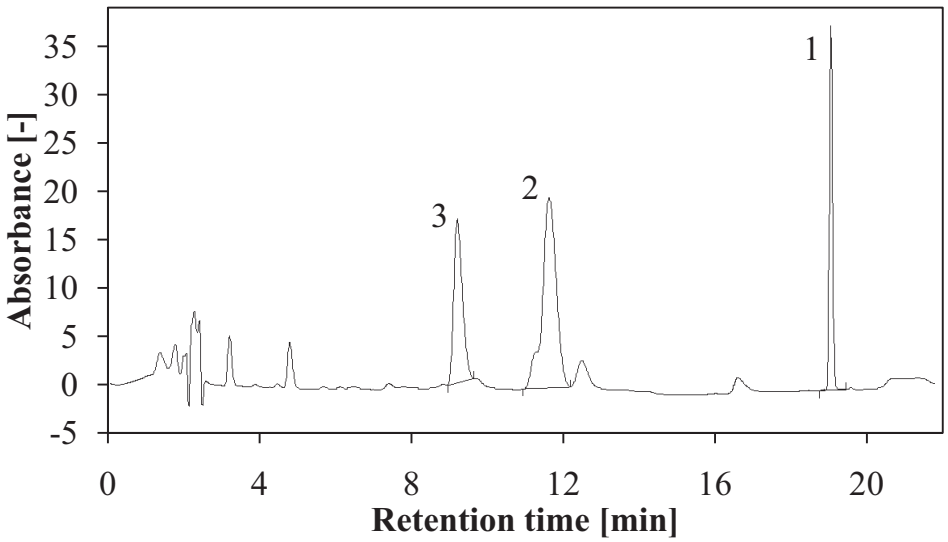

Fig. 3.25. HPLC chromatogram of the culture broth after 72 h incubation at 24 °C, 130 min^{-1}. Reactant (1), product (2) and side product (3) can clearly be seen.

The main side product could not be identified but it can be speculated to be 6-beta-11-alpha-OH-19-NorAD, a common product of secondary hydroxylation (Dulaney et al., 1955a). However, as the focus of the project is not the characterization of the specificity of the biotransformation but the overall capability of the seed culture, the reactant consumption rather than the product formation will be employed throughout this study to illustrate the activity of the culture mainly. However, the average product yield over all cultivations is 13.2 % with initial 19-NorAD concentrations of 2 g/L.

The specific effect of the sporulation environome will be presented in subchapters 4.1.8 and 4.4.7. More general, the relationship between biotransformation activity and morphology shall be investigated here. **Figure 3.26** illustrates the positive correlation of the morphology index and reactant consumption. It can be seen that lower morphology indices representing primarily mycelial growth correlate with lower reactant consumptions while higher morphology indices foster higher activities. This is not strictly linear as several exceptions can be seen in the plot as well. Further, it shall be mentioned that the preferred morphology also depends on the product of interest (Braun and Vecht-Lifshitz, 1991). The overall trend, however, becomes obvious and a postulated nonlinear regression is characterized by a stability index of 0.79. Also, a mere statistical analysis of the raw-data emphasizes this finding: The average reactant consumption over all shake flask cultivations with a morphology index below 0.5 is 39 % while the average over all cultivations with MI ≥ 0.5 is 47 % representing an increase of approx. 22 % with a statistical significance of $p < 0.001$.

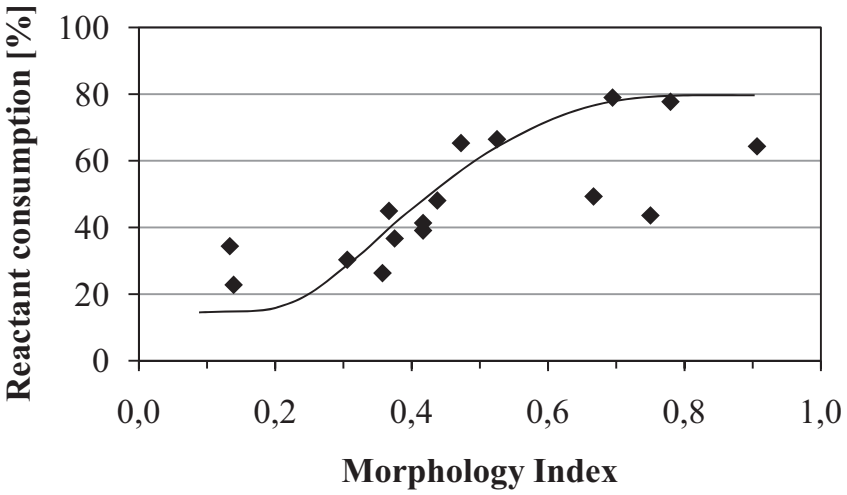

Fig. 3.26. Relative reactant consumption 1-[19-NorAD]$_i$/[19-NorAD]$_0$ as a function of the culture morphology. 30 mL CSL-SP medium, 24 °C, 130 min^{-1}, pH 5.6 [19-NorAD]$_0$ = 2 g/L. Each data point represents the arithmetic mean of 6 biological and 3 technical replicates. Mycelial growth represented by smaller indices seems to inhibit high conversion. Pellet growth correlates with higher yields.

3.10 Conclusion of the spore characterization

In the previous chapters, nine comprehensive methods for the characterization of spores were presented, validated and their significance was exemplified. It was shown that the characterization of spores which until today was merely limited to their quantification is possible. Those spore quality indicators can constitutively be applied in two ways.

First, they may serve as meaningful instruments for quality management. A routine assessment of seeding cultures can readily be implemented using all or a selection of the presented methods supporting personnel involved in the industrial exploitation of filamentous fungi. More homogenous production processes, better comparability between lots and better workload capacity utilization are potential consequences as improper spore sets can be rejected and replaced prior to their application to inoculate large scale cultivations.

Furthermore, the established indicators can be applied in the optimization of sporulation conditions and spore treatment. As they allow the determination of a spore sets characteristics without the need to conduct a full submerged cultivation in order to identify the quality of the conidia, optimization procedures can not only be accelerated but also increased in informative value. Sporulation substrates, environmental conditions or storage of conidia are no longer only judged according to their effect on subsequent submerged cultivations but moreover based on changes directly attributable to spore properties. This allows for the first time to assign specific cultivations findings to either the fermentation itself or the seeding culture. For the holistic characterization and understanding of submerged cultivations with filamentous fungi, this differentiation is crucial.

4 Influence of sporulation conditions on spores' constitution and performance

In this section, each of the established spore quality indicators will be, where possible and expedient, applied to characterize spore populations generated under different conditions. The structure of this section is hence best illustrated by table 4.1. Furthermore, and not presented in the scheme below, cross variations were conducted as well, for example varying sporulation medium and spore storage simultaneously. These cross variations are respectively shown in the subchapter where the second parameter was introduced. Further, correlations of spore quality indicators will be explained where meaningful. Additionally, selected changes that can be witnessed in germinating spores are explained in chapter 4.5.

Tab. 4.1. Structure of this section. Spore quality indicators are permutated with altered sporulation environome parameters. Resulting combinations are presented in the respective subchapter.

Spore quality indicator	Sporulation medium	Inoculum concentration	Sporulation duration	Storage
Spore yield	4.1.1	4.2.1	4.3.1	-
Spore aggregation	4.1.2	-	4.3.2	4.4.1
Spore size	-	-	-	-
Spore metabolite profile	4.1.3	-	-	4.4.2
Spore ATP content	4.1.4	-	-	4.4.3
Spore NAD(P)H distribution	4.1.5	-	-	4.4.4
Spore autofluorescence	4.1.6	-	4.3.3	4.4.5
Spore viability	4.1.7	-	4.3.4	4.4.6
Submerged culture performance	4.1.8	-	-	4.4.7

4.1 Effect of sporulation media

4.1.1 Spore yield depending on sporulation media

As indicated in chapter 1.4, the composition of the sporulation medium has a significant impact on the amount of spores produced. The optimal ingredients for conidiation vary from strain to strain and equivocal findings in the literature make it difficult to determine trends. While some suggest starvation to enhance spore production, others find rich media to give best results. Also, various complex natural substrates of unclear ingredients like millet and V8-juice have been shown to generate substantial amounts of spores. Furthermore, C:N ratios between 5:1 and 80:1 have

been reported ‘optimal’ for sporulation depending on the particular fungus of interest (Bapat et al., 2003; Gao and Liu, 2009; Harman et al., 1991; Ying and Feng, 2006).

Therefore, a multitude of substrates was evaluated for their applicability to serve as sporulation media for the production of *A. ochraceus* spores. In preliminary assessments, natural substrates and media compositions suggested by reliable sources were tested for their general potential to serve as substrates for the production of conidia. Therefore, fruits, vegetables and the different media ingredients were used in their native state or, in cases where the native state is a powder, prepared as agar plates as indicated in the reference source. As the spore suspension for inoculation cannot be spread with a spatula on chunky substrates, inoculation was achieved by spraying the conidia on the medium. For better comparability this was identically conducted on all media including the agar plates.

The substrates used in this first step and the results gained therefrom are presented in **table 4.2**. Despite their good results, carrot, peach, tomato and wheat beer were not evaluated any further as they could not readily be processed and integrated into agar plates. Also, their eventual use in industrial applications seemed unlikely. Peas, although readily incorporated into agar plates, were also not continued as they showed poor results after processing. Analysis of sporulation on corn steep liquor, despite inferior yields in the first assessments, was continued due to outstanding results previously reported (Chen et al., 2005) and possible facilitation in an industrial context where corn steep liquor is used in submerged cultivation already and would therefore reduce the number of stock media needed.

Subsequently, positively selected media were processed in order to resemble comparable conditions such as even agar surfaces and identical pH which was not adjusted in solids during preliminary tests. Only this standardization allows the correct comparison of different substrates as the medium height as well as the surface to volume ratio had been shown to influence conidiation (Georgiou and Shuler, 1986). It is also noteworthy that, as explained in Materials and Methods and chapter 4.4, spores were precultured between cryostorage and the assessment of media effects to eliminate possible bias through cryodamage. The media of those precultures were of the same composition as for the main analysis, i.e. MEA for MEA, BAA for BAA etc.

Tab. 4.2. Tested sporulation media and their results. Czapeck yeast extract agar (CYEA), malt extract yeast extract agar + 40 % (w/v) glucose (MYEGA), potato dextrose agar (PDA), yeast extract sucrose agar (YESA), yeast extract peptone glucose agar (YEPGA).

Substrate	Preparation	Biomass growth	Sporulation	Further application
Banana	Peeled, cut into pieces	Ample	Ample	Yes
Carrot	Peeled, cut into pieces	Ample	Ample	No
Chocolate	Direct use	None	None	No
Corn steep liquor	To 10 g/L in agar plates	Ample	Very poor	Yes
CYEA	According to Atlas (1993)	Average	Average	No
Lentil	Soaked in MiliQ water	Poor	Poor	No
MYEGA	According to Atlas (1993)	Good	Ample	Yes
Oatmeal	Soaked in MiliQ water	Ample	Ample	Yes
PDA	According to Atlas (1993)	Average	None	No
Pea (canned)	Direct use, slightly drained	Ample	Ample	No
Pea flour	To 30 g/L in agar plates	Average	Poor	No
Peach (fresh)	Cut into pieces	Ample	Ample	No
Soy granulate	Soaked in MiliQ water	Poor	Very poor	No
Tomato	Cut into pieces	Ample	Good	No
Wheat beer	Solidified with agar	Ample	Ample	No
Wheat bran	Soaked	Average	Ample	Yes
Wheat grain	Soaked	None	Very poor	No
YESA	According to Atlas (1993)	Average	Poor	No
YEPGA	According to Atlas (1993)	Poor	None	No

Figure 4.1 illustrates the large differences between the spore yields on different complex media. Malt extract agar (MEA) as the standard medium takes a middle position with a spore concentration in the harvest suspension of $21.0 \pm 2.0 \cdot 10^7$ spores/mL. The highest spore yield can be obtained on oat bran agar (OBA) giving $25.8 \pm 0.5 \cdot 10^7$ spores/mL. Wheat bran agar (WBA), banana agar (BAA) and glucose enriched malt extract yeast extract agar (MYEGA) with $16.8 \pm 0.2 \cdot 10^7$, $6.1 \pm 0.3 \cdot 10^7$ spores/mL and $11.4 \pm 0.5 \cdot 10^7$ spores/mL, respectively, show results below the reference medium although within the same order of magnitude. Corn steep liquor agar (CSLA), despite superior reported results for the conidiation of *C. minitans* (Chen et al., 2005), totally fails for the production of *A. ochraceus* spores. Also, CYEA, PDA YESA and YEPGA yield very low spore concentrations of 6.1, 0.1, 4.7 and $0.6 \cdot 10^7$ spores/mL respectively (data not shown). All reported differences are significant with $p < 0.05$.

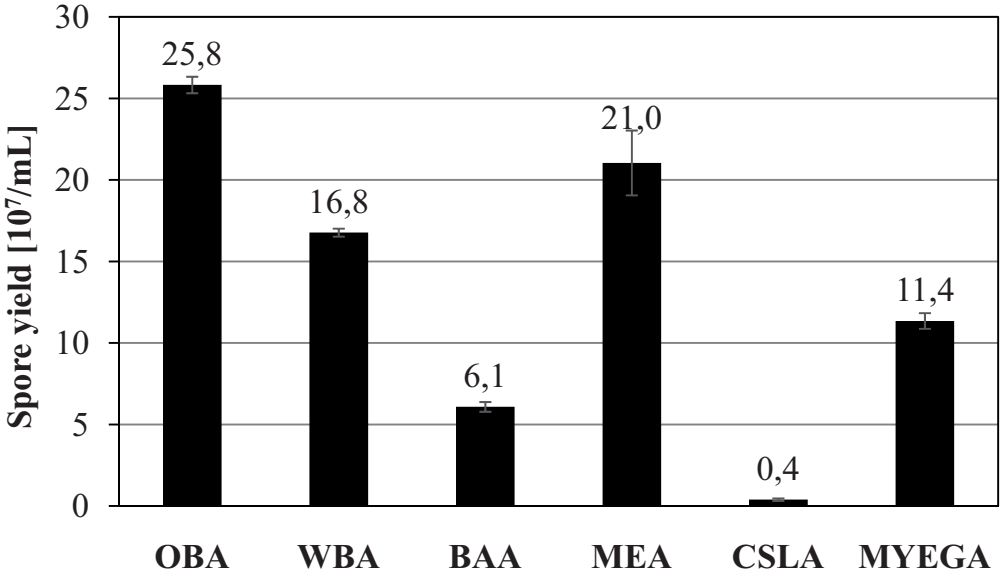

Fig. 4.1. Spore yield on different solid media after 8 d of incubation at 24 °C in the dark. Substrate height in all cases 1.6 cm, oat bran agar (OBA), wheat bran agar (WBA), banana agar (BAA), malt extract agar (MEA), corn steep liquor agar (CSLA), malt extract yeast extract agar + 40 % (w/v) glucose (MYEGA). Presented are arithmetic means of 6 biological and 3 technical replicates ± SEM.

Fig. 4.2. Growth and sporulation of A. ochraceus *on selected solid media after 8 d of incubation at 24 °C in the dark. Oat bran agar (OBA), malt extract agar (MEA), corn steep liquor agar (CSLA), banana agar (BAA), wheat bran agar (WBA). Substrate height 1.6 cm.*

These results correlate well with the naked eye observation of the sporulation plates which are illustrated in **figure 4.2**. The entire surface of OBA and WBA plates was covered with ochre to brownish spores. Also, MEA plates were coated entirely with spores although not as darkly colored. BAA showed the same pigmentation but

repeatedly exhibited blank spots where no mycelium and no spores grew while fungal growth on all other substrates was evenly spread over the entire plate without exception. Hardly any conidiation occurred on CSLA. However, intensive growth of white mycelium of up to 3 mm thickness could be noticed. This is significantly more than witnessed on any other substrate and caused the substrate to wrinkle as moisture was detracted from the agar plate. Wrinkling was not observed on control plates and to a much lesser extent, if any, on the other media.

Despite the described ongoing discussion in the literature whether carbon limitation or excess stimulates conidiation, spore yield of *A. ochraceus* is enhanced with increasing carbon content in the solid medium as shown in **table 4.3** and **figure 4.3**. This is in line with findings of Ooijkaas et al. (1999) and Vega et al. (2003) but contrary to Schisler et al. (1991). However, as the only known report about the sporulation of *A. ochraceus* describes the process for submerged conditions, no further strain specific comparison can be drawn (Broderick and Greenshields, 1981).

Tab. 4.3. Carbon concentration, nitrogen concentration and spore yield of selected complex sporulation media.

Substrate	Carbon concentration [g/L]	Nitrogen concentration [g/L]	C:N ratio	Spore yield [$\cdot 10^7$/mL]
OBA	15.40	1.38	11:1	25.8
WBA	10.08	0.75	13:1	16.8
BAA	7.73	0.14	55:1	6.1
MEA	12.40	0.73	17:1	21.0
CSLA	7.38	1.07	7:1	0.4
MYEGA	182.75	1.2	152:1	11.4

Data for the calculation of carbon and nitrogen concentrations were obtained from the website of the 'Nutrient Data Laboratory' of the 'United States Department of Agriculture'. It is clearly visible how increasing carbon concentrations foster the production of spores. Banana and corn steep liquor with carbon contents below 8 g/L show lowest spore yield. Wheat bran agar, malt extract agar and oat bran agar with 10, 12 and 15 g/L carbon, respectively, produce increasing amounts of spores. However, the yields obtained from the glucose enriched medium MYEGA with 183 g/L carbon and a harvest concentration of $11 \pm 0.5 \cdot 10^7$ spores/mL illustrate that this is not a strictly linear trend. At the same time this finding demonstrates that even very high carbon concentrations do not inhibit conidiation in contrast to results found for *C. truncatum* (Jackson and Schisler, 1992). Nonetheless, the viability of those spores was clearly impaired as will be shown in chapter 4.1.7.

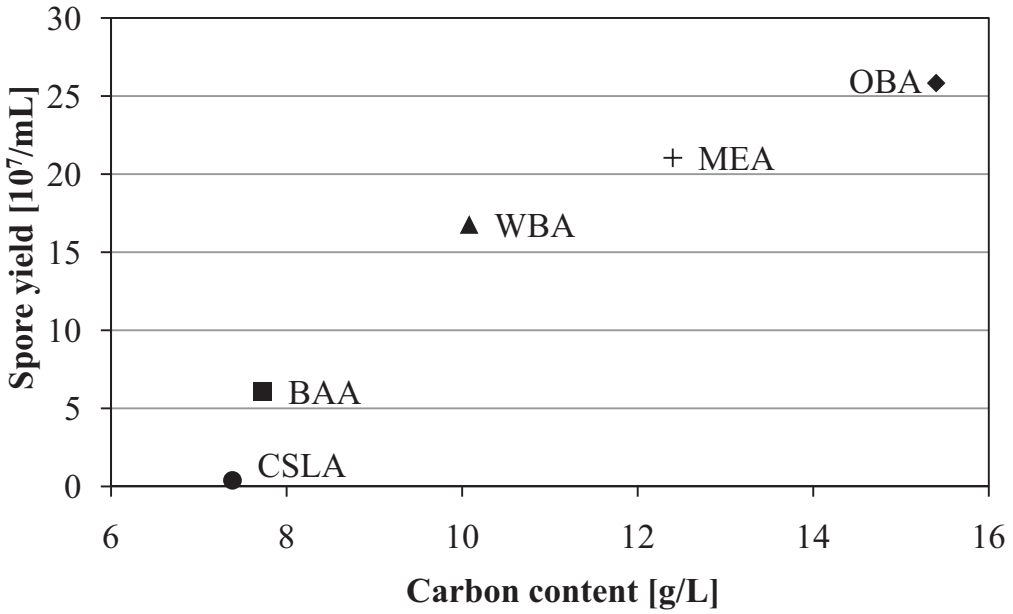

Fig. 4.3. Spore yield over carbon concentration of the sporulation substrate. MYEGA with 183 g/L glucose removed for better perceptibility. Abbr. as above.

Ooijkaas et al. (1998) reported substantially increased mycelial growth and decreasing spore yields for high substrate concentrations though it is not entirely clear whether this declaration relates to the carbon or the nitrogen content. The opposite seems to be true for *A. ochraceus* where excess mycelium is formed on CSLA with the lowest carbon concentration but not on MYEGA. Nevertheless, CSLA also has the lowest C:N ratio and hence the highest relative nitrogen content. This may suggest lower relative nitrogen levels to be beneficial for sporulation. This conclusion, however, is confuted by OBA with the highest absolute and the second highest relative nitrogen content of 1.38 g/L and 11:1, respectively, still yielding the best spore concentrations with $25.8 \cdot 10^7$ spores/mL.

It can hence be concluded that nitrogen limitation does not serve as an essential trigger for sporulation in *A. ochraceus*. Spore yield increases with increasing carbon concentration of the substrate and there is no catabolite inhibition for carbon concentrations up to 183 g/L.

Furthermore, Georgiou and Shuler (1986) predicted the thickness of the substrate to be influential on the sporulation process. The effect was therefore investigated for the standard medium MEA and results are presented in **figure 4.4**. Height of the medium was varied in five steps between 0.4 and 2.0 cm by pouring varying amounts of solid medium into the flask. Media nomination represents amount needed in mL for height adjustment.

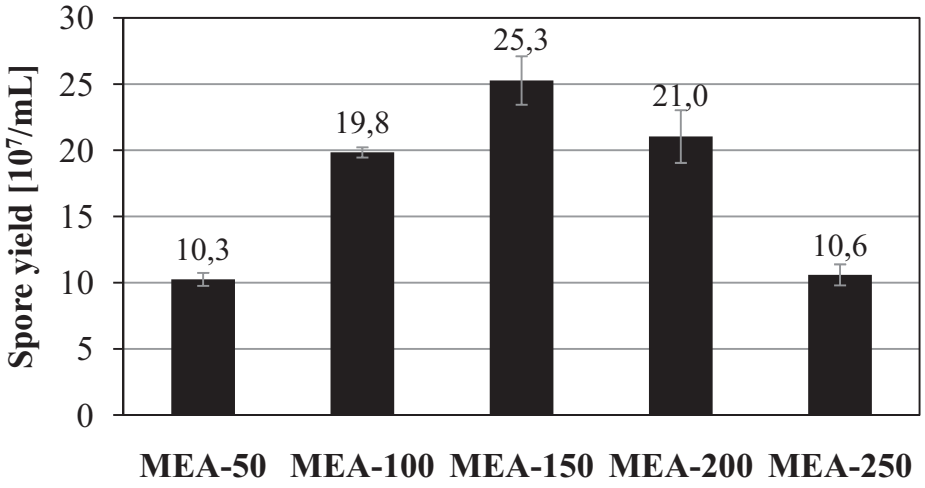

Fig. 4.4. Spore yield on MEA plates of varying height after 8 d of incubation at 24 °C. MEA-50: 0.4 cm, MEA-100: 0.8 cm, MEA-150: 1.2 cm, MEA-200: 1.6 cm, MEA-250: 2.0 cm. Presented are arithmetic means of 6 biological and 3 technical replicates ± SEM.

It can be seen that the effect of substrate thickness is in the same range as that of substrate composition. Highest yields of $25.3 \pm 1.8 \cdot 10^7$ spores/mL were obtained with a substrate height of 1.2 cm (MEA-150). The thinnest (0.4 cm) and the thickest agar plate (2 cm) generate lowest results with 10.3 and $10.6 \cdot 10^7$ spores/mL, respectively, being a factor 2.5 below the maximal yield. Sporulation for the media in between, i.e. MEA-100 with 0.8 cm and MEA-200 with 1.6 cm height, is with 19.8 and $21.0 \cdot 10^7$ spores/mL slightly less compared to the optimum.

These findings in combination with the results obtained from varied media suggest that standard cultivations on Petri dishes, which typically have a thickness of less than 0.5 cm, provide insufficient nutrient supply. On the other hand, on thick substrates no nutrient gradient will form which was emphasized to be of paramount importance for sporulation to occur (Georgiou and Shuler, 1986). Here sporulation is hence also not optimal. Best results are obtained with intermediate heights of around 1.2 cm, as illustrated in figure 4.4. However, the influence of secondary effects such as water content cannot be ruled out.

4.1.2 Spore aggregation depending on sporulation media

As described before, aggregation of conidia during the first hours of submerged cultivation is a function of pH and power input (Fujita et al., 1994; Grimm et al., 2005b; Krull et al., 2010). In this study, it is shown that yet the substrate on which the spores are generated, the sporulation medium, influences the aggregation as well.

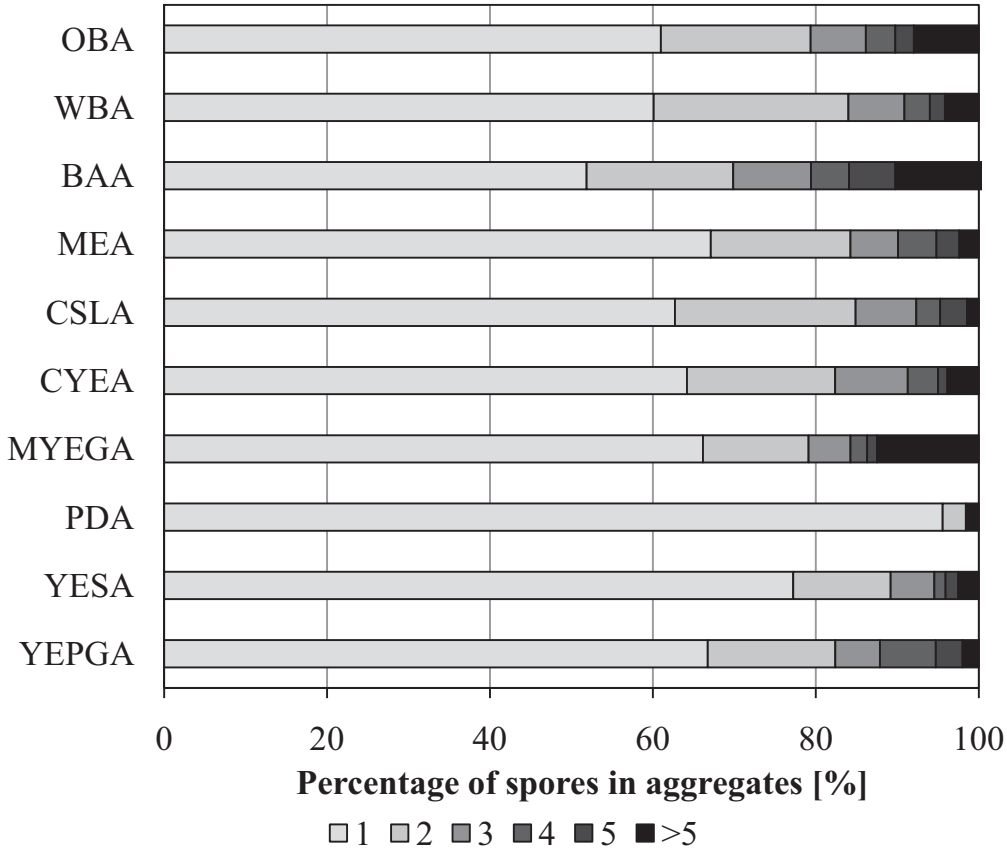

Fig. 4.5. Aggregation behavior of spores generated on different solid media during 8 d incubation at 24 °C in the dark immediately after harvesting. Oat bran agar (OBA), wheat bran agar (WBA), banana agar (WBA), malt extract agar (MEA), corn steep liquor agar (CSLA), Czapeck yeast extract agar (CYEA), malt extract yeast extract agar + 40 % (w/v) glucose (MYEGA), potato dextrose agar (PDA), yeast extract sucrose agar (YESA), yeast extract peptone glucose agar (YEPGA). Shown are the fractions of conidia found as single spores, aggregates of two, three, four, five and more. Results represent arithmetic means from 3 biological and 3 technical replicates.

Figure 4.5 shows clearly the large differences in the aggregation behavior of spores from different media. The one common attribute for conidia irrespective of sporulation medium is the predominance of single spores with a percentage of consistently over 50 %. This, however, still covers the whole range from 52 % to 96 % single spores for suspension gained from banana agar (BAA) and potato dextrose agar (PDA), respectively. Spores from BAA and glucose enriched malt and yeast extract agar (MYEGA) show a significantly increased tendency to form large aggregates with six or more spores with 11 and 12 % of spores found in those clusters, respectively. For conidia from BAA this is not only true for particularly large aggregates. Also groups of 5 (6 %), 4 (5 %) and 3 (10 %) are significantly increased compared to the average. The percentage of spores found individually is hence the lowest with only 52 %. Furthermore, it was noticed, though not statistically significant, that for spores from MEA aggregation also differs with substrate height.

Despite the large variance, no correlation can be identified allowing conclusions with regard to the medium composition or harvestable spore yield. With the exception of PDA where harvested spore yield was very low no connection between spore concentration and spore aggregation can be drawn. Also, the pH of the suspension, which is a major determining factor, can be ruled out as a relevant parameter as it was identical throughout the samples with a value of 5.5 ± 0.3 and can hence not be the cause of the variance. Moreover, no reasonable correlation of any kind can be found between the aggregation behavior and the carbon or the nitrogen content of the medium. As the results were obtained in biological and technical replicates and differences were proven significant with $p < 0.05$, it can be excluded that the phenomenon is the result of random statistical event.

It has therefore to be expected that other ingredients in the complex media may have caused the observed changes in the constitution of the spores' cell wall. These alterations may be attributed to the abundance of melanin (Gerin et al., 1993), the arrangement of surface proteins such as hydrophobins (Kershaw and Talbot, 1998), the presence of lipids (Latgé et al., 1988), the structure of glucans (Fontaine et al., 2010) or the activity of wall bound enzymes (Mouyna et al., 2000). The underlying mechanisms cannot be determined at this point. It can be speculated though that the expression of cell wall proteins and/or enzymes for the production thereof underlie a complex regulatory network. This may possibly be triggered by starvation or excess of nutrients, both causing alterations in the cAMP signal cascade and the MAP-Kinase pathway, which among others regulate cell wall assembly as suggested previously (Jeraj et al., 2005; Obaidi and Berry, 1980; Xu, 2000).

4.1.3 Spore metabolites depending on sporulation media

The metabolism of a given set of spores is strongly connected to its history and distinct clustering of different populations can be witnessed due to significant differences in the global composition of each spore set's metabolome as explained in chapter 3.4 and illustrated in figure 3.12. In contrast to the metabolic fingerprinting analysis conducted there, here a target analysis is presented.

Figure 4.6 shows the relative concentrations of nine relevant, selected metabolites detected in freshly harvested spores from oat bran agar (OBA), malt extract agar (MEA) and wheat bran agar (WBA, for a complete profile see appendix, table 7.1). Ribitol, sorbitol, inositol and trehalose could be quantified and occur in MEA spores at concentrations of 55.4, 76.1, 0.1 and 7.4 ng/10^5 spores, respectively. This is in line

with parallel conducted determinations employing HPLC analysis where concentrations between 50 and 300 ng mannitol/10^5 spores were detected. Even though no precise determination is possible for the other metabolites, they can be expected to be present at comparable concentrations due to the similarity of the molecular structure and the resulting behavior in GC-MS analysis. Inositol and myo-inositol, which are isomers and show identical biological behavior in the analyzed samples, are summarized to inositol in the following explanations for improved perceptibility.

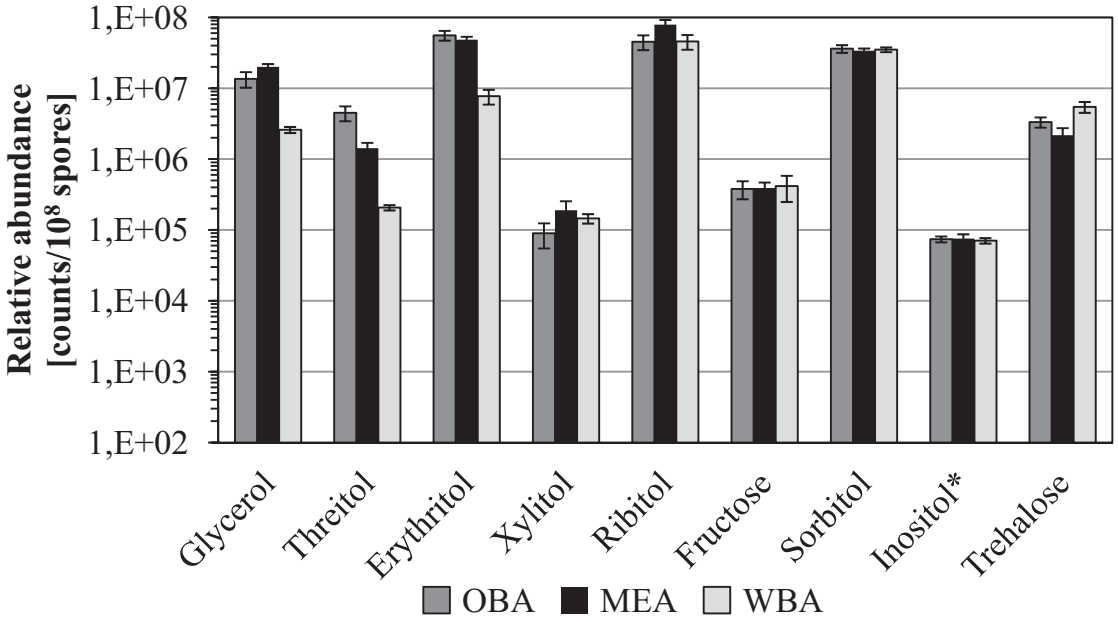

*Fig. 4.6. Relative abundance of nine dominant metabolites per 10^8 spores in fresh conidia generated on oat bran agar (OBA, dark grey), malt extract agar (MEA, black) and wheat bran agar (WBA, light grey). Presented are arithmetic means of 3 biological and 3 technical replicates ± SEM. Note the logarithmic scale and the base point of 100 of the ordinate. *Sum of the isomers inositol and myo-inositol.*

It becomes obvious that fructose, sorbitol and inositol are present in spores at identical levels irrespective of the sporulation medium. The difference between the population with the highest and the lowest content of one of those metabolites is in all cases below 10 %. In contrast, the erythritol concentrations in OBA and WBA spores differs by factor 7 and that of threitol (a diastereomer of the first) even by factor 22. Also, the concentration of glycerol varies by factor 8 depending on the substrate. While the differences between spores from OBA and MEA alternate, the concentrations of these important stress protectors and carbon stores is inferior in all cases in WBA. Similar findings had been reported for *A. nidulans* which shows significantly reduced glycerol and erythritol concentrations under altered growth conditions. However, in that study, mycelium was investigated, not fungal spores (Dijkema et al., 1985).

Even though the effect of particular polyols on particular strains may differ, it had been shown previously that generally high concentrations of polyols enhance the spores' resistance to stresses and increase the rate of germination. Particularly, glycerol and erythritol have been proven to accelerate germination of *Metarhizium anisopliae*, *Paecilomyces farinosus* and *Beauveria bassiana* (Al-Hamdani and Cooke, 1987; Pascual et al., 2003). Unlike for several other polyols, these findings have not been disputed in the literature and it can hence be expected that they can be transferred to other fungi as well showing conserved, essential functions in spores. The effect of trehalose, however, is intensively discussed and appears to be not only dependent on the species but also on the presence of further sugars or polyols (Hallsworth and Magan, 1995; Hallsworth and Magan, 1996; Harman et al., 1991; Tereshina et al., 2004). It can therefore be expected that the effect of decreased trehalose concentrations on the spores' constitution is not as disadvantageous as that of decreased threitol, erythritol and glycerol. It can therefore be expected that spores generated on WBA medium are significantly more susceptible to stress damage and may show inferior storage competence as will be discussed in chapter 4.4.

These findings emphasize the large dynamic range that metabolites of spores span and how extensive the effect of different conidiation media can be. This also once again illustrates the power of metabolite profiling to reveal differences between populations that cannot be differentiated by classical phenotype analysis but show stunning metabotypes.

Besides the metabolites detected and described above, it is also noteworthy what was not detected. Malic acid is the only TCA cycle intermediate and from the 13 detectable amino acids, none was present in freshly harvested spores. Pyruvic acid as the key intersection of primary metabolism and alanine as the simplest and second most abundant amino acid were both below detection limits in all unstored spores irrespective of the solid medium deployed for their generation. This indicates that spores are truly dormant immediately after harvest.

Despite its much discussed role as a protector against oxygen and other stresses, its role as a compatible solute or its function as a carbon and energy reservoir, mannitol could also not be detected reproducibly in the spores of any substrate. Sorbitol, an isomer of the first, however, was found at equal concentrations irrespective of the conidiation substrate.

The fact that significant differences between the metabolite profiles of conidia from different conidiation substrates become visible is remarkable. This finding illustrates

that focusing on spore yield alone during the optimization of sporulation conditions will not necessarily give the best results. Spores from different media are distinct in their carbon reservoirs and their concentrations of compatible solutes. This immediately leads to the conclusion that different spore populations can be expected to show different behaviors depending on the requirement. Spores that show ideal performance under certain conditions may be inferior under other conditions.

4.1.4 Spore ATP content depending on sporulation media

It has previously been reported that the ATP content in cells can serve as an indicator for viability (Lane et al., 1988). The effect of the conidiation conditions on the ATP content of generated spores has never been investigated though. Hence, the influence of the sporulation substrate on the ATP concentration in *A. ochraceus* spores was investigated, results are presented in **figure 4.7**.

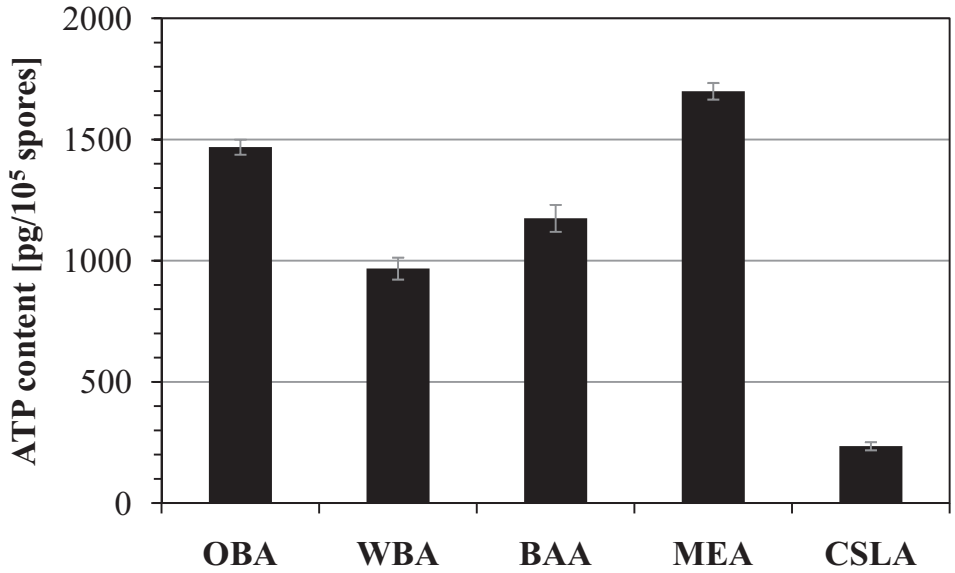

Fig. 4.7. ATP concentration in freshly harvested spores from oat bran agar (OBA), wheat bran agar (WBA), banana agar (BAA), malt extract agar (MEA) and corn steep liquor agar (CSLA). Presented are arithmetic means of 6 biological and 9 technical replicates ± SEM.

As can clearly be seen, the composition of the substrate has a significant impact on the ATP accumulation in the produced spores. The spores generated on the standard substrate malt extract agar (MEA) show the highest ATP concentration with 1 699 ± 34 pg ATP/10^5 spores. Spores produced on oat bran agar (OBA), banana agar (BAA) and wheat bran agar (WBA) are within the same range with ATP concentrations of 1 469 ± 31, 1 175 ± 55 and 968 ± 45 pg ATP/10^5 spores even though differences are significant ($p < 0.01$). Conidia formed on corn steep liquor agar (CSLA), however, show with only 235 ± 17 pg ATP/10^5 spores very low ATP

concentrations. It can therefore be expected that conidia generated on CSLA are less resistant to external stresses.

Figure 4.8 shows the correlation of the carbon content of the sporulation substrate and the ATP concentration in the generated spores. Even though not strong, a slight trend can be identified where higher ATP concentrations are achieved with an increasing carbon content of the conidiation substrate.

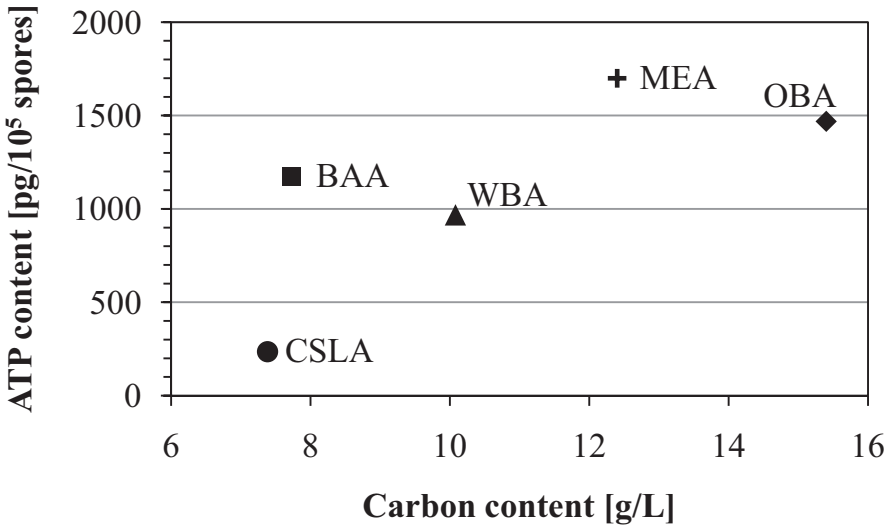

Fig. 4.8. Spore ATP concentration over carbon content of the sporulation substrate for freshly harvested spores after 8 d incubation at 24 °C on banana agar (BAA), corn steep liquor agar (CSLA), malt extract agar (MEA), oat bran agar (OBA) and wheat bran agar (WBA). Presented are arithmetic means of 6 biological and 9 technical replicates.

As the plot suggests a weak correlation between the carbon content and ATP concentration, it was tested whether the total amount of available nutrients affect the conidial ATP reservoir. **Figure 4.9** hence illustrates the ATP concentration as a function of the substrate height. It becomes visible that increasing substrate heights correlate with increasing ATP contents in the generated spores. Conidia harvested from MEA-50 with a thickness of 0.4 cm show with 134 ± 3 pg ATP/10^5 spores the lowest concentration of this relevant energy carrier. The reservoirs of the spores from MEA-100 (0.8 cm), MEA-150 (1.2 cm) and MEA-200 (1.6 cm) increase constantly with ATP concentrations of 536 ± 23, 749 ± 19 and 1 699 ± 23 pg ATP/10^5 spores. The highest ATP concentration is achieved in spores from the 2 cm thick MEA-250 conidiation substrate. These conidia contain 2 741 ± 274 pg ATP/10^5 immediately after harvesting.

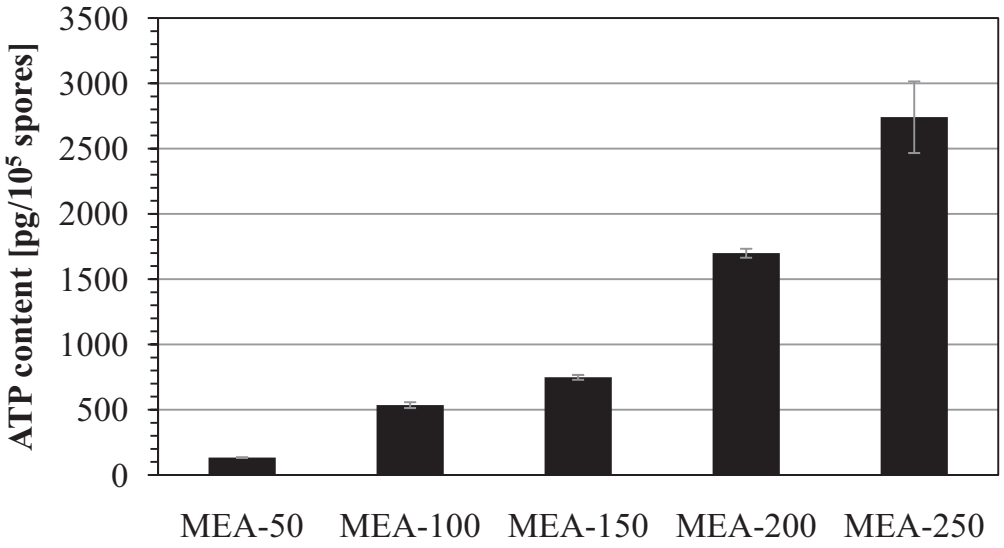

Fig. 4.9. ATP concentration in freshly harvested spores from malt extract agar (MEA) of varying substrate height. Presented are arithmetic means of 6 biological and 9 technical replicates ± SEM.

The concentration in spores of even thicker substrates cannot be tested as the sporulation yield rapidly decreased beyond this substrate height as shown in chapter 4.1.1. It may be speculated though that a sigmoid correlation would be seen.

Further, the dry weight of lyophilizated spores was determined to be 2.45 µg/10^5 spores. The concentration in freshly harvested spores from MEA-250 is hence 0.0011 g ATP/g spores. ATP thus accounts for 0.1 % (w/w) in spores.

Compared to ribitol, sorbitol, inositol and trehalose which could be determined to account for 2.3, 3.1, 0.01 and 0.3 % (w/w) in freshly harvested spores from MEA, respectively, the ATP content appears to be in a reasonable range. This once again emphasizes the applicability of the established extraction and determination methods. In subchapter 4.4.3 it will be demonstrated how storage of spores affects the conidial ATP concentration.

4.1.5 Spore NAD(P)H composition depending on sporulation media

As explained before, the fluorescence lifetime of protein bound NAD(P)H is significantly increased compared to its free state. Measurement of fluorescence decay behavior and subsequent non-linear fitting of the signals was established by the Institute for Physical and Theoretical Chemistry (Technische Universität Braunschweig), Prof. K. H. Gericke. This allowed precise determination of both, fluorescence lifetimes and relative abundance for two out of the three postulated

ingredients. While absolute concentrations, however, have to be regarded error-prone, relative amounts for free and protein bound NAD(P)H are determined readily with this method.

Table 4.4 shows the fluorescence lifetimes of free and protein bound NAD(P)H as well as the percentage of bound NAD(P)H for freshly harvested spores from MEA, OBA and WBA.

Tab. 4.4. Fluorescence lifetimes of free and protein bound NAD(P)H in freshly harvested spores from malt extract agar (MEA), oat bran agar (OBA) and wheat bran agar (WBA). Presented are arithmetic means from 2 biological and 3 technical replicates ± SEM.

	Lifetime [ps]		Fraction of protein bound NAD(P)H [%]
	NAD(P)H free	NAD(P)H bound	
MEA	814 ± 55	3 226 ± 233	10 ± 2
OBA	719±31	2 893 ± 158	11 ± 1
WBA	560 ± 24	2 351 ± 100	22 ± 1

The fluorescence lifetime of melanin is not shown as calculations yielded lifetimes of approx 50 - 100 ps. This is within the expected range (Nofsinger and Simon, 2001), however, detections and hence calculations below 0.1 ns are below the temporal resolution of the experimental setup and have therefore to be regarded as unreliable. Therefore, quantification of melanin is also not possible. Free and protein bound NAD(P)H, however, were identified through comparison with previously published data where the fluorescence lifetime of the free coenzyme was reported to be between 450 and 800 ps and that of the bound cofactor 3.41 ns, slightly varying depending on cell conditions (Lakowicz et al., 1992; Zhang et al., 2002).

Most interesting is the concentration of protein bound NAD(P)H. For spores generated on MEA, it is 10 %, for those from OBA 11 % and for conidia from WBA 22 % immediately after harvest. It can therefore be concluded that spores from WBA are significantly more active than spores from the other two substrates ($p < 0.01$). This is striking as differences between spore populations would have not been expected to differ this dramatically. At the same time, these findings are well in line with the results presented in the previous subchapters where several metabolites varied by the order of one magnitude or more between freshly harvested spores from different media. In any case, wheat bran agar spores appear extraordinary suggesting this population to be significantly different from other populations. The elevated relative concentration of protein bound NAD(P)H in WBA spores suggests an ongoing

metabolic activity in these spores rather than being dormant as commonly attributed. This in turn may explain the decreased amounts of the putative storage polyols glycerol, threitol and erythritol shown for WBA spores in chapter 4.1.3. It may be speculated that the more active conidia deplete their reservoirs faster than the more dormant spores. This immediately influences endurance during storage as well as cultivation performance of these spores as will be shown later.

It is furthermore possible to reveal variances between single spores of the same population with the established method (see figure 3.14-C). Fluorescence lifetime and proportions of bound NAD(P)H were found to vary by more than 20 % between individual spores for every conidiation substrate. This indicates large heterogeneities during the production of spores on solid medium, possibly a result of coexisting younger and older spores as well as a micro-environome on the plates. For meaningful results, TCSPC data were hence spatially integrated over an entire raster scanned image containing a minimum of 5 conidia. Randomly selected images were then regarded as technical replicates.

As a negative control, dead spores were also subjected to the same technology. Conidia sterilized for 30 min at 100 °C were tested for viability and showed no growth (data not shown). The fluorescence lifetimes fell from 814 to 448 ps for free and from 3226 to 1775 ps for bound NAD(P)H, a reduction by almost 50 % in both cases. As decreased fluorescence lifetimes represent decreased protein stabilization of the coenzyme, this reduction clearly stands for the breakdown of crucial cell structures and the hence changed intra-conidial conditions.

It can be concluded that the conidiation substrates (MEA, OBA and WBA) strongly influence the metabolic activity of the produced spores. The ratios of free and protein bound NAD(P)H vary significantly between the substrates. Particularly, the conidia generated on WBA show enhanced metabolic activity with ratios of protein bound NAD(P)H increased by factor 2 compared to the other spores. Since fluorescence lifetimes of the coenzyme also vary, it becomes obvious that the cofactor not only exists as either bound or free but can be stabilized through the interaction with other cellular compounds as well creating a near continuum of possible fluorescence lifetimes between 1 775 and 3 226 ps for bound NAD(P)H. Further, population heterogeneity as well as cell structure breakdown could be detected. Finally, based on these findings, it may be speculated that spores generated on WBA show the fastest response when left for germination under favorable conditions.

4.1.6 Spore visible longwave fluorescence depending on sporulation media

Specific autofluorescence (SAF) in the visible longwave range was measured as described in chapter 3.7 for freshly harvested spores from different sporulation media. **Figure 4.10** shows the results for conidia from oat bran agar (OBA), wheat bran agar (WBA), banana agar (BAA), malt extract agar (MEA) and corn steep liquor agar (CSLA).

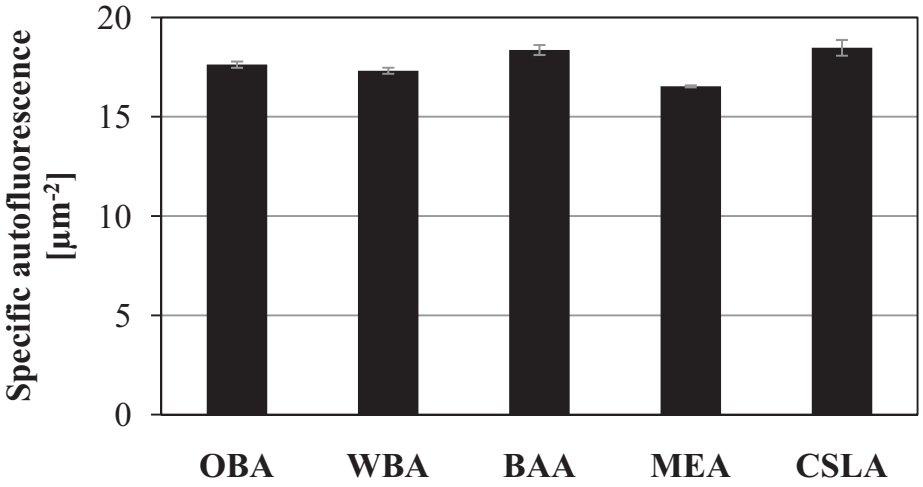

Fig. 4.10. Specific autofluorescence of spores from oat bran agar (OBA), wheat bran agar (WBA), banana agar (BAA), malt extract agar (MEA) and corn steep liquor agar (CSLA) after incubation for 8 d at 24 °C in the dark. Presented are arithmetic means of 9 biological and 3 technical replicates ± SEM. Excitation at 366 nm, emission detection > 670 nm.

The SAF of the tested spore populations ranges from 16.5 to 18.5 μm^{-2} for MEA and CSLA, respectively. The results for OBA, WBA and BAA are 17.6, 17.3 and 18.4, respectively. Due to the large number of analyzed spores (10 000 per measurement), the standard error is minute. The differences based on t-test analysis with $p < 0.01$ are hence significant. However, the mere statistical analysis does not seem appropriate for the understanding of the phenomenon. As the multiple wavelength shifts in FRET and the broad absorption of the heteropolymer melanin do not allow a more detailed allocation of the detected fluorescence signals, any further interpretation would be sheer speculation. It has hence to be concluded that based on the analysis of visible longwave autofluorescence by means of flow cytometry, spore populations generated on different sporulation substrates show similar signals. Based on the explanation given in chapter 3.7, they can therefore be expected to contain comparable compositions of secondary metabolites.

4.1.7 Spore viability as a function of sporulation media

The influence of the sporulation substrate on the viability of the generated conidia was investigated as described in chapter 3.8. It shall be mentioned again that the suggested viability assessment includes a time component as the colony forming units (CFU) were yet determined after 72 h of incubation. This procedure includes the industrially relevant factor germination time into the viability.

Figure 4.11 shows the viability of the harvested spores as a function of the conidiation medium. Highest results were obtained with potato dextrose agar (PDA), the common substrate for production of *A. niger* spores. *A. ochraceus* spores harvested therefrom after 8 d of incubation in the dark show a viability of 95 ± 2 %. Conidia harvested from yeast extract peptone glucose agar (YEPGA) are least viable with a viability of only 39 ± 3 %. Also, malt extract yeast extract glucose agar (MYEGA), the second substrate highly enriched in glucose, shows very low viabilities of only 48 ± 3 %. The recommended standard medium (malt extract agar, MEA) is in the intermediate range with viabilities of 59 %. No reliable correlation between viability and carbon or nitrogen content was found though.

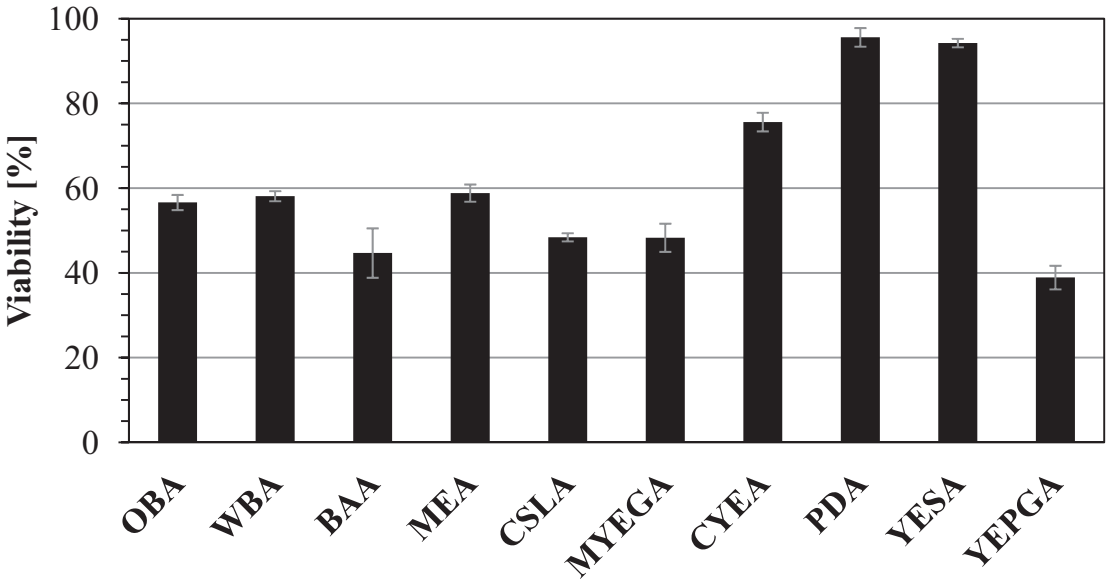

Fig. 4.11. Viability of freshly harvested spores after 8 d incubation at 24 °C in the dark as a function of sporulation medium. Oat bran agar (OBA), wheat bran agar (WBA), banana agar (BAA), malt extract agar (MEA), corn steep liquor agar (CSLA), malt extract yeast extract glucose agar (MYEGA), Czapeck yeast extract agar (CYEA), potato dextrose agar (PDA), yeast extract sucrose agar (YESA), yeast extract peptone glucose agar (YEPGA).

Reported viabilities for conidia of fungal spores have been very equivocal depending on the respective strain and the investigation method applied. A comparison of the

obtained results is hence difficult. However, published viabilities for *Aspergillus* spp. range from 32 % to 92 % (Araujo and Rodrigues, 2004; Ludemann et al., 2010) confirming the results presented in this work which are within the same range.

Figure 4.12 shows the combination of the viability and the absolute concentration of harvestable spores. The multiplication of the two indicators gives the yield of viable spores, an important measure for the characterization of spore populations for industrial applications. This is shown below:

$$\text{Spore yield } [10^7/\text{mL}] \cdot \text{Viability} = \text{Viable spore concentration } [10^7/\text{mL}] \qquad (4.1)$$

Here, it becomes obvious that neither the mere viability nor the sheer concentration of spores represents meaningful results alone. However, the combination of the two elucidates the relevant information about the amount of spores which are capable to quickly germinate and putatively form biomass.

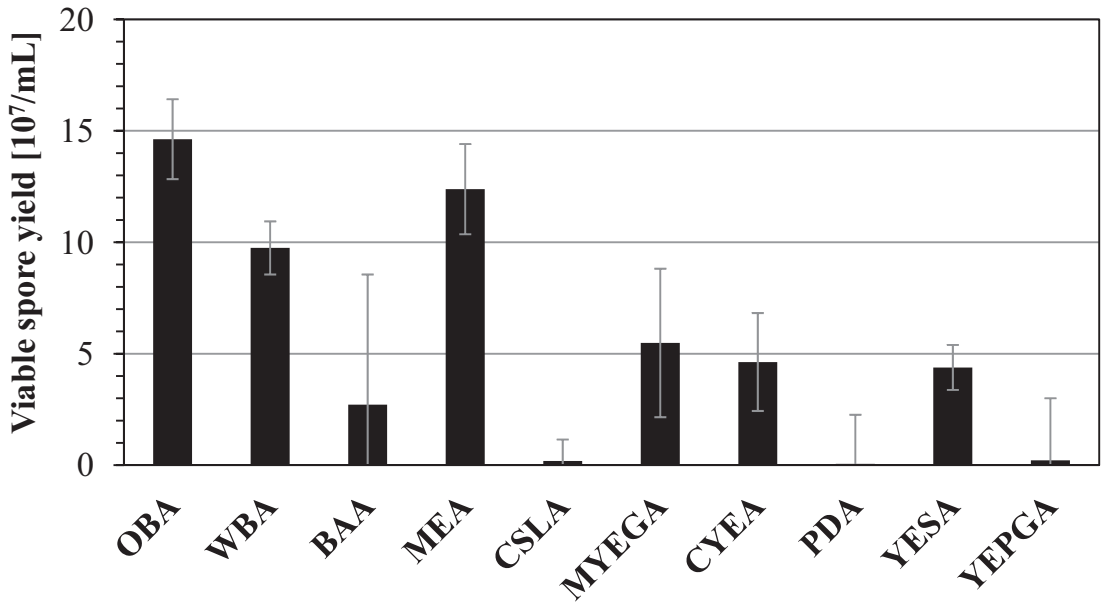

Fig. 4.12. Concentration of viable spores freshly harvested from various conidiation substrates. For abbreviations see fig. 4.11.

It can clearly be seen that oat bran agar, wheat bran agar and malt extract agar are the most promising conidiation substrates producing 14 ± 2, 10 ± 1 and 12 ± 2 · 10^7 viable spores/mL, respectively. Despite large error bars due to error propagation, most differences are still significant ($p < 0.05$).

Due to their outstanding performance and the hence suitable application in industrial processes, MEA, OBA and WBA were selected for further detailed analysis. It is noteworthy though that their absolute viability is with 59, 57 and 58 %, respectively,

virtually identical. This is particularly striking as large differences were found in the metabolite profile, the ATP content and the ratio of bound and free NAD(P)H between the spore populations generated on the different substrates as explained in the previous subchapters. It has therefore to be speculated that these differences become more relevant during storage (which will be explained in the following chapters) and that conidia have a multitude of mechanisms to compensate environmental changes while maintaining stable viabilities. The findings also suggest that spore yield and viability exist in equilibrium. Maintaining high viabilities under possibly adverse conditions results in reduced spore yields as can vividly be seen for PDA and YESA. Best activities are hence obtained with media that show intermediate performance with respect to yield and viability individually. Taken together, this combination will outperform sporulation media that are superior in one or the other characteristic.

Summarized, it can be concluded that the determination of viability is particularly meaningful in combination with the total spore yield and a time correlated component. Conidiation substrates have to be rigorously assessed for their applicability to generate large amounts of quickly germinating conidia. Chen and Sequin-Swartz (2002) stated similar imperatives but in different contexts and without suggesting appropriate investigation methods. Even though most authors give details about the amount of spores generated per substrate and some state viability assessments (Bapat et al., 2003; Ooijkaas et al., 1999; Vega et al., 2003), the combination of germination rate, viability and total spore yield has not yet been reported.

4.1.8 Shake flask performance as a function of sporulation media

The effect of the sporulation medium on the performance of the conidia in shake flask cultivations was analyzed. **Figure 4.13** shows the effect of the sporulation medium on the pH of the cultivation broth inoculated with the hence generated spores. As indicated in chapter 3.9, the rise of the pH from its initial value of 5.6 can be attributed to the degradation of feed-peptides and subsequent deamination of amino acid. It is hence a criterion for metabolic activity. Cultures inoculated with spores from wheat bran agar (WBA) show with a pH of 8.7 ± 0.1 the highest increase indicating that WBA spores show the highest activity. Lowest activity was detected for cultivations inoculated with MEA spores reaching a pH of 8.2 ± 0.0 after cultivation for 72 h.

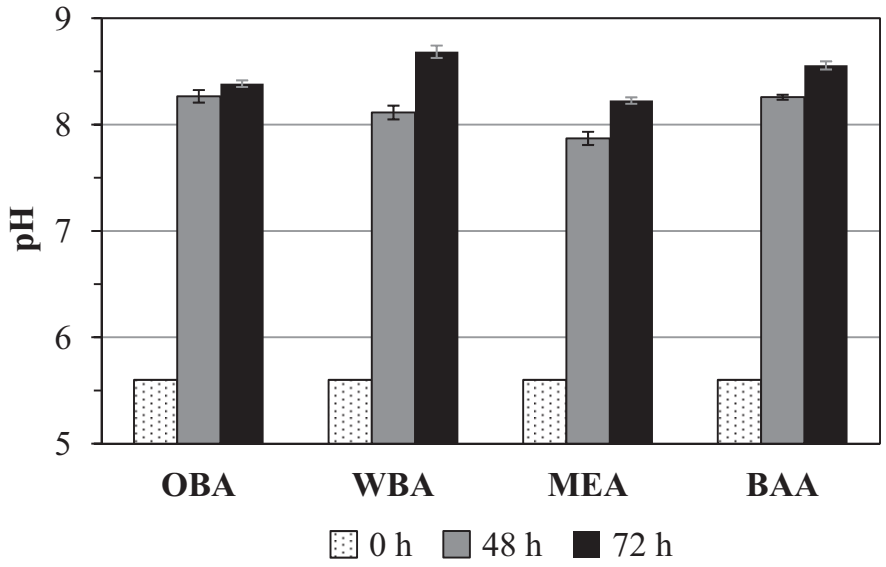

Fig. 4.13. pH of the cultivation broth 0 h (dotted columns), 48 h (grey columns) and 72 h after inoculation (black columns). CSL-SP medium, 30 mL, 24 °C, 130 min^{-1}, pH 5.6. Oat bran agar (OBA), wheat bran agar (WBA), malt extract agar (MEA), banana agar (BAA). Presented are arithmetic means of 6 biological and 3 technical replicates ± SEM.

Further, the dry biomass, the wet volume of biomass and the culture morphology were determined. **Figure 4.14** shows the morphology index for cultures inoculated with freshly harvested OBA, WBA, MEA and BAA spores after 72 h of cultivation. It can be seen that cultures inoculated with freshly harvested spores from WBA show the highest morphology index reaching 0.7 ± 0.1 which indicates that in average approx. 70 % of the biomass exists as pellets. This is noteworthy as the same cultures also exhibit the highest pH increase as shown in the previous figure. The dry biomass formation, however, is the smallest with 1.45 g/L while wet volume of biomass formation is second highest with 0.29 mL/mL (data not shown). Subsequently, these cultures are characterized by lowest biomass concentrations that exist in high-volume pellets. In summary, cultivations inoculated with freshly harvested WBA spores generate large, fluffy pellets. It has to be stated though that the correlation of pH and morphology is not strictly linear: MEA shows the smallest pH increase reaching a pH of 8.2 after 72 h of cultivation but still the second highest morphology index with 0.5 ± 0.1. Further input parameters must hence be involved.

However, the formation of pellets in cultures inoculated with WBA spores is not only due to the self-induced pH ascent. As was explained in subchapter 4.1.2, freshly harvested WBA conidia are characterized by the second lowest fraction of single spores (60 %) and the largest fraction of spores that exist in pairs (24 %). It can hence be concluded that WBA spores show a relatively strong aggregation tendency due to

specific spore wall properties which further fosters the formation of pellets. The correlation of the aggregation behavior and the resulting morphology in subsequent cultivations was already explained in subchapter 3.9.3.

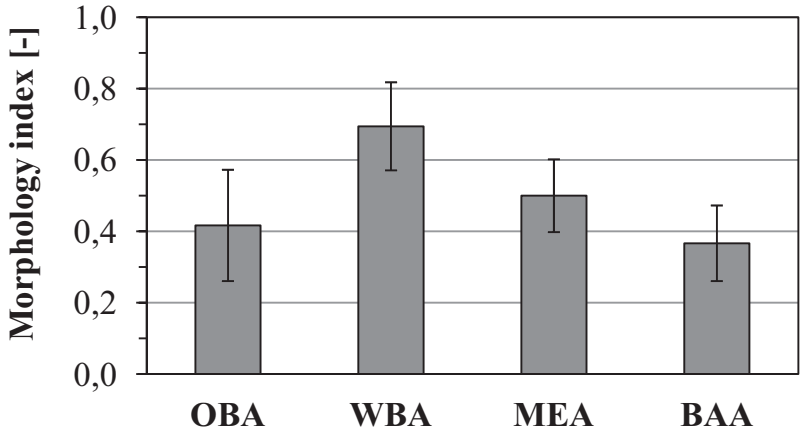

Fig. 4.14. Morphology index of the cultivation broth 72 h after inoculation with seed cultures generated on different sporulation substrates (8 d, 24 °C, darkness): Oat bran agar (OBA), wheat bran agar (WBA), malt extract agar (MEA), banana agar (BAA). Submerged cultivation: CSL-SP medium, 30 mL, 24 °C, 130 min^{-1}, pH 5.6. Presented are arithmetic means of 6 biological and 3 technical replicates ± SEM.

Most interesting, however, is the product formation and the reactant consumption during submerged cultivations. **Figure 4.15** shows the reactant consumption over the course of cultivations, that have been inoculated with spores harvested from 4 different conidiation media: banana agar, malt extract agar, oat bran agar and wheat bran agar. It can be seen that the culture inoculated with WBA spores clearly outperforms any other cultivation. Reactant consumption after 72 h of cultivation is 79 ± 5 % and therefore approx. twice as high as in OBA, BAA and MEA cultivations reaching 41, 45 and 34 %, respectively. The same trend could be observed for the product formation (data not shown).

The outstanding performance of inocula generated on WBA is the result of several factors: Due to increased aggregation tendency and increased auto-alkalization of the cultivation broth, the culture biomass is predominantly present in the morphology of fluffy pellets which has been reported previously to lower transfer resistances and hence increase productivity (El-Enshasy et al., 1999; Hille et al., 2005; Lin et al., 2010). Additionally, the portion of protein bound, and therefore active, NAD(P)H is in freshly harvested WBA spores with 22 % twice as high as in MEA and OBA spores with 10 and 11 %, respectively, as explained in chapter 4.1.5. This is perfectly in line with the reactant consumption witnessed in the cultivation and represents a unique and novel finding. NAD(P)H composition is hence a remarkable indicator for inoculum quality and subsequent product formation.

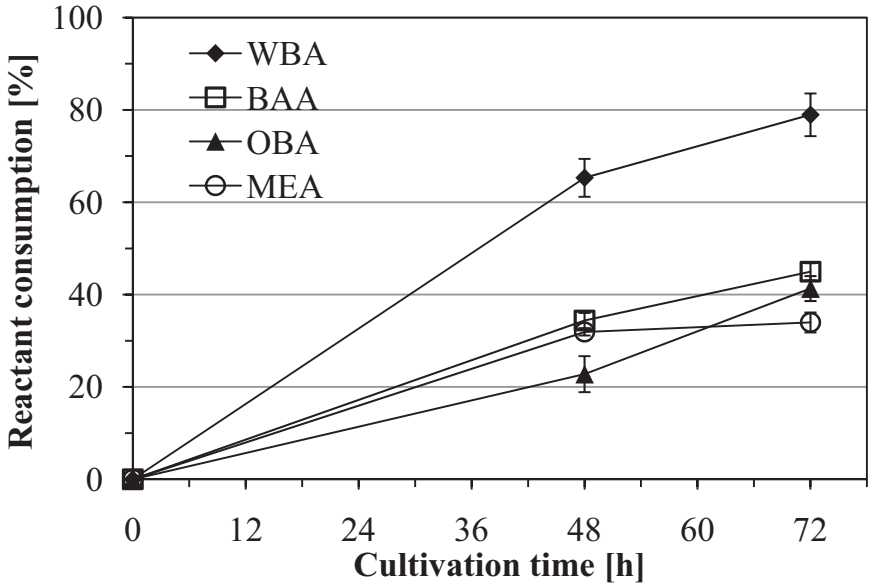

Fig. 4.15. Reactant consumption over the course of shake flask cultivations. Inocula generated on wheat bran agar (WBA), banana agar (BAA) oat bran agar (OBA) and malt extract agar (MEA) during 8 d sporulation at 24 °C in the dark. Submerged cultivation: CSL-SP medium, 30 mL, 24 °C, 130 min^{-1}, pH 5.6. Presented are arithmetic means of 6 biological and 3 technical replicates ± SEM.

4.2 Influence of inoculum concentration on solid media

4.2.1 Spore yield depending on inoculum concentration

Reports about germination behavior of filamentous fungi on solid media as a function of inoculum concentration have been controversial due to the individual needs of differing strains. It has been reported that a minimum inoculum density must be exceeded while too high concentrations lead to germination inhibition through 'crowding' (Lax et al., 1985; Lingappa et al., 1973). Araujo and Rodrigues (2004) found inhibition for *A. fumigatus* in liquid culture at concentrations higher than 10^6 spores/mL (area unknown) though Beyer (2004) found no effect of spore density on germination of *Fusarium graminearum* on solid media between approx. 2 and 20 spores per mm^2. Lately, investigations have revealed some information about the mechanisms and involved signaling pathways of this quorum sensing effect in fungi, however, no generalizable trend could be detected so far (Hogan, 2006).

Based on the typical in-house protocol for conidiation of *A. niger*, agar plates of an inner diameter of approx. 13 cm were initially inoculated with 100 µl of a 10^7 spores/mL concentrated suspension. Subsequently, the volume was diluted to 1.5 mL allowing automated distribution. Then, five concentrations were tested for their influence on the conidiation of *A. ochraceus*. The number of spores is most relevant

related to the area they are applied to. **Figure 4.16** therefore shows the harvestable concentration of spores as a function of seeded spores per mm² of the solid medium.

It becomes visible that the effect of varying spore seeding densities is relatively small. With one exception, the average harvested spore yields were approx. $19 \pm 2 \cdot 10^7$ spores/mL over the entire tested seeding range of 40 to 750 spores/mm² and are hence within the standard error and not significant ($p > 0.05$). Only at the highest density of 750 spores/mm², the spore yield decreases significantly ($p < 0.05$) to $11 \cdot 10^7$ spores/mL affirming literature findings predicting germination inhibition through 'crowding' for too high inoculation densities for Aspergilli (Barrios-González et al., 1989). This has also been confirmed by a more copious analysis conducted in parallel (Sommer, personal communication).

For all future investigations, inoculation was therefore conducted with a concentration of 320 spores/mm² which was achieved by spreading 1.5 mL of a $2.8 \cdot 10^6$ spores/mL suspension per agar plate with an inner diameter of 13 cm.

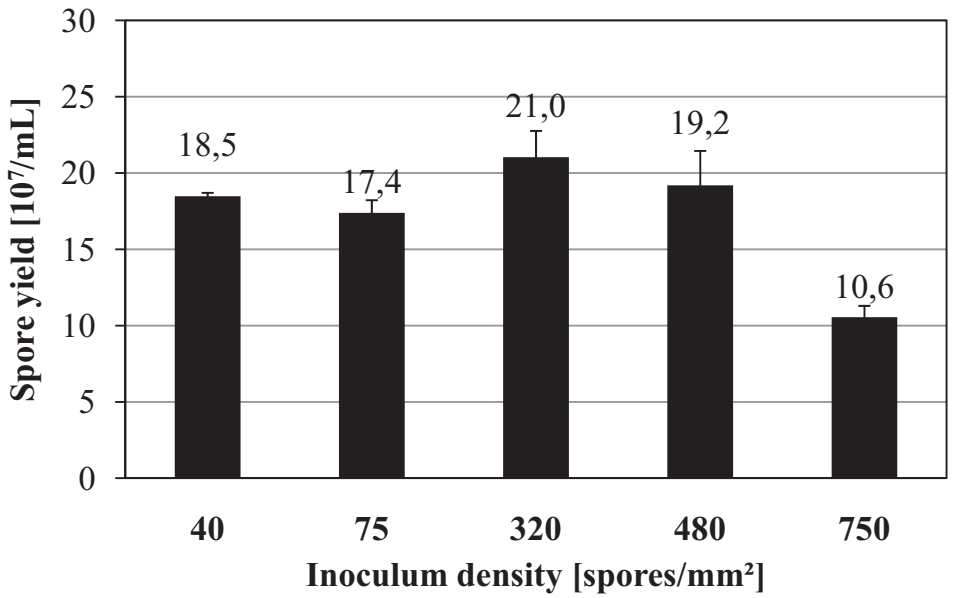

Fig. 4.16. Spore yield on MEA plates of varying inoculum concentration after 8 d of incubation at 24 °C. Presented are arithmetic means of 2 biological and 3 technical replicates ± SEM.

4.2.2 Effect of inoculum concentration on further quality indicators

The effect of a varying inoculum concentration on further quality indicators including aggregation behavior, viability and ATP content was assessed but showed no significant changes. Further analyses such as shake flask cultivation, metabolome analysis and autofluorescence were therefore not conducted.

4.3 Influence of sporulation duration

The effect of the incubation time during which conidiation is conducted on the constitution of the produced spores will be analyzed in this chapter. Naturally, this duration includes the time for germination and sporulation which are successive processes. As they can hardly be investigated individually and this study focuses on the identification of optimal sporulation conditions, those two phases are regarded as one phase, referred to as incubation on solid medium or sporulation time synonymously including the inevitable germination time into the sporulation time.

4.3.1 Spore yield depending on sporulation duration

Germination and sporulation speed of conidia of filamentous fungi highly depend on the specific strain. While *N. crassa*, for example, is reported to form visible colonies within hours, *C. minitans* takes several weeks to reproduce (Galagan et al., 2003; Ooijkaas et al., 1998).

Figure 4.17 shows the course of spore production over the sporulation time. Spore formation starts from day three onwards and an almost continuous increase can be witnessed. While no spores can be harvested 2 d after inoculation of the agar plate, at day three $5.9 \pm 1.1 \cdot 10^7$ spores can be harvested upon flooding the agar surface with 25 mL sterile saline solution. A continuous, though not strictly linear increase can be observed with 10.8 ± 1.0, 14.5 ± 0.8, 15.4 ± 2.1, 16.1 ± 0.9, 18.1 ± 1.1 and $22.3 \pm 1.3 \cdot 10^7$ spores/mL from day 4 through day 9, respectively.

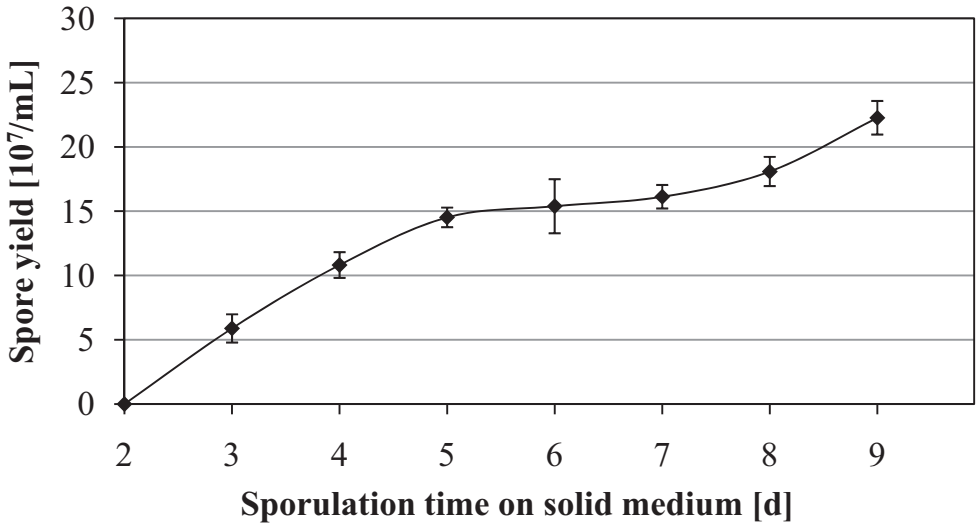

Fig. 4.17. Increase of spore yield with increasing incubation time on 1.6 cm thick MEA plates incubated at 24 °C in the dark. Presented are arithmetic means of 3 biological and 3 technical replicates ± SEM. For day 7 through 9, data base is reduced to 4 and 3 plates, respectively, as some plates could not be harvested due to severe crevices.

It can be speculated that conidiation continues after day 9 and possibly even higher spore yields can be obtained thereafter. However, the substrate significantly dries out during the incubation. Also, addition of large water containers to the incubator did not overcome this problem. As the agar wrinkles, shrinks and forms crevices when it dries, harvesting is strongly hindered after longer incubation and yet at day 9 spore harvest was impaired. It is hence recommended to incubate agar plates only for 8 d and further analyses within this study will based on an 8 day incubation period on solid medium.

4.3.2 Spore aggregation depending on sporulation duration

It was assessed whether the sporulation time, i.e. the time the culture is incubated at 24 °C in the dark on solid MEA medium has not only an effect on the amount of produced spores but also on the aggregation behavior of those spores. **Figure 4.18** shows that the fraction of spores present as single spores as well as those that are found in groups of 2, 3, 4, 5 or more is relatively constant throughout the incubation time during which the spores are produced. Two exception, however, can be identified: After 9 d of incubation the number of single spores decreases to 62 % and more conidia are found in aggregates of two or three, 19.4 and 8 %, respectively, while all other variations remain within the standard error. This indicates that conidia that have been left on the conidiation medium longer have an increased tendency to aggregate.

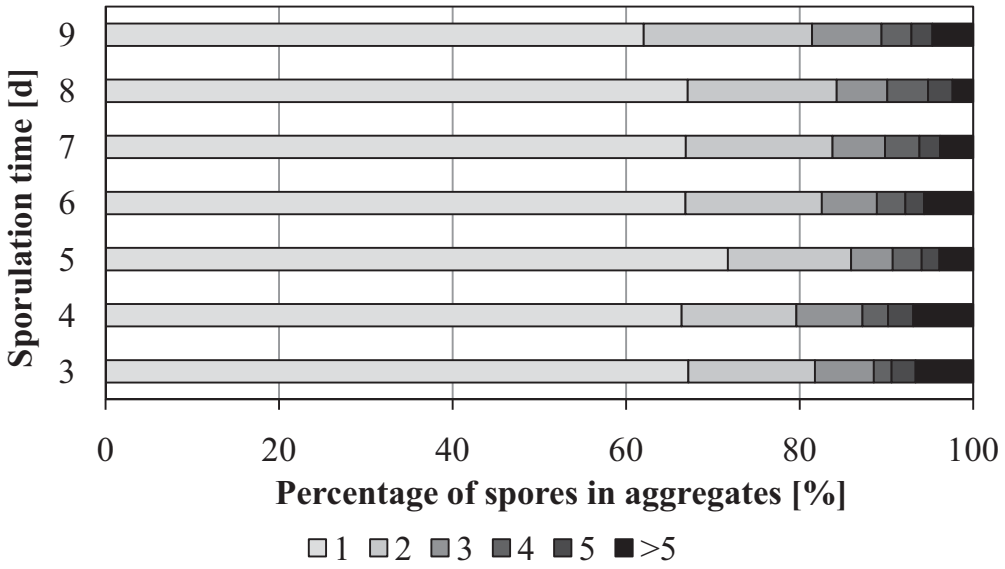

Fig. 4.18. Aggregation behavior of spores harvested from malt extract agar after varying incubation times at 24 °C in the dark. Shown are the fractions of conidia found as single spores, aggregates of two, three, four, five and more. Results represent arithmetic means from 3 biological and 3 technical replicates. Variation after 5 d storage is statistically significant ($p < 0.05$).

The second exception is even more striking. It can be seen that after 5 d of incubation, a slightly but significant increase of single spores can be witnessed which is not detectable after a sporulation time of 4 or 6 d. While the fraction of single spores varies between 66.7 ± 0.4 % for an incubation duration of 3, 4, 6, 7 and 8 d, it is 71.7 % for spores harvested after 5 d. Statistical variation can be excluded because results are pooled from 3 biological and 3 technical replicates and no outliers were found in the underlying statistical population with WALSH's outlier test. Further, the t-test yields a p-value of 0.02 and hence renders results significant. Finally, a repetition under slightly changed conditions (Petri dishes instead of flasks) still confirmed the finding. It has therefore to be concluded that the aggregation behavior of spores changes during the course of conidiation. It can, however, not be determined at this point whether the behavior of all spores present on the substrate at that time changes, whether that of a certain sub-population changes or whether those conidia that are generated precisely on day 5 differs from the conidia generated before and after the event. The fact which makes it even more remarkable is that the decreased aggregation tendency vanishes after day 5 and even more as the phenomenon was not seen to this extend and significance on other media though a tendency was still visible (data not shown).

4.3.3 Spore visible longwave fluorescence depending on sporulation time

Figure 4.19 shows the effect of the sporulation time on the specific visible longwave autofluorescence (SAF) of freshly harvested spores. Analysis was conducted as described in chapter 3.7. It can be seen that the SAF increases significantly over the incubation time. Spores harvested from MEA after 3 d show a specific autofluorescence of 5.8 ± 0.6 μm^{-2}, while those harvested 8 d after inoculating the solid medium are characterized by an almost threefold increased autofluorescence of 16.5 ± 0.5 μm^{-2}. The increase is almost linear with a minor decrease at day 4 with 5.4 ± 0.8 μm^{-2}. The trend also levels off towards day 9, where a decrease can also be witnessed. The analysis of spores generated for more than 9 d was not possible because the agar plates showed severe crevices and harvest of spores was hence not possible as described above.

The shown progression of the SAF supports the previously proposed hypothesis that the detected visible longwave fluorescence is a result of accumulated secondary metabolites, primarily of the porphyrine and the flavin family as well as associated complexes (Dichtel et al., 2004). It had been demonstrated that conidia undergo a ripening process during conidiation in which the cell wall is rearranged and significant

(though not further specified) changes occur regarding the ingredients of the spore (Kawanabe, 1986). It is therefore coherent to expect the amount of secondary metabolites to increase in the conidia which subsequently results in increasing SAF in the visible longwave range. As will be shown in the next subchapter, these findings are in line with conidial viability. The detection of increasing amounts of secondary metabolites in spores is hence a meaningful indicator for the rapid analysis of spore quality. Also, the correlations between SAF and viability will be presented in the following subchapter.

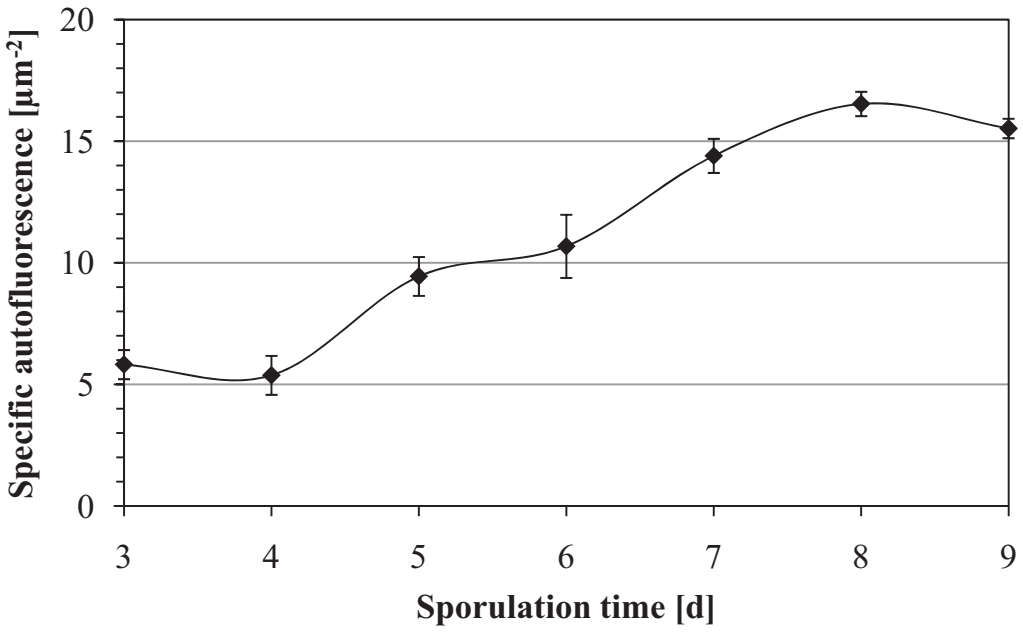

Fig. 4.19. Specific autofluorescence of spores from malt extract agar after varying incubation at 24 °C in the dark. Presented are arithmetic means of 9 biological and 3 technical replicates ± SEM. Excitation at 366 nm, emission detection > 670 nm.

4.3.4 Spore viability depending on sporulation duration

Araujo and Rodrigues (2004) found equivocal results when investigating the effect of sporulation duration on the germination rate of *A. fumigatus*, *A. niger* and *A. flavus*. While the first two strains showed faster germination, i.e. increased viability for younger conidia (5 d incubation) and impaired growth for older conidia (11 d incubation), *A. flavus* was not affected by sporulation duration. Kawanabe (1986), however, reported a more detailed analysis of the correlation of sporulation duration and viability for *N. crassa*. Highest viabilities of approx. 60 % were found for cultures left for 3 to 5 d sporulation. Shorter and longer sporulation generates spores with impaired germination rates. Also, Hall et al. (1994) demonstrated higher viabilities for young conidia of several pest control fungi. Spores harvested after 2 d of sporulation

showed up to 5-fold increased infection rates compared to spores harvested after 7 d. Porcel et al. (2006), in contrast, reported increased activities for older spores of *A. terreus* (though not further specified). As indicated above, sporulation rates vary tremendously between different species. Comparisons have therefore to be conducted most carefully. While a 5 day incubation may be considered too long for one strain, it may represent the time where other species show first conidiation. The findings reported by Kawanabe (1986) are hence the most relevant as they also show too short sporulation times rather than the plain finding of young conidia outperforming older spores.

Figure 4.20 shows the development of the viability of *A. ochraceus* spores over sporulation time on solid MEA substrate and compares it to Kawanabe's findings for *N. crassa*. Most interestingly, both strains exhibit their optimum after 5 d of sporulation. However, they still show very distinct developments. While the viability of *Neurospora* increases continuously from day 2 through day 5 reaching its maximum of 60 % and decreases thereafter, the sporulation behavior of *A. ochraceus* differs significantly. Most remarkable is the sudden though highly reproducible viability increase at day 5 with 64 ± 2 % while viabilities at day 4 and 6 are 40 ± 4 and 46 ± 6 %, respectively. Germination potential thereafter increases again reaching a second maximum at day 8 (59 ± 2 %) and eventually decreasing towards day 9. At this point, the underlying mechanism and regulation for this phenomenon is unclear.

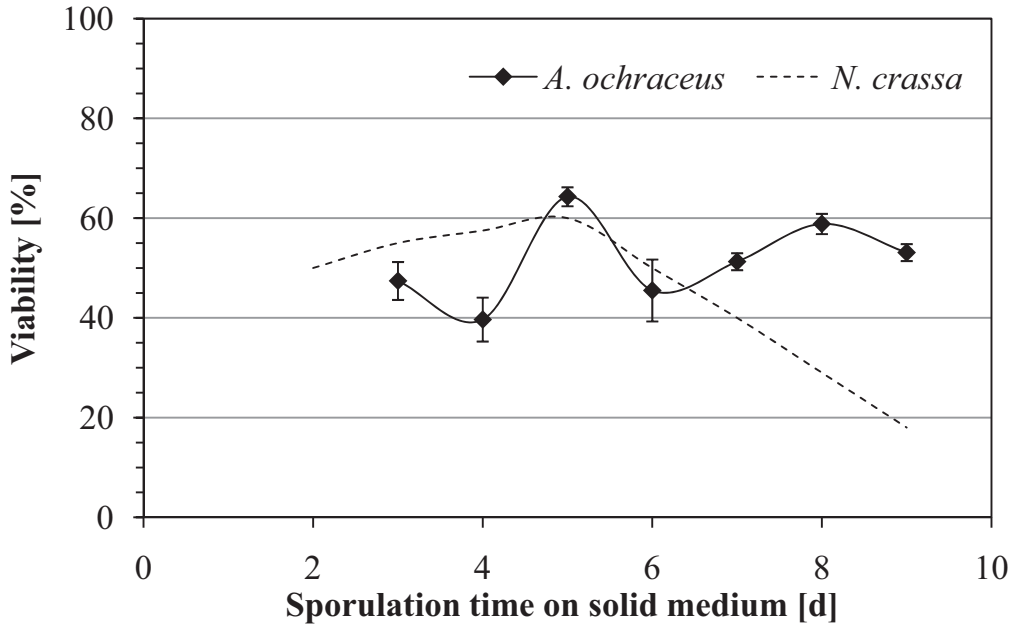

Fig. 4.20. Progression of viability of spores generated on malt extract agar over sporulation time for A. ochraceus *(solid line) and* N. crassa *(dashed line, adapted from Kawanabe, 1986).*

However, this finding is well in line with the out of range behavior found for aggregation (see subchapter 4.3.2). There spores harvested after 5 d of incubation were found to show a decreased aggregation tendency and a subsequent increased fraction of single conidia that was only present after 5 d of incubation. As will be shown later, the effect was inverted after storage and could be eliminated by vigorous washing of spores indicating to be a surface related occurrence. However, this can be excluded for the increased viability after 5 d of sporulation as the effect persisted vigorous washing. I.e., the viability curve appears similar for spores that have been washed prior to the assessment of their viability (CFU). This indicates an interior accumulation of secondary metabolites and/or metabolites that have not yet been identified by means of GC-MS to be responsible for the observed, interesting phenomenon. As sporulation times exceeding 9 d could not be analyzed due to the drying of the agar plates, a long-term trend cannot be determined at this point. Also, comparisons to previously published reports are difficult as their findings are equivocal. However, it became obvious that the effect of sporulation duration on viability is highly specific to the strain under investigation.

Figure 4.21 shows the correlation of viability and visible longwave autofluorescence of spores freshly harvested from malt extract agar. The relationship is noteworthy as both graphs are parallel, except that the specific autofluorescence does not follow the sharp decrease of the viability from day 5 to day 6. Instead it hardly changes during this interval and subsequently from day 6 onwards continues to follow the viability at an ‘elevated level’. This indicates, as suggested previously, that the SAF is a measure for accumulated secondary metabolites within the spore. The viability, however, can be expected to be a function of intrinsic metabolite reservoirs and several additional effects. While one of those effects, for example the rearrangement of spore wall properties (in line with the altered aggregation behavior at the same time), may have caused the decrease of viability, the specific autofluorescence is not affected by this sway. The viability hence collapses briefly while the specific autofluorescence continues unaffected. This indicates that for the holistic characterization of a spore population not only absolute measures are relevant but also developments of the culture over time. Also, more than one indicator is necessary to analyze the properties of a spore population. While, in the stated example, the mere analysis of viability would have neglected the unaltered metabolite reservoir while exclusive application of fluorescence analysis would have ignored the drastic loss of viability.

In conclusion, it can be stated that the sporulation duration significantly affects the viability of the generated spores. Further, a correlation of viability and conidial specific autofluorescence in the visible longwave range could be determined. However, assessment of SAF alone is not sufficient to explain the observed changes.

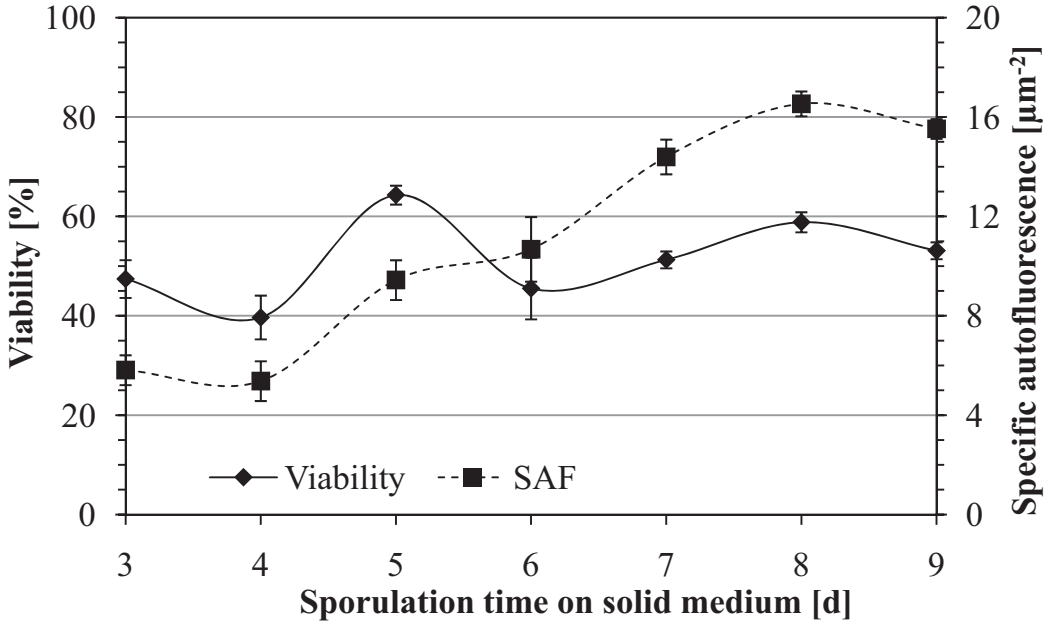

Fig. 4.21. Correlation of spore viability and specific autofluorescence at $\lambda > 670$ nm over sporulation time. Incubation at 24 °C in the dark on malt extract agar.

4.4 Effect of storage on the constitution of conidia

Reports about the effect of spore storage have been, again, equivocal. While some find conidia to be unaltered after storage (Beyer et al., 2004), others witnessed a decrease in thermo tolerance (Ying and Feng, 2006) and again others found increasing germination rates (Porcel et al., 2006). As before, this can most likely be attributed to different strains and even more to different investigated aspects. While the viability may be unaffected, the infectious efficacy, a consequence of particular surface proteins, can be altered.

No effect, however, was clearly witnessed for the repeated subculturing of *A. ochraceus* for up to 40 passages (Vezina et al., 1963). Therefore, cryostocks were plated and brought to sporulation on precultures whose harvest was successively cultured and subject to further analyses. By this any bias of possibly introduced spore alteration through prolonged storage at -80 °C was eliminated and the effect of spore storage was limited to the controlled storage under investigation.

4.4.1 Spore aggregation after storage

The aggregation behavior of spores changes significantly when they are stored. This is not surprising as the formation of aggregates is mediated by the properties of the cell wall which is the most susceptible to extrinsic sways. Release of melanin, degradation of cell wall proteins or rearrangement of the glucan structure may be provoked during the storage, possibly affecting the aggregation of the conidia. Also, as described before (see chapter 1.5) and as will be explained later (see subchapter 4.4.2), spores are metabolically active during storage in suspension at 4 °C. As an active metabolism almost immediately requires an exchange of substrates between the cells and their surrounding, the spore wall has to be dynamic rather than a solid, static and inert structure. This in turn proposes that aggregation behavior is not just a function of unchangeable physical properties but a result of active cell wall alterations. Therefore, the aggregation was analyzed as a function of storage duration with all other parameters kept constant. Next, it was analyzed as a function of covaried sporulation time and storage duration and finally with covaried sporulation medium.

Changes in conidial aggregation during storage

Fontaine et al. (2010) provided evidence that aggregation of conidia is mediated through glucans in the intermediate wall of fungal spores. It was also recently shown that the negatively charged melanin present in the conidial wall is responsible for aggregation during the first hour of submerged cultivation (Eisenman et al., 2007, Priegnitz, personal communication). It had also been proven before that hydrophobins cause conidial aggregation and initiate the formation of pellets in aqueous environments (Dynesen and Nielsen, 2003). Hence, three factors of the cell wall have been shown to be relevant for aggregation. As shown in previous chapters, the constitution of the conidial wall is altered during storage. It may hence be expected that the storage of spores in suspension also affects the aggregation behavior.

Figure 4.22 shows how the aggregation behavior continuously changes over the course of three weeks during which spores were stored suspended in saline solution at 20 °C. Germination was prevented by the absence of nutrients and in random examinations no germ tubes were visible. It can be seen in the plot how the portion of single spores decreases constantly from 67.1 % single spores in suspension immediately after harvesting the conidia to 49.3 % after 21 d of storage. In parallel, the abundance of aggregates increases. There is, however, no trend detectable towards the formation of a particular class of aggregates. Only the presence of 15 % of the conidia in aggregates larger than 5 after 21 d of storage is statistically significant.

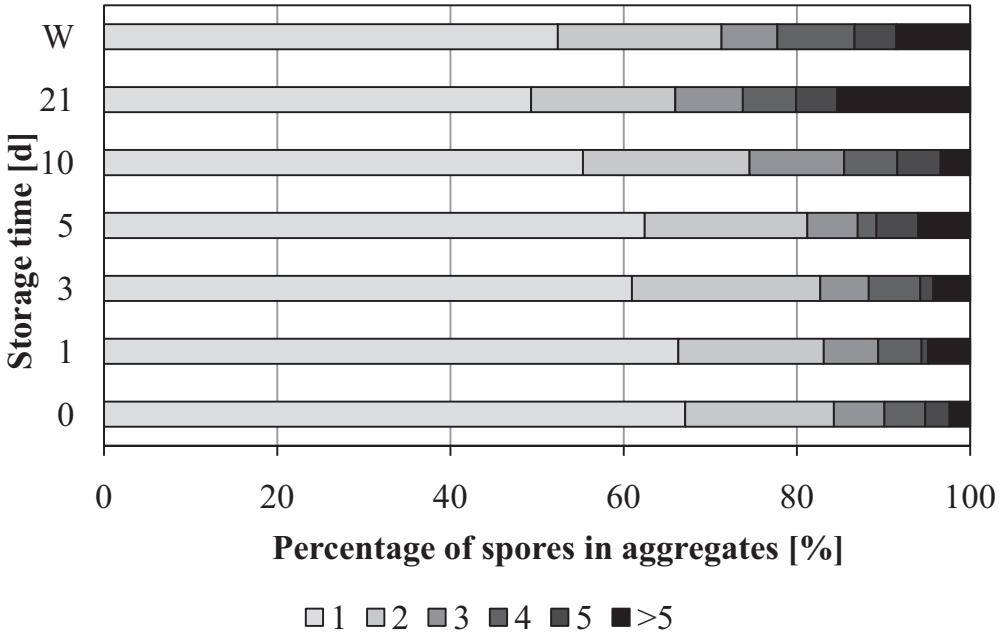

Fig. 4.22. Aggregation behavior of spores harvested from solid media after incubation at 24 °C in the dark and subsequent storage in saline suspension at 20 °C. 'W' represents freshly harvested spores, vigorously washed. Shown are the fractions of conidia found as single spores, aggregates of two, three, four, five and more. Results represent arithmetic means from 3 biological and 3 technical replicates.

Assuming a linear correlation during the investigated period, the daily loss of single spores is 0.84 percentage points. Even better correlation can be achieved with polynomial fitting, which is also more likely to represent natural behavior as otherwise all spores would have to be aggregated after three months which is unlikely. Polynomial fitting hence explains the behavior as shown below:

$$\text{Percent single spores} = 67.05 - 1.409 \cdot d + 0.0268 \cdot d^2 \qquad (4.2)$$

where d is the storage time in days.

It was further tested if the effect is triggered by the release of cell wall material such as melanin and hydrophobins as suggested previously. Therefore, spores were washed 5 times with cold saline solution. Before analysis, they were left to settle 30 min to allow 'reaggregation' as vortexing during washing per se broke most aggregates. The result is also depicted in figure 4.22 (indicated with 'W') and it can be seen that storage can be resembled by washing the spores even in absence of detergents.

It can hence be concluded that the loss of conidial wall material mediates aggregation of spores in aqueous solution. However, whether this is primarily a result of the reduced repulsion of spores covered with negatively charged melanin, as suggested by Priegnitz, or primarily the consequence of exposed glucans, as proposed by Fontaine et

al. (2010), cannot be concluded at this point. It is likely, however, that it is a combination of both while the effect of hydrophobins, as described by Dynesen et al (2003), seems to play only a minor role.

Changes in conidial aggregation during storage with covaried sporulation time

The effect of varying storage duration was also analyzed with covaried sporulation time. Here, the interesting finding reported in chapter 4.3.2 was affirmed, however, in an unexpected manner: **Figure 4.23** depicts the fraction of single spores over the storage duration (0 to 21 d) for conidia harvested 3, 5 or 7 d after inoculation shown in grey, black and striped, respectively. While the portion of single spores is significantly higher in populations harvested after 5 d that were not stored, it dramatically decreases for all tested storage durations. As can be seen, yet after storage of 1 d, the fraction of single spores from cultures that were incubated for 5 d drops from 71.7 to 53.2 %. During the following storage period, aggregation increases further until after 21 d the percentage of single spores has fallen to 41.1 %.

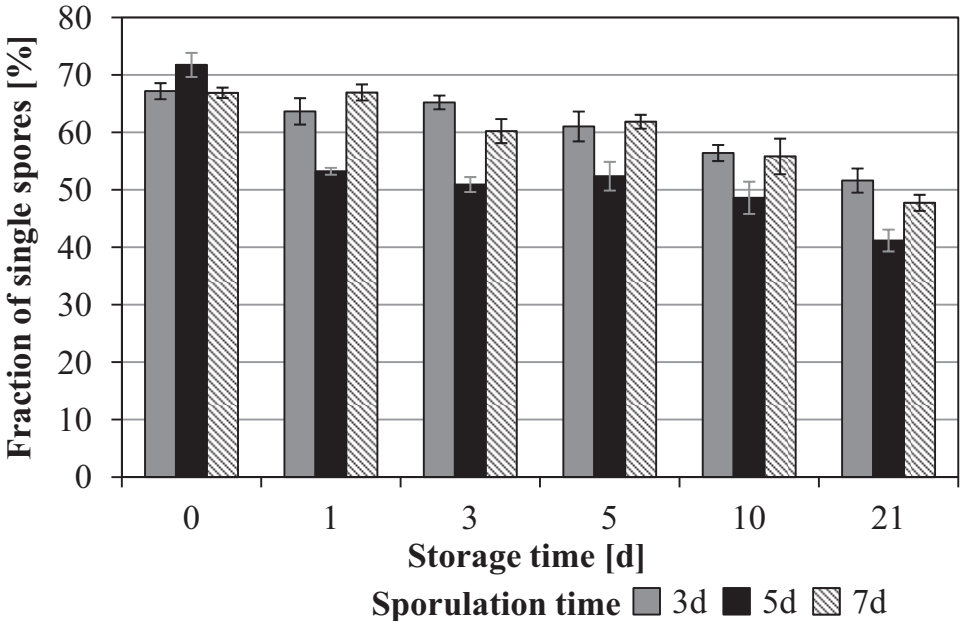

Fig. 4.23. Aggregation behavior of spores harvested from solid media after incubation at 24 °C in the dark for 3 d (grey), 5 d (black) or 7 d (striped) and subsequent storage in saline suspension at 20 °C for 0 to 21 d. Shown are the fractions of conidia found as single spores, aggregates of two, three, four, five and more. Results represent arithmetic means from 3 biological and 3 technical replicates.

The above suggested polynomial fit of equation 4.2 describes the data for the populations harvested at day 3 and 7 with a correlation index of above 90 %. The conidial population from day 5, however, cannot adequately be described with the linear or the polynomial fit. Also, removal of the first data point still does not allow correlation indices above 70 %.

For the explanation of this remarkable population, the hypothesis is proposed that spores which have germinated for 5 d are coated with an aggregation impairing substance. This putative substance is highly efficient in maintaining single spores and it replaces melanin (or other putative 'standard' aggregation inhibitors) to a certain extent. However, it is released readily during storage. Again, the effect of washing was assessed and resembled the findings explained above. It seems therefore likely that the population from day 5 loosely carries an additional substance that prevents aggregation rather than the explanation that those conidia lack a substance which is later restored through metabolic activities of the spores themselves during the first day of storage.

Changes in conidial aggregation during storage with covaried sporulation medium

Further, it was analyzed whether conidia that have been generated on different conidiation substrates are differently affected by storage. Therefore, spores from MEA, OBA and WBA were stored at 4 °C for 7 d and the aggregation behavior was determined before and after storage. The results are compared in **Figure 4.24**. It can be seen that spores which were initially generated on MEA show the largest change of their aggregation behavior after storage. Here, the fraction of single spores decreases from 67.1 to 42.1 %. Also, the percentage of spores that can be found in pairs of 2 decreases slightly from 17.1 to 15.0 %. Particularly, aggregates with four and those larger than 5 spores increase significantly from 4.7 to 11.5 and from 2.4 to 21.4 %, respectively. The change which OBA spores undergo is similar but not as drastic. Single spores decrease from 60.9 to 57.4 and couples of spores decrease from 18.4 to 14.6 %, respectively. Larger aggregates with 3, 4, 5 or more spores increase by approx. 2 percentage points each. This, however, is not the case for WBA spores. Here the fraction of single spores increases from 60.1 to 65.2 % during the storage period. Spores in pairs of 2 decrease from 23.9 to 18.0 %. Only aggregates with 4 spores also show an increase from 3.1 to 7.7 %.

The aggregation behavior of spores from MEA and OBA can hence be summarized in the way that during cooled storage in suspension the fractions of single spores and those in pairs of two decrease while larger aggregates become more common. Overall, the tendency to form aggregates increases. WBA spores, on the other hand, show a contrary behavior. Their tendency to form aggregates slightly decreases and hence the fraction of single spores increases. It has therefore to be expected that the composition of the conidial wall with respect to the aggregation determining factors melanin, glucan and hydrophobin differs between different spore populations. As some compounds are more stable and possibly show stronger resistance against washout

than others, a differing shift can be observed between spore populations. For MEA and OBA, it can be expected that washout of melanin and/or hydrophobins during storage fosters aggregation through changed surface charge and exposure of glucans as suggested by Fontaine et al. (2010) and Priegnitz (personal communication). WBA spores, in turn, show stronger pigmentation and can hence be expected to have larger amounts of melanin incorporated into their cell wall which, as described before, impairs aggregation. It is also plausible that an additional compound other than melanin, glucan and hydrophobins, e.g. a putative 'aggregation-protein', is present on or in the wall of spores from WBA which promotes aggregation. This protein also underlies extrinsic sways and is degraded or washed out during storage. While in spores from MEA and OBA the washout of melanin may prevail and therefore determine the increased aggregation behavior, the washout of melanin may be overcompensated by the degradation and/or loss of this putative 'aggregation-protein' in spores from WBA. This, even though speculative, is in line with results presented in chapter 3.2.2 where three (though faint) high molecular weight proteins were detected in the wall of fresh spores from WBA that were neither found in spores from MEA nor in stored spores from WBA.

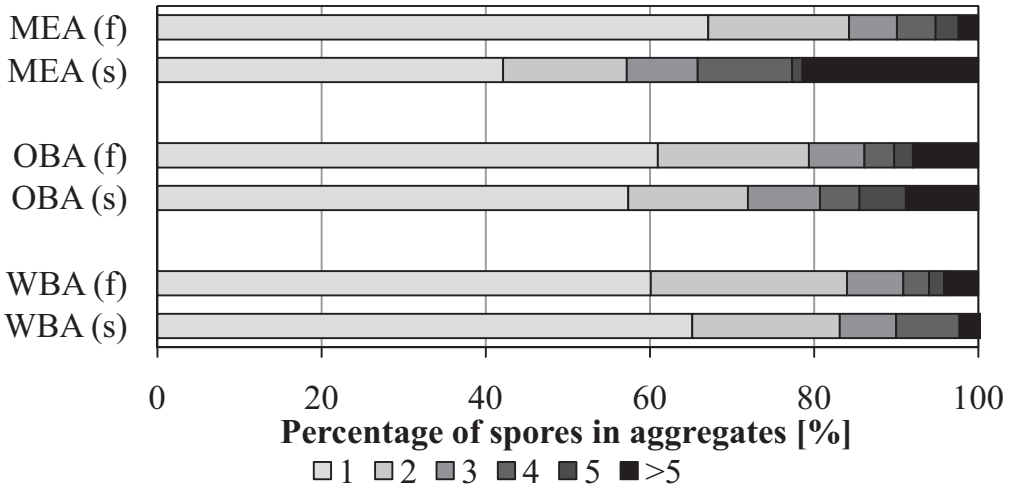

Fig. 4.24. Aggregation behavior of spores from malt extract agar (MEA), oat bran agar (OBA) and wheat bran agar (WBA) freshly harvested (f) compared to aggregation after subsequent storage in saline suspension at 4 °C for 7 d (s). Shown are the fractions of conidia found as single spores, aggregates of two, three, four, five and more. Results represent arithmetic means from 3 biological and 3 technical replicates.

It is therefore suggested here that the aggregation behavior of fungal conidia is not only determined by the ratio and exposure of melanin, hydrophobins and glucans as described previously but a fourth parameter may be involved. This putative aggregation protein may be located on the outer wall, may promote aggregation and its expression is dependent on particular growth conditions during conidiation.

From an ecological and evolutionary perspective, it is of greatest importance for an organism to be able to respond to changing environmental conditions in a multitude of patterns. As spores, among others, serve the survival of adverse conditions and the dispersal to more favorable habitats, it appears sensible that differing growth conditions cause different molecular responses and hence generate variations of the fungal phenotype. This increases the possibility to successfully escape poor growth environments and colonize new haunts.

4.4.2 Spore metabolite profile after storage

Spores generated on MEA before and after storage

When comparing the metabolite profile of spores freshly harvested from MEA to those that have been stored for 7 d at 4 °C, drastic changes become visible. The targeted approach described in chapter 3.4 allows the comparison of 41 metabolites between fresh and stored spores. Out of those, 20 appear after storage that have not been detectable before. In contrast, only 5 metabolites decrease during storage and another 4 disappear entirely being no longer detectable. 12 metabolites remain relatively unchanged during storage. Of the 20 emerging metabolites, 14 are TCA cycle intermediates, amino acids or closely related molecules. This vividly illustrates that spores are much more than a dormant, negligible state. It proves on a metabolic level that ungerminated spores show a distinct metabolism and catabolize intrinsic reservoirs. **Figure 4.25** shows the changes for 10 selected metabolites.

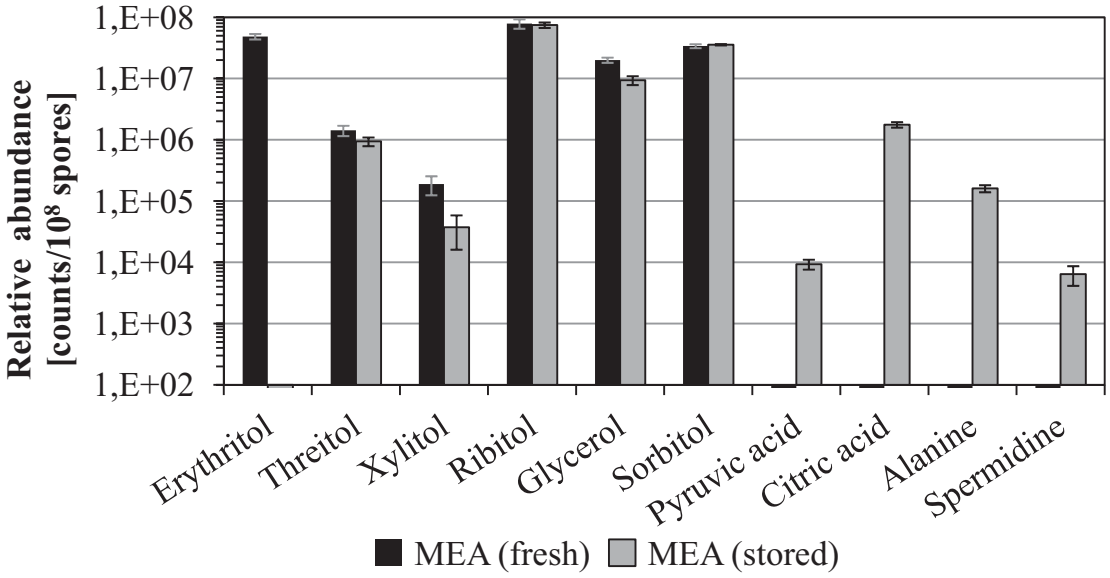

Fig. 4.25. Abundance of dominant metabolites in freshly harvested spores (black) and spores that have been stored for 7 d at 4 °C (grey) from malt extract agar (MEA). Presented are arithmetic means of 3 biological and 3 technical replicates ± SEM. Note the logarithmic scale and the base point of 100 of the ordinate.

One of the most striking observations is the fact that erythritol (along with three others, see appendix) reproducibly disappears from spores over the course of one week at 4 °C. Before storage, it was found in concentrations of up to 20 ng/10^5 spores though differing significantly between the different populations generated on MEA, OBA and WBA substrate (see subchapter 4.1.3). As there was no erythritol found in the storage suspension, leakage of the spores can be excluded. The loss of this 4-carbon polyol can therefore only be explained by its metabolic usage. This is indicative for its role as a carbon and energy reservoir rather than primarily functioning as a compatible solute. However, it is unclear at this point whether it was metabolized completely for the supply of energy, whether it was converted into one or several other polyols or whether it was converted to building blocks of the cellular metabolism. Still, as none of the detected polyols showed an increase after storage, it is most likely that erythritol serves as a reservoir of carbon and energy for the metabolic activities of spores. This is in line with erythritol's role suggested by Dijkema et al. (1985) in their pioneering work. However, those studies were conducted with fungal mycelium grown in submerged cultivation rather than spores. Further, it is noteworthy that threitol, a diastereomer of erythritol, remains virtually unchanged during storage. This indicates that the cataplerosis of erythritol is conducted by an enzyme specifically responsible for the metabolization of erythritol.

It was further witnessed that xylitol, a 5-carbon polyol, decreases by factor 5 while its isomer ribitol remains unaltered during storage. Like with freshly harvested spores, mannitol was still not detected though its isomer sorbitol remains unchanged at high levels. This again is interesting as sorbitol, a 6-carbon polyol, is the least soluble in this homologous series and is therefore expected to serve primarily as a carbon store where the smaller representatives like erythritol act as compatible solutes. The here presented findings suggest that the opposite is true for spores of *A. ochraceus*. Glycerol, the smallest member of the group, however, is highly abundant in fresh and stored spores and only shows a minor decrease throughout keeping of spores suspended in saline solution for 7 d.

Pyruvic acid, lactic acid, succinic acid and citric acid all arise after storage. Also, alanine, valine, serine, glycine, aspartic acid and phenylalanine were below detection limits in freshly harvested spores but emerged after storage, all emphasizing the onset of cellular metabolism. Further, urea, a byproduct of amino acid degradation, is also only present after storage. This may be indicative for protein breakdown as it had been suggested previously that under certain conditions, proteins may serve as the main energy reservoir in spores (Cliquet and Jackson, 2005).

The appearance of spermidine in spores stored at 4 °C for 7 d is also of interest. It has been shown for *A. nidulans* that the germination rate of strains incapable of synthesizing this relatively large polyamine is dramatically decreased but can be restored by the addition of spermidine to the medium (Jin et al., 2002). Besides its known role for DNA stabilization (Nsoukpoe-Kossi et al., 2008), it has been proposed that spermidine is involved in the complex signal transduction pathways regulating sporulation and germination in dependence of available nutrients, light and other parameters (Guzmán-de-Peña et al., 1998; Leroy et al., 1997). Variations in its concentration within the spore may therefore be important indicators for germination and further development of the particular spore population.

Combining the semi-quantitative results in a very preliminary manner, it can be stated that the total emergence of amino acids, TCA cycle intermediates and related metabolites accounts for 47 % of the total loss of storage compounds, such as erythritol. These findings which have to be verified by truly quantitative measures suggest that 53 % of the storage reservoirs are converted to energy, carbon dioxide and water while 47 % can be found in converted forms within the cellular metabolism. Further, it has to be stated that the applied separation and detection methodology of GC-TOF-MS is most suitable for the detection of substrates from the primary metabolism. Complex molecules from secondary metabolism which are better monitored by means of LC-TOF-MS may be lost in this analysis and account for a portion of the difference between storage reservoir's decrease and the appearance of primary metabolites.

Comparison of stored spores from MEA, OBA and WBA

The abundance of citric and pyruvic acid is similar for stored spores from OBA, WBA and MEA irrespective of the conidiation substrate. For the latter, the concentration could be determined to approx. 0.1 ng/10^5 spores. Amongst the metabolites appearing during spore storage, 4-aminobutyric acid (also known as gamma-aminobutyric acid, GABA) plays an outstanding role. It shows a factor five lower concentration in stored spores from WBA compared to analogues from OBA. Even though this non-proteinogenic amino acid is mostly characterized as an inhibitory neurotransmitter in mammals, a few reports elucidate its role in fungi. Its concentration was for example found to increase during acidogenesis in parallel with citric acid formation in manganese deficient cultures of *A. niger* (Kubicek et al., 1979). It has also been shown that glutamate decarboxylase (GAD, generating GABA from glutamate) is significantly upregulated during germination of *Bacillus* spores, replenishing succinate

and hence accelerating the TCA cycle (Foerster and Foerster, 1973). It is hence not surprising that in stored spores from WBA the concentration of succinate (in this catabolytic pathway downstream of GABA) is also significantly lower compared to the succinate concentration in spores from OBA though the decrease is only factor three (and no longer five). This confirms the connection between GABA and succinate for *A. ochraceus* affirming its role in driving the TCA cycle. Principally, the direct introduction of desaminated glutamate into the TCA cycle at alpha-ketoglutarate would also be possible. However, the link to glutamate (upstream of GABA) which at least in *N. crassa* spores had been shown to be the most important nitrogen store (Kumar and Punekar, 1997) cannot be drawn as virtually no glutamate was detected in fresh or stored spores. It has therefore to be speculated that GABA in *A. ochraceus* is either fueled from a different (unknown) source or that glutamate is stored for example as a polymer. This is likely as numerous microorganisms have been proven capable of producing polyglutamic acid and it has been found particularly in the spores of *Bacillus* spp. (Shih and Van, 2001). The fact that stored WBA spores show the highest concentrations of urea, a byproduct of protein degradation, also argues in favor for this speculation. Finally, the addition of glutamic acid to the sporulation medium has been shown to significantly increase spore yield and quality, again supporting this speculation (Sommer, personal communication).

For *N. crassa*, it had been shown that GAD is one of the key enzymes allowing fungi to catabolize amino acid reservoirs and hence provide energy, conveniently sized carbon skeletons as well as nitrogen, but does not decarboxylate glutamate despite simultaneous presence until the onset of germination. Even more remarkable is the finding that its activity constantly declines during germination and does not reappear until the asexual life cycle has completed entirely (Christensen and Schmit, 1980). This, once more, supports the proposal that differences introduced during conidiation affect the entire ‘future’ of a spore and the mycelium developing out of it as it was also observed in this study.

As illustrated in **figure 4.26**, succinic acid and malic acid show significant changes between the differentially generated spore populations. WBA spores contain the lowest and OBA spores the largest reservoir of those TCA cycle intermediates. However, the relatively similar concentration of pyruvic and citric acid, also key intermediates in the TCA cycle, suggests that the anaplerotic and/or cataplerotic pathways may be regulated differentially between the spore populations. Citric acid exits the TCA cycle as a precursor for fatty acid synthesis while malic acid can be replenished from amino acid breakdown via fumaric acid or serve as a starting point

for gluconeogenesis itself. The parallel response of malic and succinic acid with an overall higher concentration of malic acid has also been reported for mycelial growth of *A. niger* in submerged cultivation (Scherling and Driouch, personal communication). Also, threitol which in MEA spores remains unchanged during storage shows dramatically decreased concentrations in WBA spores.

The arousal of shikimic acid in stored spores compared to fresh spores not containing shikimic acid is also noteworthy as it is not only the precursor for aromatic amino acids but also a building block for ochratoxin A (O'Callaghan et al., 2003). The concentration differs by a factor of 25 between the populations of stored spores from different substrates. The exact pathway of ochratoxin formation from shikimic acid, however, is unclear and therefore no further conclusions can be drawn at this point.

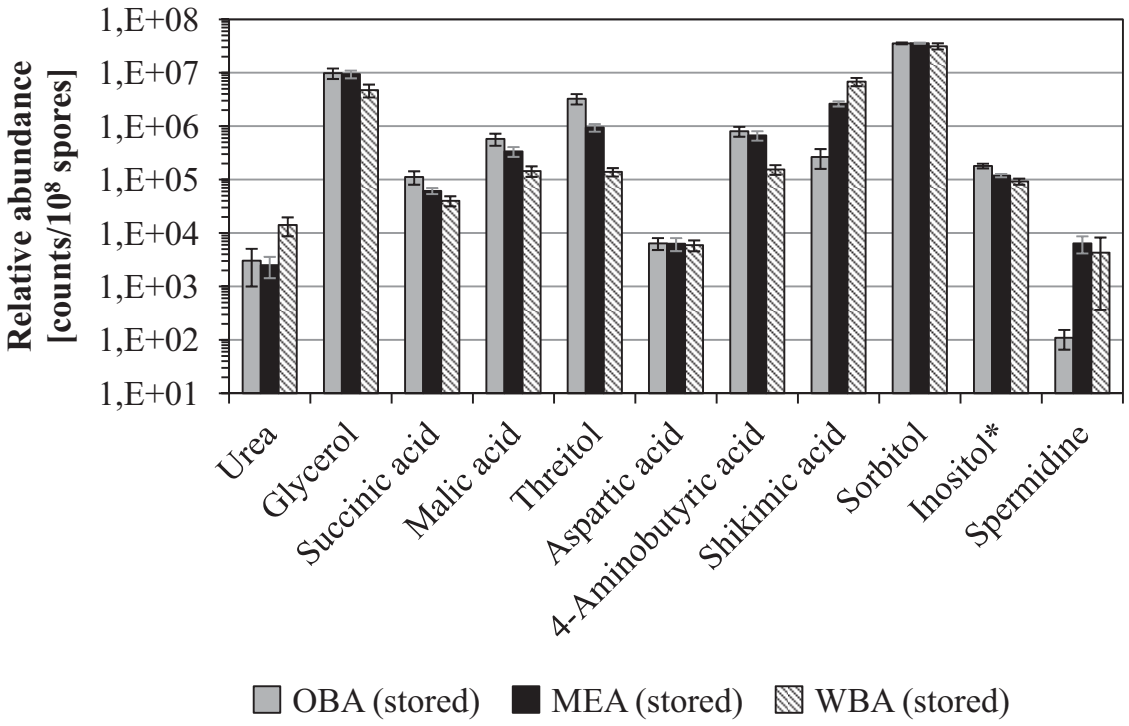

*Fig. 4.26. Abundance of the most relevant metabolites in spores from oat bran agar (OBA, grey), malt extract agar (MEA, black) and wheat bran agar (WBA, striped) that have been stored at 4 °C for 7 d. Presented are arithmetic means of 3 biological and 3 technical replicates ± SEM. Note the logarithmic scale and the base point of 10 of the ordinate. *Sum of the isomers inositol and myo-inositol.*

Despite the described significant differences between stored spores from WBA, OBA and MEA, some metabolites are similar irrespective of the conidiation substrate. Aspartic acid, as one of the detected amino acid, and ribitol, a 5-carbon polyol, were for example found at comparable concentrations over all populations of stored spores.

Overall, it can be concluded that spores show tremendously increased metabolic activity after storage at 4 °C for 7 d in saline solution. With almost the entire set of TCA cycle intermediates and amino acids detectable, it is no longer justifiable to call spores 'dormant'. It has rather to be recognized that conidia of *A. ochraceous* are highly active and that their components see significant changes during this time. It has previously been shown that spores are capable of catalyzing complex reactions (Wolken et al., 2003), now metabolic evidence from within the spores is provided. In fact, storage may be looked at from a totally different perspective, like Dillon and Charnley (1990) suggested: They found tremendously increased germination rates with increasing duration of 'soaking' rather than storage. It is further most interesting that vast differences between the metabolite profile of stored spores from different conidiation substrates were detected.

4.4.3 Spore ATP content after storage

Figure 4.27 shows the decline of intra-conidial ATP reservoirs during storage in suspension at 4 °C after 7 d. It can clearly be seen that the ATP concentration is significantly reduced in all samples.

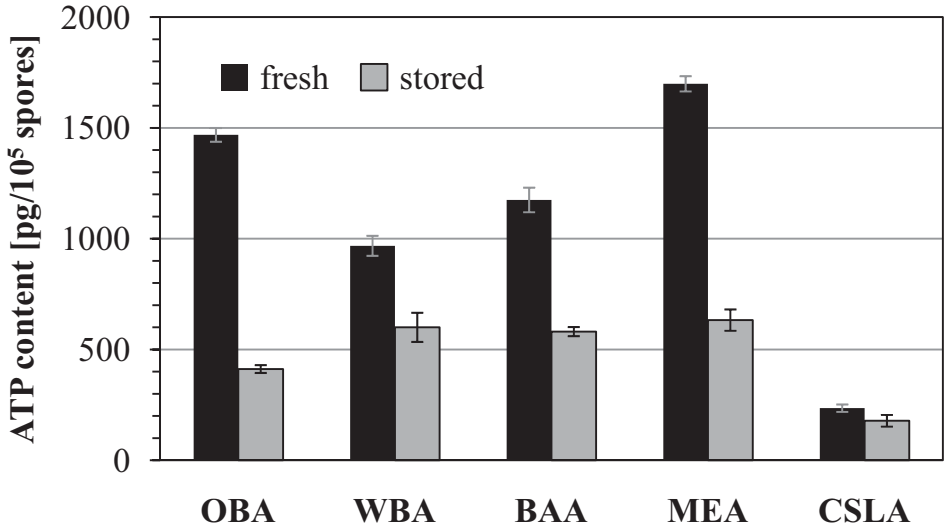

Fig. 4.27. ATP concentration in spores from different conidiation substrates. Oat bran agar (OBA), wheat bran agar (WBA), banana agar (BAA), malt extract agar (MEA), corn steep liquor agar (CSLA) after harvesting (black columns) and after subsequent storage in saline solution (7 d, 4 °C, grey columns).

Spores generated on OBA exhibit the largest decrease. The initial concentration of 1 469 ± 31 pg ATP/10^5 spores drops by 72 % to 412 ± 18 pg ATP/10^5 spores. The smallest decrease is witnessed for spores from CSLA where loss is only 24 % to 178 ± 26 pg ATP/10^5 spores compared to 235 ± 17 before storage. ATP content decreases significantly irrespective of the initial sporulation substrate. It is noticeable

that, except for spores from CSLA, the ATP concentration differences between the conidia are leveled off during storage. The range between the highest and the lowest ATP concentration (except for CSLA) before storage is 968 to 1 699 pg/10^5 spores, hence a variance of 55 % around the mean. After storage, variance is only 40 % around the mean of the 4 presented populations (except CSLA). This may be caused through differences in the conidial activity: Assuming biological ATP degradation during storage to be a first order reaction dependent on the concentration of ATP, the observed behavior can readily be explained. The reaction rate would be higher in spores with high ATP concentrations resulting in faster breakdown of the reservoir. Conidia with low initial ATP concentrations in contrast show low conversion rates right from the start. This also explains the minimal decrease of the ATP reservoir in spores from CSLA. The observable result is an alignment of the ATP pools of spores from different conidiation substrates. At the same time, this hypothesis suggests that no further regulatory mechanism is active in the spore. As explained above, spores stored in suspension show tremendous metabolic activity (Wolken et al., 2003). At the same time, respiration is limited to a minimum through the crystalline conidial wall and pseudo-anaerobic storage conditions. Regeneration of metabolized ATP through the respiratory chain cascade is hence not possible and a constant depletion of the ATP pool is subsequently witnessed, in line with prediction previously published (Giulivi et al., 2006). However, to this point, no correlation to findings regarding the metabolome could be drawn.

It has also previously been reported that the ATP content in spores decreases as conidia are stored over several months. The breakdown was reduced through storage at very low temperatures. The authors attribute this finding to the fact that the metabolism is no longer active below 0 °C and only physico-chemical degradation occurs (Gindro and Pezet, 2001). These findings are in line with the results presented in this work. Furthermore, several authors find positive correlations between the ATP concentration and the viability of cells in general and spores in particular (Gindro and Pezet, 2001; Lane et al., 1988; Przybylski and Bullerman, 1980). Based on the findings of Lai et al. (2011) who demonstrated ATP's relevance under conditions of external stresses, it has to be expected though that spores with yet initially low ATP concentrations are less capable to withstand stress.

Even though colder storage at e.g. -20 °C may decelerate ATP breakdown, this freeze-thawing would represent an additional external stress per se (Beyer et al., 2004) and hence introduce further damage. Therefore, the common short term storage of conidia at 4 °C between harvest and inoculation has to be regarded most suitable.

4.4.4 Spore NAD(P)H composition after storage

The effect of storage on the ratio of free and protein bound NAD(P)H in conidia of *A. ochraceus* was analyzed by means of two-photon fluorescence microscopy. **Table 4.5** shows the relevant results for stored spores and compares them to freshly harvested spores from MEA, OBA and WBA.

Tab. 4.5. Fluorescence lifetimes of free and protein bound NAD(P)H in freshly harvested spores from malt extract agar (MEA), oat bran agar (OBA) and wheat bran agar (WBA) compared to stored spores originating from the same conidiation substrate (storage: 7 d, 4 °C in suspension). Presented are arithmetic means from 2 biological and 3 technical replicates ± SEM.

	Lifetime [ps]		Fraction of protein bound NAD(P)H [%]
	NAD(P)H free	NAD(P)H bound	
MEA fresh	814 ± 55	3 226 ± 233	10 ± 2
MEA stored	796 ± 8	3 823 ± 62	23 ± 1
OBA fresh	719 ± 31	2 893 ± 158	11 ± 1
OBA stored	617 ± 46	2 855 ± 201	20 ± 1
WBA fresh	560 ± 24	2 351 ± 100	22 ± 1
WBA stored	158 ± 26	1 436 ± 61	13 ± 1

It becomes clearly visible that stored MEA spores have an activated metabolism compared to freshly harvested, unstored MEA spores. With 23 % of the conidial NAD(P)H bound to proteins after storing the spores for 7 d in suspension at 4 °C, the ratio of bound NAD(P)H has increased significantly from its initial value at 10 %. This can be the result of two processes. Either, more NAD(P)H of an unchanged total pool is bound altering the numerator of the ratio. Or the concentration of unbound coenzyme has decreased, for example through breakdown or leakage. Yet Vezina et al. (1963), however, demonstrated the ability of ungerminated *A. ochraceus* spores to catalyze the hydroxylation of steroids. Even though, the actual metabolism of spores was not investigated, numerous further activities of ungerminated spores have been reported since then (Wolken et al., 2003). It is therefore profound to speculate that the increased ratio of bound NAD(P)H in conidia which have been stored in suspension for 7 d at 4 °C is a result of increasing metabolic activity and hence of a shift of the coenzyme towards the bound state through increasing protein interactions. For the determination of absolute concentrations, however, further elaborate investigations are necessary.

It can further be seen that the behavior differs significantly for spores from different conidiation substrates. In spores from OBA, the portion of bound NAD(P)H increases similar to the effect described above for MEA spores. The portion of bound cofactor increases from 11 to 20 % while the fluorescence lifetime of free and bound NAD(P)H remains unchanged within the measuring tolerance. The shift of NAD(P)H from the free state towards its protein bound state by almost factor 2 unmistakably indicates increased stabilization and metabolic activity.

WBA spores, however, show the contrary behavior. Here, a drastic decrease of protein bound NAD(P)H from 22 to 13 % can be witnessed accompanied by an also dramatic decrease of the fluorescence lifetimes of free and protein bound NAD(P)H from 560 to 158 and 2 351 to 1 436 ps, respectively. It becomes obvious that the activity of the spores is decreased throughout the storage period of 7 d at 4 °C in suspension. This is again perfectly in line with the findings presented in the previous subchapters, where decreased concentrations for threitol and GABA were reported for WBA spores.

It can be concluded that spores from MEA and OBA show increasing activities during storage in suspension. After 7 d, increased amounts of protein bound NAD(P)H representing high metabolic activity were detected. In contrast, spores generated on WBA show high activity prior to storage and decreased metabolic activity after storage with very low amounts of protein bound NAD(P)H. This is parallel to decreasing amounts of storage substances explained above and can therefore be attributed to an overall depletion of carbon and/or energy reservoirs within spores.

4.4.5 Spore visible longwave fluorescence after storage

Specific autofluorescence of conidia in the visible longwave range as a function of storage was analyzed. As described above, the autofluorescence detected by means of flow cytometry in the wavelength bandwidth > 670 nm can be correlated to the abundance of high molecular secondary metabolites, primarily flavins and porphyrins.

Figure 4.28 illustrates how the spores' SAF increases during the first 3 d of storage in suspension from 16.5 μm^{-2} to 18.6 μm^{-2} and 18.5 μm^{-2} for the population kept at 4 °C and the one kept at 30 °C, respectively. Interestingly, this trend is independent of the storage temperature but the increase is slightly faster for the population kept at 30 °C (higher SAF after 1 d storage). After day 3, conidial SAF decreases for both storage temperatures. Autofluorescence of the cooled spores returns to its initial value after 10 d and hardly changes during prolonged storage for 21 d. The population kept at 30 °C shows a significant decrease of SAF to 11.6 μm^{-2} after storage for 10 d and

further to 5.2 µm^{-2} after 21 d at 30 °C. Based on previous explanations, it can be speculated that the detected effect is caused by the accumulation, activation and possible final degradation of secondary metabolites in the spores during storage.

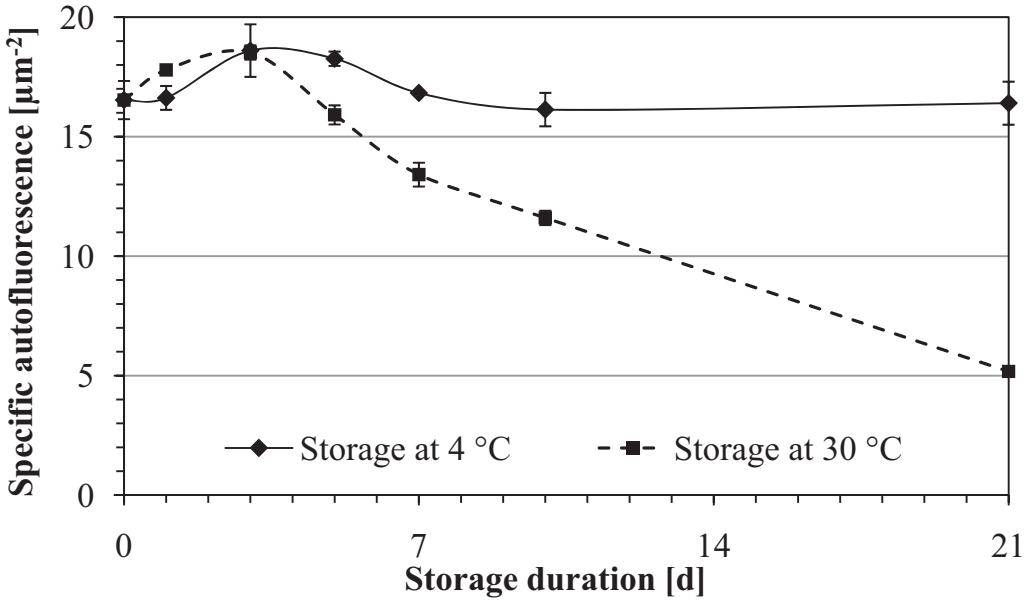

Fig. 4.28. Specific autofluorescence of stored spores. Conidiation on malt extract agar, incubation 8 d, 24 °C in the dark. Subsequent varying storage at 4 °C (solid line) and 30 °C (dashed line). Presented are arithmetic means of 9 biological and 3 technical replicates ± SEM. Excitation at 366 nm, emission detection > 670 nm.

Multiple explanations for the cause of conidial autofluorescence focus on the contribution of flavins and their role in the respiratory chain for the regeneration of ATP (Laflamme et al., 2006). Even though flavoproteins are of utmost importance in the cell and contribute to the overall fluorescence, the direct link between autofluorescence and ATP regeneration (Amat et al., 2005) has to be questioned. As shown in subchapter 4.4.3, the ATP pool is drastically decreased after storage of spores for 7 d. Autofluorescence, however, is still within the same range as before, especially for conidia stored under cooled conditions. **Figure 4.29** shows the SAF of conidia from different substrates that were stored at 4 °C for 7 d. It can be seen that the SAF is virtually unchanged for all populations. Moreover, a tendency towards increasing autofluorescences can be witnessed while the ATP concentrations of the same populations were drastically depleted to approx. 50 % (see figure 4.27).

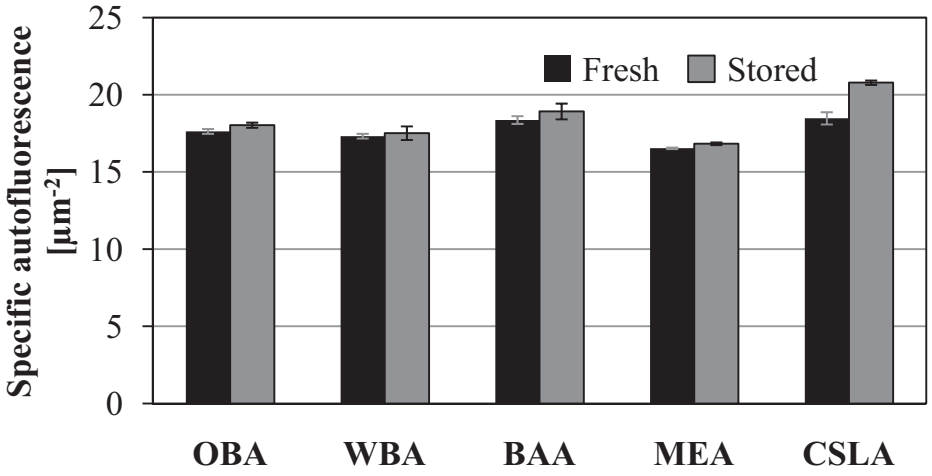

Fig. 4.29. Specific autofluorescence of stored spores (suspension, 7 d, 4 °C), harvested from oat bran agar (OBA), wheat bran agar (WBA), banana agar (BAA), malt extract agar (MEA) and corn steep liquor agar (CSLA). Presented are arithmetic means of 9 biological and 3 technical replicates ± SEM. Excitation at 366 nm, emission detection > 670 nm.

Hence, no conclusion to the activity of the respiratory chain may be drawn from the SAF alone. However, flavins and porphyrins, the most relevant fluorophores in conidia, are involved in a multitude of enzymes and reactions, for example the hydroxylation of steroids by Cyt P450 which is highly active in spores as has been stated previously. The specific autofluorescence can hence serve as an indicator for the metabolic potential of a spore. This again is in line with the increased metabolism during storage in suspension at 4 °C compared to freshly harvested spores (see chapter 4.4.2).

4.4.6 Spore viability after storage

Figure 4.30 shows the development of conidial viability during storage at 4 , 20 and 30 °C over a period of 21 d. While cooled storage for 21 d in suspension does not affect the viability of *A. orchaceus* conidia, uncooled storage at 20 and 30 °C significantly decreases the viability of the spores. Initial viability of freshly harvested spores from MEA is 59 ± 2 %. During cooled storage at 4 °C, the viability slightly increases to 61 ± 2 % after 7 d and subsequently decreases to its initial value. According to t-test analysis, the change is not significant ($p > 0.05$). Also, conidia stored at 20 °C experience a slight increase of viability during the first 10 d to 63 %. Continued storage eventually causes the viability to decrease to 36 % though. The viability increase during short-term storage can also be witnessed for conidia stored at 30 °C. Here the maximum is significantly higher, in contrast to the previous observations significant with $p < 0.05$ and also reached faster. After 3 d of storage, viability reaches 69 ± 2 %. However, it rapidly and almost linearly decreases subsequently to 3.5 ± 1 % after storage for a total of 21 d.

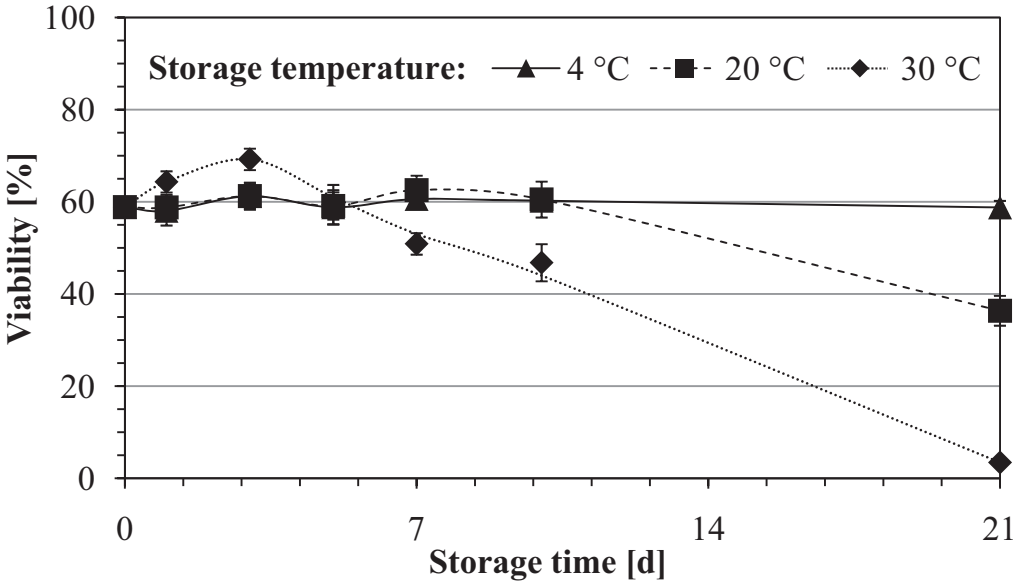

Fig. 4.30. Viability of conidia stored in suspension at 4 °C (triangle, solid line), 20 °C (square, dashed line) or 30 °C (diamond, dotted line) for up to 21 d post harvest from MEA. Presented are arithmetic means of 9 biological and 3 technical replicates ± SEM.

These results are well in line with previously reported findings. Beyer et al. (2004), for example, found no effect of age (19 to 98 d) when assessing conidia activity of *Fusarium graminearum* on solid media. Also, Vezina et al. (1963) found no effect of cooled storage on biotransformation rates with ungerminated spores. Similar results are found investigating the viability of stored conidia of different media as shown in **figure 4.31**.

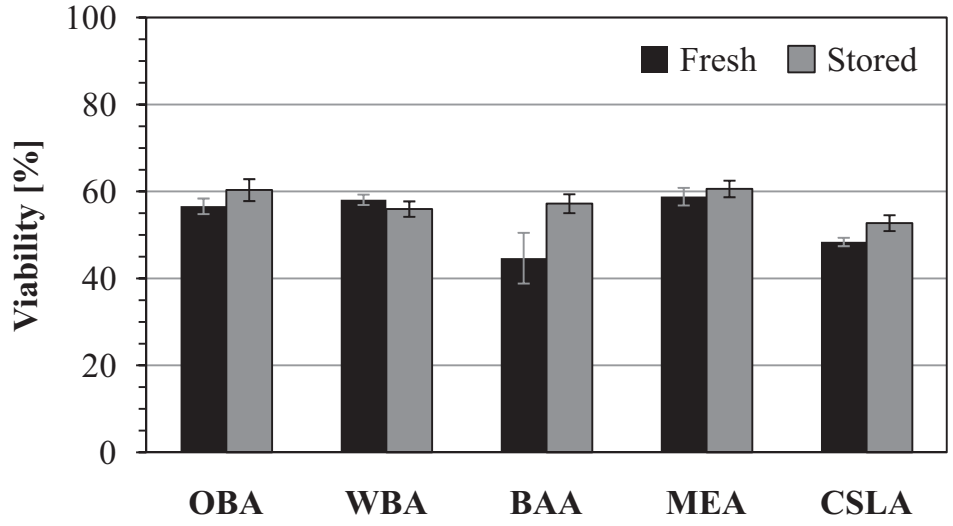

Fig. 4.31. Viability of conidia generated on oat bran agar (OBA), wheat bran agar (WBA), banana agar (BAA), malt extract agar (MEA) and corn steep liquor agar (CSLA) freshly after harvesting (8 d, 24 °C in the dark, black columns) and after subsequent storage (7 d, 4 °C, saline suspension).

It can be seen that except for wheat bran agar (WBA) all tested spore populations show slightly increased viability after storage for 7 d in suspension at 4 °C. Even though this is only significant for spores from banana agar ($p < 0.05$), the trend is obvious throughout the analysis. As indicated in the previous subchapters, the perspective may hence have to be changed and 'storage' in suspension shall rather be regarded as 'soaking' as suggested by Dillon and Charnley (1990). They found increased germination rates for spores that were soaked in distilled water prior to inoculation. In subchapters 4.4.2, 4.4.3 and 4.4.4, it was further elucidated that significant metabolic activity occurs in conidia during their storage as can be seen by high ratios of TCA cycle intermediates and increased interaction of NAD(P)H with proteins. All this affirms the perception that spores are not 'dormant' during storage but they are preparing for rapid germination upon detection of favorable conditions.

It can be said though that the spore takes a risk when maintaining the metabolism on relatively high levels. It was shown in the previous subchapters that the intracellular level of ATP and several important storage metabolites significantly decreases during storage. A parallel decrease of intracellular ATP concentrations and viability during storage for up to 50 d at 4 and 20 °C was previously reported for blastospores of *Paecilomyces farinosus* (Lane et al., 1988). It was also stated that declining ATP concentrations do not affect conidial viability unless it falls below a certain threshold. Minor losses seem not to impair conidial activity. However, prolonged storage with high metabolic activities may lead to depleted reservoirs and cause spore death.

Hence, it is not surprising that spores with longer sporulation times show better resistance against loss of viability during storage. **Figure 4.32** shows the course of viability over storage at 30 °C for conidia harvested after 4, 5, 7 or 8 d of incubation. The spores that had more time to accumulate metabolite reservoirs during sporulation show significantly higher viabilities. The population harvested from the conidiation substrate after 8 d has 46 ± 4 % viable spores after storage for 7 d at 30 °C in suspension. In contrast, spores that were harvested yet after 4 d and were subjected to subsequent storage for 7 d at 30 °C in suspension only have 20 ± 3 viable spores. Partly, this is again in line with the results presented by Kawanabe (1986) explaining the beneficial effect of secondary metabolite accumulation during prolonged conidiation. Further, Tereshina et al. (2004) related better storage survival to larger carbohydrate reservoirs in *A. niger* spores.

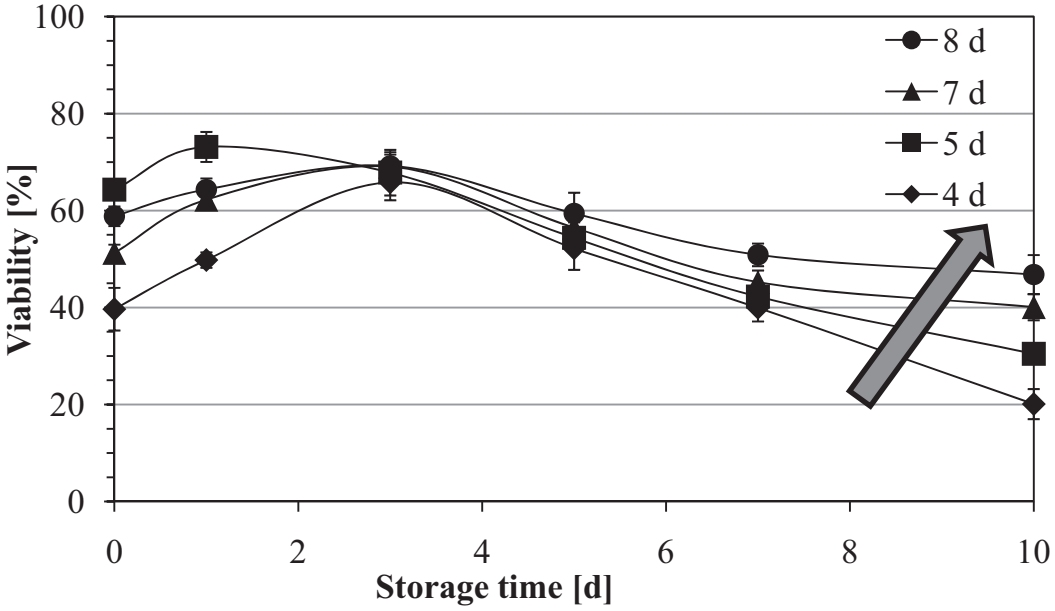

Fig. 4.32. Viability as a function of storage time (0 – 10 d) and previous sporulation time (4 – 8 d). Sporulation conditions: MEA, 24 °C in the dark for all cases. Subsequent storage in suspension at 4 °C.

Even though the declining viability of wheat bran agar spores after storage is statistically not significant, it is interesting as it is the only decreasing viability of the analyzed media. This is particularly striking as spores from wheat bran agar also show significantly lower initial concentrations of glycerol, threitol and erythritol as extensively discussed in subchapter 4.1.3. Polyols have been reported to be important carbon reservoirs and stress protectors at the same time. Decreased viability post storage may hence be expected for those populations with the smallest initial reservoirs of polyols. Further, glycerol, threitol and inositol show decreased concentrations in WBA spores after storage, strongly suggesting that the decreased viability in WBA spores is a result of low initial polyol reservoirs.

At the same time, it is noteworthy that the decrease in viability is only 2 percentage points (58 to 56 %) while the total initial carbohydrate reservoir is decreased to 50 %. This suggests that compensation mechanisms regulate the activity and maintain the spores' viability despite reduced carbon reservoirs. Additionally, as also suggested in previous subchapters, conidia generated on wheat bran agar may have alternative reservoirs such as the proposed oligopeptide polyglutamic acid.

The presented findings correlate well with the observed specific autofluorescence over the course of storage. **Figure 4.33** shows SAF and viability over the course of 21 d storage at 30 °C in suspension. It can clearly be seen how both characteristics initially increase to reach their maximum after 3 d and subsequently almost linearly decline. The initial rise is indicative of increasing metabolic activity, particularly fostered through the high temperature of 30 °C. Spores, however, did not germinate as the storage suspension was sterile 0.9 % NaCl solution and did hence not contain any nutrients. Germination was also excluded by random sampling and microscopic investigation. The following decline in putative secondary metabolites, reservoirs, metabolic activity and viability is vividly illustrated by the almost parallel decrease of the two graphs from day 3 until day 21.

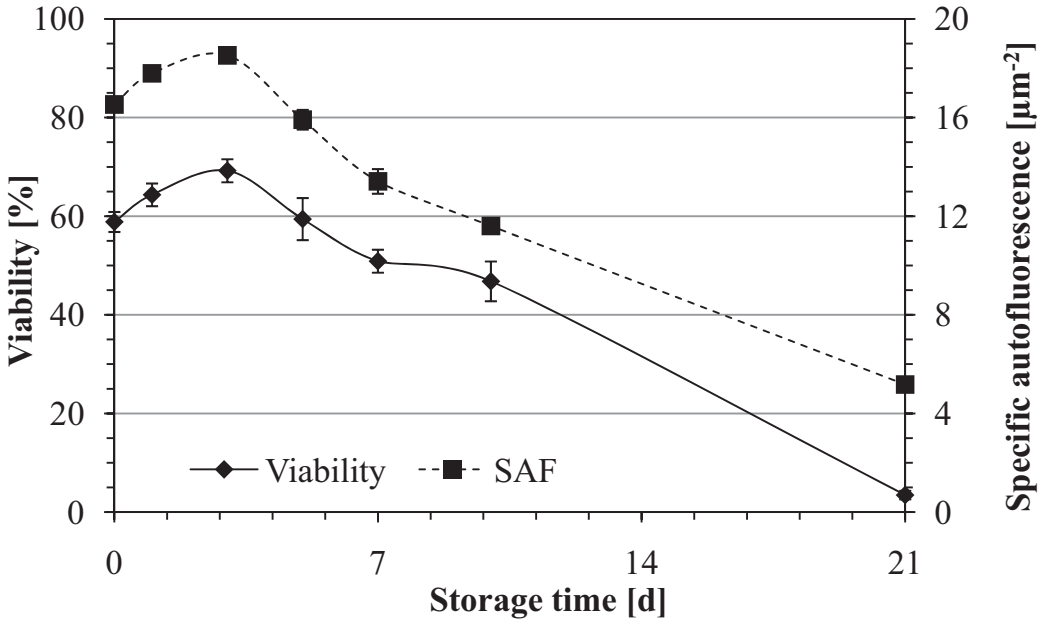

Fig. 4.33. Viability and specific autofluorescence of A. ochraceus *conidia over storage in suspension at 30 °C. Presented are arithmetic means of 3 biological and 3 technical replicates ± SEM.*

Overall, it became obvious that spore viability is a function of sporulation medium, sporulation time and storage temperature. Strong correlations can be drawn between the viability and the metabolite analysis and hence the specific autofluorescence of the respective spore. However, the correlation to the spores' ATP concentration is despite previous reports not as obvious. Further, the suggested viability assessment includes the industrially relevant factor germination time. In combination with the total spore yield, this introduces the total viable spore concentration and is a meaningful criterion for the characterization of conidial populations and sporulation substrates.

4.4.7 Shake flask performance after storage

It was not only analyzed whether the storage of conidia in suspension at 4 °C over 7 d affects the properties of the spores but also whether it influences the performance of the spores in a subsequent submerged cultivation. This is relevant as it is common in industrial applications that conidia have to be stored for one or several days. Typically, this is executed believing that spores are not affected by short term storage in cooled conditions. However, as will be shown here, this is not the case.

As described in chapter 3.9, all parameters were monitored over the course of the shake flask cultivations but for better perceptibility end-point determinations will be presented here. **Figure 4.34** shows the pH of the cultivation broth 72 h after inoculation. The differences between cultures inoculated with freshly harvested spores and conidia that have been stored in suspension for 7 d at 4 °C can be seen. Further, the effect is displayed for spore populations generated on four different sporulation substrates. It becomes obvious that storage has no significant effect on the cultivations' pH for most sporulation substrates. Cultivations inoculated with spores from WBA, however, show a sharp decrease. While spores freshly harvested from WBA cause the largest increase in pH (reaching 8.7), stored spores exhibit the weakest response, reaching a pH of 8.1 ± 0.1. A pH of 8.6 ± 0.0 and hence highest activity is now observed in cultivations inoculated with spores from BAA.

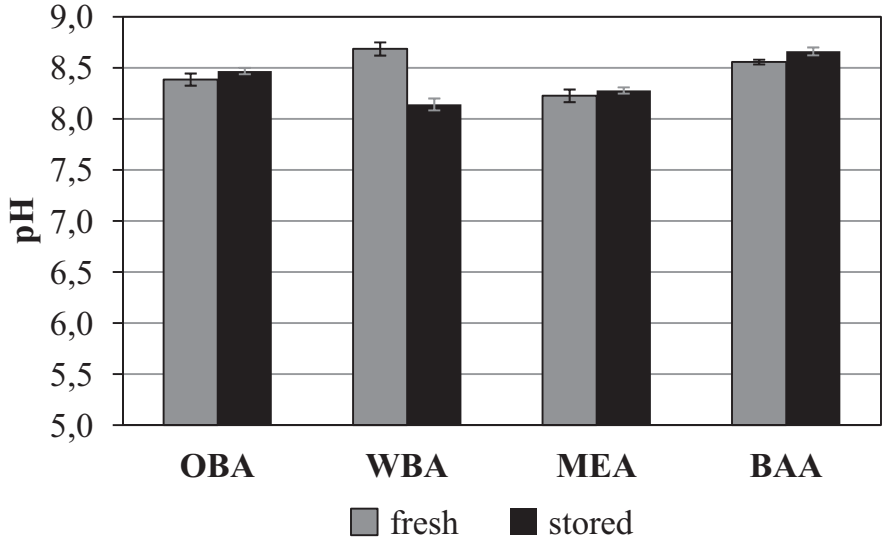

Fig. 4.34. pH of the cultivation broth 72 h after inoculation. Freshly harvested spores (grey columns) and spores that have been stored in suspension (4 °C, 7 d, black columns) were used as inocula. CSL-SP medium, 30 mL, 24 °C, 130 min^{-1}, pH 5.6. Conidiation on oat bran agar (OBA), wheat bran agar (WBA), malt extract agar (MEA), banana agar (BAA). Presented are arithmetic means of 6 biological and 3 technical replicates ± SEM.

Recalling that rapid alkalization was discussed as an indicator for metabolic activity, this finding suggests spores from WBA to be adversely affected by storage. In fact, this is confirmed by the reactant consumption. While freshly harvested WBA spores showed the highest activity and transformed 80 % of the reactant during the first 72 h (shown in chapter 4.1.8, figure 4.15), stored WBA spores only convert 40 % during the same interval and with all further parameters being unchanged. **Figure 4.35** shows clearly how stored spores from WBA exhibit by far the weakest performance of all stored inocula.

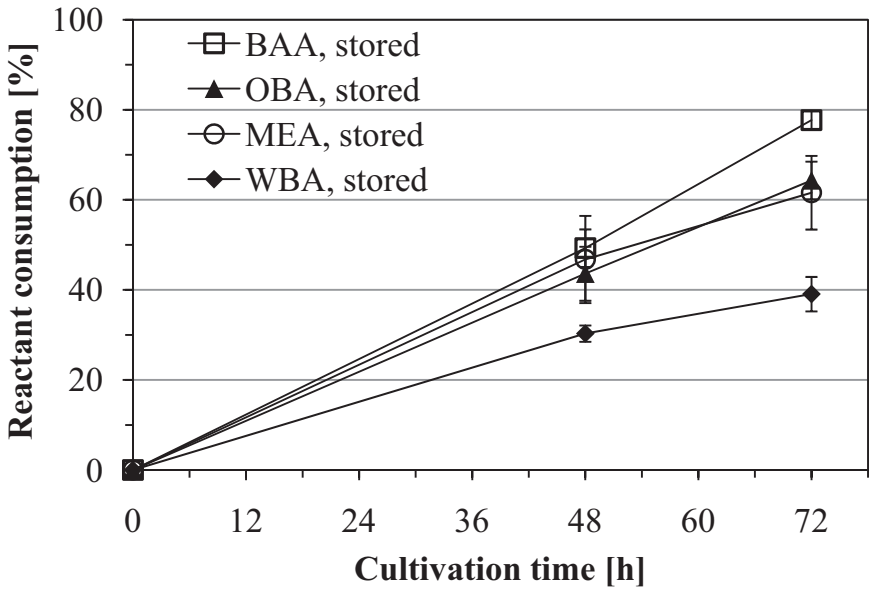

Fig. 4.35. Reactant consumption over the course of shake flask cultivations. Inocula generated on banana agar (BAA), oat bran agar (OBA), malt extract agar (MEA) and wheat bran agar (WBA) during 8 d sporulation at 24 °C in the dark were subsequently stored for 7 d in suspension at 4 °C. Submerged cultivation: CSL-SP medium, 30 mL, 24 °C, 130 min^{-1}, [19-NorAD]$_0$ = 2 g/L. pH 5.6. Presented are arithmetic means of 6 biological and 3 technical replicates ± SEM.

The finding becomes even more obvious when comparing the morphology index and the reactant consumption after 48 and 72 h of submerged cultivation for all four sporulation media as shown in **figure 4.36** and **figure 4.37.** It clearly becomes obvious that both, morphology index and reactant consumption, increase over the duration of the cultivation and then again when comparing cultivations inoculated with stored spores to their counterpart with freshly harvested spores. This indicates that the morphology shifts towards more pellet growth during the course of the cultivation and that stored spores show a stronger tendency to form pellets upon the start of the cultivation. Most interestingly, the reactant consumption is drastically increased through storing the inoculum at 4 °C for 7 d. Even though surprising at first, this is well in line with results presented earlier in the study as well with previously reported

findings. For example, Porcel et al. (2006) found increased lovastatin production for briefly stored spores. Further, Vezina et al. (1963) reported steroid conversion with *A. ochraceus* conidia to be unaffected by prior storage of the same.

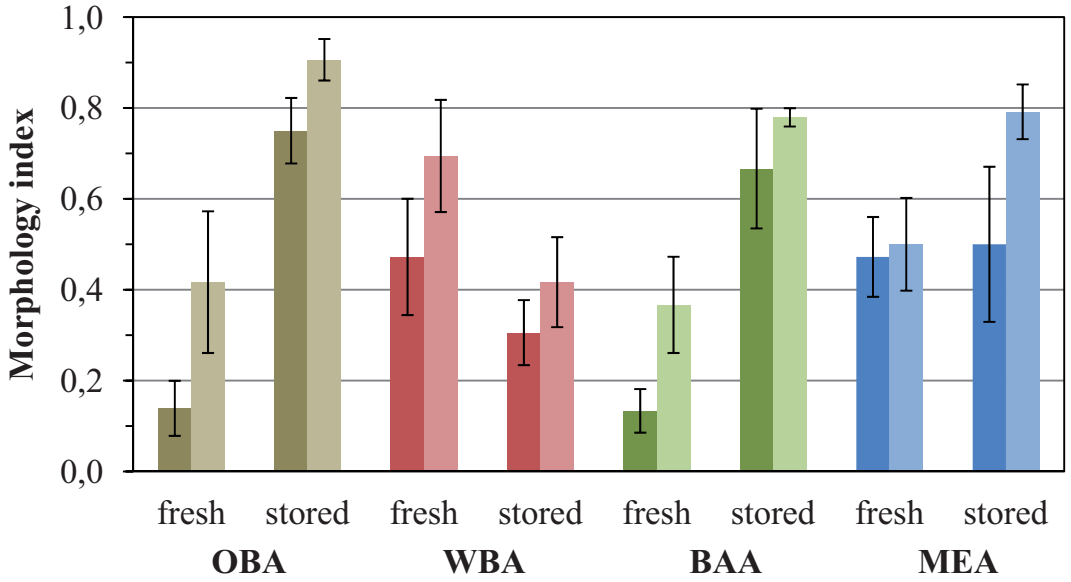

Fig. 4.36. Morphology index of shake flask cultures after 48 h (darker colored columns) and 72 h (lighter colored columns) inoculated with spores generated on oat bran agar (OBA), wheat bran agar (WBA), banana agar (BAA) and malt extract agar (MEA). Sporulation at 24 °C for 8 d in the dark. Further, cultivations inoculated with freshly harvested spores can be distinguished from those that have been stored for 7 d at 4 °C in suspension in the dark. Submerged cultivation: CSL-SP medium, 30 mL, 24 °C, 130 min^{-1}, $[19\text{-NorAD}]_0$ = 2 g/L. pH 5.6. Presented are arithmetic means of 6 biological and 3 technical replicates ± SEM.

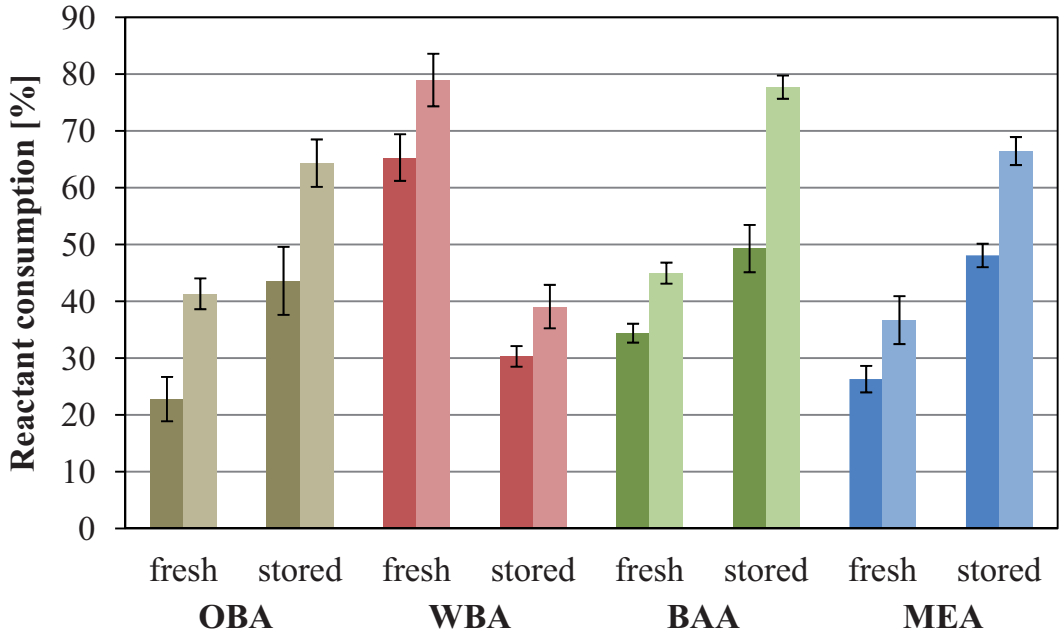

Fig. 4.37. Reactant consumption for shake flask cultivations. All other details as in the figure above.

It was shown in subchapter 4.4.2 that conidia exhibit a highly active metabolism during storage, possibly preparing for faster germination upon detection of favorable conditions. The poor cultivation performance of cultures inoculated with stored spores from WBA can hence readily be explained with their inferior metabolite profile, showing reduced concentrations of carbon reservoirs and TCA cycle intermediates. Further, the ratio of bound NAD(P)H drops from 22 to 13 % in spores from WBA during storage while it rises roughly in the same range in spores from OBA and MEA. Eventually, also the pellet formation tendency of conidia from WBA decreases, possibly due to altered surface protein properties. This represents a novel and remarkable correlation between inherent spore properties and cultivation results.

However, shifting the focus from the predominant drop in WBA spores' performance, it is just as noteworthy how productivity increases for OBA, BAA and MEA spores after storage. In average, the fraction of single spores, determined as described in chapter 3.2, decreases from 65 to 55 % during 7 d storage in suspension at 4 °C (data not shown) while the portion of aggregates of three or more spores increases from 17 to 27 % indicating significantly increasing aggregation tendency. Even though the hence generated primary aggregates are several orders of magnitude smaller than pellets, yet they determine, in combination with pH and mechanical power input, the morphological development of the cultivation of this coagulative fungus as they represent starting points for pellet formation.

It has to be stated though that uncooled storage is clearly detrimental for spores and impairs productivity in subsequent cultivations. **Figure 4.38** shows the course of the reactant consumption and the pH of a cultivation that has been inoculated with 7 d old spores that were stored at 30 °C rather than 4 °C. For comparison, aliquots of the fresh population were stored at 4 °C and are depicted in the same graph. It can clearly be seen how the cultivations significantly differ and the inoculum stored at 30 °C shows dramatically decreased metabolic activity. While cultivation inoculated with the cooled spores transforms 66 % of the reactant, its counterpart only transforms 21 %. Also, the pH rises only to 6.7 instead of 8.3 for the cooled seed culture. Results for biomass are similar (not shown). A simple generalization that storing spores prior to their application increases the yield is hence not possible. Moreover, this finding vividly shows how important proper spore treatment is for reproducible, high cultivation yields.

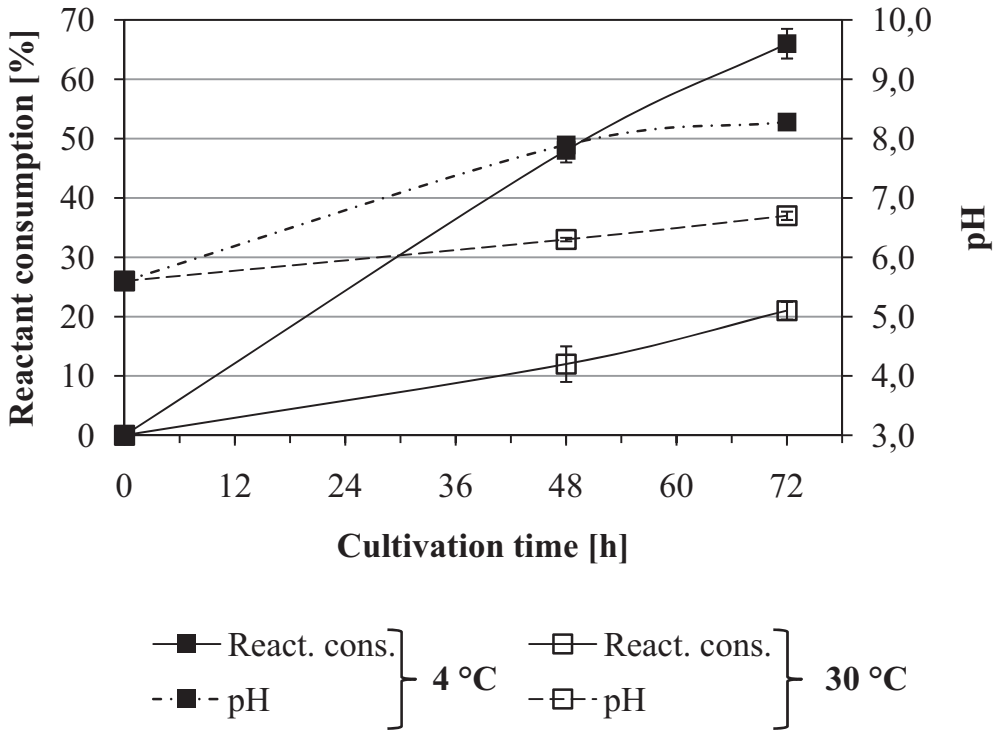

Fig. 4.38. Reactant consumption (solid line) and pH (dashed line) over the course of shake flask cultivations. Inoculum: Spores generated on media and subsequently stored for 7 d at 4 °C (full squares) or at 30 °C (open squares). Submerged cultivation: CSL-SP medium, 30 mL, 24 °C, 130 min^{-1}, $[19\text{-NorAD}]_0$ = 2 g/L. pH 5.6. Presented are arithmetic means of 3 biological and 3 technical replicates ± SEM.

4.5 Effect of early germination

4.5.1 Change of metabolite profile during early germination

Conidia from *A. ochraceus* were incubated in liquid medium under standard conditions. The analysis of the metabolite profile revealed a significant increase of intermediates from the primary metabolism accompanied by the decrease of storage components, similar but not identical to the findings with stored spores presented in subchapter 4.4.2. However, some dramatic differences were uncovered between germinating spores from different conidiation substrates, between spores that have been left for germination for 4, 6 and 12 h as well as between spores left for germination in the presence and absence of the reactant steroid 19-NorAD. These findings will be presented in the following subchapters.

Metabolite profile of germinating spores from MEA, OBA and WBA

Figure 4.39 shows how the entire TCA cycle awakes during germination and cellular metabolism emerges. As seen with fresh and stored spores in the previous chapters, conidia produced on OBA and MEA show similar behavior over the majority of metabolites. WBA, however, is no longer inferior but shows activity at the same or an increased level. Pyruvic acid, the main metabolic intersection, is present in all three populations at comparable levels. This is in line with the findings reported for stored spores in subchapter 4.4.2. Further, with citric acid, alpha-ketoglutarate, succinic acid and malic acid almost all of the TCA cycle intermediates could be detected (data not shown).

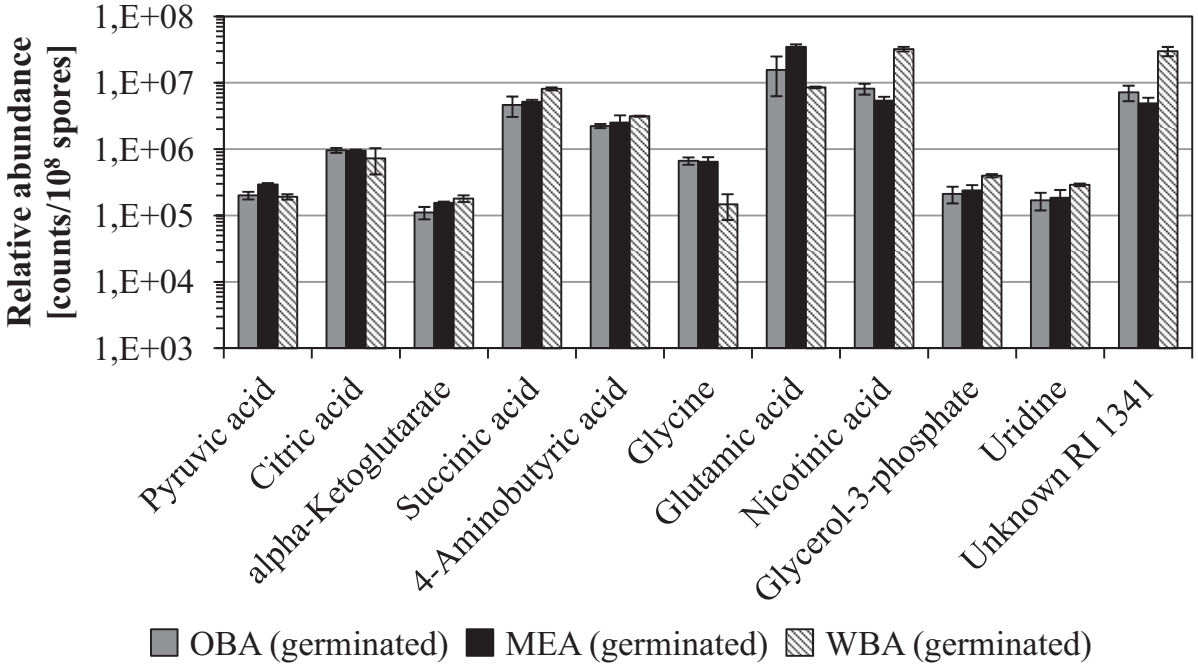

Fig. 4.39. Abundance of the most relevant metabolites in spores from oat bran agar (OBA, grey), malt extract agar (MEA, black) and wheat bran agar (WBA, striped) after germination in liquid culture (MEL medium, 30 mL, 24 °C, 130 min^{-1}, 6 h). Presented are arithmetic means of 3 biological replicates ± SEM. Note the logarithmic scale and the base point of the ordinate of 1 000.

The interesting difference, however, is that spores from WBA show no longer decreased concentrations of TCA cycle intermediates in the second half (alpha-ketoglutarate, succinic acid and malic acid) but the highest abundance of those metabolites compared to OBA and MEA spores. Furthermore, 4-aminobutyric acid (GABA), which is alongside with alpha-ketoglutarate a major link to amino acid metabolism, also shows highest concentrations in germinated WBA spores. Additionally, the concentrations of kojic acid (a common by-product of fungal cultivations), nicotinic acid (an important building block for the generation of the cofactors NADH and NADPH), uridine (for RNA synthesis) and glycerol-3-phosphate

(for phospholipid synthesis) are increased in fresh, germinating WBA spores compared to their OBA and MEA counterparts.

These results fuel the speculation that spores generated on WBA show a shifted composition with regard to their carbon, energy and nitrogen storage. As shown in subchapter 4.1.3, WBA spores have smaller polyol reservoirs. Larger peptide pools are here postulated. During storage at 4 °C, these peptide pools are then not as stable and show less protection against environmental stresses compared to polyols. Peptides are thus depleted for maintenance metabolism or subject of other breakdown mechanisms over the course of the storage period. Therefore, spores from wheat bran agar, show inferior composition and performance after storage. However, when fresh WBA spores are left for germination, they make use of those readily available reservoirs serving as building blocks and energy supply concomitantly. This renders WBA spores ideal for immediate germination after harvesting but inferior when conidia are required to be stored between harvest and application.

An over interpretation of the results has to be avoided though as the differences between the levels of concentration are around factor 2 which is the threshold commonly chosen to speak of significant changes in the up- and downregulation of metabolism. Also, two important amino acids (glutamic acid and glycine, see figure 4.39) are found at lower concentrations in spores from WBA undermining the above stated hypothesis. Furthermore, wheat bran shows an intermediate nitrogen level in the same range as malt extract and oat bran. For detailed information, flux analyses with ^{13}C labeled carbon would hence have to be conducted as only these allow the precise tracking of reservoirs and subsequent metabolization thereof.

Metabolite profiles of spores germinating for 4, 6 and 12 hours

Freshly harvested spores from MEA were left for germination under standard conditions for 4, 6 and 12 h. The metabolite profile was subsequently assessed as described before. **Figure 4.40** shows the changes of the most relevant metabolites of unstored spores immediately after harvest as well as after 4, 6 and 12 h of germination in liquid culture. Erythritol and ribitol which are both highly abundant in untreated spores from MEA show a constant decrease during early germination. This resembles the expected. However, compared to conidia that have been kept at 4 °C for 7 d, this states a remarkable difference. There, the 4-carbon polyol erythritol is depleted entirely over the course of one week whereas ribitol, a 5-carbon polyol, remains absolutely unchanged throughout the storage period (see chapter 4.4.2).

Therefore, it can be stated that erythritol serves as a carbon and energy supply during storage and germination while ribitol is retained and only consumed during germination. This indicates that they cater distinct functions within the conidial metabolism and are not interchangeable.

The observation that pyruvic acid, succinic acid, malic acid and lactic acid show parallel increasing concentrations is a clear indicator for the onset of the central carbon metabolism in more and more spores during the first 12 h of germination. Of those, malic acid, however, is the only TCA cycle intermediate that was already detectable in freshly harvested spores.

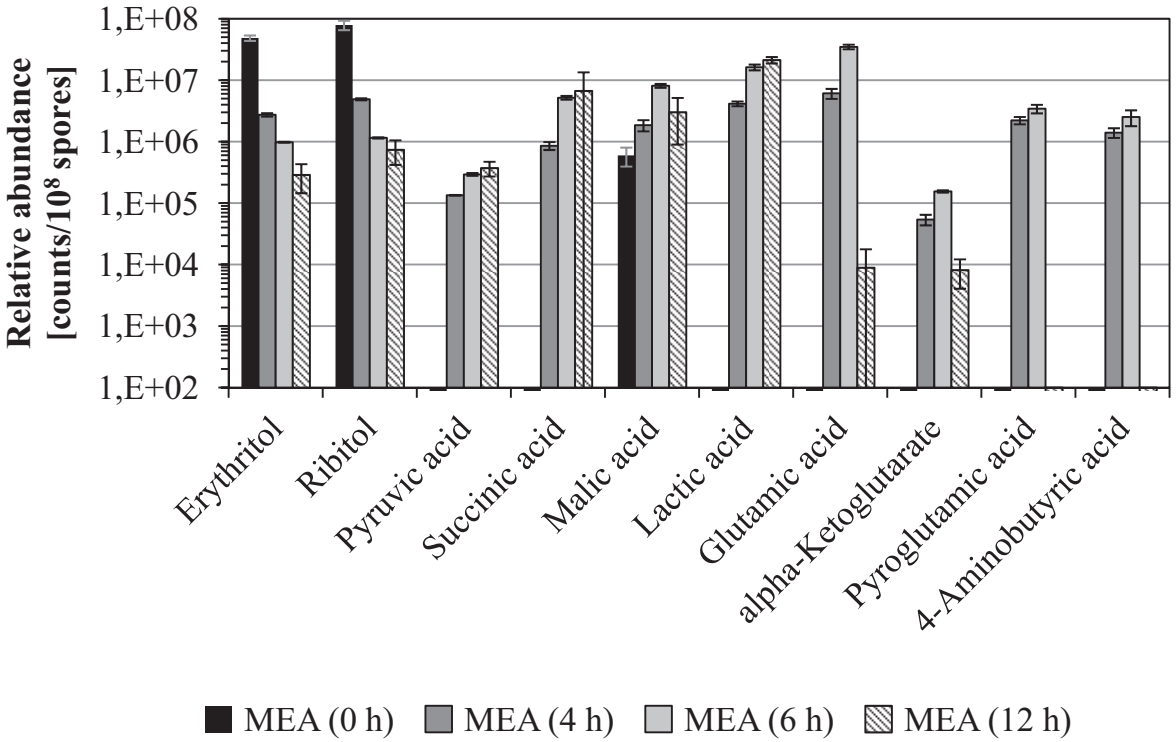

Fig. 4.40. Abundance of the most relevant metabolites in freshly harvested spores from malt extract agar (MEA). Untreated (black), germinated in liquid culture for 4 h (dark grey), 6 h (light grey) and 12 h (striped). Presented are arithmetic means of 3 biological replicates ± SEM. Note the logarithmic scale and the base point of 100 of the ordinate.

The behavior of glutamic acid, alpha-ketoglutarate, pyroglutamic acid and 4-aminobutyric acid (GABA) is outstanding. While none of those metabolites can be detected in untreated spores, they very rapidly appear after 4 h of germination, rise towards 6 h and then decrease. Glutamic acid and alpha-ketoglutarate, which serve central roles in the normal cellular metabolism, fall to intermediate concentrations. Pyroglutamic acid and GABA, however, disappear entirely. It can hence be suspected that these metabolites are intermediates of peptide catabolism and amino acid degradation. Therefore, they only appear during the short period where the degradation

rate of the putative reservoir-oligomer exceeds the consumption by downstream pathways. This represents a novel concept for the explanation of reservoir changes in fungal spores during germination. However, for bacterial spores it had been shown that hexosamine containing peptides are secreted into the suspending medium during germination (Powell and Strange, 1953; Strange and Powell, 1954). Aimanianda et al. (2009) found that hydrophobins, typically covering the dormant spore, are not released into the suspending medium during germination but entirely degraded. The fact that hydrophobins are small proteins with highly conserved, repeating amino acid motives would make rapid degradation for the supply of building blocks additionally convenient for germinating conidia. As shown in chapter 3.2.2, changes of the proteins in the conidial wall were also reported within this work. Further, the composition of spore wall proteins of *Syncephalastrum racemosum* has been reported to be rich in aspartic acid, glutamic acid, glycine and serine, all representing amino acids that are readily metabolized (Hobot and Gull, 1981a). Also, Lamarre et al. (2008) found parallel upregulation of GAD and isocitrat dehydrogenase in germinating spores of *A. fumigatus* suggesting the close link between the regulation of TCA cycle and amino acid metabolism. These findings can be regarded as further indications in favor of the suggested theory.

In summary, the presented findings support the hypothesis that amino acid based reservoirs with distinct roles during the onset of germination and metabolism are likely to be present in fungal spores.

Metabolite profile of spores germinating in the presence of 19-NorAD

Significant differences between germinating MEA spores in the presence and absence of the reactant steroid 19-NorAD were revealed. As shown previously, several steroids exhibit strong anti-fungal activity, particularly on germinating spores (Deacon and Mitchell, 1985). Lately, it has been reported that progesterone may even convey its inhibitory effects via G protein coupled signaling pathways in mycelia (Jeraj et al., 2005). Furthermore, 19-NorAD is dissolved in dimethylformamide (DMF) which has also proven toxic (Stratton, 1985). It can hence be expected that spores germinating in the presence of the reactant show an impaired response and slower growth. The results, however, exceed the anticipation and are depicted in **figure 4.41**.

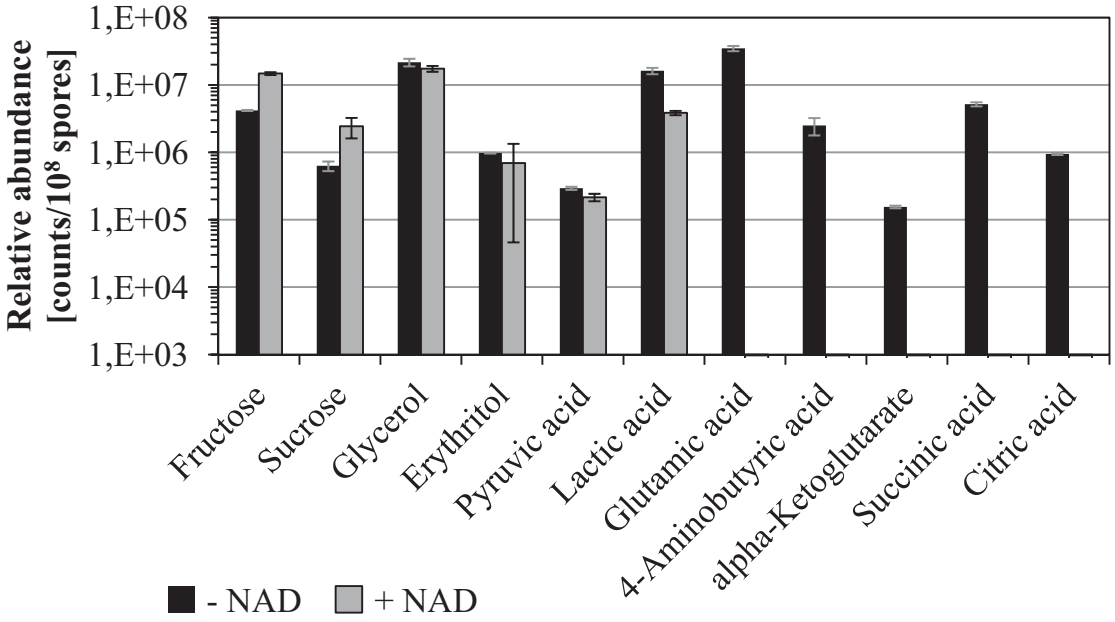

Fig. 4.41. Abundance of selected metabolites in 6 h germinating spores in the absence (black) and presence (grey) of the reactant steroid 19-NorAD. Presented are arithmetic means of 3 biological replicates ± SEM. Note the logarithmic scale and the base point of 1 000 of the ordinate.

Of the 45 detected metabolites, 22 were only present in the culture grown without steroid addition, 19 were abundant in similar or lower concentrations in the shake flasks with added steroid and 4 were found in higher concentrations in the 19-NorAD positive cultures (data not shown). Interestingly, the 4 metabolites found in higher concentration are sucrose, glucose and fructose as well as an unknown substance. This is especially noteworthy as the liquid medium has no added sugars. Also, lactose, trehalose, isomaltose, maltotriose, glycerol, erythritol, xylitol, ribitol, sorbitol and inositol are found at comparable levels. Interestingly, pyruvic acid and lactic acid also show only minor differences between the two germination conditions. However, amino acid and related metabolites (e.g. alanine, valine, serine, threonine, glycine, glutamic acid and pyroglutamic acid) as well as TCA cycle intermediates (succinic acid, malic acid, alpha-ketoglutarate and citric acid) were not found in germinating spores with added 19-NorAD but only in cultures in the absence of the reactant.

However, as cultivations were readily conducted in the presence of 19-NorAD, both, from the beginning as well as added after germination, it has to be concluded that the steroid does not inhibit but delay and/or retard the onset of fungal growth. This indicates that cultivations are better conducted with the steroid absent during the initial phase, so that conidia germinate faster and develop rapidly into active mycelium. Later addition of the steroid should therefore allow faster transformation rates as also lately suggested for biotransformations in general (Adams et al., 2003).

4.5.2 Change of NAD(P)H distribution during early germination

Germinating spores of *A. ochraceus* were investigated by means of two-photon fluorescence microscopy in order to reveal changes in the NAD(P)H distribution. Measurements were taken after incubating the spores for 6 h in submerged culture in malt extract liquid medium (MEL). Figure 3.14-D and **figure 4.42** illustrate that at this point spores are still clearly visible while very few germ tubes and short hyphae can also already be witnessed. As described before though, image analysis was conducted for entire images integrating TCSPC decays over the whole scan. The results of the subsequent fit and data analysis are presented in **table 4.6**.

It becomes visible that germinating spores show high ratios of protein bound NAD(P)H and hence high metabolic acitivities. Irrespective of the conidiation substrate, the portion of free NAD(P)H decreases while the bound NAD(P)H becomes more abundant. MEA showed with an increase from 10 to 22 % the largest shift towards the bound coenzyme. Also, spores from OBA increased significantly from 11 % bound NAD(P)H immediately after the harvest to 17 % during germination. Even WBA spores that showed with a ratio of 22 % bound NAD(P)H in freshly harvested spores already the level of metabolic activity that MEA spores reached after 6 h of germination increased further. They now show a ratio of protein bound NAD(P)H of 29 %, the highest abundance of bound cofactor determined in this study.

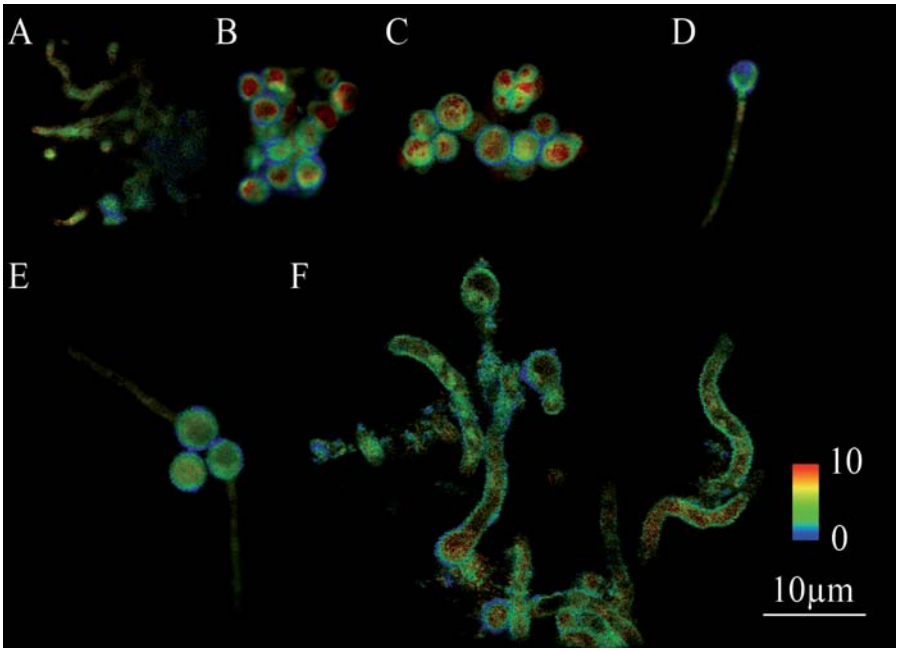

Fig. 4.42. Fluorescent lifetime images (FLIM) of A. ochraceus *spores germinated for 12 h. Color code represents average fluorescence lifetime per pixel in ns. Data acquisition and analysis with SymPhoTime.*

Tab. 4.6. Fluorescence lifetimes of free and protein bound NAD(P)H in germinating spores (MEL, 6 h, 24 °C, 100 min^{-1}) originally harvested from malt extract agar (MEA), oat bran agar (OBA) and wheat bran agar (WBA). Presented are arithmetic means from 2 biological and 3 technical replicates ± SEM.

	Lifetime [ps]		Fraction of protein bound NAD(P)H [%]
	NAD(P)H free	NAD(P)H bound	
MEA germinated	532 ± 19	3 285 ± 37	22 ± 0
OBA germinated	427 ± 18	3 310 ± 83	17 ± 0
WBA germinated	546 ± 15	3 714 ± 41	29 ± 2

It is further noteworthy that some FLIM images also exhibited comparably reliable results for biexponential fitting (instead of triexponential) indicating the abundance of melanin in the cell wall to be decreasing during germination. Detailed analyses, however, were not possible as the fluorescence lifetime of melanin is too short to be resolved reliably.

These findings are again very well in line with the results presented in the previous subchapter where the onset of conidial metabolism during early germination is described based on the metabolite profile. It can be seen how TCA cycle intermediates as well as numerous additional metabolites increase. With the hence increasing overall metabolic activity, the rapid generation of NADH in glycolysis and TCA cycle as well as cell growth, as depicted in figures 3.14 and 4.42, more NAD(P)H is therefore bond to active enzymes. It may be speculated that the shift towards protein associated cofactors is exponential until it reaches its maximum because the abundance of enzymes increases during germination and hence the concentration of possible partners for interaction. At least during the first hours, this will immediately accelerate transcription and translation of early germination genes, again increasing the concentration of possible binding sites (Lamarre et al., 2008). Only when the required enzymes for the generation of NAD(P)H become available and the total pool of NAD(P)H is increased in a regulated manner, this process will turn into a dynamic equilibrium.

It will hence be interesting to investigate the entire germination process until the formation of hyphae and mycelium. Also, the scrutiny of the effect of different growth conditions (power input, oxygen supply, nutrient availability) appears fascinating as the localization of metabolically active and inactive hyphal regions should be detectable due to high or low ratios of NAD(P)H, respectively in the mycelium. Due to its unique properties, two-photon fluorescence microscopy is particularly practical for

such analysis. The low energy infrared excitation light can readily penetrate fungal structures and hence provide information about the inside of pellets. The hurdle to overcome for this task though is the immobilization of the pellet.

In this study, for the first time, the distribution of NAD(P)H in conidia was shown by means of two-photon fluorescence microscopy. It was not only possible to demonstrate differences between spores of different media (MEA, OBA and WBA) but also between spores in different growth states (freshly harvested, stored and germinated). Further, even differences between individual spores could be revealed and analyzed. The findings are well in line with the metabolite profiles of the corresponding spores and emphasize the meaningful applicability of two-photon fluorescence for the detection, the visualization of localization and the determination of relative concentrations of free and protein bound NAD(P)H which is a suitable, versatile indicator for fungal metabolic activity.

5 Summary and conclusion

The goal of this study was the comprehensive characterization of fungal spores in order to correlate their properties with the outcome of submerged cultivations inoculated with these spores. Therefore, spore quality indicators had to be determined and methods for their respective assessment had to be established. Subsequently, this allowed the revelation of the triad between sporulation environome, spore properties and cultivation performance. Seven major spore quality indicators were verified as meaningful and validated for the portrayal of a conidia population. It could be shown that the spore aggregation tendency, readily assessed microscopically, correlates with the later morphology during the cultivation, possibly through altered spore wall properties. In order to allow the analysis of the ingredients of spores a method for the preservative extraction of spore metabolites was established and successfully applied, permitting metabolic profiling in fungal spores for the first time and giving deep insights into the reactions inside the spores that have been claimed 'dormant' for many years. Further, the metabolically relevant co-factor NAD(P)H was spatially resolved and semi-quantitatively determined by means of two-photon fluorescence microscopy (2pFLIM). Especially the ratio of free and protein bound NAD(P)H proved to be a valuable indicator for the quality of a seed culture. Similar trends could be found when studying the visible longwave fluorescence. While being not as specific as the 2pFLIM measurements, their determination can be conducted rapidly and routinely. The same is true for the here presented methods for the ATP analysis as well as the determination of the spore viability. Hence, a comprehensive set of methods was established to investigate spore quality indicators for quality control assessments and fundamental research alike.

In a second step, the effect of the sporulation environome, which also had not been previously described as such, on these spore quality indicators was elucidated. It was shown that the carbon content of the sporulation medium positively correlates with the concentration of harvestable conidia within reasonable boundaries. The highest spore yield of $26 \cdot 10^7$ spores/mL was achieved using oat bran agar (OBA) with a carbon concentration of 15 g/L. Increasing the carbon content to 183 g/L through the addition of glucose though did not further foster conidiation but did also not inhibit the same. The effect of nitrogen appears to be minor.

Further, fresh spores were found to contain high concentrations of several polyols and sugars. Individual polyol species, such as inositol and ribitol, were detected at concentrations between 0.1 and 55 ng/10^5 spores, respectively, each representing

between 0.05 and 2 % of the spore matter. While fructose, inositol, and sorbitol for example are present at almost identical concentrations across the tested spore populations independent of the sporulation medium, glycerol, threitol and erythritol vary significantly with differences of up to factor 22. In these cases, spores generated on wheat bran agar (WBA) showed the lowest concentrations of those important metabolites that mediate stress tolerance and serve as carbon reservoirs compared to those from malt extract agar (MEA) and OBA. The metabolite profile of spores that have been stored in saline solution for 7 d at 4 °C doubtlessly reveals the onset of the TCA cycle and amino acid metabolism. For example, pyruvic acid, citric acid, alanine and spermidine are found in large concentrations in stored spores while they were below detection limits in freshly harvested conidia. Their generation is observed at the expense of reservoir compounds which significantly decrease during storage. This finding has relevant implications for industrial applications as the short term storage of spores at 4 °C was generally expected to not alter the spores' properties.

Also, fresh spores originating from WBA show the highest ratio of protein bound NAD(P)H. While only 10 % of all NAD(P)H in spores from MEA and OBA was conjugated with proteins, the fraction is at 22 % in spores from WBA indicating an increased metabolic readiness. However, this observation changed entirely after storing the spores for 7 d at 4 °C in suspension. Spores from WBA then show low levels of protein bound NAD(P)H while spores from the other substrates exhibit higher activities with fractions of bound NAD(P)H up to 20 %.

This behavior was mirrored completely by the performance in subsequent submerged biotransformations. Cultivations inoculated with fresh spores from WBA showed the largest reactant consumption of approx. 80 % after 72 h. Those started with spores from banana agar (BAA), MEA or OBA only converted approx. 40 %. In line with the findings for NAD(P)H distribution and metabolite profile, this revolves after storage: Performance of stored spores from WBA decreases while the activity of cultivations inoculated with stored spores from all other substrates increases significantly. For stored spores, best results were obtained with conidia generated on banana agar converting 78 % of the reactant after 72 h of cultivation. This again emphasizes the significant changes that spore populations undergo during storage.

Furthermore, reactant turnover in the cultivation broth could be related to the culture morphology which itself is a result of the conidial aggregation behavior. It was revealed that yet the primary aggregation of spores influences the morphology of the following cultivation. It could be demonstrated that the fraction of single spores

decreases from 67 to 42 % during storage of conidia. Subsequently, cultivations inoculated with stored spores show a considerable shift towards pellet morphology which in turn positively correlates with the culture productivity. Aggregation is hence no longer only a function of the pH, the power input and the addition of microparticles but also of the spore properties.

It became obvious that the selection of the optimal sporulation substrate depends on the required application of the conidia. For immediate inoculation, spores freshly harvested from WBA are recommended as therewith the highest metabolic activity, reactant consumption and product formation were witnessed. Sporulation on OBA is favorable if the sheer concentration of spores is of largest relevance. If spores are needed to show a well-balanced performance and stability during storage, MEA is the recommended conidiation substrate.

This illustrates that the evaluation of a conidiation medium only by the amount of harvestable spores is inadequate. Also, the description of a spore population's quality by the mere assessment of their viability can only serve as a preliminary indicator. As the ultimate culture performance is a function of several conidial properties, the determination of a single criterion would in any case not be sufficient for the holistic characterization of the spore population. Only the combined analysis of macroscopic changes such as aggregation behavior and molecular properties like the NAD(P)H distribution and the metabolite profile allows a comprehensive understanding of the spore population. This work hence represents a relevant step towards a better understanding of fungal cultivation processes as it represents the first elucidation of an important but previously neglected parameter in this multivariant system.

The fact that these findings were also related to the performance of subsequent submerged cultivations makes the results additionally interesting for industrial applications. Routine introduction of selected techniques may aid in the detection of inferior seed cultures. Early discharge of those inocula may consequently reduce suboptimal cultivation runs, improve workload capacity utilization and ultimately minimize costs.

6 Outlook

The knowledge of the significant influence of the sporulation environome on the properties of conidia and their subsequent behavior in submerged cultivations opens a large field for future investigations. In order to understand the underlying genetic reasons for the observed differences, the changes of mRNA level in mycelia and conidia during the formation of spores are of largest interest. As currently international efforts are being combined to understand the overall genetic regulation of sporulation, a fruitful intercommunication can be expected here. However, the extraction of intact mRNA from conidia for subsequent qRT-PCR analysis has proven difficult in the past.

Also, knowledge about the development of the metabolome over the course of spore formation would be an important keystone for the interpretation and subsequent optimization of conidiation processes. Particularly, the introduction of LC-MS analysis for the improved detection of secondary metabolites appears promising. Further, the determination of absolute concentrations of NAD(P)H in spores would provide a deeper insight into the conidial composition of cofactors. In addition, the existing model for the correlation of aggregation and morphology may be extended to include the influence of the primary aggregation. Therefore, it may be of interest to further assess the spore wall properties (particularly glucan, melanin and hydrophobins) and how they are affected by the sporulation environome.

Also, the application of defined media would assist in the understanding of intracellular processes and exhibit the possibility to correlate the found changes to individual ingredients of the sporulation medium. As shown, spores yet within a given population still show significant variances, for example in NAD(P)H distribution and size. This has to be attributed to the existence of a putative ‘micro-environome’ during sporulation on solid media. It would therefore be beneficial to select individual spores for the inoculation of successive cultivations. This may for example be achieved by means of fluorescence activated cell sorting. Additionally, it shall be investigated whether the micro-environome can be controlled for.

For the holistic understanding of the overall process, the final step would be the inclusion of the determined results into a comprehensive mathematical model. This shall incorporate cultivation parameters, such as pH and power input, as well as sporulation parameters and spore characteristics, like the ATP content or the aggregation behavior. The model would then allow the prediction of the cultivation outcome only based on these input parameters.

7 References and appendix

7.1 References

Adams, A; Demyttenaere, JCR and De Kimpe, N (2003). Biotransformation of (R)-(+)- and (S)-(-)-limonene to [alpha]-terpineol by *Penicillium digitatum* - investigation of the culture conditions. Food Chem **80**(4): 525-534.

Adams, TH; Wieser, JK and Yu, J-H (1998). Asexual Sporulation in *Aspergillus nidulans*. Microbiol Mol Biol Rev **62**(1): 35-54.

Agger, T; Spohr, AB; Carlsen, M and Nielsen, J (1998). Growth and product formation of *Aspergillus oryzae* during submerged cultivations: Verification of a morphologically structured model using fluorescent probes. Biotechnol Bioeng **57**(3): 321-329.

Aimanianda, V; Bayry, J; Bozza, S; Kniemeyer, O; Perruccio, K; Elluru, SR; Clavaud, C; Paris, S; Brakhage, AA; Kaveri, SV, et al. (2009). Surface hydrophobin prevents immune recognition of airborne fungal spores. Nature **460**(7259): 1117-21.

Al-Anati, L and Petzinger, E (2006). Immunotoxic activity of ochratoxin A. J Vet Pharmacol Ther **29**(2): 79-90.

Al-Hamdani, AM and Cooke, RC (1987). Effects of water potential on accumulation and exudation of carbohydrates and glycerol during sclerotium formation and myceliogenic germination in *Sclerotinia sclerotiorum*. T Brit Mycol Soc **89**(1): 51-60.

Allen, MJ; Voelker, DR and Mason, RJ (2001). Interactions of Surfactant Proteins A and D with *Saccharomyces cerevisiae* and *Aspergillus fumigatus*. Infect Immun **69**(4): 2037-2044.

Amat, A; Rigau, J; Waynant, RW; Ilev, IK; Tomas, J and Anders, JJ (2005). Modification of the intrinsic fluorescence and the biochemical behavior of ATP after irradiation with visible and near-infrared laser light. J Photochem Photobiol B **81**(1): 26-32.

Ammor, M (2007). Recent Advances in the Use of Intrinsic Fluorescence for Bacterial Identification and Characterization. J Fluoresc **17**(5): 455-459.

Apoga, D; Ek, B and Tunlid, A (2001). Analysis of proteins in the extracellular matrix of the plant pathogenic fungus *Bipolaris sorokiniana* using 2-D gel electrophoresis and MS/MS. FEMS Microbiol Lett **197**(2): 145-50.

Araujo, R and Rodrigues, AG (2004). Variability of germinative potential among pathogenic species of *Aspergillus*. J Clin Microbiol **42**(9): 4335-7.

Asif, AR; Oellerich, M; Amstrong, VW; Riemenschneider, B; Monod, M and Reichard, U (2006). Proteome of conidial surface associated proteins of *Aspergillus fumigatus* reflecting potential vaccine candidates and allergens. J Proteome Res **5**(4): 954-62.

Atkins, P and de Paula, J (2006). Physical Chemistry: 8e. Oxford, Oxford University Press.

Atlas, RM (1993). Handbook of Microbiological Media. Boca Raton, CRC Press.

Axelrod, DE (1972). Kinetics of differentiation of conidiophores and conidia by colonies of *Aspergillus nidulans*. J Gen Microbiol **73**(1): 181-4.

Baker, NR (2008). Chlorophyll Fluorescence: A Probe of Photosynthesis *In Vivo*. Annu Rev Plant Biol **59**(1): 89-113.

Bapat, PM; Kundu, S and Wangikar, PP (2003). An optimized method for *Aspergillus niger* spore production on natural carrier substrates. Biotechnol Prog **19**(6): 1683-8.

Barrios-González, J; Martínez, C; Aguilera, A and Raimbault, M (1989). Germination of concentrated suspensions of spores from *Aspergillus niger*. Biotechnol Lett **11**(8): 551-554.

Beaurepaire, E and Mertz, J (2002). Epifluorescence Collection in Two-Photon Microscopy. Appl Opt **41**(25): 5376-5382.

Bennett, JW (1998). Mycotechnology: the role of fungi in biotechnology. J Biotechnol **66**(2-3): 101-107.

Berg, JM; Tymoczko, JL and Stryer, L (2003). Biochemie. Heidelberg, Spektrum Akademischer Verlag.

Beyer, M; Röding, S; Ludewig, A and Verreet, JA (2004). Germination and Survival of *Fusarium graminearum* Macroconidia as Affected by Environmental Factors. J Phytopathol **152**(2): 92-97.

Beyer, M; Verreet, J-A and Ragab, WSM (2005). Effect of relative humidity on germination of ascospores and macroconidia of *Gibberella zeae* and deoxynivalenol production. Int J Food Microbiol **98**(3): 233-240.

Billinton, N and Knight, AW (2001). Seeing the Wood through the Trees: A Review of Techniques for Distinguishing Green Fluorescent Protein from Endogenous Autofluorescence. Anal Biochem **291**(2): 175-197.

Bochenek, K and Gudowska-Nowak, E (2003). Electronic Properties of Random Polymers: Modelling Optical Spectra of Melanins. Acta Phys Pol B **34**(5): 2775.

Bolten, CJ; Kiefer, P; Letisse, F; Portais, J-C and Wittmann, C (2007). Sampling for Metabolome Analysis of Microorganisms. Anal Chem **79**(10): 3843-3849.

Bowman, SM and Free, SJ (2006). The structure and synthesis of the fungal cell wall. BioEssays **28**(8): 799-808.
Braun, S and Vecht-Lifshitz, SE (1991). Mycelial morphology and metabolite production. Trends Biotechnol **9**(2): 63-68.
Broderick, AJ and Greenshields, RN (1981). Sporulation of *Aspergillus niger* and *Aspergillus ochraceus* in Continuous Submerged Liquid Culture. J Gen Microbiol **126**(1): 193-202.
Bruneau, J-M; Magnin, T; Tagat, E; Legrand, R; Bernard, M; Diaquin, M; Fudali, C and Latgé, J-P (2001). Proteome analysis of *Aspergillus fumigatus* identifies glycosylphosphatidylinositol-anchored proteins associated to the cell wall biosynthesis. Electrophoresis **22**(13): 2812-2823.
Cahagnier, B; Lesage, L and Richard-Molard, D (1993). Mould growth and conidiation in cereal grains as affected by water activity and temperature. Lett Appl Microbiol **17**(1): 7-13.
Canepa, L; Ferraris, AM; Miglino, M and Gaetani, GF (1991). Bound and unbound pyridine dinucleotides in normal and glucose-6-phosphate dehydrogenase-deficient erythrocytes. BBA-Gen Subjects **1074**(1): 101-104.
Capozzi, V; Perna, G; Carmone, P; Gallone, A; Lastella, M; Mezzenga, E; Quartucci, G; Ambrico, M; Augelli, V; Biagi, PF, et al. (2006). Optical and photoelectronic properties of melanin. Thin Solid Films **511-512**: 362-366.
Carlin, JB and Doyle, LW (2001). Basic concepts of statistical reasoning: Hypothesis tests and the t-test. J Paediatr Child Health **37**(1): 72-77.
Champe, SP; Rao, P and Chang, A (1987). An Endogenous Inducer of Sexual Development in *Aspergillus nidulans*. J Gen Microbiol **133**(5): 1383-1387.
Chance, B; Legallais, V and Schoener, B (1962). Metabolically Linked Changes in Fluorescence Emission Spectra of Cortex of Rat Brain, Kidney and Adrenal Gland. Nature **195**(4846): 1073-1075.
Chang, C; Sud, D and Mycek, M (2007). Fluorescence Lifetime Imaging Microscopy. Digital Microscopy. Eds.: G. Sluder and D. E. Wolf, Academic Press (Elsevier). **81:** 495-524.
Chelack, WS; Borsa, J; Szekely, JG; Marquardt, RR and Frohlich, AA (1991). Variants of *Aspergillus alutaceus* var. *alutaceus* (formerly *Aspergillus ochraceus*) with altered ochratoxin A production. Appl Environ Microbiol **57**(9): 2487-2491.
Chen, CY and Seguin-Swartz, G (2002). A rapid method for assessing the viability of fungal spores. Can J Plant Pathol **24**(2): 230 - 232.
Chen, X; Li, Y; Du, G and Chen, J (2005). Application of response surface methodology in medium optimization for spore production of *Coniothyrium minitans* in solid-state fermentation. World J Microbiol Biotechnol **21**(4): 593-599.
Christensen, M (1982). The *Aspergillus ochraceus* Group: Two New Species from Western Soils and a Synoptic Key. Mycologia **74**(2): 210-225.
Christensen, RL and Schmit, JC (1980). Regulation and glutamic acid decarboxylase during *Neurospora crassa* conidial germination. J Bacteriol **144**(3): 983-990.
Clark, A; Blissett, K and Oliver, R (2003). Investigating the role of polyols in *Cladosporium fulvum* during growth under hyper-osmotic stress and in planta. Planta **216**(4): 614-619.
Cliquet, S and Jackson, MA (2005). Impact of carbon and nitrogen nutrition on the quality, yield and composition of blastospores of the bioinsecticidal fungus *Paecilomyces fumosoroseus*. J Ind Microbiol Biotechnol **32**(5): 204-210.
Crolla, A and Kennedy, KJ (2001). Optimization of citric acid production from *Candida lipolytica* Y-1095 using n-paraffin. J Biotechnol **89**(1): 27-40.
Da Costa, CE; Comasseto, JV; Crusius, IHS; Andrade, LH and Porto, ALM (2007). Biotransformation of ß-hydroxyphenyl selenides, diphenyldiselenide and benzeneseleninic acid by whole cells of *Aspergillus terreus*. J Mol Catal B-Enzym **45**(3-4): 135-139.
Dague, E; Alsteens, D; Latge, JP and Dufrene, YF (2008). High-resolution cell surface dynamics of germinating *Aspergillus fumigatus* conidia. Biophys J **94**(2): 656-60.
Dahlberg, KR and Etten, JLV (1982). Physiology and Biochemistry of Fungal Sporulation. Annu Rev Phytopathol **20**(1): 281-301.
Davis, RH and Perkins, DD (2002). *Neurospora*: a model of model microbes. Nat Rev Genet **3**(5): 397-403.
Deacon, JW and Mitchell, RT (1985). Toxicity of oat roots, oat root extracts, and saponins to zoospores of *Pythium* spp. and other fungi. T Brit Mycol Soc **84**(3): 479-487.
Demain, AL (2000). Small bugs, big business: the economic power of the microbe. Biotechnol Adv **18**(6): 499-514.
Denk, W; Strickler, JH and Webb, WW (1990). Two-photon laser scanning fluorescence microscopy. Science **248**(4951): 73-76.
Desjardin, DE; Oliveira, AG and Stevani, CV (2008). Fungi bioluminescence revisited. Photoch Photobio Sci **7**(2): 170-182.
Diassi, PA and Westfield, NJ (1970). Hydroxy, Acycloxy, and 11-keto-1,3,5(10),7 Estratetranes. US-Patent.

Dichtel, WR; Serin, JM; Edder, C; Frechet, JMJ; Matuszewski, M; Tan, L-S; Ohulchanskyy, TY and Prasad, PN (2004). Singlet Oxygen Generation via Two-Photon Excited FRET. J Am Chem Soc **126**(17): 5380-5381.

Dijkema, C; Kester, HC and Visser, J (1985). 13C NMR studies of carbon metabolism in the hyphal fungus *Aspergillus nidulans*. PNAS **82**(1): 14-18.

Dillon, RJ and Charnley, AK (1990). Initiation of germination in conidia of the entomopathogenic fungus, *Metarhizium anisopliae*. Mycol Res **94**(3): 299-304.

Dreyer, B; Morte, A; Perez-Gilabert, M and Honrubia, M (2006). Autofluorescence detection of arbuscular mycorrhizal fungal structures in palm roots: an underestimated experimental method. Mycol Res **110**(8): 887-897.

Dulaney, EL; McAleer, WJ; Koslowski, M; Stapley, EO and Jaglom, J (1955a). Hydroxylation of progesterone and 11-desoxy-17-hydroxycorticosterone by *Aspergillus* and *Penicillium*. Appl Microbiol **3**(6): 336-40.

Dulaney, EL; Stapley, EO and Hlavac, C (1955b). Hydroxylation of Steroids, Principally Progesterone, by a Strain of *Aspergillus ochraceus*. Mycologia **47**(4): 464-474.

Dunn, KW and Young, PA (2006). Principles of Multiphoton Microscopy. Nephron Exp Nephrol **103**(2): e33-44.

Dunn, P; Wells, AS and Williams, MT (2010). Green Chemistry in the Pharmaceutical Industry. Weinheim, WILEY-VCH.

Dutta, D; Ghosh, DK; Mishra, AK and Samanta, TB (1983). Induction of benzo(a)pyrene hydroxylase in *Aspergillus ochraceus* TS: Evidences of multiple forms of cytochrome P-450. Biochem Biophys Res Commun **115**(2): 692-699.

Dutta, TK; Datta, J and Samanta, TB (1993). Onset of new catalytic activity in immobilized spores of *Aspergillus ochraceus* TS due to in situ germination: C17-C20 lysis accompanies 11 alpha-hydroxylation of steroid. Biochem Biophys Res Commun **192**(1): 119-23.

Dutta, TK and Samanta, TB (1999). Bioconversion of Progesterone by the Activated Immobilized Conidia of *Aspergillus ochraceus* TS. Curr Microbiol **39**(6): 309-312.

Dynesen, J and Nielsen, J (2003). Surface hydrophobicity of *Aspergillus nidulans* conidiospores and its role in pellet formation. Biotechnol Prog **19**(3): 1049-52.

Eisenman, HC; Mues, M; Weber, SE; Frases, S; Chaskes, S; Gerfen, G and Casadevall, A (2007). *Cryptococcus neoformans* laccase catalyses melanin synthesis from both D- and L-DOPA. Microbiology **153**(12): 3954-3962.

El-Enshasy, H; Hellmuth, K and Rinas, U (1999). Fungal morphology in submerged cultures and its relation to glucose oxidase excretion by recombinant *Aspergillus niger*. Appl Biochem Biotechnol **81**(1): 1-11.

El-Kady, IA and Youssef, MS (1993). Survey of mycoflora and mycotoxins in Egyptian soybean seeds. J Basic Microb **33**(6): 371-378.

Engelkes, CA; Nuclo, RL and Fravel, DR (1997). Effect of Carbon, Nitrogen, and C:N Ratio on Growth, Sporulation, and Biocontrol Efficacy of *Talaromyces flavus*. Phytopathology **87**(5): 500-505.

Fiehn, O (2002). Metabolomics - the link between genotypes and phenotypes. Plant Mol Biol **48**(1): 155-171.

Foerster, CW and Foerster, HF (1973). Glutamic Acid Decarboxylase in Spores of *Bacillus megaterium* and its Possible Involvement in Spore Germination. J Bacteriol **114**(3): 1090-1098.

Fontaine, T; Simenel, C; Dubreucq, G; Adam, O; Delepierre, M; Lemoine, J; Vorgias, CE; Diaquin, M and Latgé, J-P (2000). Molecular Organization of the Alkali-insoluble Fraction of *Aspergillus fumigatus* Cell Wall. J Biol Chem **275**(36): 27594-27607.

Fontaine, T; Magnin, T; Melhert, A; Lamont, D; Latgé, J-P and Ferguson, MAJ (2003). Structures of the glycosylphosphatidylinositol membrane anchors from *Aspergillus fumigatus* membrane proteins. Glycobiology **13**(3): 169-177.

Fontaine, T; Beauvais, A; Loussert, C; Thevenard, B; Fulgsang, CC; Ohno, N; Clavaud, C; Prevost, M-C and Latgé, J-P (2010). Cell wall [alpha]1-3glucans induce the aggregation of germinating conidia of *Aspergillus fumigatus*. Fungal Genet Biol **47**(8): 707-712.

Fried, J; Thoma, RW; Gerke, JR; Herz, JE; Donin, MN and Perlman, D (1952). Oxidation of Steroids by Microorganisms. II. 1 Hydroxylation in Positin 11 and Synthesis of Cortisone from Reichstein's Compound S. J Am Chem Soc **74**(15): 3962-3963.

Friedl, MA; Kubicek, CP and Druzhinina, IS (2008). Carbon Source Dependence and Photostimulation of Conidiation in *Hypocrea atroviridis*. Appl Environ Microbiol **74**(1): 245-250.

Fujita, M; Iwahori, K; Tatsuta, S and Yamakawa, K (1994). Analysis of pellet formation of *Aspergillus niger* based on shear stress. J Ferment Bioeng **78**(5): 368-373.

Galagan, JE; Calvo, SE; Borkovich, KA; Selker, EU; Read, ND; Jaffe, D; FitzHugh, W; Ma, L-J; Smirnov, S; Purcell, S, et al. (2003). The genome sequence of the filamentous fungus *Neurospora crassa*. Nature **422**(6934): 859-868.

Gao, L and Liu, X (2009). A novel two-stage cultivation method to optimize carbon concentration and carbon-to-nitrogen ratio for sporulation of biocontrol fungi. Folia Microbiol **54**(2): 142-146.

Geiser, DM (2009). Sexual structures in *Aspergillus*: morphology, importance and genomics. Med Mycol **47**(s1): S21-S26.
Georgiou, G and Shuler, ML (1986). A computer model for the growth and differentiation of a fungal colony on solid substrate. Biotechnol Bioeng **28**(3): 405-416.
Gerin, PA; Dufrene, Y; Bellon-Fontaine, MN; Asther, M and Rouxhet, PG (1993). Surface properties of the conidiospores of *Phanerochaete chrysosporium* and their relevance to pellet formation. J Bacteriol **175**(16): 5135-5144.
Giepmans, BNG; Adams, SR; Ellisman, MH and Tsien, RY (2006). The Fluorescent Toolbox for Assessing Protein Location and Function. Science **312**(5771): 217-224.
Gil, ML; Casanova, M; Martinez, JP and Sentandreu, R (1991). Antigenic cell wall mannoproteins in *Candida albicans* isolates and in other *Candida* species. J Gen Microbiol **137**(5): 1053-1061.
Gindro, K and Pezet, R (2001). Effects of long-term storage at different temperatures on conidia of *Botrytis cinerea*. FEMS Microbiol Lett **204**(1): 101-104.
Giulivi, C; Kato, K and Cooper, CE (2006). Nitric oxide regulation of mitochondrial oxygen consumption I: cellular physiology. Am J Physiol Cell Physiol **291**(6): C1225-1231.
Göppert-Mayer, M (1931). Über Elementarakte mit zwei Quantensprüngen. Ann Phys **401**(3): 273-294.
Gouterman, M (1961). Spectra of porphyrins. J Mol Spectrosc **6**: 138-163.
Grimm, LH; Kelly, S; Hengstler, J; Göbel, A; Krull, R and Hempel, DC (2004). Kinetic studies on the aggregation of *Aspergillus niger* conidia. Biotechnol Bioeng **87**(2): 213-218.
Grimm, LH; Kelly, S; Krull, R and Hempel, DC (2005a). Morphology and productivity of filamentous fungi. Appl Microbiol Biotechnol **69**(4): 375-84.
Grimm, LH; Kelly, S; Völkerding, II; Krull, R and Hempel, DC (2005b). Influence of mechanical stress and surface interaction on the aggregation of *Aspergillus niger* conidia. Biotechnol Bioeng **92**(7): 879-888.
Guzmán-de-Peña, D; Aguirre, J and Ruiz-Herrera, J (1998). Correlation between the regulation of sterigmatocystin biosynthesis and asexual and sexual sporulation in *Emericella nidulans*. A van Leeuw J Microb **73**(2): 199-205.
Hall, RA; Peterkin, DD; Ali, B and Lopez, VF (1994). Influence of culture age on rate of conidiospore germination in four deuteromycetous entomogenous fungi. Mycol Res **98**(7): 763-768.
Hallsworth, JE and Magan, N (1994). Effect of carbohydrate type and concentration on polyhydroxy alcohol and trehalose content of conidia of three entomopathogenic fungi. Microbiol **140**(10): 2705-2713.
Hallsworth, JE and Magan, N (1995). Manipulation of intracellular glycerol and erythritol enhances germination of conidia at low water availability. Microbiol **141**(5): 1109-1115.
Hallsworth, JE and Magan, N (1996). Culture Age, Temperature, and pH Affect the Polyol and Trehalose Contents of Fungal Propagules. Appl Environ Microbiol **62**(7): 2435-2442.
Harman, GE; Jin, X; Stasz, TE; Peruzzotti, G; Leopold, AC and Taylor, AG (1991). Production of conidial biomass of *Trichoderma harzianum* for biological control. Biol Control **1**(1): 23-28.
Haugland, RP (2005). A Guide to Fluorescent Probes and Labeling Technologies. Eugene, USA, Molecular Probes.
Hawker, LE (1965). Fine structure of fungi as revealed by electron microscopy. Biol Rev **40**(1): 52-91.
He, X; Wang, Y; Hu, H; Wu, Y and Zeng, X (2010). Novel bioconversion products of andrographolide by *Aspergillus ochraceus* and their cytotoxic activities against human tumor cell lines. J Mol Catal B-Enzym **68**(1): 89-93.
Helmchen, F and Denk, W (2005). Deep tissue two-photon microscopy. Nat Methods **2**(12): 932-940.
Herzenberg, LA; Parks, D; Sahaf, B; Perez, O; Roederer, M and Herzenberg, LA (2002). The history and future of the fluorescence activated cell sorter and flow cytometry: a view from Stanford. Clin Chem **48**(10): 1819-27.
Hibbett, DS; Binder, M; Bischoff, JF; Blackwell, M; Cannon, PF; Eriksson, OE; Huhndorf, S; James, T; Kirk, PM; Lücking, R, et al. (2007). A higher-level phylogenetic classification of the Fungi. Mycol Res **111**(5): 509-547.
Hildebrandt, H (1994). Pschyrembel Klinisches Wörterbuch. Berlin, Verlag Walter de Gruyter.
Hille, A; Neu, TR; Hempel, DC and Horn, H (2005). Oxygen profiles and biomass distribution in biopellets of *Aspergillus niger*. Biotechnol Bioeng **92**(5): 614-23.
Hirshfield, KM; Toptygin, D; Packard, BS and Brand, L (1993). Dynamic Fluorescence Measurements of Two-State Systems: Applications to Calcium-Chelating Probes. Anal Biochem **209**(2): 209-218.
Hobot, JA and Gull, K (1981a). Structure and biochemistry of the spore surface of *Syncephalastrum racemosum*. Curr Microbiol **5**(3): 183-185.
Hobot, JA and Gull, K (1981b). Changes in the organisation of surface rodlets during germination of *Syncephalastrum racemosum* sporangiospores. Protoplasma **107**(3): 339-343.
Hogan, DA (2006). Talking to Themselves: Autoregulation and Quorum Sensing in Fungi. Eukaryot Cell **5**(4): 613-619.
Hölker, U and Lenz, J (2005). Solid-state fermentation - are there any biotechnological advantages? Curr Opin Microbiol **8**(3): 301-306.

Holland, HL and Weber, HK (2000). Enzymatic hydroxylation reactions. Curr Opin Biotechnol **11**(6): 547-53.
Huffman, JA; Treutlein, B and Pöschl, U (2009). Fluorescent biological aerosol particle concentrations and size distributions measured with an Ultraviolet Aerodynamic Particle Sizer (UV-APS) in Central Europe. Atmos Chem Phys **10**: 3215-3233.
Imanishi, Y; Lodowski, KH and Koutalos, Y (2007). Two-Photon Microscopy: Shedding Light on the Chemistry of Vision. Biochemistry **46**(34): 9674-9684.
Jackson, MA and Bothast, RJ (1990). Carbon Concentration and Carbon-to-Nitrogen Ratio Influence Submerged-Culture Conidiation by the Potential Bioherbicide *Colletotrichum truncatum* NRRL 13737. Appl Environ Microbiol **56**(11): 3435-3438.
Jackson, MA and Schisler, DA (1992). The Composition and Attributes of *Colletotrichum truncatum* Spores Are Altered by the Nutritional Environment. Appl Environ Microbiol **58**(7): 2260-2265.
Janssen, MHA (2006). Properties of immobilised penicillin G Acylase in beta-lactam antibiotic synthesis. Delft, Technische Universiteit Delft.
Jeraj, N; Lenasi, H and Breskvar, K (2005). The involvement of cAMP in the growth inhibition of filamentous fungus *Rhizopus nigricans* by steroids. FEMS Microbiol Lett **242**(1): 147-154.
Jin, Y; Bok, JW; Guzman-de-Peña, D and Keller, NP (2002). Requirement of spermidine for developmental transitions in *Aspergillus nidulans*. Mol Microbiol **46**(3): 801-812.
Kanaani, H; Hargreaves, M; Smith, J; Ristovski, Z; Agranovski, V and Morawska, L (2008). Performance of UVAPS with respect to detection of airborne fungi. J Aerosol Sci **39**(2): 175-189.
Kardinahl, S; Rabelt, D and Reschke, M (2006). Biotransformation: Von der Vision zur Technologie! Chem Ing Tech **78**(3): 209-217.
Kawanabe, Y (1986). Responsiveness of *Neurospora crassa* conidia to auxin and gibberellin in relation to culture age. Agr Biol Chem **50**(3): 757-758.
Kershaw, MJ and Talbot, NJ (1998). Hydrophobins and Repellents: Proteins with Fundamental Roles in Fungal Morphogenesis. Fungal Genet Biol **23**(1): 18-33.
Kniemeyer, O; Lessing, F; Scheibner, O; Hertweck, C and Brakhage, A (2006). Optimisation of a 2-D gel electrophoresis protocol for the human-pathogenic fungus *Aspergillus fumigatus*. Curr Genet **49**(3): 178-189.
Koolman, J and Röhm, K-H (1998). Taschenatlas der Biochemie. Stuttgart, Georg Thieme Verlag.
Kouskoumvekaki, I; Yang, Z; Jonsdottir, S; Olsson, L and Panagiotou, G (2008). Identification of biomarkers for genotyping Aspergilli using non-linear methods for clustering and classification. BMC Bioinformatics **9**(59): 1-11.
Kozakiewicz, Z (1990). CMI Descriptions of Pathogenic Fungi and Bacteria. Mycopathologia **109**(3): 183-202.
Krasniewski, I; Molimard, P; Feron, G; Vergoignan, C; Durand, A; Cavin, J-F and Cotton, P (2006). Impact of solid medium composition on the conidiation in *Penicillium camemberti*. Process Biochem **41**(6): 1318-1324.
Krull, R; Cordes, C; Horn, H; Kampen, I; Kwade, A; Neu, TR and Nörtemann, B (2010). Morphology of filamentous fungi - Linking cellular biology to process engineering using *Aspergillus niger*. Biosystems Engineering II – Linking Cellular Networks and Bioprocesses. Eds.: C. Wittmann and R. Krull. Heidelberg, Springer Verlag. **121**.
Kubicek, CP; Hampel, W and Röhr, M (1979). Manganese deficiency leads to elevated amino acid pools in citric acid accumulating *Aspergillus niger*. Arch Microbiol **123**(1): 73-79.
Kumar, S and Punekar, NS (1997). The metabolism of 4-aminobutyrate (GABA) in fungi. Mycol Res **101**(4): 403-409.
Kwak, MY and Rhee, JS (1992). Cultivation characteristics of immobilized *Aspergillus oryzae* for kojic acid production. Biotechnol Bioeng **39**(9): 903-906.
Laflamme, C; Verreault, D; Lavigne, S; Trudel, L; Ho, J and Duchaine, C (2005). Autofluorescence as a viability marker for detection of bacterial spores. Front Biosci **10**: 1647-53.
Laflamme, C; Verreault, D; Ho, J and Duchaine, C (2006). Flow cytometry sorting protocol of *Bacillus* spore using ultraviolet laser and autofluorescence as main sorting criterion. J Fluoresc **16**(6): 733-7.
Lai, T; Li, B; Qin, G and Tian, S (2011). Oxidative Damage Involves in the Inhibitory Effect of Nitric Oxide on Spore Germination of *Penicillium expansum*. Current Microbiology **62**(1): 229-234.
Laible, PD; Knox, RS and Owens, TG (1998). Detailed Balance in Förster-Dexter Excitation Transfer and Its Application to Photosynthesis. J Phys Chem B **102**(9): 1641-1648.
Lakowicz, JR; Szmacinski, H; Nowaczyk, K and Johnson, ML (1992). Fluorescence lifetime imaging of free and protein-bound NADH. PNAS **89**(4): 1271-1275.
Lakowicz, JR (2006). Principles of Fluorescence Spectroscopy: 3e. Berlin, Springer.
Lamarre, C; Sokol, S; Debeaupuis, J-P; Henry, C; Lacroix, C; Glaser, P; Coppee, J-Y; Francois, J-M and Latge, J-P (2008). Transcriptomic analysis of the exit from dormancy of *Aspergillus fumigatus* conidia. BMC Genomics **9**(1): 417.

Lane, BS; Humphreys, AM; Thompson, K and Trinci, APJ (1988). ATP content of stored spores of *Paecilomyces farinosus* and the use of ATP as a criterion of spore viability. T Brit Mycol Soc **90**(1): 109-111.

Larroche, C (1996). Microbial growth and sporulation behaviour in solid state fermentation. J Sci Ind Res **55**(5-6): 408-423.

Larroche, C and Gros, J-B (1997). Special transformation processes using fungal spores and immobilized cells. Adv Biochem Eng/Biotechnol **55**: 179-220.

Larsen, TO; Gareis, M and Frisvad, JC (2002). Cell Cytotoxicity and Mycotoxin and Secondary Metabolite Production by Common Penicillia on Cheese Agar. J Agric Food Chem **50**(21): 6148-6152.

Latgé, J-P (2007). The cell wall: a carbohydrate armour for the fungal cell. Mol Microbiol **66**(2): 279-290.

Latgé, JP; Bouziane, H and Diaquin, M (1988). Ultrastructure and composition of the conidial wall of *Cladosporium cladosporioides*. Can J Microbiol **34**(12): 1325-1329.

Lax, AR; Templeton, GE and Meyer, WL (1985). Isolation, Purification, and Biological Activity of a Self-Inhibitor from Conidia of *Colletotrichum gloeosporioides*. Phytopathology **75**(4): 386-390.

Leroy, D; HerichE, J-K; Filhol, O; Chambaz, EM and Cochet, C (1997). Binding of Polyamines to an Autonomous Domain of the Regulatory Subunit of Protein Kinase CK2 Induces a Conformational Change in the Holoenzyme. J Biol Chem **272**(33): 20820-20827.

Liewen, MB and Marth, EH (1985). Viability and ATP content of conidia of sorbic acid-sensitive and-resistant strains of *Penicillium roqueforti* after exposure to sorbic acid. Appl Microbiol Biotechnol **21**(1): 113-117.

Lin, P-J; Scholz, A and Krull, R (2010). Effect of volumetric power input by aeration and agitation on pellet morphology and product formation of *Aspergillus niger*. Biochem Eng J **49**(2): 213-220.

Lin, S-J and Guarente, L (2003). Nicotinamide adenine dinucleotide, a metabolic regulator of transcription, longevity and disease. Curr Opin Cell Biol **15**(2): 241-246.

Lin, S-J; Tan, H-Y; Kuo, C-J; Wu, R-J; Wang, S-H; Chen, W-L; Jee, S-H and Dong, C-Y (2009). Multiphoton autofluorescence spectral analysis for fungus imaging and identification. Appl Phys Lett **95**(4): 043703-3.

Lingappa, BT; Lingappa, Y and Bell, E (1973). A self-inhibitor of protein synthesis in the conidia of *Glomerella cingulata*. Arch Microbiol **94**(2): 97-107.

Lodish, H; Berk, A; Zipursky, SL; Matsudaira, P; Baltimore, D and Darnell, J (2000). Molecular Cell Biology. New York, W. H. Freeman and Co.

Lopez-Ribot, JL; Casanova, M; Martinez, JP and Sentandreu, R (1991). Characterization of cell wall proteins of yeast and hydrophobic mycelial cells of *Candida albicans*. Infect Immun **59**(7): 2324-2332.

Lottspeich, F and Engels, JW (2006). Bioanalytik. Heidelberg, Spektrum Akad. Verlag.

Ludemann, V; Greco, M; Rodriguez, MP; Basilico, JC and Pardo, AG (2010). Conidial production by *Penicillium nalgiovense* for use as starter cultures in dry fermented sausages by solid state fermentation. LWT Food Sci Technol **43**(2): 315-318.

Mahato, SB and Garai, S (1997). Advances in microbial steroid biotransformation. Steroids **62**(4): 332-345.

Mainen, ZF; Maletic-Savatic, M; Shi, SH; Hayashi, Y; Malinow, R and Svoboda, K (1999). Two-Photon Imaging in Living Brain Slices. Methods **18**(2): 231-239.

Maus, M; Rousseau, E; Cotlet, M; Schweitzer, G; Hofkens, J; Van der Auweraer, M; De Schryver, FC and Krueger, A (2001). New picosecond laser system for easy tunability over the whole ultraviolet/visible/near infrared wavelength range based on flexible harmonic generation and optical parametric oscillation. Rev Sci Instrum **72**(1): 36-40.

McIntyre, M; Dynesen, J and Nielsen, J (2001). Morphological characterization of *Aspergillus nidulans*: growth, septation and fragmentation. Microbiol **147**(1): 239-246.

Meredith, P and Riesz, J (2004). Radiative relaxation quantum yields for synthetic eumelanin. Photochem Photobiol **79**(2): 211-6.

Metz, B and Kossen, NWF (1977). The growth of molds in the form of pellets - a literature review. Biotechnol Bioeng **19**(6): 781-799.

Mizeret, J (1998). Cancer detection by endoscopic frequency-domain fluorescence lifetime imaging. Lausanne, École Polytechnique Federale de Lausanne. **PhD**.

Moo-Young, M; Moreira, AR and Tengerdy, RP (1983). Principles of solid-substrate fermentation. The filamentous fungi. Eds.: J. E. Smith, D. R. Berry and B. Kristiansen. London, Arnold. **4:** 117.

Morgenthal, K; Wienkoop, S; Scholz, M; Selbig, J and Weckwerth, W (2005). Correlative GC-TOF-MS-based metabolite profiling and LC-MS-based protein profiling reveal time-related systemic regulation of metabolite-protein networks and improve pattern recognition for multiple biomarker selection. Metabolomics **1**(2): 109-121.

Morris, SC and Nicholls, PJ (1978). An Evaluation of Optical Density to Estimate Fungal Spore Concentrations in Water Suspensions. Phytopathology **68**(8): 1240-1242.

Mouyna, I; Fontaine, T; Vai, M; Monod, M; Fonzi, WA; Diaquin, M; Popolo, L; Hartland, RP and Latge, JP (2000). Glycosylphosphatidylinositol-anchored glucanosyltransferases play an active role in the biosynthesis of the fungal cell wall. J Biol Chem **275**(20): 14882-9.

Muñoz, GA; Agosin, E; Cotoras, M; Martin, RS and Volpe, D (1995). Comparison of aerial and submerged spore properties for *Trichoderma harzianum*. FEMS Microbiol Lett **125**(1): 63-69.

Nanou, K; Roukas, T and Kotzekidou, P (2007). Role of hydrolytic enzymes and oxidative stress in autolysis and morphology of *Blakeslea trispora* during β-carotene production in submerged fermentation. Appl Microbiol Biotechnol **74**(2): 447-453.

Nelson, DL and Cox, M (2005). Lehninger Biochemie. Berlin, Springer.

Nielsen, N-PV; Smedsgaard, J and Frisvad, JC (1999). Full Second-Order Chromatographic/Spectrometric Data Matrices for Automated Sample Identification and Component Analysis by Non-Data-Reducing Image Analysis. Anal Chem **71**(3): 727-735.

Niesner, R; Peker, B; Schluesche, P and Gericke, K-H (2004). Noniterative Biexponential Fluorescence Lifetime Imaging in the Investigation of Cellular Metabolism by Means of NAD(P)H Autofluorescence. ChemPhysChem **5**(8): 1141-1149.

Nighswander-Rempel, SP; Riesz, J; Gilmore, J; Bothma, JP and Meredith, P (2005). Quantitative fluorescence excitation spectra of synthetic eumelanin. J Phys Chem B **109**(43): 20629-35.

Nofsinger, JB and Simon, JD (2001). Radiative Relaxation of Sepia Eumelanin is Affected by Aggregation. Photochem Photobiol **74**(1): 31-37.

Nsoukpoe-Kossi, CN; Ouameur, AA; Thomas, T; Shirahata, A; Thomas, TJ and Tajmir-Riahi, HA (2008). DNA Interaction with Antitumor Polyamine Analogues: A Comparison with Biogenic Polyamines. Biomacromolecules **9**(10): 2712-2718.

O'Callaghan, J; Caddick, MX and Dobson, ADW (2003). A polyketide synthase gene required for ochratoxin A biosynthesis in *Aspergillus ochraceus*. Microbiology **149**(12): 3485-3491.

O'Callaghan, J; Stapleton, PC and Dobson, AD (2006). Ochratoxin A biosynthetic genes in *Aspergillus ochraceus* are differentially regulated by pH and nutritional stimuli. Fungal Genet Biol **43**(4): 213-21.

Obaidi, ZS and Berry, DR (1980). cAMP concentration, morphological differentiation and citric acid production in *Aspergillus niger*. Biotechnol Lett **2**(1): 5-10.

Ooijkaas, LP; Ifoeng, CJ; Tramper, J and Buitelaar, RM (1998). Spore Production of *Coniothyrium minitans* during Solid-State Fermentation on Different Nitrogen Sources with Glucose or Starch as Carbon Source. Biotechnol Lett **20**(8): 785-788.

Ooijkaas, LP; Wilkinson, EC; Tramper, J and Buitelaar, RM (1999). Medium optimization for spore production of *Coniothyrium minitans* using statistically-based experimental designs. Biotechnol Bioeng **64**(1): 92-100.

Ormerod, MG (2000). Flow cytometry: a practical approach. Oxford, Oxford University Press.

Paoli, J; Smedh, M; Wennberg, A-M and Ericson, MB (2007). Multiphoton Laser Scanning Microscopy on Non-Melanoma Skin Cancer: Morphologic Features for Future Non-Invasive Diagnostics. J Invest Dermatol **128**(5): 1248-1255.

Papagianni, M and Moo-Young, M (2002). Protease secretion in glucoamylase producer *Aspergillus niger* cultures: fungal morphology and inoculum effects. Process Biochem **37**: 1271-1278.

Papagianni, M (2004). Fungal morphology and metabolite production in submerged mycelial processes. Biotechnol Adv **22**(3): 189-259.

Paris, S; Debeaupuis, J-P; Crameri, R; Carey, M; Charles, F; Prevost, MC; Schmitt, C; Philippe, B and Latgé, JP (2003). Conidial Hydrophobins of *Aspergillus fumigatus*. Appl Environ Microbiol **69**(3): 1581-1588.

Parshetti, GK; Kalme, SD; Gomare, SS and Govindwar, SP (2007). Biodegradation of Reactive blue-25 by *Aspergillus ochraceus* NCIM-1146. Bioresource Technol **98**(18): 3638-3642.

Pascual, S; De Cal, A; Magan, N and Melgarejo, P (2000). Surface hydrophobicity, viability and efficacy in biological control of *Penicillium oxalicum* spores produced in aerial and submerged culture. J Appl Microbiol **89**(5): 847-853.

Pascual, S; Melgarejo, P and Magan, N (2003). Water availability affects the growth, accumulation of compatible solutes and the viability of the biocontrol agent *Epicoccum nigrum*. Mycopathologia **156**(2): 93-100.

Peterson, DH and Murray, HC (1952). Microbiological Oxygenation of Steroids at Carbon 11. J Am Chem Soc **74**(7): 1871-1872.

Pollak, N; Doelle, C and Ziegler, M (2007). The power to reduce: pyridine nucleotides - small molecules with a multitude of functions. Biochem J **402**(2): 205-218.

Porcel, E; López, J; Ferrón, M; Pérez, J; Sánchez, J and Chisti, Y (2006). Effects of the sporulation conditions on the lovastatin production by *Aspergillus terreus*. Bioproc Biosyst Eng **29**(1): 1-5.

Powell, JF and Strange, RE (1953). Biochemical changes occurring during the germination of bacterial spores. Biochem J **54**(2): 205-209.

Przybylski, KS and Bullerman, LB (1980). Influence of sorbic acid on viability and ATP content of conidia of *Aspergillus parasiticus*. J Food Sci **45**(2): 375-376.

Punt, PJ; van Biezen, N; Conesa, A; Albers, A; Mangnus, J and van den Hondel, C (2002). Filamentous fungi as cell factories for heterologous protein production. Trends Biotechnol **20**(5): 200-6.
Rahardjo, YSP; Korona, D; Haemers, S; Weber, FJ; Tramper, J and Rinzema, A (2004). Limitations of membrane cultures as a model solid-state fermentation system. Lett Appl Microbiol **39**(6): 504-508.
Rakotonirainy, MS; Heraud, C and Lavedrine, B (2003). Detection of viable fungal spores contaminant on documents and rapid control of the effectiveness of an ethylene oxide disinfection using ATP assay. Luminescence **18**(2): 113-21.
Rittle, J and Green, MT (2010). Cytochrome P450 Compound I: Capture, Characterization, and C-H Bond Activation Kinetics. Science **330**(6006): 933-937.
Roessner, U; Wagner, C; Kopka, J; Trethewey, RN and Willmitzer, L (2000). Simultaneous analysis of metabolites in potato tuber by gas chromatography-mass spectrometry. Plant J **23**(1): 131-142.
Rubart, M (2004). Two-Photon Microscopy of Cells and Tissue. Circ Res **95**(12): 1154-1166.
Ruelle, P; Farina-Cuendet, A and Kesselring, UW (1997). The mobile order solubility equation applied to polyfunctional molecules: The non-hydroxysteroids in aqueous and non aqueous solvents. Int J Pharm **157**(2): 219-232.
Ruelle, P; Fariña-Cuendet, A and Kesselring, U (2000). Hydrophobic and solvation effects on the solubility of hydroxysteroids in various solvents: Quantitative and qualitative assessment by application of the mobile order and disorder theory. Perspect Drug Discov **18**(1): 61-112.
Ruijter, GJ; Bax, M; Patel, H; Flitter, SJ; van de Vondervoort, PJ; de Vries, RP; vanKuyk, PA and Visser, J (2003). Mannitol is required for stress tolerance in *Aspergillus niger* conidiospores. Eukaryot Cell **2**(4): 690-8.
Rydjord, B; Namork, E; Nygaard, UC; Wiker, HG and Hetland, G (2007). Quantification and characterisation of IgG binding to mould spores by flow cytometry and scanning electron microscopy. J Immunol Methods **323**(2): 123-31.
Samanta, TB and Ghosh, DK (1987). Characterization of progesterone 11 alpha-hydroxylase of *Aspergillus ochraceus* TS: a cytochrome P-450 linked monooxygenase. J Steroid Biochem **28**(3): 327-32.
Saratale, GD; Kalme, SD and Govindwar, SP (2006). Decolorisation of textile dyes by *Aspergillus ochraceus* (NCIM-1146) Indian J Biotechnol **5**(3): 407-410.
Schisler, DA; Jackson, MA and Bothast, RJ (1991). Influence of nutrition during conidiation of *Colletotrichum truncatum* on conidial germination and efficacy in inciting disease in *Sesbania exaltata*. Phytopathology **81**: 458-461.
Schleg, MC and Knight, SG (1962). The Hydroxylation of Progesterone by Conidia from *Aspergillus ochraceus*. Mycologia **54**(3): 317-319.
Schwantes, HO (1996). Biologie der Pilze. Stuttgart, Verlag Eugen Ulmer.
Schweitzer, D; Quick, S; Klemm, M; Hammer, M; Jentsch, S and Dawczynski, J (2010). Zeitaufgelöste Autofluoreszenz bei retinalen Gefäßverschlüssen. Ophthalmologe **37**: 1-8.
Scott, DW (1979). On optimal and data-based histograms. Biometrika **66**(3): 605-610.
Scott, TG; Spencer, RD; Leonard, NJ and Weber, G (1970). Synthetic spectroscopic models related to coenzymes and base pairs. V. Emission properties of NADH. Studies of fluorescence lifetimes and quantum efficiencies of NADH, AcPyADH, [reduced acetylpyridineadenine dinucleotide] and simplified synthetic models. J Am Chem Soc **92**(3): 687-695.
Secrist, JA; Barrio, JR; Leonard, NJ and Weber, G (1972). Fluorescent modification of adenosine-containing coenzymes. Biological activities and spectroscopic properties. Biochemistry **11**(19): 3499-3506.
Sharma, R; Katoch, M; Srivastava, P and Qazi, G (2009). Approaches for refining heterologous protein production in filamentous fungi. World J Microbiol Biotechnol **25**(12): 2083-2094.
Shibahara, M; Moody, JA and Smith, LL (1970). Microbial hydroxylations V. 11-alpha-hydroxylation of progesterone by cell-free preparations of *Aspergillus ochraceus*. Biochim Biophys Acta, Lipids Lipid Metab **202**(1): 172-179.
Shih, I-L and Van, Y-T (2001). The production of poly-([gamma]-glutamic acid) from microorganisms and its various applications. Bioresource Technol **79**(3): 207-225.
Shull, GM and Kita, DA (1955). Microbiological Conversion of Steroids. I. Introduction of the 11-beta-Hydroxyl Group into C21 Steroids. J Am Chem Soc **77**(3): 763-764.
Solomon, PS; Waters, ODC; Jörgens, CI; Lowe, RGT; Rechberger, J; Trengove, RD and Oliver, RP (2006). Mannitol is required for asexual sporulation in the wheat pathogen *Stagonospora nodorum* (glume blotch). Biochem J **399**(2): 231-239.
Solomon, PS; Waters, ODC and Oliver, RP (2007). Decoding the mannitol enigma in filamentous fungi. Trends Microbiol **15**(6): 257-262.
Stopa, PJ (2000). The flow cytometry of *Bacillus anthracis* spores revisited. Cytometry **41**(4): 237-44.
Strange, RE and Powell, JF (1954). Hexosamine-containing peptides in spores of *Bacillus subtilis*, *B. megaterium* and *B. cereus*. Biochem J **58**(1): 80-87.
Stratton, GW (1985). The influence of solvent type on solvent-pesticide interactions in bioassays. Arch Environ Con Tox **14**(6): 651-658.

Sugata, K; Sakai, S; Noriaki, N; Osanai, O; Kitahara, T and Takema, Y (2010). Imaging of melanin distribution using multiphoton autofluorescence decay curves. Skin Res Technol **16**(1): 55-59.
Sulc, M; Peslova, K; Zabka, M; Hajduch, M and Havlicek, V (2009). Biomarkers of *Aspergillus* spores: Strain typing and protein identification. Int J Mass Spectrom **280**(1-3): 162-168.
Sumner, LW; Mendes, P and Dixon, RA (2003). Plant metabolomics: large-scale phytochemistry in the functional genomics era. Phytochemistry **62**(6): 817-836.
Svoboda, K and Yasuda, R (2006). Principles of Two-Photon Excitation Microscopy and Its Applications to Neuroscience. Neuron **50**(6): 823-839.
Swe, KH; Alimon, AR and Ramin, M (2009). Effect of Delaying Sporulation by Addition of Ammonium Sulphate on the Fermentation of Palm Kernal Cake Based Substrate by *Aspergillus niger*. Am J Agr Biol Sci **4**(4): 262-265.
Takahashi, J and Yamada, K (1959). Studies on the effect of some physical conditions on the submerged mold culture: Part II. On the two types of pellet formation in the shaking culture. J Agr Chem Soc Jpn **33**: 707–709.
Tereshina, VM; Kovtunenko, AV; Memorskaya, AS and Feofilova, EP (2004). Effect of Carbohydrate Composition of the Cytosol of *Aspergillus niger* Conidia on Their Viability During Storage. Appl Biochem Microbiol **40**(5): 454-459.
Timberlake, WE (1990). Molecular Genetics of *Aspergillus* Development. Annu Rev Genet **24**(1): 5-36.
Tran, ML; Powell, BJ and Meredith, P (2006). Chemical and structural disorder in eumelanins: a possible explanation for broadband absorbance. Biophys J **90**(3): 743-52.
Tung, JW; Heydari, K; Tirouvanziam, R; Sahaf, B; Parks, D, R.; Herzenberg, L, A. and Herzenberg, L, A. (2007). Modern flow cytometry : A practical approach. Clin Lab Med **27**: 453-468.
Tyo, KE; Alper, HS and Stephanopoulos, GN (2007). Expanding the metabolic engineering toolbox: more options to engineer cells. Trends Biotechnol **25**(3): 132-137.
van der Aa, BC; Asther, M and Dufrêne, YF (2002). Surface properties of *Aspergillus oryzae* spores investigated by atomic force microscopy. Colloid Surface B **24**(3-4): 277-284.
Van Der Merwe, KJ; Steyn, PS; Fourie, L; Scott, DB and Theron, JJ (1965). Ochratoxin A, a Toxic Metabolite produced by *Aspergillus ochraceus* Wilh. Nature **205**(4976): 1112-1113.
Veech, RL; Eggleston, LV and Krebs, HA (1969). The redox state of free nicotinamide-adenine dinucleotide phosphate in the cytoplasm of rat liver. Biochem J **115**(4): 609-619.
Vega, FE; Jackson, MA; Mercadier, G and Poprawski, TJ (2003). The impact of nutrition on spore yields for various fungal entomopathogens in liquid culture. World J Microbiol Biotechnol **19**(4): 363-368.
Velez, H; Glassbrook, NJ and Daub, ME (2007). Mannitol metabolism in the phytopathogenic fungus *Alternaria alternata*. Fungal Genet Biol **44**(4): 258-268.
Verma, M; Brar, SK; Tyagi, RD; Surampalli, RY and Valéro, JR (2007). Antagonistic fungi, *Trichoderma* spp.: Panoply of biological control. Biochem Eng J **37**(1): 1-20.
Vesper, S; McKinstry, C; Hartmann, C; Neace, M; Yoder, S and Vesper, A (2008). Quantifying fungal viability in air and water samples using quantitative PCR after treatment with propidium monoazide (PMA). J Microbiol Meth **72**(2): 180-184.
Vezina, C; Sehgal, SN and Singh, K (1963). Transformation of Steroids by Spores of Microorganisms: I. Hydroxylation of Progesterone by Conidia of *Aspergillus ochraceus*. Appl Environ Microbiol **11**(1): 50-57.
Villas-Bôas, SG; Delicado, DG; Åkesson, M and Nielsen, J (2003). Simultaneous analysis of amino and nonamino organic acids as methyl chloroformate derivatives using gas chromatography-mass spectrometry. Anal Biochem **322**(1): 134-138.
Villas-Bôas, SG; Mas, S; Åkesson, M; Smedsgaard, J and Nielsen, J (2005). Mass spectrometry in metabolome analysis. Mass Spectrom Rev **24**(5): 613-646.
Vishwasrao, HD; Heikal, AA; Kasischke, KA and Webb, WW (2005). Conformational Dependence of Intracellular NADH on Metabolic State Revealed by Associated Fluorescence Anisotropy. J Biol Chem **280**(26): 25119-25126.
Walsh, JE (1950). Some Nonparametric Tests of Whether the Largest Observations of a Set are too Large or too Small. Ann Math Stat **21**(4): 583-592.
Wang, XF; Kitajima, S; Uchida, T; Coleman, DM and Minami, S (1990). Time-Resolved Fluorescence Microscopy Using Multichannel Photon Counting. Appl Spectrosc **44**: 25-30.
Wessels, JGH; de Vries, OMH; Asgeirsdottir, SA and Schuren, FHJ (1991). Hydrophobin Genes Involved in Formation of Aerial Hyphae and Fruit Bodies in *Schizophyllum*. Plant Cell **3**(8): 793-799.
Wolken, WAM; Tramper, J and van der Werf, MJ (2003). What can spores do for us? Trends Biotechnol **21**(8): 338-345.
Wösten, HAB (2001). Hydrophobins: Multipurpose Proteins. Annu Rev Microbiol **55**(1): 625-646.
Wucherpfennig, T; Kiep, KA; Driouch, H; Wittmann, C and Krull, R (2010). Morphology and Rheology in Filamentous Cultivations. Advances in Applied Microbiology. Eds.: A. I. Laskin, S. Sariaslani and G. M. Gadd. Burlington, Academic Press. **Volume 72:** 89-136.

Xu, C; Zipfel, W; Shear, JB; Williams, RM and Webb, WW (1996). Multiphoton fluorescence excitation: new spectral windows for biological nonlinear microscopy. PNAS **93**(20): 10763-10768.
Xu, J-R (2000). MAP Kinases in Fungal Pathogens. Fungal Genet Biol **31**(3): 137-152.
Ying, SH and Feng, MG (2006). Medium components and culture conditions affect the thermotolerance of aerial conidia of fungal biocontrol agent *Beauveria bassiana*. Lett Appl Microbiol **43**(3): 331-335.
Ying, W (2008). NAD^+/NADH and $NADP^+$/NADPH in Cellular Functions and Cell Death: Regulation and Biological Consequences. Antioxid Redox Sign **10**(2): 179-206.
Yu, Q and Heikal, AA (2009). Two-photon autofluorescence dynamics imaging reveals sensitivity of intracellular NADH concentration and conformation to cell physiology at the single-cell level. J Photochem Photobiol B **95**(1): 46-57.
Yu, X; Hallett, SG; Sheppard, J and Watson, AK (1997). Application of the Plackett-Burman experimental design to evaluate nutritional requirements for the production of *Colletotrichum coccodes* spores. Appl Microbiol Biotechnol **47**(3): 301-305.
Yuste, R (2005). Fluorescence microscopy today. Nat Methods **2**(12): 902-904.
Zhang, Q; Piston, DW and Goodman, RH (2002). Regulation of Corepressor Function by Nuclear NADH. Science **295**(5561): 1895-1897.
Zipfel, WR; Williams, RM; Christie, R; Nikitin, AY; Hyman, BT and Webb, WW (2003a). Live tissue intrinsic emission microscopy using multiphoton-excited native fluorescence and second harmonic generation. PNAS **100**(12): 7075-80.
Zipfel, WR; Williams, RM and Webb, WW (2003b). Nonlinear magic: multiphoton microscopy in the biosciences. Nat Biotechnol **21**(11): 1369-77.

7.2 List of metabolites

Tab 7.1. Detected metabolites, their retention index (RI), quantifying mass (QM) and occurrence (y = present, 0 = not found). Sorted by RI.

Metabolite	RI	QM	Category	Fresh	Stored	Germinating
Pyruvic acid	1036.7	174	Glycolysis/TCA (and related)	0	y	y
Lactic acid	1042.8	117	Glycolysis/TCA (and related)	0	y	y
Glycolic acid	1062.3	205 +177	Glycolysis/TCA (and related)	y	y	y
Alanine	1086.6	116	Amino acid (and related)	0	y	y
Butyro-1,4-lactam	1142.7	142	Amino acid (and related)	0	y	0
Unknown RI 1163	1164.2	84	unknown	y	y	y
Succinic semialdehyde	1178.8	113	Glycolysis/TCA (and related)	0	0	y
Valine	1207.8	144 +218	Amino acid (and related)	0	y	y
Butanoic acid	1231.0	147	Glycolysis/TCA (and related)	0	0	y
Unknown #sst-cgl-008	1237.6	110	unknown	0	0	y
Urea	1241.9	189 +171	Amino acid (and related)	0	y	0
Serine	1255.1	116 +132	Amino acid (and related)	0	y	y
Glycerol	1267.2	205	Fat (and related)	y	y	y
Phosphoric acid	1267.9	299	Multiple Functions	y	y	y
Nicotinic acid	1279.1	106	Vitamin	y	y	y
Threonine	1292.4	117	Amino acid (and related)	0	0	y
Glycine	1303.7	174	Amino acid (and related)	0	y	y
Succinic acid	1312.0	147 +247	Glycolysis/TCA (and related)	0	y	y
Unknown RI 1341	1338.3	106	unknown	y	y	y
Unknown RI 1401	1406.3	147	unknown	y	y	y
Erythrose	1438.4	117	Sugar/Polyol (and related)	0	0	y
Malic acid	1478.7	73	Glycolysis/TCA (and related)	y	y	y

		+233				
Threitol	1487.3	103	Sugar/Polyol (and related)	y	y	0
Erythritol	1493.1	217	Sugar/Polyol (and related)	y	0	y
Aspartic acid	1513.1	232	Amino acid (and related)	0	y	0
Pyroglutamic acid	1521.2	156	Amino acid (and related)	0	y	y
4-Aminobutyric acid	1525.0	174	Amino acid (and related)	0	y	y
Glutamic acid	1530.5	84	Amino acid (and related)	0	0	y
2-Hydroxyglutaric acid	1568.9	129 +203+247	Glycolysis/TCA (and related)	0	y	y
alpha-Ketoglutarate	1572.6	198	Glycolysis/TCA (and related)	0	0	y
Unknown RI 1612	1612.8	138	unknown	y	0	0
Phenylalanine	1632.0	218	Amino acid (and related)	0	y	0
Kojic acid	1661.2	271	Fungus specific	0	0	y
Xylitol	1690.9	217 +103	Sugar/Polyol (and related)	y	y	0
Ribitol	1712.2	103	Sugar/Polyol (and related)	y	y	y
Putrescine	1738.8	174	Stabilization	0	y	y
Shikimic acid	1752.6	204	Amino acid (and related)	0	y	0
Glycerol-3-phosphate	1756.7	299	Fat (and related)	0	0	y
Citric acid	1811.9	273	Glycolysis/TCA (and related)	0	y	y
Fructose	1857.4	103	Glycolysis/TCA (and related)	y	y	y
Gluconic acid-1,5-lactone	1875.5	220	Sugar/Polyol (and related)	y	0	y
Glucose	1883.9	160	Sugar/Polyol (and related)	0	0	y
Sorbitol	1913.2	319	Sugar/Polyol (and related)	y	y	y
Inositol	2015.3	318	Sugar/Polyol (and related)	y	y	y
Hexadecanoic acid	2045.7	117	Fat (and related)	0	y	y
myo-Inositol	2080.7	217	Sugar/Polyol (and related)	y	y	y
Spermidine	2192.9	174 +200	Stabilization	0	y	0
Octadecanoic acid	2242.7	117	Fat (and related)	y	y	y
Uridine	2468.4	217	Other	0	0	y
Sucrose	2623.5	361	Sugar/Polyol (and related)	0	y	y
Disaccharide RI 2663	2663.4	361	Sugar/Polyol (and related)	y	0	0
Lactose	2722.7	204	Sugar/Polyol (and related)	0	0	y
Trehalose	2726.7	191	Sugar/Polyol (and related)	y	y	y
Isomaltose	2846.7	361	Sugar/Polyol (and related)	0	0	y
Maltotriose	3496.2	204	Sugar/Polyol (and related)	0	0	y

8 Eidesstattliche Erklärung (Originality statement)

Hiermit erkläre ich, dass ich die vorliegende Dissertation „Influence of the Environome on the Production and Quality of Seed Cultures" selbständig verfasst, sowie die benutzten Quellen und Hilfsmittel vollständig angegeben habe. Die Arbeit ist in dieser oder einer ähnlichen Form noch nicht als Prüfungsleistung eingereicht worden.

With this statement I declare, that I have independently completed the above doctoral thesis. The thoughts taken directly or indirectly from external sources are properly marked as such. This thesis was not previously submitted to another academic institution and has also not yet been published

Braunschweig, 3. Januar 2011

Band 1 **Sunder, Matthias**: Oxidation grundwasserrelevanter Spurenverunreinigungen mit Ozon und Wasserstoffperoxid im Rohrreaktor. 1996. FIT-Verlag · Paderborn, ISBN 3-932252-00-4

Band 2 **Pack, Hubertus**: Schwermetalle in Abwasserströmen: Biosorption und Auswirkung auf eine schadstoffabbauende Bakterienkultur. 1996. FIT-Verlag · Paderborn, ISBN 3-932252-01-2

Band 3 **Brüggenthies, Antje**: Biologische Reinigung EDTA-haltiger Abwässer. 1996. FIT-Verlag · Paderborn, ISBN 3-932252-02-0

Band 4 **Liebelt, Uwe**: Anaerobe Teilstrombehandlung von Restflotten der Reaktivfärberei. 1997. FIT-Verlag · Paderborn, ISBN 3-932252-03-9

Band 5 **Mann, Volker G.**: Optimierung und Scale up eines Suspensionsreaktorverfahrens zur biologischen Reinigung feinkörniger, kontaminierter Böden. 1997. FIT-Verlag · Paderborn, ISBN 3-932252-04-7

Band 6 **Boll Marco**: Einsatz von Fuzzy-Control zur Regelung verfahrenstechnischer Prozesse. 1997. FIT-Verlag · Paderborn, ISBN 3-932252-06-3

Band 7 **Büscher, Klaus**: Bestimmung von mechanischen Beanspruchungen in Zweiphasenreaktoren. 1997. FIT-Verlag · Paderborn, ISBN 3-932252-07-1

Band 8 **Burghardt, Rudolf**: Alkalische Hydrolyse – Charakterisierung und Anwendung einer Aufschlußmethode für industrielle Belebtschlämme. 1998. FIT-Verlag · Paderborn, ISBN 3-932252-13-6

Band 9 **Hemmi, Martin**: Biologisch-chemische Behandlung von Färbereiabwässern in einem Sequencing Batch Process. 1999. FIT-Verlag · Paderborn, ISBN 3-932252-14-4

Band 10 **Dziallas, Holger**: Lokale Phasengehalte in zwei- und dreiphasig betriebenen Blasensäulenreaktoren. 2000. FIT-Verlag · Paderborn, ISBN 3-932252-15-2

Band 11 **Scheminski, Anke**: Teiloxidation von Faulschlämmen mit Ozon. 2001. FIT-Verlag · Paderborn, ISBN 3-932252-16-0

Band 12 **Mahnke, Eike Ulf**: Fluiddynamisch induzierte Partikelbeanspruchung in pneumatisch gerührten Mehrphasenreaktoren. 2002. FIT-Verlag · Paderborn, ISBN 3-932252-17-9

Band 13 **Michele, Volker**: CDF modeling and measurement of liquid flow structure and phase holdup in two- and three-phase bubble columns. 2002. FIT-Verlag · Paderborn, ISBN 3-932252-18-7

Band 14 **Wäsche, Stefan**: Einfluss der Wachstumsbedingungen auf Stoffübergang und Struktur von Biofilmsystemen. 2003. FIT-Verlag · Paderborn, ISBN 3-932252-19-5

Band 15 **Krull Rainer**: Produktionsintegrierte Behandlung industrieller Abwässer zur Schließung von Stoffkreisläuren. 2003. FIT-Verlag · Paderborn, ISBN 3-932252-20-9

Band 16 **Otto, Peter**: Entwicklung eines chemisch-biologischen Verfahrens zur Reinigung EDTA enthaltender Abwässer. 2003. FIT-Verlag · Paderborn, ISBN 3-932252-21-7

Band 17 **Horn, Harald**: Modellierung von Stoffumsatz und Stofftransport in Biofilmsystemen. 2003. FIT-Verlag · Paderborn, ISBN 3-932252-22-5

Band 18 **Mora Naranjo, Nelson**: Analyse und Modellierung anaerober Abbauprozesse in Deponien. 2004. FIT-Verlag · Paderborn, ISBN 3-932252-23-3

Band 19 **Döpkens, Eckart**: Abwasserbehandlung und Prozesswasserrecycling in der Textilindustrie. 2004. FIT-Verlag · Paderborn, ISBN 3-932252-24-1

Band 20 **Haarstrick, Andreas**: Modellierung millieugesteuerter biologischer Abbauprozesse in heterogenen problembelasteten Systemen. 2005. FIT-Verlag · Paderborn, ISBN 3-932252-27-6

Band 21 **Baaß, Anne-Christina**: Mikrobieller Abbau der Polyaminopolycarbonsäuren Propylendiamintetraacetat (PDTA) und Diethylentriaminpentaacetat (DTPA). 2004. FIT-Verlag · Paderborn, ISBN 3-932252-26-8

Band 22 **Staudt, Christian**: Entwicklung der Struktur von Biofilmen. 2006. FIT-Verlag · Paderborn, ISBN 3-932252-28-4

Band 23 **Pilz, Roman Daniel**: Partikelbeanspruchung in mehrphasig betriebenen Airlift-Reaktoren. 2006. FIT-Verlag · Paderborn, ISBN 3-932252-29-2

Band 24 **Schallenberg, Jörg**: Modellierung von zwei- und dreiphasigen Strömungen in Blasensäulenreaktoren. 2006. FIT-Verlag · Paderborn, ISBN 3-932252-30-6

Band 25 **Enß, Jan Hendrik**: Einfluss der Viskosität auf Blasensäulenströmungen. 2006. FIT-Verlag · Paderborn, ISBN 3-932252-31-4

Band 26 **Kelly, Sven**: Fluiddynamischer Einfluss auf die Morphogenese von Biopellets filamentöser Pilze. 2006. FIT-Verlag · Paderborn, ISBN 3-932252-32-2

Band 27 **Grimm, Luis Hermann**: Sporenaggregationsmodell für die submerse Kultivierung koagulativer Myzelbildner. 2006. FIT-Verlag · Paderborn, ISBN 3-932252-33-0

Band 28 **León Ohl, Andrés**: Wechselwirkungen von Stofftransport und Wachstum in Biofilsystemen. 2007. FIT-Verlag · Paderborn, ISBN 3-932252-34-9

Band 29 **Emmler, Markus**: Freisetzung von Glucoamylase in Kultivierungen mit *Aspergillus niger*. 2007. FIT-Verlag · Paderborn, ISBN 3-932252-35-7

Band 30 **Leonhäuser, Johannes**: Biotechnologische Verfahren zur Reinigung von quecksilberhaltigem Abwasser. 2007. FIT-Verlag · Paderborn, ISBN 3-932252-36-5

Band 31 **Jungebloud, Anke**: Untersuchung der Genexpression in *Aspergillus niger* mittels Echtzeit-PCR. 1996. FIT-Verlag · Paderborn, ISBN 978-3-932252-37-2

Band 32 **Hille, Andrea**: Stofftransport und Stoffumsatz in filamentösen Pilzpellets. 2008. FIT-Verlag · Paderborn, ISBN 978-3-932252-38-9

Band 33 **Fürch, Tobias**: Metabolic characterization of recombinant protein production in *Bacillus megaterium*. 2008. FIT-Verlag · Paderborn, ISBN 978-3-932252-39-6

Band 34 **Grote, Andreas Georg**: Datenbanksysteme und bioinformatische Werkzeuge zur Optimierung biotechnologischer Prozesse mit Pilzen. 2008. FIT-Verlag · Paderborn, ISBN 978-3-932252-40-120

Band 35 **Möhle, Roland Bernhard**: An Analytic-Synthetic Approach Combining Mathematical Modeling and Experiments – Towards an Understanding of Biofilm Systems. 2008. FIT-Verlag · Paderborn, ISBN 978-3-932252-41-9

Band 36 **Reichel, Thomas**: Modelle für die Beschreibung das Emissionsverhaltens von Siedlungsabfällen. 2008. FIT-Verlag · Paderborn, ISBN 978-3-932252-42-6

Band 37 **Schultheiss, Ellen**: Charakterisierung des Exopolysaccharids PS-EDIV von *Sphingomonas pituitosa*. 2008. FIT-Verlag · Paderborn, ISBN 978-3-932252-43-3

Band 38 **Dreger, Michael Andreas**: Produktion und Aufarbeitung des Exopolysaccharids PS-EDIV aus *Sphingomonas pituitosa*. 1996. FIT-Verlag · Paderborn, ISBN 978-3-932252-44-0

Band 39 **Wiebels, Cornelia**: A Novel Bubble Size Measuring Technique for High Bubble Density Flows. 2009. FIT-Verlag · Paderborn, ISBN 978-3-932252-45-7

Band 40 **Bohle, Kathrin**: Morphologie- und produktionsrelevante Gen- und Proteinexpression in submersen Kultivierungen von *Aspergillus niger*. 2009. FIT-Verlag · Paderborn, ISBN 978-3-932252-46-2

Band 41 **Fallet, Claas**: Reaktionstechnische Untersuchungen der mikrobiellen Stressantwort und ihrer biotechnologischen Anwendungen. 2009. FIT-Verlag · Paderborn, ISBN 978-3-932252-47-1

Band 42 **Vetter, Andreas**: Sequential Co-simulation as Method to Couple CFD and Biological Growth in a Yeast. 2009. FIT-Verlag · Paderborn, ISBN 978-3-932252-48-8

Band 43 **Jung, Thomas**: Einsatz chemischer Oxidationsverfahren zur Behandlung industrieller Abwässer. 2010. FIT-Verlag· Paderborn, ISBN 978-3-932252-49-5

Band 45 **Herrmann, Tim**: Transport von Proteinen in Partikeln der Hydrophoben Interaktions Chromatographie. 2010. FIT-Verlag · Paderborn, ISBN 978-3-932252-51-8

Band 46 **Becker, Judith**: Systems Metabolic Engineering of *Corynebacterium glutamicum* towards improved Lysine Prodction. 2010. Cuvillier Verlag · Göttingen, ISBN 978-3-86955-426-6

Band 47 **Melzer, Guido**: Metabolic Network Analysis of the Cell Factory *Aspergillus niger*. 2010. Cuvillier Verlag · Göttingen, ISBN 978-3-86955-456-3

Band 48 **Bolten J., Christoph**: Bio-based Production of L-Methionine in *Corynebacterium glutamicum*. 2010. Cuvillier Verlag · Göttingen, ISBN 978-3-86955-486-0

Band 49 **Lüders, Svenja**: Prozess- und Proteomanalyse gestresster Mikroorganismen. 2010. Cuvillier Verlag · Göttingen, ISBN 978-3-86955-435-8

Band 50 **Wittmann, Christoph**: Entwicklung und Einsatz neuer Tools zur metabolischen Netzwerkanalyse des industriellen Aminosäure-Produzenten *Corynebacterium glutamicum*. 2010. Cuvillier Verlag · Göttingen, ISBN 978-3-86955-445-7

Band 51 **Edlich, Astrid**: Entwicklung eines Mikroreaktors als Screening-Instrument für biologische Prozesse. 2010. Cuvillier Verlag · Göttingen, ISBN 978-3-86955-470-9

Band 52 **Hage, Kerstin**: Bioprozessoptimierung und Metabolomanalyse zur Proteinproduktion in *Bacillus licheniformis*. 2010. Cuvillier Verlag · Göttingen, ISBN 978-3-86955-578-2

Band 53 **Kiep, Katina Andrea**: Einfluss von Kultivierungsparametern auf die Morphologie und Produktbildung von *Aspergillus niger*. 2010. Cuvillier Verlag · Göttingen, ISBN 978-3-86955-632-1

Band 54 **Fischer, Nicole**: Experimental investigations on the influence of physico-chemical parameters on anaerobic degradation in MBT residual waste. 2011. Cuvillier Verlag · Göttingen, ISBN 978-3-86955-679-6

Band 55 **Schädel, Friederike**: Stressantwort von Mikroorganismen. 2011. Cuvillier Verlag· Göttingen, ISBN 978-3-86955-750-2

Band 56 **Wichter, Johannes:** Untersuchung der L-Cystein-Biosynthese in Escherichia coli mit Techniken der Metabolom- und ^{13}C-Stoffflussanalyse. 2011. Cuvillier-Verlag · Göttingen, ISBN 978-3-86955-750-2

Band 57 **Knappik, Irena Isabell:** Charakterisierung der biologischen und chemischen Reaktionsprozesse in Siedlungsabfällen. 2011. Cuvillier-Verlag · Göttingen, ISBN 978-3-86955-760-1

Band 58 **Driouch, Habib**: Systems Biotechnology of Recombinant Protein Production in *Aspergillus niger*. 2011. Cuvillier Verlag · Göttingen, ISBN 978-3-86955-808-0